Chem Soc Rev

REVIEW ARTICLE

View Article Online
View Journal

Cite this: DOI: 10.1039/d0cs01466d

Enroute sustainability: metal free C–H bond functionalisation

Sayan Roy,[a] Subir Panja,[a] Sumeet Ranjan Sahoo,[a] Sagnik Chatterjee[a] and Debabrata Maiti *[ab]

Received 7th November 2022

DOI: 10.1039/d0cs01466d

rsc.li/chem-soc-rev

The term "C–H functionalisation" incorporates C–H activation followed by its transformation. In a single line, this can be defined as the conversion of carbon–hydrogen bonds into carbon–carbon or carbon–heteroatom bonds. The catalytic functionalisation of C–H bonds using transition metals has emerged as an atom-economical technique to engender new bonds without activated precursors which can be considered as a major drawback while attempting large-scale synthesis. Replacing the transition-metal-catalysed approach with a metal-free strategy significantly offers an alternative route that is not only inexpensive but also environmentally benign to functionalize C–H bonds. Recently metal free synthetic approaches have been flourishing to functionalize C–H bonds, motivated by the search for greener, cost-effective, and non-toxic catalysts. In this review, we will highlight the comprehensive and up-to-date discussion on recent examples of ground-breaking research on green and sustainable metal-free C–H bond functionalisation.

1. Introduction

Synthetic organic chemistry has experienced tremendous development during the last century with its notable application in medicinal, pharmaceutical, agrochemical, materials science as well as biochemistry disciplines.[1,2] In this aspect, C–H and C–C bonds are the most abundant linkages in nature. However, the robust nature and the lack of reactivity of C–H bonds have become the most fundamental as well as practical challenge to synthetic chemists.[3] The insufficient reactivity of C–H bonds is often attributed to their high bond energies (typically 90–100 kcal mol^{-1}) and very low acidity (pK_a = 45–60). Thereafter, the C–H functionalisation was heralded as the one 'holy grail' in organic synthesis which discriminatively activates a typically inert C–H bond into a latent functional group.[4–9] The term "C–H functionalisation" thus includes a C–H activation step followed by C–H transformation thereby reducing the number of transformations in multi-step synthesis consisting of long and laborious protection–deprotection sequences as well as undesired by-products. The significance of selective bond formation between carbon and other atoms using transition

[a] Department of Chemistry, Indian Institute of Technology Bombay, Powai, Mumbai-400076, India. E-mail: dmaiti@iitb.ac.in; Web: https://www.dmaiti.com
[b] Department of Interdisciplinary Program in Climate Studies, Indian Institute of Technology Bombay, Powai, Mumbai, 400076, India

Sayan Roy

Dr Sayan Roy was born and raised in Kolkata, West Bengal, India. He received his PhD from the Centre of Biomedical Research (CBMR), Lucknow, in 2020 under the supervision of Prof. Saumen Hajra. Then he joined Prof. Maiti's group at IIT Bombay as a post-doctoral fellow. His research interests are focused on photo-redox catalysed cross electrophile coupling. Currently, he is a post-doctoral fellow at Purdue University, USA.

Subir Panja

Dr Subir Panja was born in West Bengal, India. He received his PhD from IACS, Kolkata, in 2020 under the supervision of Prof. Brindaban C. Ranu and Dr. Joyram Guin. Then he moved to Prof. Maiti's group at IIT Bombay as a post-doctoral fellow. His research interests are focused on the development of new and sustainable synthetic and catalytic methods via electrocatalysis.

metals has been acknowledged by the Nobel Prize in Chemistry in 2010.[10] Following this, a lot of effort was put in the pursuit of a more refined method of activating C–H bonds, which has gone from being an aspirational idea to being widely employed in both academia and industry. Nevertheless, the catalytic functionalisation of C–H bonds mostly depends on the power of precious transition metals like Pd, Ir, Rh, and Ru which can be a considerable drawback while attempting large-scale synthesis.[11–14] This catalytic activity of these metals is further enhanced using electronically as well as sterically tuned ligands. Unfortunately, these noble transition metals are not only cost-intensive but are also generally rather toxic. Indeed, the level of residual trace metal impurities in pharmaceutical industries, organic electronic devices and crop protecting agents constitutes a significant challenge in terms of applications of noble-transition-metal catalysis. However, the ever-increasing recognition and ubiquitous usage of C–H activation processes continuously drive the synthetic chemist to improve the sustainability of C–H reactions from an environmental standpoint. In this context, replacing this transition-metal-catalysed approach by a metal-free strategy significantly offers an alternative inexpensive as well as environmentally benign route to C–H functionalisation.[15–17] Therefore, the metal-free catalysis has been thriving recently, inspired by the aspiration for a greener, cheaper, and less toxic environment, and consequently the recent development of elegant and boundary-pushing ideas on various metal-free C–H functionalisation reactions is the focal point of this review.

Sumeet Ranjan Sahoo

Sumeet Ranjan Sahoo was born in Odisha, India. He obtained his Integrated BS-MS Dual Degree from the Indian Institute of Science Education and Research (IISER), Kolkata, in 2019, under the supervision of Prof. Swadhin Kumar Mandal, where he worked at the Development of Earth Abundant Metal-Based Catalysts for Homogeneous Catalysis. After working as a research assistant at IIT Bombay on Metal-Mediated Remote C–H Bond Functionalisation of Aliphatic Systems, under the supervision of Prof. Debabrata Maiti, he joined the Department of Chemistry at Purdue University as a graduate student. Currently he is working under the supervision of Prof. Christopher Uyeda at Purdue University.

2. Evolution from noble to mild metal to metal free approach

C–H activation has emerged as a rapidly developing field within homogeneous catalysis over the past two decades, shaping the field of organometallic catalysis as well as synthetic organic chemistry. The initial efforts in this field were mainly devoted to the discovery of noble metal catalysts that can insert into the C–H bond. But owing to the inert nature of the C–H bond, typically harsh reaction conditions are required which apparently hampered the wide functional group tolerance. Moreover, due to the use of precious metals and a stoichiometric amount of the oxidant, C–H activation has not yet found widespread applications in the synthesis of complex molecules and natural products. Thus, today's researchers are focused on finding ways to improve its practicality and implement less expensive and environmentally damaging alternatives. In preparation for the next generation of C–H activation, many research groups have focused on developing reactions that take a more benign route. To achieve 'mildness in the methodology', chemists have introduced comprehensive and path-breaking ideas for C–H functionalisation. In this context, earth-abundant 3d-transition metal catalysts such as Sc, V, Mn, Co, Cu, Fe, Zn, *etc*. have experienced a strong demand for the development of powerful C–H functionalisation methods not only due to their environmentally friendly nature,[18–20] but also because they are less toxic than their 4d and 5d counterparts, leading to these 3d metals gaining prominence also in enzymatic processes. As an

Sagnik Chatterjee

Sagnik Chatterjee was born and raised in Kolkata, India. He completed his Bachelor's in Chemistry from St. Xavier's College, Kolkata, in 2020. After that, he obtained his Master's in Chemistry from Indian Institute of Technology, Bombay, in the year 2022. During his Master's, he worked under the tutelage of Prof. Dr Debabrata Maiti towards his Master's thesis. His research interests encompass developing sustainable methodologies using photocatalytic techniques.

Debabrata Maiti

Prof. Debabrata Maiti received his PhD from John Hopkins University (USA) in 2008 under the supervision of Prof. Kenneth D. Karlin. After postdoctoral studies at Massachusetts Institute of Technology (MIT) with Prof. Stephen L. Buchwald (2008–2010), he joined the Department of Chemistry at IIT Bombay in 2011, where he is currently Institute Chair Professor. His research interests are focused on the development of new and sustainable synthetic and catalytic methods.

added bonus, the cost-effectiveness of using these 3d-transition metals is directly correlated with their abundance on Earth. Taking a step forward, further progress has been achieved by employing milder reaction conditions as well as the usage of main group elements quite recently. Since the pioneering invention that the Frustrated Lewis Pair (FLP) can heterolytically split molecular hydrogen, this main group ambiphilia has been taken into consideration for the fruitful C–H bond activation in the last five years.[21,22] Moreover, to avoid all toxic metals and stoichiometric oxidants, scientists are continuously involved in the discovery of complete metal free greener approaches in the arena of C–H activation. In this regard, aerobic oxidation as well as photocatalytic metal free C–H functionalisation has emerged as a complementary approach to the classical transition metal catalysed transformations. This review will provide an up-to-date discussion on recent examples of ground-breaking research on metal-free activation of C–H bonds to achieve green and sustainable C–H bond functionalisation.

3. Metal free oxidative C–H functionalisation

The development of C–H functionalisation methods under benign conditions is an ongoing challenge for the synthetic chemists as discussed earlier. Clearer than ever before, synthetic organic chemistry needs to prioritise energy efficiency and waste management in light of growing environmental concerns and climatic shifts.[23] The principles of green chemistry have led to a focus on metal-free and metal-oxidant-free C–H functionalization as a direct result. Oxidative coupling reaction has been the focus of extensive research in this area in the past decade. Chemical oxidants such as DDQ and TBHP are frequently used in various cross dehydrogenative coupling (CDC) reactions. Furthermore, molecular oxygen is an environmentally benign oxidant in this regard. In this technique, free radical intermediates play a crucial role in selective C–H bond activation.

3.1 Aerobic/oxygen-initiated C–H functionalisation

The discovery of auto-oxidation of aldehydes is the cornerstone which enabled the mild and selective formation of acyl radicals utilizing only molecular oxygen as a reagent (Scheme 1). In order to achieve green and sustainable C–H bond functionalization, researchers have begun to consider the use of dioxygen to activate C–H bonds by generating radical species. In this regard, different research groups have applied different orchestrations to introduce oxygen gas in their reaction, *i.e.* the use of a pressurised environment of dioxygen through an autoclave (>1 atm) or *via* a balloon (1 atm) or even purging compressed air into the reaction mixture in an inert environment, or by simple exposure of the reaction to atmospheric dioxygen. Apart from aldehydes, dioxygen induced C–H bond functionalisation reactions have also utilised ethers, benzylamines and glycine derivatives as antecedents for aerobic activation.

3.1.1 Aldehyde as a precursor for aerobic C–H functionalisation. Due to its auto-oxidation in the presence of molecular oxygen and the pervasiveness of the acyl group in molecular architecture, aldehyde is the most recommended substrate to achieve the C–H functionalisation reaction. Radical C–H functionalisation is a convenient approach in this regard due to the susceptible hydrogen abstraction of aldehydic C–H bonds. This powerful synthetic potential of aldehyde offers a formidable approach to aerobic C–H activation followed by its further exploitation in C–C bond formation.

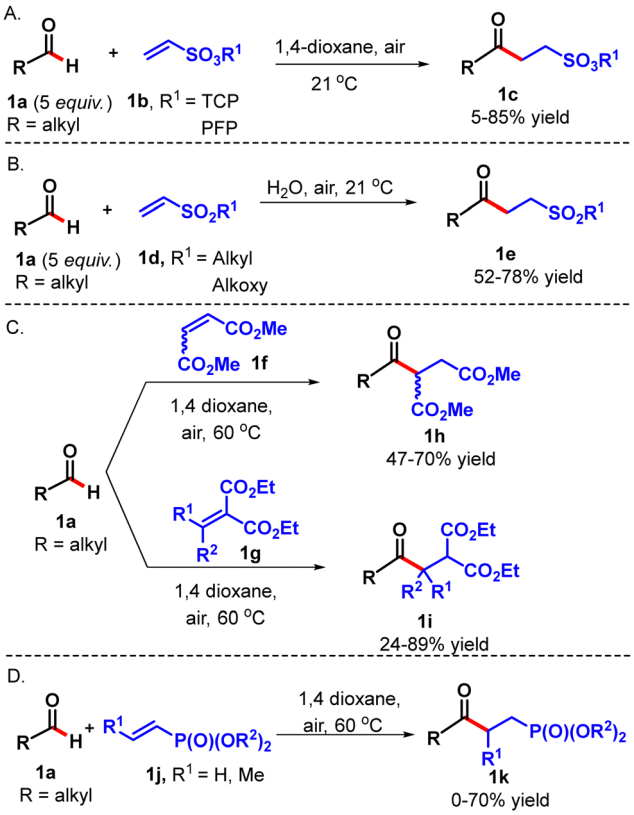

Scheme 1 Hydroacylation of activated olefin *via* aerobic C–H activation (Fitzmaurice *et al.*,[24] Chudasama *et al.*[25–27]).

In 2009, Caddick and co-workers first accomplished the direct C–H activation of aldehyde **1a** and the concomitant addition of the acyl radical to vinyl sulfonates **1b** to afford unsymmetrical ketones **1c** in moderate to good yields (5–85%) (Scheme 1A).[24] The isolated yield of the ketone **1c** was found to be optimum with 5 equiv. of aldehyde **1a** and the corresponding TCP (2,4,6-trichloro phenyl) derived olefin **1b**. In addition, the radical mechanism was established by the complete inhibition of the reaction in the presence of radical inhibitor BHT (2,6-di-*tert*-butyl-4-methylphenol).

Later they utilised the "on-water" air promoted C–H activation of aliphatic aldehydes to achieve hydroacylation of various vinyl sulfones **1d** that introduced the ideal "green" environment with high yields (52–78%) (Scheme 1B).[25]

The Caddick group further expanded the scope of this hydroacylation methodology of aliphatic aldehydes to α,β-unsaturated esters **1f**/**1g** to afford 1,4-dicarbonyls **1h**/**1i** in up to 89% yield (Scheme 1C).[26] In general, raising the reaction temperature to 60 °C provided the efficient transformation

by presumably lowering the dissolved oxygen in the reaction mixture.

Again, they scrutinized the scope of vinyl phosphonates **1j** as an acyl radical acceptor to provide γ-ketophosphonates **1k** (Scheme 1D).[27] The optimum yield of this reaction was obtained at 60 °C at a concentration of 1.00 mol dm^{-3}.

In 2015, the Guin group outlined an operationally simple protocol for the alkylation of electrophilic nitrogen heterocycles employing air promoted (oxygen balloon) aldehydic C–H bond activation (Scheme 2).[28] However, they applied an elevated reaction temperature (115 °C) to access the alkyl radicals through facile decarbonylation. This methodology provided a diverse class of biologically relevant nitrogen-rich alkylated heterocycles by using various aldehydes and nitrogen heterocycles in good yields (26–90%). A plausible mechanism was suggested, according to which the autooxidation of aldehyde followed by decarbonylation afforded the alkyl radical which was intercepted with the protonated heterocycles to generate the radical cation, which upon rearomatization with O_2 or the hydroperoxide radical rendered the alkylated product.

Recently, the same group again illustrated the molecular oxygen promoted radical acylarylation of substituted acrylamides to afford acylated oxindoles with good yield (25–95%) (Scheme 3).[29] Unlike the previous report, radical acylation reaction was carried out at lower temperature (90 °C instead of 115 °C) to lower the tendency of decarbonylation, thereby minimizing the competitive alkylation process. Furthermore, the kinetic study revealed about the existence of a lag phase during the initial 10–12 h of the reaction. After the lag phase, sharp improvement in the rate of reaction was observed which suggested about the longer reaction time to obtain high yield. Thus, fine-tuning of the reaction conditions and proper selection of aldehyde are the key behind the success of this reaction.

3.1.2 Ether/benzylamine/glycine derivative as a precursor for aerobic C–H functionalisation. Ether, benzylamine and glycine are uncommon antecedents for aerobic C–H functionalisation unlike aldehydes. Although the auto-oxidation of ether is well known due to its widespread use as solvent, aerobically induced C–H bond activation utilising these substrates is limited except for some recent explorations.

In 2010, Troisi *et al.* reported the tetrahydrofuranylation of simple (phenol, benzylic) as well as complex (cholesterol) alcohols by exploiting the aerobic C–H bond activation of the freshly distilled and unstabilized THF (Scheme 4).[30] At slightly higher temperature, atmospheric oxygen initiated tetrahydrofuranyl radical generation and an allyl radical helped in the propagation step. For mechanistic proof, the reaction was carried out in the absence of allyl chloride and the product was formed in traces. Furthermore, the reaction with deaerated THF did not yield any product. These two experiments validated the need of oxygen as the initiator and allyl chloride as the propagator of the radical chain. Complete retardation of the reaction in the presence of TEMPO provided further evidence of the radical mechanism. They have also expanded the scope of reaction with imine and alkyne functionalities using allyl chloride as the radical chain propagator.

In 2011, Fu *et al.* developed a metal-free aerobic oxidative coupling of amines to imines by refluxing aerated suspensions of water and amines (Scheme 5).[31] No product formation under a nitrogen atmosphere highlighted the significance of dioxygen in the reaction. A plausible mechanism was suggested according

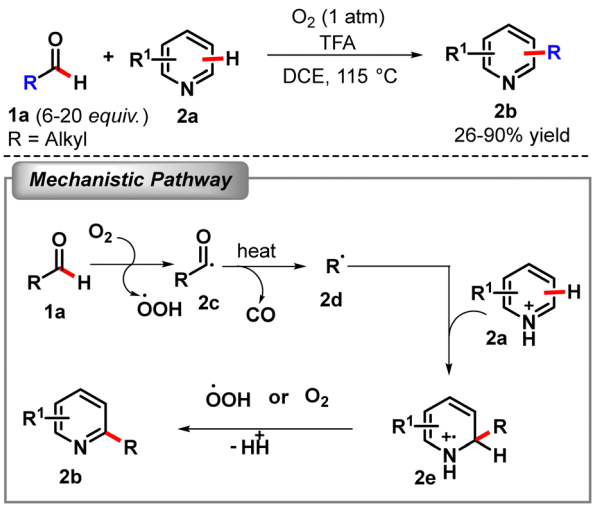

Scheme 2 Aerobic C–H alkylation of nitrogen heterocycles with aldehydes (Paul *et al.*[28]).

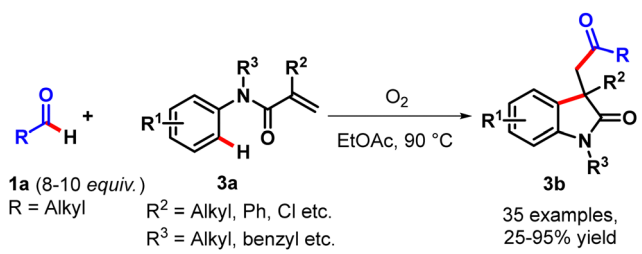

Scheme 3 Aerobic radical acylarylation reaction of *N*-alkyl-*N*-arylacrylamide (Biswas *et al.*[29]).

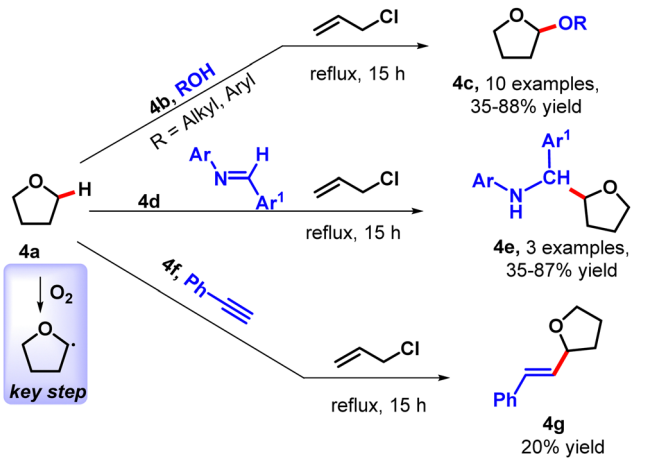

Scheme 4 Aerobic tetrahydrofuranylation of alcohol, imine and alkyne (Troisi *et al.*[30]).

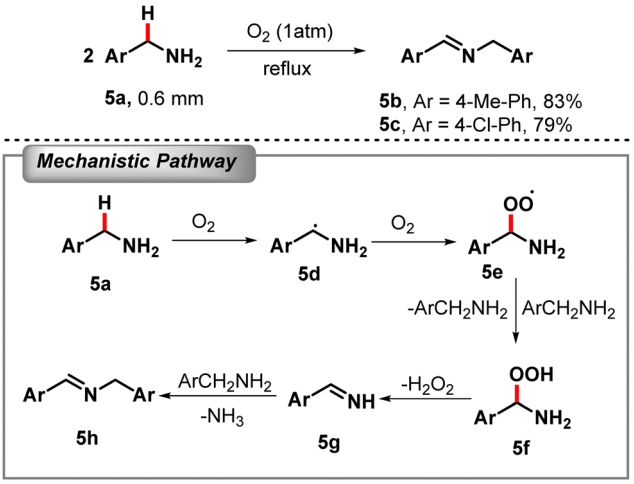

Scheme 5 Aerobic αC–H activation of benzylamine (Liu *et al.*[31]).

to which a benzyl radical was formed by the aerobic αC–H activation of benzylamine. This benzyl radical further reacted with oxygen to form a peroxide complex and a subsequent elimination of hydrogen peroxide afforded the imine.

In 2013, the Nyugen group utilized the aerobic auto-oxidation of benzyl amine for the synthesis of benzimidazoles by heating a mixture of benzylamine and *o*-phenylenediamine (Scheme 6).[32] Elevated reaction temperature (110 °C) and the use of a catalytic amount (20 mol%) of acetic acid fetched the product in good yield (25–87%).

In 2014, the Huo group demonstrated the auto-oxidative cross-coupling reaction of glycine derivatives in a simple mixed organic solvent in the presence of oxygen or air (Scheme 7).[33] The mechanism of glycine auto-oxidation is like that of benzylamines in which an imine intermediate is formed by the expulsion of H_2O_2. This *in situ* generated imine was exploited for the cross dehydrogenative coupling with the indole nucleophile. It is noteworthy that freshly distilled DCE decreased the efficiency of the reaction whereas stored DCE (for 3 to 5 weeks) offered reproducible results. The generation of trace amounts of an acidic impurity in the process of storage of DCE might promote a facile auto-oxidation reaction.

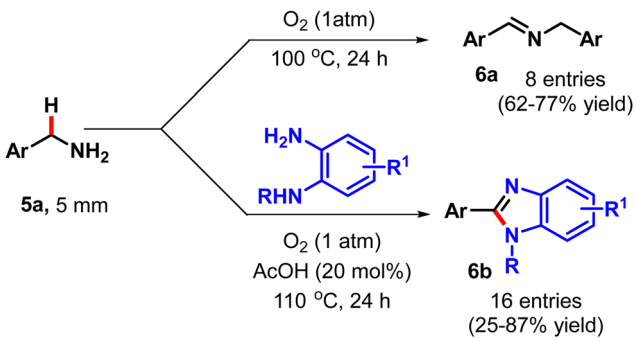

Scheme 6 Synthesis of benzimidazoles by aerobic autooxidation of benzylamine (Nguyen *et al.*[32]).

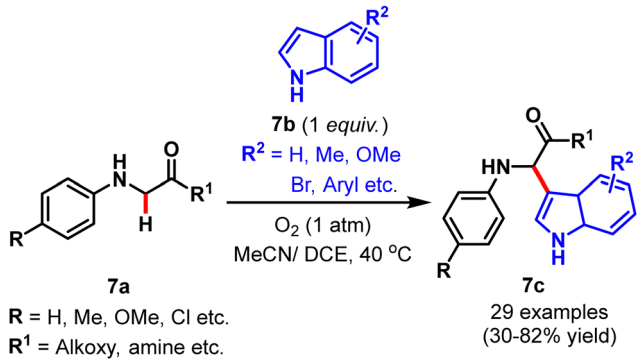

Scheme 7 Aerobic C–H activation of glycine derivatives (Huo *et al.*[33]).

3.2 Oxidant mediated C–H functionalisation

The direct construction of C–C or C-heteroatom bonds by means of C–H bond functionalisation has generated considerable enthusiasm due to step and time efficiency and atom economy. Although metal-catalyzed cross dehydrogenative coupling (CDC) reactions have been studied extensively, the use of oxidants in the absence of metal to promote CDC is the preferred method due to its environmental friendliness. These reactions are feasible in the presence of different oxidants such as DDQ (2,3-dichloro-5,6-dicyanobenzoquinone), DCP (dicumyl peroxide), DTBP (di-*tert*-butyl peroxide), BPO (benzoyl peroxide), CHP (cumene hydroperoxide), TAHP (*tert*-amyl hydroperoxide), TBHP (*tert*-butyl hydroperoxide), *etc.*, that act as a radical initiator in general.

3.2.1 Metal-free direct oxidative C–C bond coupling. In 2009, Itami and Li first reported the new oxidative CDC between two different C–H bonds in the absence of any transition metal (Scheme 8).[34] The reaction of pyridine *N*-oxide and alkane under the influence of DTBP furnished the 2,6-dialkylated product in moderate yield (55–81%). It is to be noted that the nitrogen activation of pyridine was the key behind the success of this coupling reaction since a trace amount of the product was obtained when pyridine was used under similar reaction conditions. Furthermore, increasing the amount of alkene afforded 2,4,6-trialkylated pyridine *N*-oxide as well. It has to be mentioned that DTBP acted as a radical promoter which generated the alkyl radical from the corresponding alkane at higher temperature.

In the same year, Liu *et al.* demonstrated TBHP initiated C(sp^3)–H bond activation of alcohol followed by coupling of the corresponding α-hydroxyalkyl radicals to alkynes for the synthesis of allylic alcohols *via* direct C(sp^2)–C(sp^3) bond formation (Scheme 9).[35] Besides aliphatic alcohols, THF and 1,4-dioxane were also tested for this transformation. A plausible mechanism

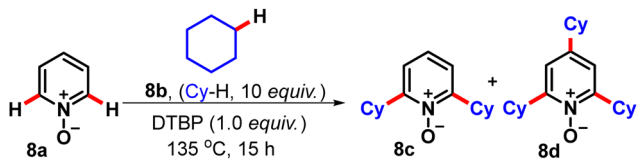

Scheme 8 Oxidative cross dehydrogenative coupling (Deng *et al.*[34]).

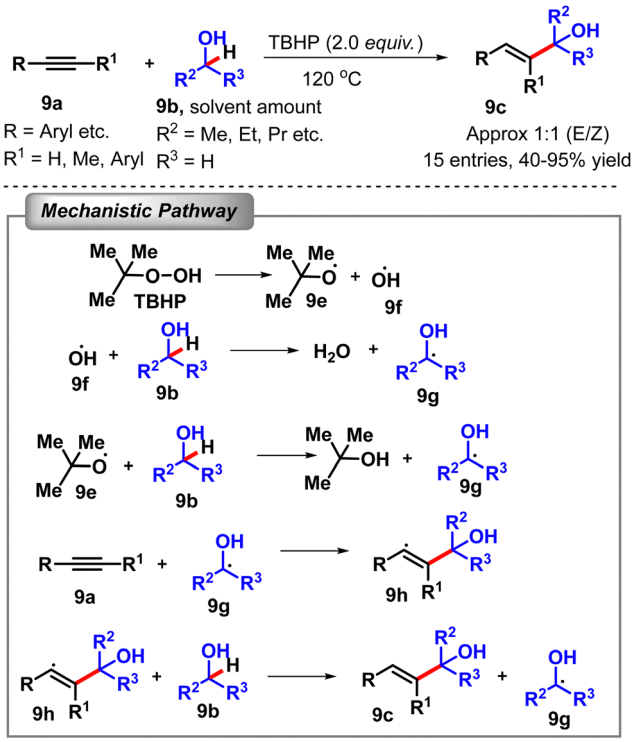

Scheme 9 TBHP initiated C(sp^3)–H bond activation of alcohol (Liu *et al.*[35]).

was suggested the involvement of the radical generated by the homolytic cleavage of the TBHP actually assisted α-hydroxyalkyl radical generation from alcohol **9b** followed by its addition to alkyne **9a** to render the alkenyl radical **9h**. This alkenyl radical abstracted the hydrogen from alcohol to furnish allylic alcohols.

In 2011, the Wang group developed an efficient method for the C2-alkylation of azoles by a similar kind of oxidative C(sp^3)–H bond activation of alcohols and ethers and subsequent cross dehydrogenative C(sp^3)–C(sp^2) coupling with azole (Scheme 10).[36] A plausible mechanism was proposed in that the radicals

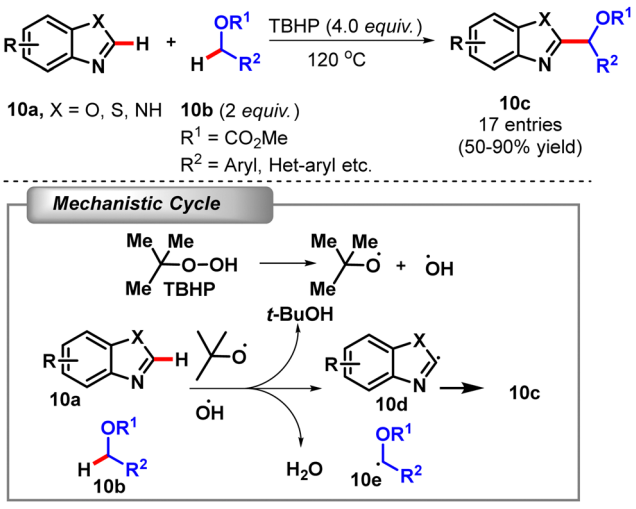

Scheme 10 TBHP initiated C2-alkylation of azoles (He *et al.*[36]).

generated by the homolytic cleavage of TBHP at higher temperature abstracted the hydrogens from the 2-position, *i.e.* sp^2 C–H of benzothiazole and the sp^3 C–H of alcohol, forming the corresponding free radicals. Finally, these two radicals were quenched by desired cross-coupling to afford the C2-alkylated azole as a major product.

Garcia Mancheno *et al.* explored the direct oxidative C(sp^3)–H α-alkylation/cyclisation cascade reaction of simple carbamates with nonactivated olefins to afford a wide range of oxazinones in moderate to excellent yield (38–99%) (Scheme 11).[37] They used the 4-acetamido derivative of TEMPO salt as the oxidant and the adamantyl (Ad) group as a substituent on the carbamate moiety owing to its high leaving group ability to achieve an excellent yield of the desired product. The *N*-acyliminium ion was formed by the initial oxidative C(sp^3)–H α-oxidation of the carbamate by the influence of TEMPO salt. This N-acyliminium ion experienced the nucleophilic addition of olefin followed by a subsequent expulsion of the adamantyl group and the concomitant attack of the carbamate oxygen atom at the carbocation to afford the oxazinone. Moreover, a high kinetic isotope effect (KIE) of 4.6 suggested the C–H bond cleavage to be the rate determining step.

In 2012, Qu and Guo developed an excellent methodology for the synthesis of 8-cycloalkylpurines **12c by** employing DTBP mediated oxidative C(sp^3)–H activation of cycloalkanes (Scheme 12).[38] Here they had manifested the reaction with a wide variety of modified purines and purine nucleosides, including a non-sugar carbon substituent at N9 to afford the desired 8-cycloalkyl purine derivatives in moderate to high yields. A similar free radical pathway was proposed and a significant isotopic effect (KIE 3.8) suggested the C–H bond cleavage of cycloalkane as the rate determining step.

A $K_2S_2O_8$ promoted oxidative spirocyclization of hydroxymethylacrylamide **13a** with 1,3-dicarbonyl compounds **13b** *via* a

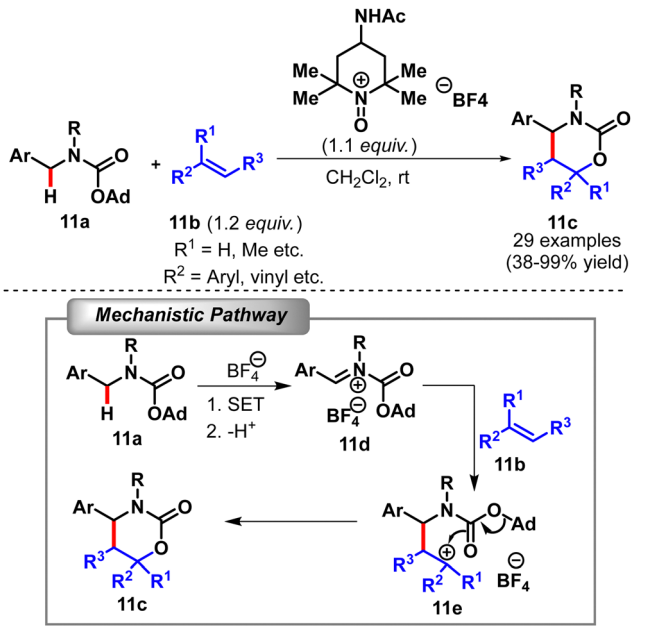

Scheme 11 Tandem α-alkylation/cyclization of *N*-benzyl carbamates with simple olefin (Richter *et al.*[37]).

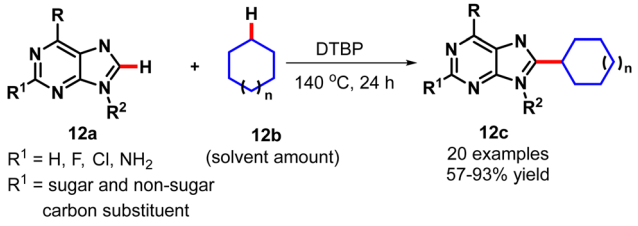

Scheme 12 DTBP mediated oxidative C(sp^3)–H activation of cycloalkane (Xia *et al.*[38]).

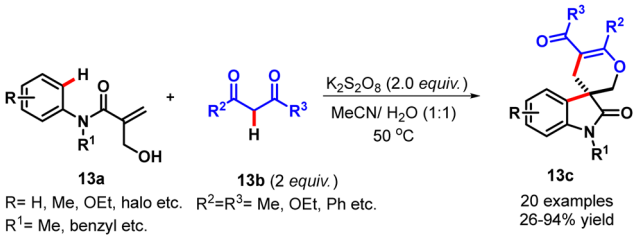

Scheme 13 Metal-free oxidative spirocyclization of hydroxymethylacrylamide with 1,3-dicarbonyl compounds (Wang *et al.*[39]).

tandem dual sp^3 C–H and sp^2 C–H functionalisation and intramolecular dehydration was achieved by Guo and Duan in 2013 for the straightforward access to spirooxindoles **13c** (Scheme 13).[39] Cyclic β-diketone provided better results than the acyclic counterpart. Surprisingly, 1,3-cyclopentanedione was unable to supply the desired product under the optimized reaction conditions.

In 2014, Han and co-workers established DTBP mediated oxidative C(sp^3)–H bond functionalisation of simple alkanes and their concomitant conjugate addition to chromone **14a** for direct preparation of 2-alkylchromanones **14c** in good yield (50–83%) (Scheme 14).[40] While secondary and primary alkanes experienced smooth transformation, tertiary sp^3 C–H functionalisation could not be observed due to steric hindrance. The radical mechanism was established by the inhibition of the reaction in the presence of TEMPO and the observation of the TEMPO-cycloalkane adduct. A high KIE of 5.25 similarly indicated the C(sp^3)–H bond cleavage as the rate determining step.

The Ji group developed a *tert*-butyl peroxybenzoate (TBPB) initiated sequential C(sp^3)–H/C(sp^2)–H bond functionalisation and dual C–C bond formation for the construction of 6-alkyl phenanthridines **15c** with moderate to good yield (24–89%). The foundation of the reaction was laid on the oxidative C(sp^3)–H

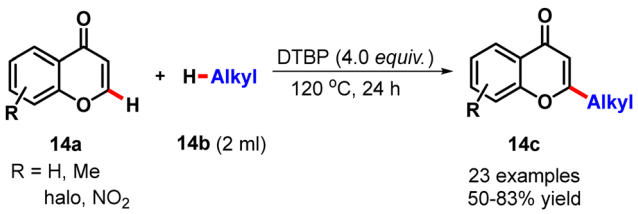

Scheme 14 Metal-free oxidative C(sp^3)–H bond functionalisation of alkanes and conjugate addition to chromone (Zhao *et al.*[40]).

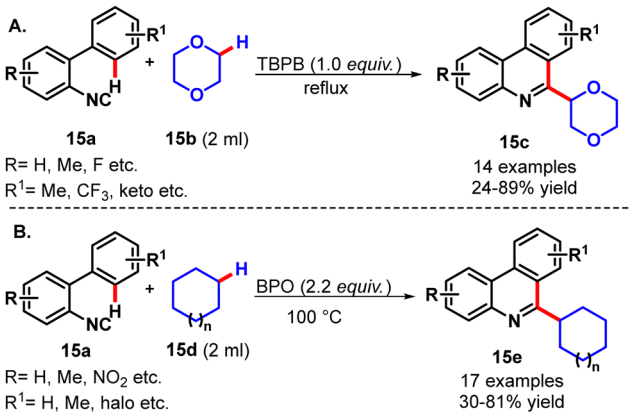

Scheme 15 Oxidative sequential C(sp^3)–H/C(sp^2)–H bond functionalisation (Cao *et al.*,[41] Sha *et al.*[42]).

bond functionalisation of 1,4-dioxane **15b** followed by somophilic isocyanide insertion and the cascade heterolytic aromatic substitution (HAS) process (Scheme 15A).[41] Parallel to the time period, Cheng *et al.* also reported the same α-phenanthridinylation of ether by isocyanide using benzoyl peroxide (BPO) as an oxidant (Scheme 15B).[42] Unlike the previous method, a variety of cyclic and acyclic hydrocarbons and ethers also provided fruitful outcomes. The reaction also followed a similar radical pathway as earlier and a large KIE was observed for THF, suggesting the cleavage of the sp^3 C–H bond rather than the sp^2 C–H bond as the rate-determining step for the transformation.

Later the Ji group again utilised the same method of *tert*-butylperoxybenzoate (TBPB) mediated oxidative C(sp^3)–H bond functionalisation of simple ethers **16b** with α,α-diaryl allylic **16a** for the facile access of α-aryl-β-oxyalkylated carbonyl ketones (Scheme 16).[43] The reaction proceeded with the ethereal radical addition to the allylic alcohol followed by the 1,2-aryl migration cascade process. Remarkably, the preferable migration of the more electron-poor aryl groups suggested the involvement of the radical (neophyl) rearrangement mechanism. It has to be highlighted that the presence of two aryl groups was necessary for such addition-migration process. The mechanism suggested that the TBPB initiated addition of α-carbon-centered radical **16e** to allylic alcohol and a subsequent intramolecular radical addition to the aryl group engendered the spiro[2,5]octadienyl radical **16f**. Next the preferential migration of the electron-deficient aryl group and further oxidation finally resulted in accomplishment of the α-aryl-β-oxyalkylated carbonyl ketones **16c**.

In 2015, Liu and colleagues established an I_2-catalysed sp^3 C–H bond activation of 3-substituted-2-oxindoles **17a** and its concomitant CDC with alkenes **17b** to afford 3-alkenyl-2-oxindoles in moderate to excellent yields (41–98%) (Scheme 17).[44] In this reaction a catalytic amount of I_2 was used as a radical initiator and atmospheric oxygen acted as the re-oxidant to complete the catalytic cycle. A probable mechanism was suggested, namely, the generation of 2-oxindole radical **17d** by iodine and its immediate trapping by styrene **17b** to form a benzyl radical intermediate **17e**. This benzyl radical was quenched by the previously formed iodine radical and a subsequent elimination of hydrogen iodide yielded the

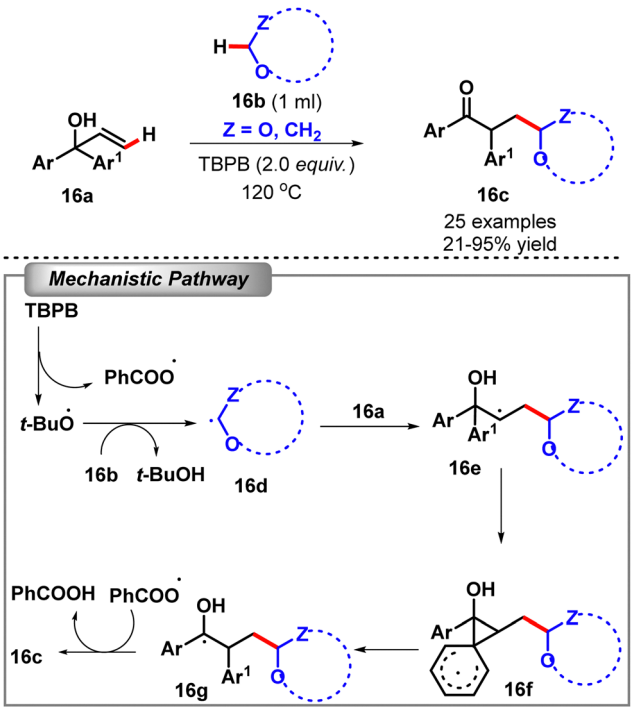

Scheme 16 Oxidative direct C(sp^3)–H bond functionalisation of ethers with α,α-diaryl allylic alcohols (Chu *et al.*[43]).

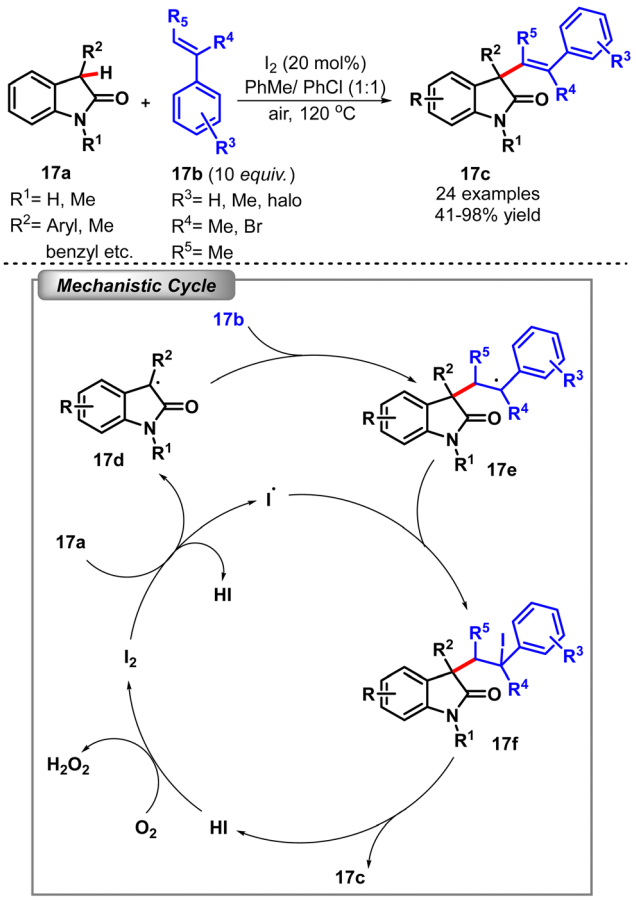

Scheme 17 I_2-catalysed sp^3 C–H bond activation of 3-substituted-2-oxindoles (Huang *et al.*[44]).

desired coupling product **17c**. Meanwhile, the generated HI was reoxidised by the atmospheric oxygen to regenerate iodine.

In the same year, Li and co-workers described a TBPB mediated dual sp^3 C–H oxidative functionalisation and radical [2 + 2 + 1] carbocyclization of benzene-linked 1,*n*-enynes **18a** to achieve a variety of fused five-membered carbocyclic hydrocarbons **18c** (Scheme 18).[45] Majorly O- and S containing cycloalkanes **18b** were found to be compatible in this reaction, whereas amine functionality failed to deliver the desired cyclization. A plausible mechanism was suggested involving the TBPB initiated generation of alkyl radical **18d** by the activation of the C(sp^3)–H bond adjacent to the heteroatom under heating conditions. This alkyl radical encountered a subsequent addition to the C–C double bond of the enyne followed by cyclization with the alkyne to afford the vinyl radical intermediate **18f**. The vinyl radical then underwent a 1,5-H shift through a second sp^3 C–H activation, followed by a radical cyclization with the C–C double bond to afford the radical intermediate **18h** selectively. The intermediate **18h** was then oxidised by TBPB and a subsequent proton loss provided the cyclized product **18c**.

In 2015, Zhu and co-workers demonstrated a dicumyl peroxide (DCP) mediated alkane C(sp^3)–H bond activation followed

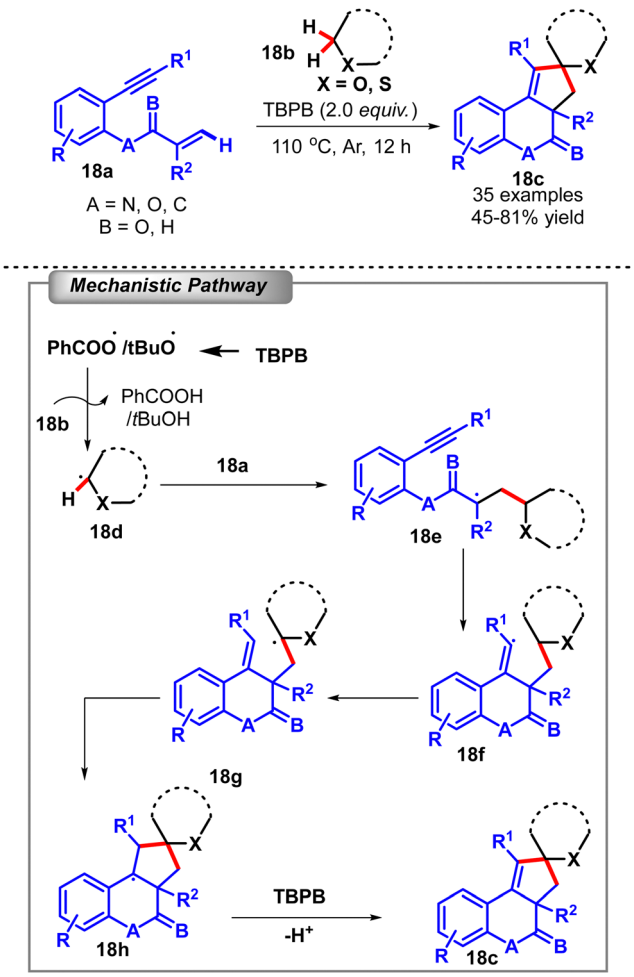

Scheme 18 Oxidative dual sp^3 C–H oxidative functionalisation and radical [2 + 2 + 1] carbocyclization (Hu *et al.*[45]).

by addition of the alkyl radical to *N*-aryl-*N*-tosylmethacrylamide **19a**, elimination of SO_2 and C–C bond formation cascade reaction (Scheme 19).[46] A plausible mechanism was suggested according to which under heating conditions DCP generates a cumyloxyl radical that abstracts a hydrogen atom from the alkane **19b** to form an alkyl radical **19d**. This alkyl radical then added to the acrylamide double bond **19a** followed by a 5-*ipso*-cyclization on the aromatic ring and a rapid desulfonylation to afford the key amidyl radical **19f**. Finally, the amidyl radical afforded the desired product after hydrogen abstraction. Furthermore, a KIE of 3.8 again suggested the involvement of C (sp^3)–H bond cleavage in the rate limiting step.

Later in 2016 the same group reported a TBPB promoted tandem oxidative C (sp^3)–H bond functionalisation of cycloalkanes **20b** followed by alkylation-initiated radical dearomative spiro-cyclization of *N*-phenyl-cinnamamides **20a** for the direct access of alkylated 1-azaspiro [4.5]decanes **20c** involving the formation of two C(sp^3)–C(sp^3) bonds with excellent regioselectivity and diastereoselectivity (Scheme 20).[47]

In 2017, Liu and Tang described a TBHP mediated oxidative C (sp^3)–H bond functionalisation of ether **21b** and its concomitant addition/ring opening/cyclization to methyl cyclopropane **21a** for the synthesis of diverse 2-substituted 3,4-dihydronaphthalenes **21c** with high yield (up to 80%) (Scheme 21).[48] A wide variety of cyclic as well as acyclic ethers were scrutinized under the optimized reaction condition that afforded the desired products

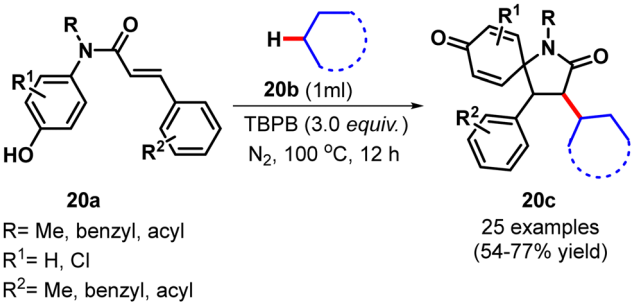

Scheme 20 Tandem oxidative C(sp^3)–H bond functionalisation of alkanes and dearomatization of *N*-phenyl-cinnamamides (Zhang *et al.*[47]).

except tetrahydropyran and tetrahydrothiopyran. As usual the alkyl radical **21d** was formed from THF by a single electron transfer (SET) from TBHP under heating conditions. The alkyl radical then reacted with the carbon–carbon double bond of MCPs **21a** to generate the more stable benzyl radical intermediate **21e**, which underwent a ring-opening of cyclopropane and the successive alkyl radical then directly cyclized with the aromatic ring to afford intermediate **21g**. Finally, this intermediate experienced oxidation followed by rearomatization by hydrogen abstraction to afford 2-substituted 3,4-dihydronaphthalene **21c**.

In 2019, Westwood *et al.* reported the Minisci type direct sp^2 C–H acylation/carbamoylation of heterocycles **22a** by ammonium persulfate $(NH_4)_2S_2O_8$ mediated decarboxylative addition of the acyl/carbamoyl radical to heterocycles (Scheme 22).[49] DMSO had been used as a solvent in this reaction due to its ability to readily

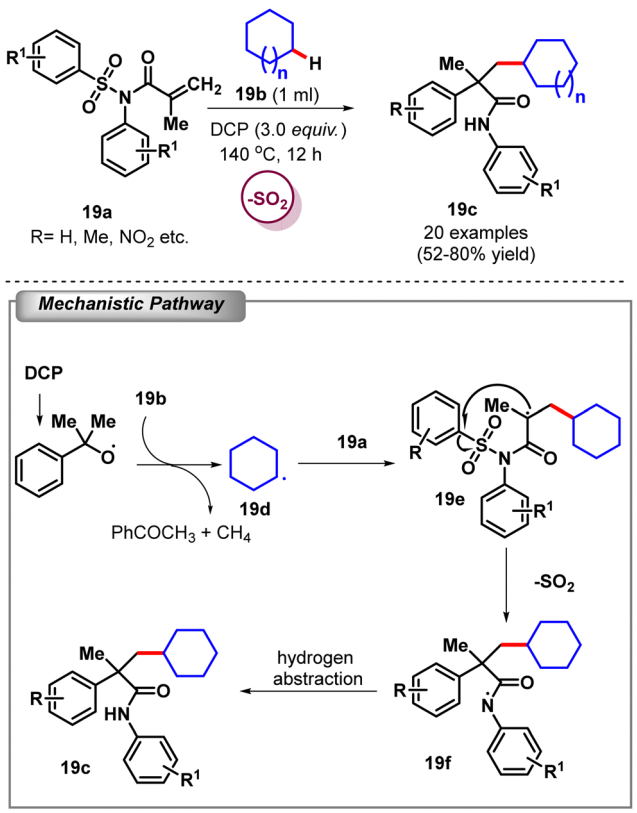

Scheme 19 Metal-free cascade construction of C–C bonds by activation of the inert C(sp^3)–H bond of alkanes (Zhang *et al.*[46]).

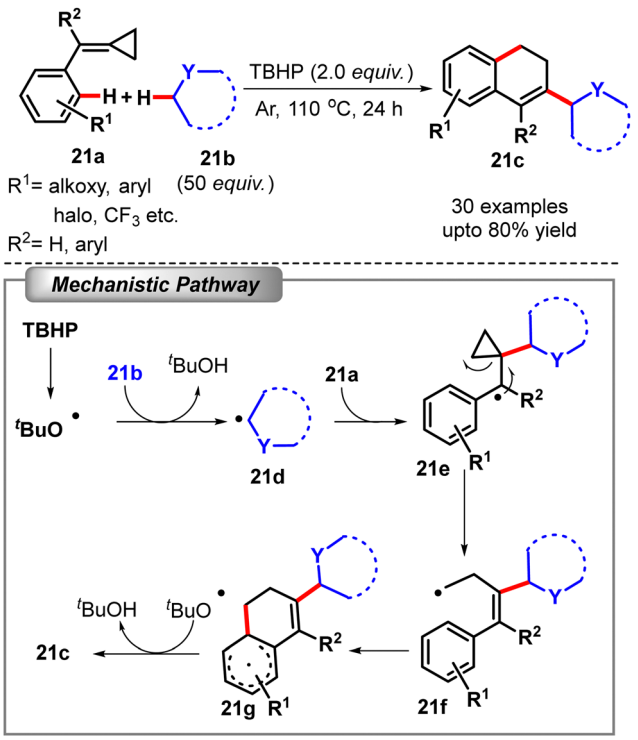

Scheme 21 Oxidative C–C bond functionalisation of methylenecyclopropanes with ethers (Liu *et al.*[48]).

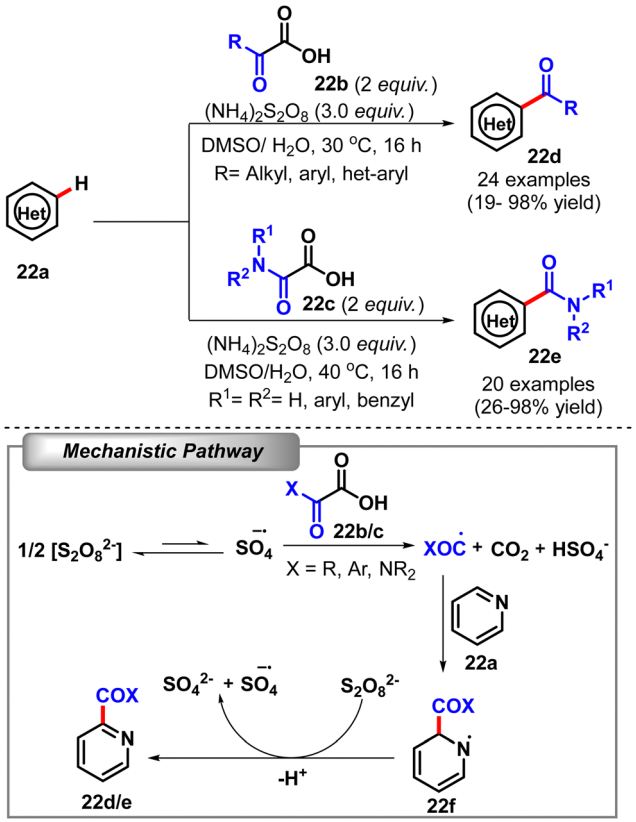

Scheme 22 Oxidative direct C–H acylation and carbamoylation of heterocycles (Westwood *et al.*[49]).

decompose the persulfate. The sulphate radical anion performed the hydrogen atom transfer with α-keto acid **22b** or oxamic acid **22c** to generate the acyl or carbamoyl radical by decarboxylation. Minisci type radical addition to heterocycles followed by hydrogen radical abstraction afforded the desired compound **22d** or **22e**.

3.2.2 Metal-free direct oxidative C–N bond formation. In 2012, the Venkateswarlu group reported a DDQ mediated allylic/benzylic C (sp^3)–H bond functionalisation followed by coupling with amides and sulfonamides **23c** to afford the corresponding amide by means of C–N bond formation in good yield (60–87%) (Scheme 23).[50] The reaction in nitromethane solvent at 80 °C with 5 equiv. of benzylic or allylic substrate was found to be optimum. Although a wide range of benzylic and allylic substrates **23a** or **23b** successfully yielded the desired C–N bond formation, the reaction with toluene and isopropyl benzene was found to be ineffective.

In 2015, Liu *et al.* communicated a similar type of DDQ mediated oxidative C–N coupling of benzylic C–H with amines to afford various amines **24c** in good yield in DCE solvent (37–87%) (Scheme 24).[51] The inclusion of molecular sieves in the reaction medium increased the selectivity by inhibiting the formation of the corresponding ketone as a side product. A plausible mechanism was suggested involving the DDQ mediated SET pathway for the formation of benzylic radical **24d** which could be further oxidized to benzylic cation **24e,** and a subsequent addition of amide to the benzylic cation rendered C–N bond formation.

3.2.3 Metal-free direct oxidative C–P bond formation. In 2011, Wan and co-workers developed a DDQ mediated C(sp^3)–H bond functionalisation of *N*-aryl tetrahydroisoquinolines **25a** followed by concomitant CDC with phosphonates **25b** to afford α-aminophosphonates **25c** by means of C–P bond formation (Scheme 25).[52] Notably, excellent yield (51–99%) of α-aminophosphonates was obtained irrespective of the electronic and sterical effects on the *N*-protected phenyl group of tetrahydroisoquinoline.

3.2.4 Metal-free direct oxidative C–S/–Se/–SCN bond formation. In 2011, Xiang and Li presented a TBHP assisted oxidative thiolation of the C (sp^3)–H bond adjacent to a nitrogen atom of amide **26a** with diaryl disulphide **26b** (Scheme 26).[53] It is noteworthy that the yield of the product was enhanced in the presence of molecular sieves which suggested their role as a weak base to promote the reaction by adjusting the pH value of the reaction solution.

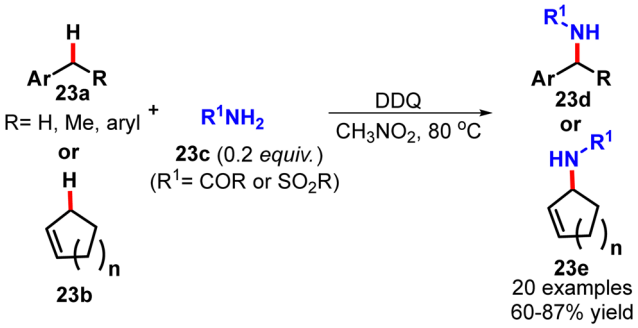

Scheme 23 Oxidative allylic/benzylic C(sp^3)–H bond functionalisation for C–N bond formation (Ramesh *et al.*[50]).

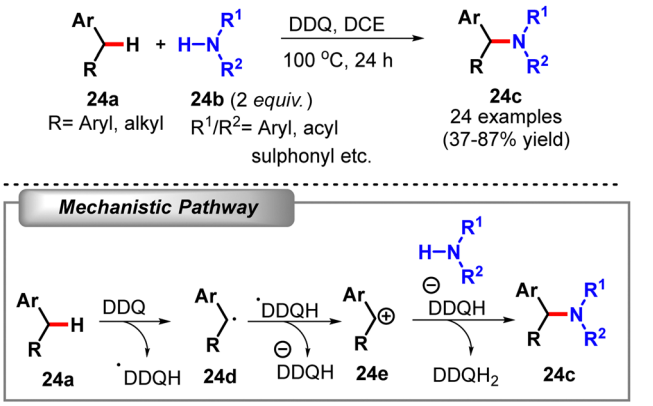

Scheme 24 DDQ mediated oxidative C–N coupling of benzylic C–H with amides (Liu *et al.*[51]).

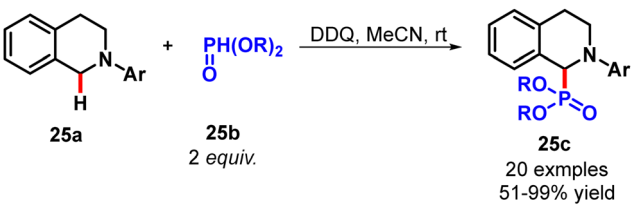

Scheme 25 DDQ mediated C(sp^3)–H bond functionalisation for C–P bond formation (Wang *et al.*[52]).

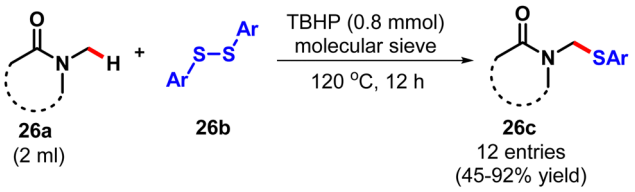

Scheme 26 TBHP-mediated oxidative thiolation of the sp^3 C–H bond (Tang *et al.*[53]).

Furthermore, the *N*-CH2 group reacted preferentially over the *N*-Me group in this reaction.

Two years later they again demonstrated a similar DTBP mediated C(sp^3)–H thiolation adjacent to an oxygen atom of ethers **27a** with diaryl disulfides **26b** for the synthesis of alkyl aryl sulphides **27b** (51–92%) (Scheme 27).[54] Unlike the previous case, here molecular sieves slightly reduced the yield. The proposed mechanism suggested that the *tert*-butoxyl radical generated by the decomposition of DTBP abstracted a hydrogen atom from the ether **27a** to produce the alkoxy radical **27c** which immediately reacted with disulfide **26b** to provide the desired diaryl disulfides **27b**. Again, the quenching of sulphide and alkoxy radicals also furnished the same product by radical chain termination.

In 2014, Lei *et al.* achieved an oxidative C(sp^3)–H/S–H coupling between hydrocarbons **28a** and aryl sulfide **28b** to construct C(sp^3)–S bonds (33–90%). This reaction was successful under the influence of I_2 as a catalyst and DTBP as an oxidant (Scheme 28).[55] A KIE value of 3.0 indicated that the C(sp^3)–H bond activation might be involved in the rate determining step. Moreover, further mechanistic studies inferred the generation of disulphide from the mercaptane in the presence of the I_2 catalyst during the reaction.

In the same year, the Sun group developed a DTBP mediated C(sp^3)–H bond activation of alkanes **29a** and their concomitant reaction with diaryl disulphide or diaryl diselenide to afford

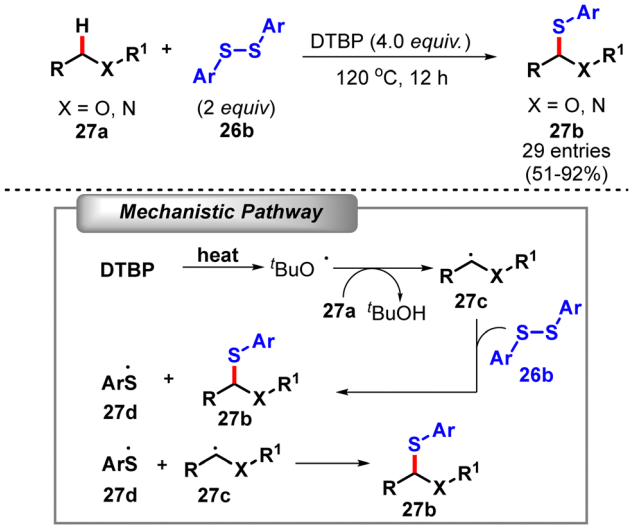

Scheme 27 Oxidative thiolation of the sp^3 C–H bond adjacent to an oxygen atom (Guo *et al.*[54]).

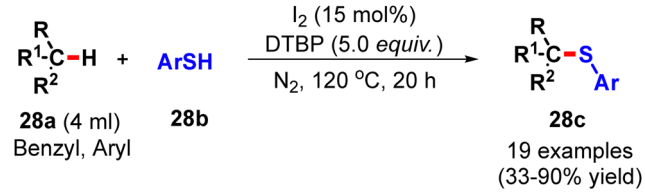

Scheme 28 Oxidative thioarylation of the sp^3 C–H bond of hydrocarbons (Yuan *et al.*[55]).

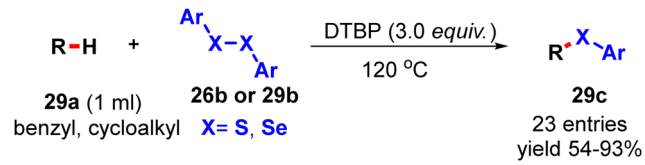

Scheme 29 Oxidative thiolation/selenylation of alkanes (Du *et al.*[56]).

organosulphides or selenides **29c** in moderate to good yields (54–93%) (Scheme 29).[56] A plausible mechanism was suggested according to which the *tert*-butoxyl radical generated by the homolytic cleavage of DTBP abstracted a hydrogen from the C(sp^3)–H bond of alkanes to afford the alkyl radical which reacted with disulphide or diselenide to provide the product as described previously.

Lee and colleagues described a DTBP-promoted C–H thiolation of aryl aldehydes **30a** with disulphides in good to excellent yield (40–99%) (Scheme 30).[57] Besides diaryl disulphides, this group also tested the dialkyl disulphide for this successful C–S bond formation reaction. However, alkyl aldehydes could not provide the desired coupling. A potential mechanism was proposed involving the generation of the aldehydic radical in the presence of DTBP at high temperature and a subsequent addition to disulphide to yield the thioester.

Recently in 2019, the Yotphan group delineated a potassium persulfate ($K_2S_2O_8$) mediated C(sp^2)–H thiolation and thiocyanation of *N*-substituted pyrazolones **31a** with the corresponding disulphide **31b** and thiocyanate salt **31c** (Scheme 31).[58] In this process, the C–H thiolation required an additional 1 equiv. of potassium iodide for the highest level of yield. Indeed, molecular iodine might serve as well. A wide variety of diaryl as well as dialkyl disulphides were tested under the optimized reaction condition. However, for C–H thiocyanation, no additional iodide salt was required. 1.5 equiv. of ammonium thiocyanate salt effectively provided the desired product in excellent yield even at room temperature. A possible mechanistic explanation suggested the generation of thiyl and thiocyanate radical species

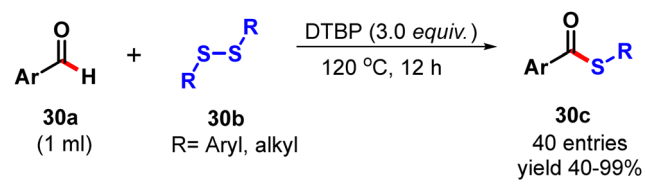

Scheme 30 Oxidative thiolation of aryl aldehydes (Zeng *et al.*[57]).

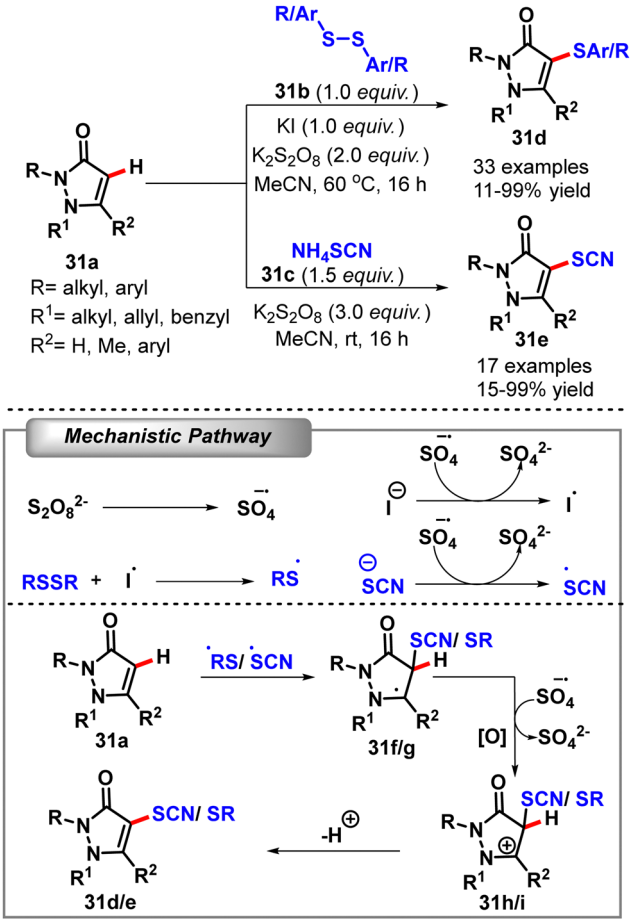

Scheme 31 Oxidative C(sp^2)–H thiolation and thiocyanation of N-substituted pyrazolones (Kittikool *et al.*[58]).

in the presence of persulfate and their concomitant addition to pyrazolone followed by oxidation of the newly generated radical and deprotonation to give the final products **31d** and **31e** respectively.

4. Hypervalent iodine mediated oxidative C–H functionalisation

Hypervalent iodine reagents (HIRs) have grown exponentially in popularity over the past few decades because of their many desirable properties, including high reactivity, low toxicity, high stability, and safety for the environment. It has been well established that the polyvalent iodine compounds have comparable efficiency to classical transition metal catalysts in coupling reactions and hence these HIRs are the green alternative to toxic metals. Phenyliodine(III)diacetate (PIDA), phenyliodine(III) bis(trifluoroacetate) (PIFA), phenyliodine(III) dipivaloate (PIDP), phenyliodine(III) bis(m-chlorobenzoate) (PhI(mCPBA)2), [hydroxy-(tosyloxy)iodo]-benzene (HTIB; Koser's reagent), iodosylbenzene (PhIO), bisimido iodobenzenes as well as recently developed chiral hypervalent iodine reagents are frequently used nowadays. Various research groups across the globe have applied hypervalent iodine(III) reagents in C–H activation followed by cross-dehydrogenative coupling (CDC) reactions to afford numerous C–C as well as C-heteroatom bonds.

4.1 C–C bond formation

4.1.1 Intramolecular direct Csp^2–Csp^2 bond formation. In 1996, the Kita group first reported the oxidative intramolecular phenolic biaryl coupling through C–H bond functionalisation by utilising hypervalent iodine(III) reagent PIFA and $BF_3{\cdot}OEt_2$ as the activator of HIR (Scheme 32A).[59] The probable mechanism for the biaryl coupling involved the one-electron oxidation of

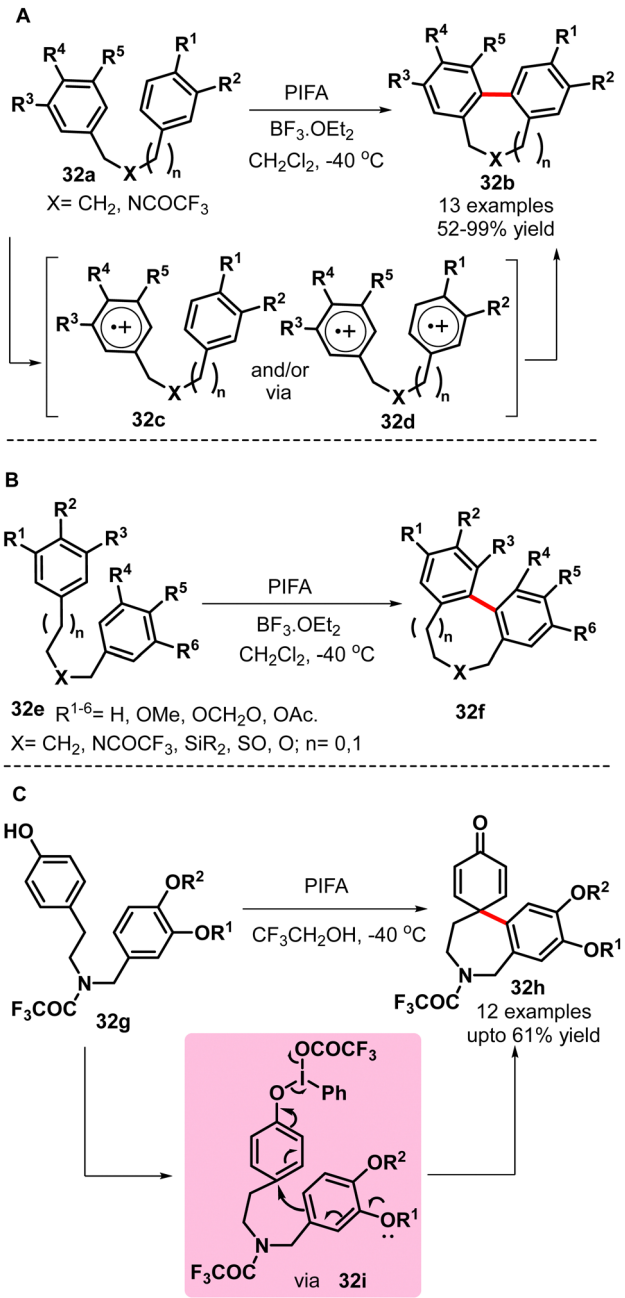

Scheme 32 HIR-mediated oxidative intramolecular phenolic biaryl coupling (Kita *et al.*,[59] Takada *et al.*,[60] Kita *et al.*[61]).

the electron-rich aromatic ring of **32a** with PIFA and $BF_3{\cdot}OEt_2$. The nucleophilic attack by the other aromatic rings on the cation radical **32c** or a radical dimerization between the dication radical intermediate **32d** offered the biaryl product **32b**. Two years later, they provided a full account of their studies on the hypervalent iodine(III)-induced intramolecular biaryl coupling reaction of phenol ether derivatives as well as nonphenolic derivatives **32e** for the synthesis of various dibenzo heterocyclic compounds **32f** (Scheme 32B).[60] By employing the HIR in poorly nucleophilic polar solvents such as 2,2,2-trifluoroethanol, they also synthesized the azacarbocyclic spirodienones **32h** from phenol derivatives as well as the spirodienone compound from norbelladine derivatives **32g** (Scheme 32C).[61]

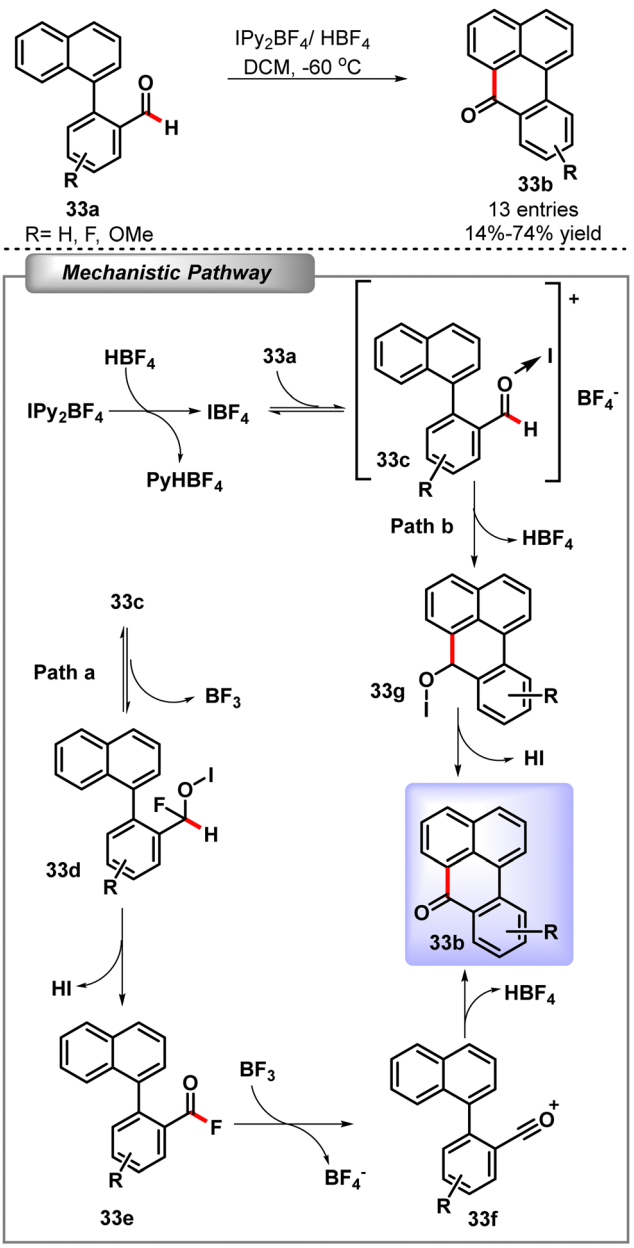

Scheme 33 IPy_2BF_4/HBF_4 mediated direct intramolecular arylation of aldehydes (Barluenga *et al.*[62]).

In 2006, Barluenga *et al.* reported an IPy_2BF_4/HBF_4 mediated intramolecular arylation of aldehyde for the synthesis of benzocyclic ketone in moderate to good yield (14–74%).[62] Based on the authors' proposed mechanism, the aldehydes **33a** to **33c** are activated by a reactive iodonium species (IBF4) formed from the reaction of IPy2BF4/HBF4 (Scheme 33). Subsequently, the formal addition of iodonium fluoride (IF) to the activated aldehyde **33c** would give **33d**, which undergoes oxidation to convert to acyl fluoride intermediate **33e** by liberating hydrogen iodide (HI). *In situ* activation of the resulting acyl fluoride by BF_3 to acyl cation and a subsequent cyclization afforded the cyclic ketone **33b** (path a). In an alternative pathway, a direct addition of the arene to the activated aldehyde **33c** followed by the elimination of HI would lead to the product (path b).

Du and Zhao applied the same strategy in 2014 to achieve the synthesis of biologically important acridone skeletons by PIDA-mediated intramolecular aryl-aldehyde Csp^2–Csp^2 bond formation of 2-(*N*-arylamino) aldehydes (40–82% yield) (Scheme 34).[63] In this reaction a substoichiometric amount of benzoyl peroxide (BPO) was used along with PIDA as a radical initiator. Moreover, the complete inhibition of the reaction in the presence of radical scavenger TEMPO suggested the radical mechanism.

The same group in 2008 presented the synthesis of functionalized indoles **35b** *via* PIDA-mediated oxidative Csp^2–Csp^2 bond formation of *N*-aryl enamines **35a** (33–91% yield) (Scheme 35).[64] It was proposed that the reaction proceeded through the intramolecular SN2′-type cyclization mechanism. Firstly, the substrate reacted with PIDA to form a N–I bond and a concomitant electrocyclic ring closure and the subsequent proton elimination and tautomerization afforded the product.

In 2013, again they demonstrated a PIFA mediated oxidative $C(sp^2)$-$C(sp^2)$ bond formation along with a simultaneous aryl migration of *N*-arylacrylamide derivatives for the efficient synthesis of 3-arylquinolin-2-ones (Scheme 36).[65] In this reaction 1 equiv. of $BF_3{\cdot}OEt_2$ and 10 equiv. of trifluoroacetic acid (TFA) as additives and DCE as solvent at a concentration of 0.025 M had been used for the excellent yield of the product (30–90% yield). A possible mechanistic pathway was proposed which involved the nucleophilic attack on the hypervalent iodine by the carbonyl oxygen of the amide moiety **36a** followed by an electrocyclic ring closure and the subsequent proton elimination to provide the intermediate **36d**. This intermediate underwent a nitrogen loan pair assisted concerted 1,2-aryl shift for the cleavage of the O–I bond and the removal of a proton to give the 3-arylquinolin-2-one **36b**.

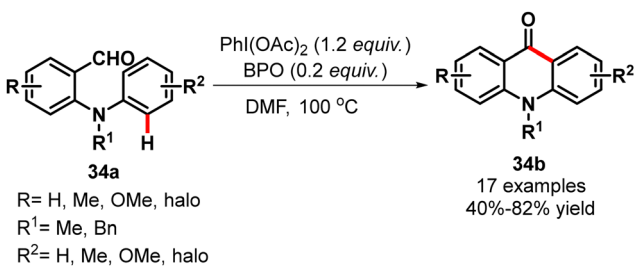

Scheme 34 HIR-mediated intramolecular oxidative Csp^2–Csp^2 bond formation (Zheng *et al.*[63]).

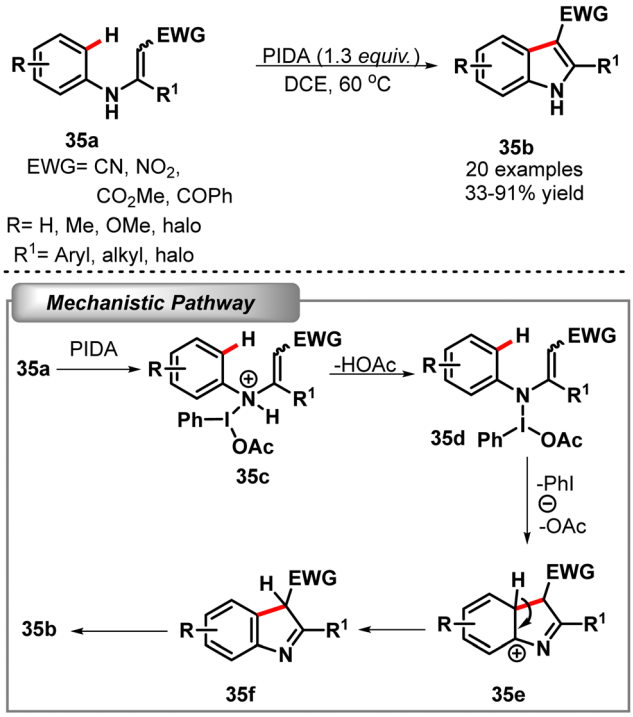

Scheme 35 PIDA-mediated oxidative Csp^2–Csp^2 bond formation of *N*-aryl enamines (Yu *et al.*[64]).

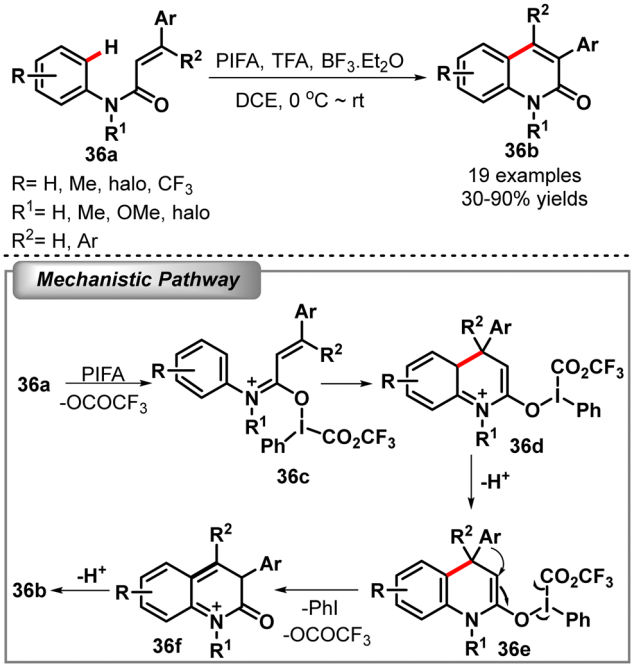

Scheme 36 PIFA-mediated C–C bond formation with a concomitant 1,2-aryl shift (Liu *et al.*[65]).

4.1.2 Intramolecular direct Csp^2–Csp^3 bond formation. In 2009, the Zhang group first reported a PIDA mediated oxidative $C(sp^2)$–$C(sp^3)$ bond formation of phenolic amides **37a** for the synthesis of oxindole derivatives **37b** (Scheme 37).[66] First the

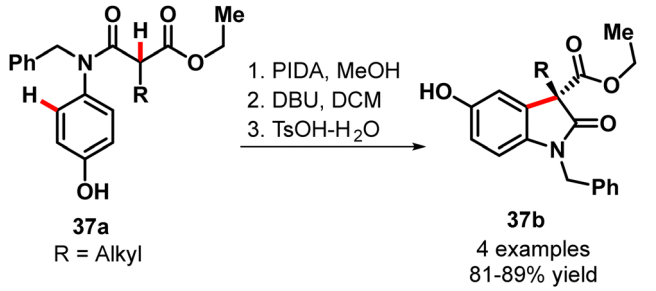

Scheme 37 PIDA mediated oxidative $C(sp^2)$–$C(sp^3)$ bond formation of phenolic amides (Liang *et al.*[66]).

oxidative dearomatization step provided the 4-methoxyl cyclohexadienenones which underwent a subsequent Michael addition followed by Brønsted acid mediated rearomatization to furnish the all-carbon quaternary oxindoles in high yield (81–89%).

Later in 2012 Du and Zhao described a PIFA mediated oxidative $C(sp^2)$–$C(sp^3)$ bond formation, followed by oxidative hydroxylation or spirocyclization cyclization of a variety of anilides **38a**/**b** (Scheme 38).[67] Depending upon the substitution pattern, the anilides with terminal ester substituents **38a** led to the oxidative hydroxylation to afford 3-hydroxy-2-oxindole derivatives **38c** and those with amide groups at the terminal carbon offered the spirooxindoles **38d**. A plausible mechanism was suggested according to which the nucleophilic attack on the iodine(III) center by the carbonyl oxygen of the amide moiety in **38a** afforded the intermediate **38e**. Then the released trifluoroacetate anion captured the acidic α-proton of imine salt **38e** to convert into enamine **38f** which underwent an electrocyclic ring closure through the cleavage of the I–O bond and subsequent aromatization to afford the oxindole **38g**. Further oxidation of oxindole by PIFA followed a similar sequence to give the iminium intermediate and a successive nucleophilic attack of the trifluoroacetate anion and the alcoholysis of the ester group in the presence of trifluoroethanol afforded the hydroxylated oxindole **38c**. On the other hand, instead of the trifluoroacetate anion addition, second intramolecular ring-closure reaction by the adjacent phenyl ring in the side chain furnished the spirooxindole **38d**.

In 2014, Wu *et al.* performed the catalytic asymmetric version of this intramolecular oxidative cross-coupling reaction (Scheme 39).[68] The reaction of diphenylmalonamide **39a** in the presence of 15 mol% of chiral organoiodine **39b**, 2 equiv. of trifluoroacetic acid as an activator and 4 equiv. of ethaneperoxoic acid as an oxidant rendered the spiro bi(indoline)-2,2′-dione **39c** in good ee (26–90% ee). The Si face of the 2-indololate moiety is open to a favourable nucleophilic attack by the benzene ring providing the (*S*)-isomer by the syn addition-elimination process.

The very next year, they again revealed a chiral organoiodine **40b** catalysed enantioselective dearomative spirocyclization of 1-hydroxy-*N*-aryl-2-naphthamide derivatives **40a** for the synthesis of spirooxindole derivative **40c** with an all-carbon quaternary centre in good yield and ee (42–80% yield, 80–92% ee) (Scheme 40).[69] 15 mol% of chiral organoiodine, 1.3 equiv. of mCPBA as the oxidant and 50 equiv. of trifluoroethanol (TFE)

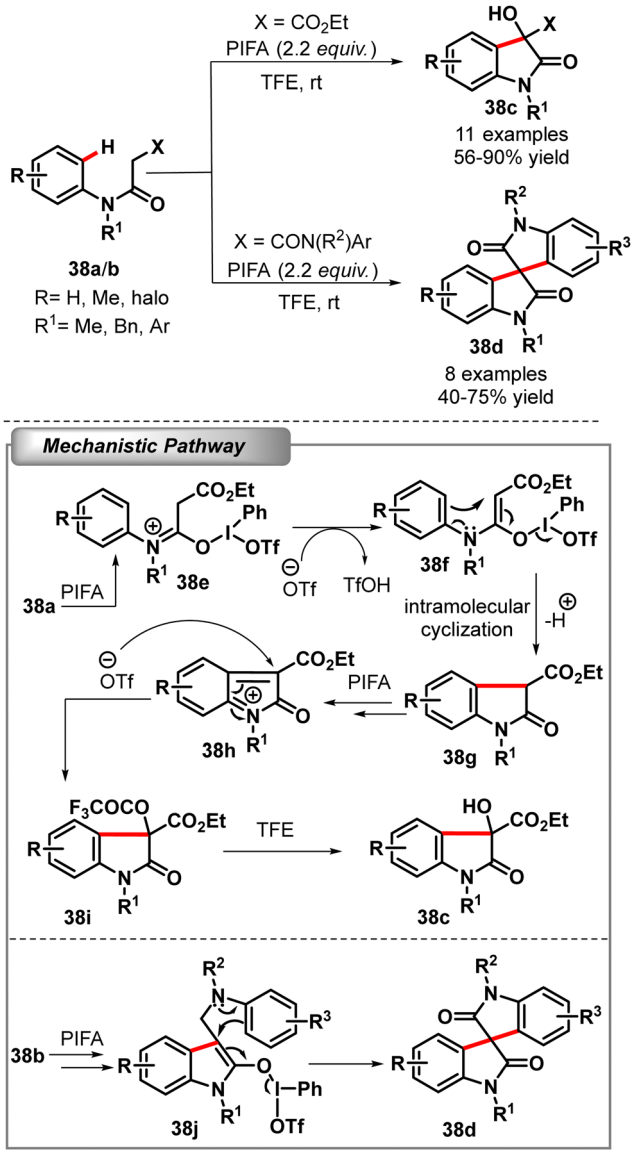

Scheme 38 PIFA mediated cascade oxidation of anilide derivatives (Wang *et al.*[67]).

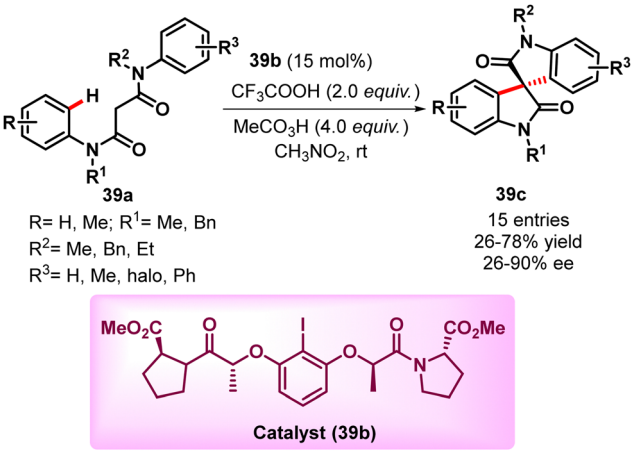

Scheme 39 Asymmetric organocatalytic intramolecular oxidative cross-coupling reaction (Wu *et al.*[68]).

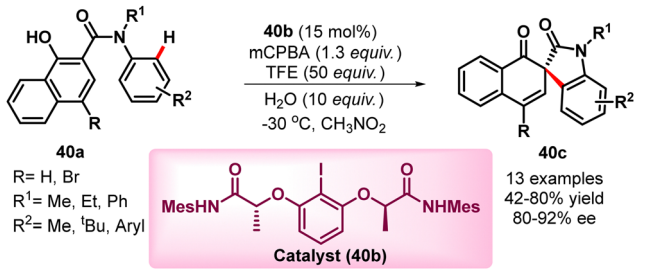

Scheme 40 Chiral iodine-catalyzed dearomative spirocyclization (Zhang *et al.*[69]).

permitted the reaction to fetch the best results in terms of both yield and enantiomeric excess.

Recently in 2019, Zhen *et al.* synthesized a class of spirooxindole compounds **41b** by the direct intramolecular oxidative C(sp^2)–C(sp^3) bond formation of *N*-arylamide derivatives **41a** (Scheme 41).[70] They utilized one of the least known HIR $PhI(OMe)_2$ as an oxidant which could be formed *in situ* from the reaction between PhIO and MeOH. The mechanism suggested an initial keto-enol tautomerization followed by nucleophilic attack on the iodine center of $PhI(OMe)_2$ by the enol to afford the O–I intermediate **41c** which was converted to the I–C intermediate **41d** *via* 1,3-migration. Intramolecular cyclization to furnish the C–C bond and the subsequent rearomatization finally provided the spirooxindole compounds **41b**.

4.1.3 Intermolecular direct Csp^2–Csp^2 bond formation. In 2002, Kita *et al.* introduced a PIFA and $BF_3{\cdot}OEt_2$ mediated oxidative homocoupling reaction of alkylarenes for the efficient

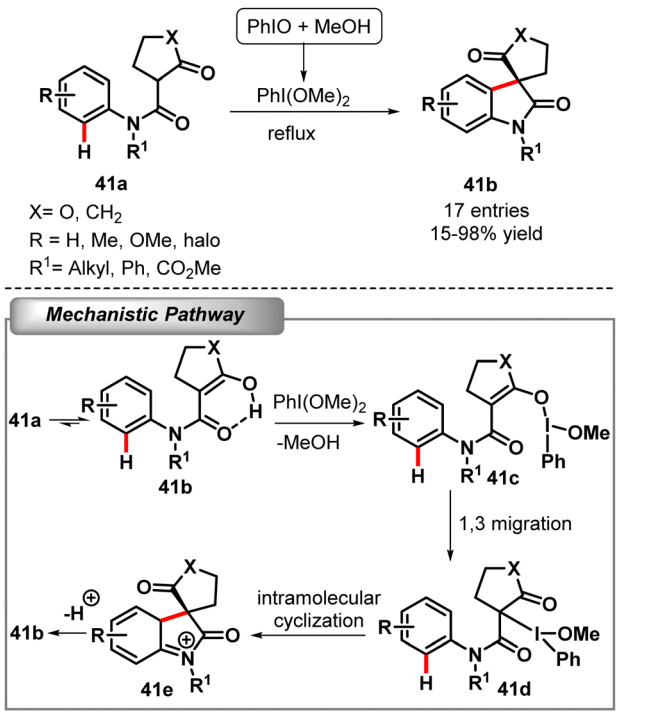

Scheme 41 Intramolecular oxidative C(sp^2)–C(sp^3) bond formation of *N*-arylamide derivatives (Zhen *et al.*[70]).

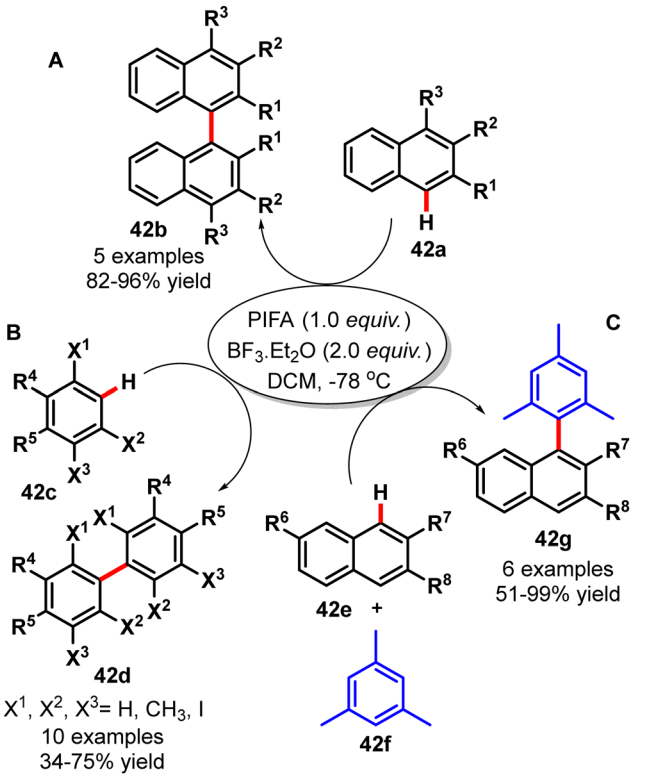

Scheme 42 Intermolecular oxidative $C(sp^2)$–$C(sp^2)$ bond formation (Tohma *et al.*,[71] Mirk *et al.*,[72] Dohi *et al.*[73]).

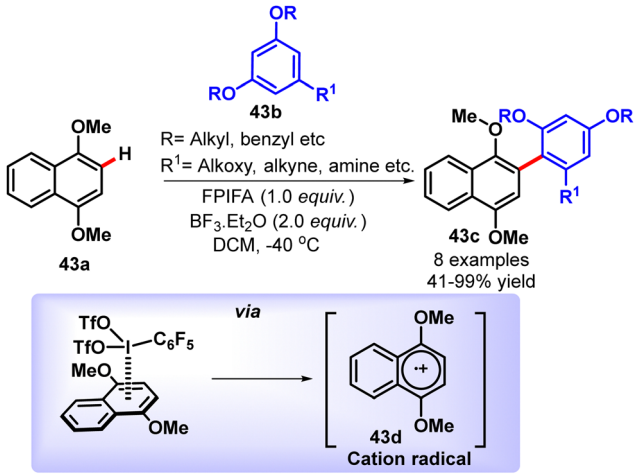

Scheme 43 Intermolecular oxidative naphthalene-benzene linked biaryls (Dohi *et al.*[74]).

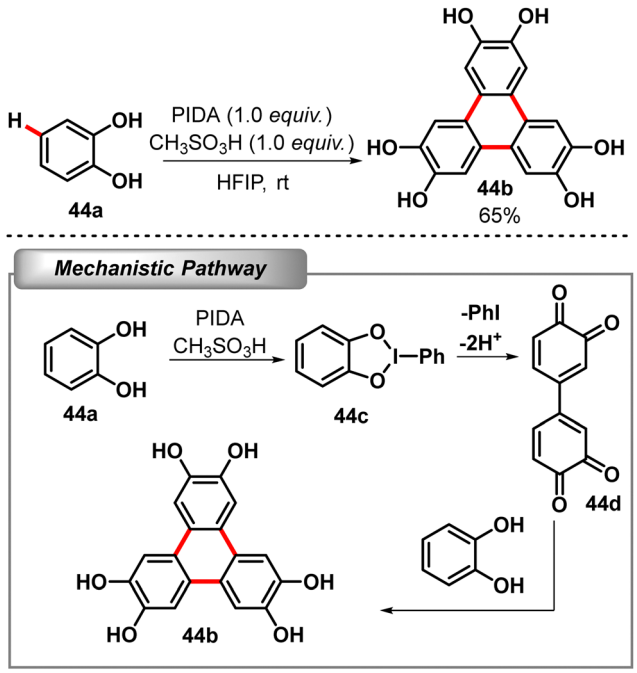

Scheme 44 Oxidative trimerization of catechol (Morimoto *et al.*[75]).

synthesis of alkylbiaryls (82–96% yield) (Scheme 42A).[71] Unfortunately, the coupling of inactive monoalkyl-benzenes such as toluene and *t*-butyl benzene did not go through under the reaction conditions. The reaction also followed the cation radical pathway as discussed earlier. Later the Waldvogel group also utilised the same technique for the synthesis of various iodinated biaryls from iodoarene by dehydrodimerization reaction (34–75% yield) (Scheme 42B).[72] In 2008, Kita and co-workers again reported an efficient PIFA mediated oxidative cross coupling of naphthalene with effective nucleophile mesitylene (51–99% yield) (Scheme 42C).[73] Notably, this reaction was the first successful report of selective cross-coupling between unfunctionalized arenes by the single-electron transfer (SET) pathway by using hypervalent iodine.

Later in 2011, Kita and co-workers again reported the extremely selective intermolecular C–H cross-coupling between the aromatic ethers for the synthesis of naphthalene-benzene linked biaryls **43c** (41–99% yield) (Scheme 43).[74] The remarkable high affinity of the perfluorinated PIFA (FPIFA) towards naphthalene ethers over phenolic ethers for the generation of a charge transfer complex successfully delivered the desired cross-coupling product by complete exclusion of undesired homocoupling.

Synthesis of hexahydroxytriphenylene **44b** was accomplished once more in 2013 by PIDA mediated oxidative trimerization of catechol **44a** (Scheme 44).[75] A tentative mechanism was proposed wherein the initial interaction between the hypervalent iodine reagent and catechol followed by the formation of quinone dimer **44d** and a subsequent Michael addition of another catechol to this quinone dimer finally materialized the trimerization.

2,2′-Bithiophene is one of the most important precursors of poly-thiophene derivatives that have important physical properties like electrical conductivity and electroluminescence. As a result, the synthesis of 2,2′-bithiophene was of great demand until Kita *et al.*'s systematic metal free oxidative cross coupling studies. In 2003, they first developed the PIFA and $BF_3{\cdot}OEt_2$ assisted coupling of alkylthiophene derivatives for the synthesis of corresponding 2,2′-bithiophene derivatives (Scheme 45A).[76] However they were unable to control the head-to-head (H–H) or head to tail (H–T) selectivity. In 2005, they were able to

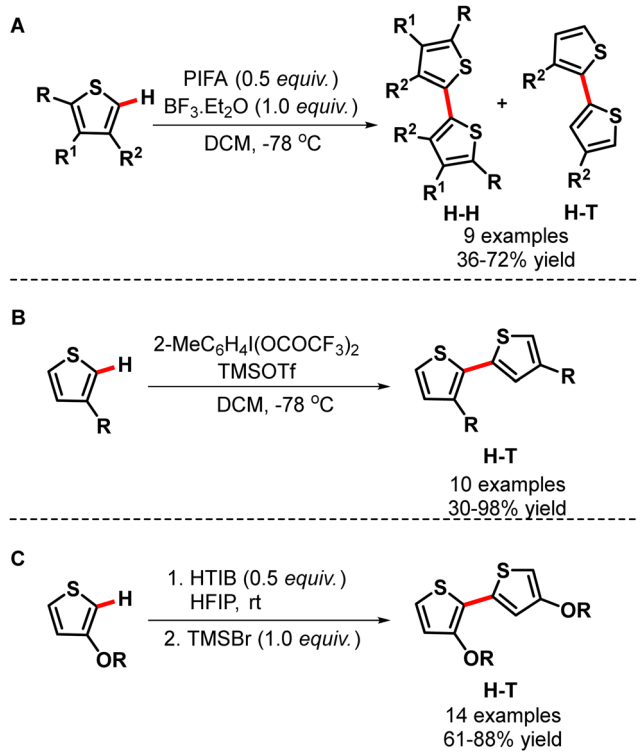

Scheme 45 Synthesis of 2,2′-bithiophene by intermolecular oxidative coupling (Tohma *et al.*,[76] Dohi *et al.*,[77] Morimoto *et al.*[78]).

overcome the selectivity issue. This time the H–T dimers were achieved selectively by the oxidative coupling reaction of 3-substituted thiophenes utilizing a substituted PIFA (Ar = 2-Me C_6H_4) and relatively week Lewis acid trimethylsilyl trifluoromethanesulfonate as an activator (Scheme 45B).[77] Surprisingly, 3-trimethylsilylthiophene selectively resulted in the construction of the H–H dimer instead of the H–T dimer. Again in 2010, they achieved the synthesis of highly regioselective H-T bithiophenes *via* Koser's reagent (PhI(OH)OTs) and TMSBr activator mediated cross coupling of 3-substituted thiophene (Scheme 45C).[78] The reaction progressed *via* the formation of the iodonium salt of 3-substituted thiophene at C-2 position by the treatment of Koser's reagent in HFIP. Hence the other 3-substituted thiophene reacted through its C-2 centre to the remaining C-5 position of the iodonium salt for the successful synthesis of H–T dimer with controlled regioselectivity in good yield.

Meanwhile, in 2006, Kita and colleagues selectively synthesized α-linked bipyrroles *via* PIFA and TMSBr mediated oxidative coupling of pyrroles (52–82% yield) (Scheme 46).[79] The protecting

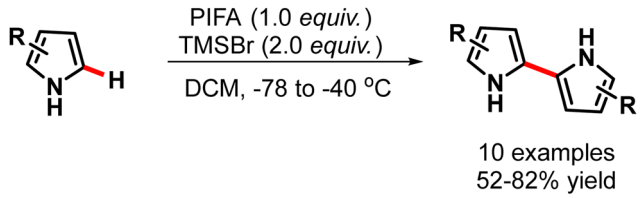

Scheme 46 Synthesis of bipyrrole by intermolecular oxidative coupling of pyrrole (Dohi *et al.*[79]).

group on the pyrrole nitrogen had great impact on the regioselectivity of the product. While unprotected pyrrole offered 2,2′-bipyrrole, *N*-phenyl pyrrole afforded the 2,3′-isomer in good yield. However, the electron deficient group on pyrrole nitrogen could not react at all.

In 2009, they reported an excellent strategy for the selective synthesis of hetero-biaryls **47d/e** *via* Koser's reagent (PhI(OH)OTs) and TMSBr mediated oxidative cross coupling of thiophenes and a wide range of arenes (Scheme 47).[80] This reaction proceeded through the formation of α-thienyl iodonium(III) salt-OTs **47f** by the treatment of Koser's reagent in HFIP. A subsequent addition of arene in the presence of TMSBr selectively produced the mixed biaryl in excellent yield.

In 2010, they again came up with an excellent idea of *ipso* substitution of diaryl iodonium salt **48a** by the SET oxidising pathway (Scheme 48).[81] In the previous report they had introduced the aromatic nucleophiles to the γ-position of the iodine(III)–carbon bond. To overcome this drawback, they tried to find a suitable acid additive that accelerated the reaction by activating the thiophene iodonium salt. Finally, after thorough screening they found that 2 equiv. of TMSOTf as the acid additive enabled successful transformation with good yield (50–81%). The mechanism suggested that the addition of TMSOTf played a crucial role in inducing the SET pathway and facilitated the initial interaction

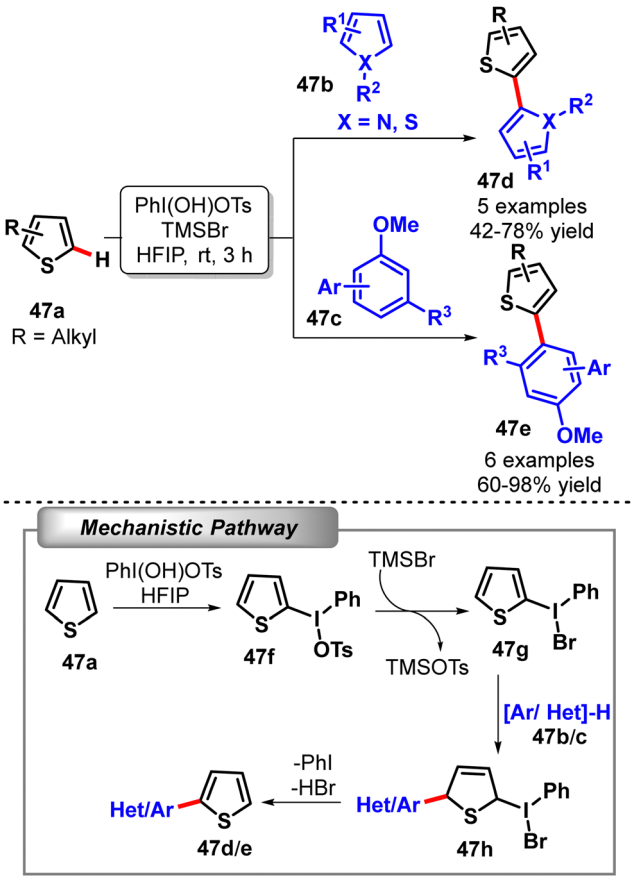

Scheme 47 Synthesis of heterobiaryls by intermolecular oxidative coupling (Kita *et al.*[80]).

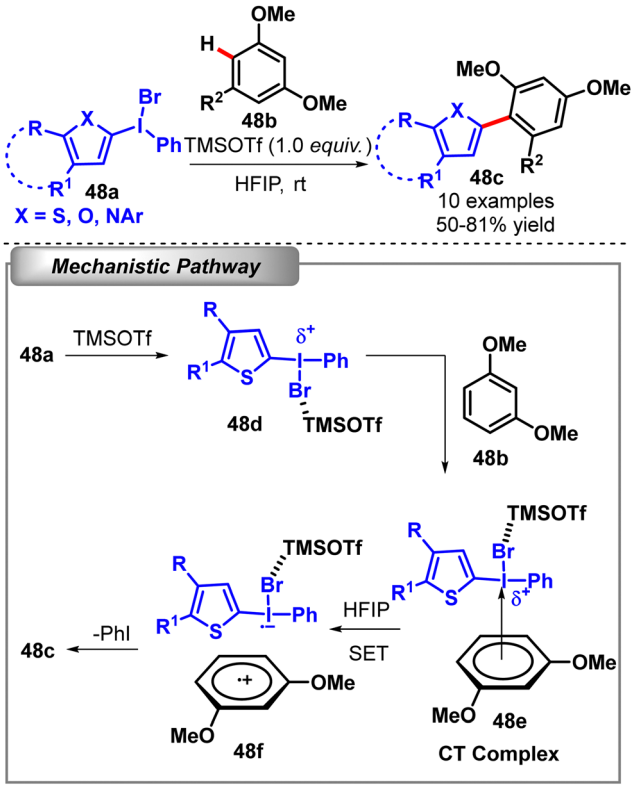

Scheme 48 Synthesis of heterobiaryls by intermolecular oxidative coupling (Dohi *et al.*[81]).

of diaryl iodonium salt with the aromatic nucleophile to form a CT complex **48e** by enhancing the electrophilicity of the iodine atom through coordination with the bromo atom. The electron-rich hetero arene was then transferred to the cation radical to finally furnish the *ipso* substitution.

In 2011, Ackermann *et al.* reported a direct arylation of indoles and pyrroles by utilising diaryl iodonium salt **49b** in DMF solvent (Scheme 49).[82] In the case of unsymmetrically substituted diaryliodonium salts, it was found that the less sterically hindered as well as the less electron rich aromatic moiety was preferentially transferred for the C-3 arylation.

Subsequently in 2012, Yu and Zhang developed a similar type of direct arylation of arene and N-heteroarenes **50a**/**b** with diaryliodonium salt **50c** (12–93% yield) (Scheme 50).[83] This cross-coupling reaction is efficiently promoted by the addition of an inorganic base (NaOH). It is noteworthy that less electron-rich

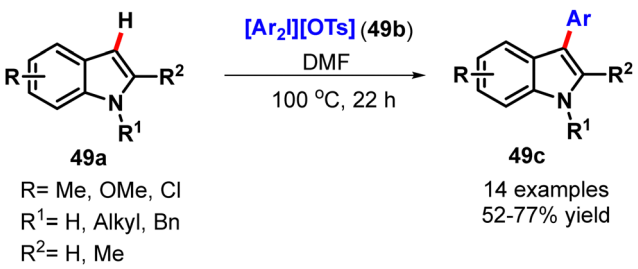

Scheme 49 C-3 arylation of indole and pyrrole (Ackermann *et al.*[82]).

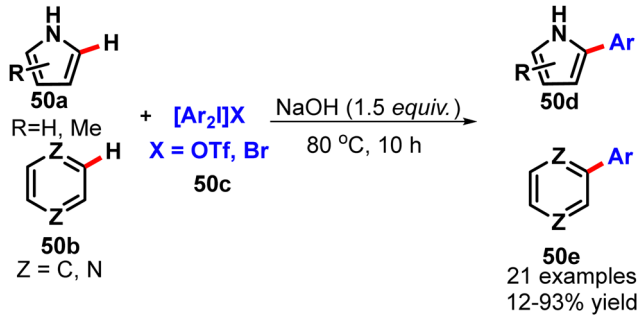

Scheme 50 Direct arylation of arene and heteroarene (Wen *et al.*[83]).

aromatic moieties were favoured as an arylating agent like the earlier one. Based on the radical trapping experiment using TEMPO, the authors indicated the involvement of the aryl radical intermediate in this reaction.

In 2016, again Kita and co-workers successfully established the oxidative biaryl coupling of pyrrole and electron rich arene (Scheme 51).[84] This reaction proceeded with the *in situ* generation of stabilized pyrrolyl iodonium(III) salt by the interaction of 4-F PIDA and pyrrole followed by arylation in the presence of TMSCl as an activator.

In 2010, Gu and Wang developed a PIFA and $BF_3{\cdot}OEt_2$ mediated direct oxidative cross-coupling of *N*-acetylindoles **52a** with anisoles **52b** for the synthesis of C-3 arylindoles **52c** (23–85% yield) (Scheme 52).[85] It is noteworthy that the coupling reaction happened at the *p*-position of anisole and no C-2 arylindole was observed. Moreover, electron withdrawing substituents on the indole moiety reacted efficiently with high yield than the electron donating groups.

Meanwhile in 2007, Canesi and coworkers reported a PIDA mediated oxidative coupling of aniline derivatives **53a** and thiophenes **53b** for the synthesis of mixed biaryls **53c** (58–84% yield)

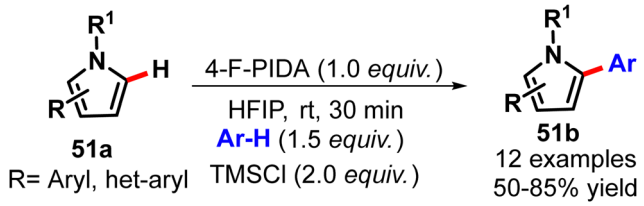

Scheme 51 Oxidative biaryl coupling of pyrrole and electron rich arene (Morimoto *et al.*[84]).

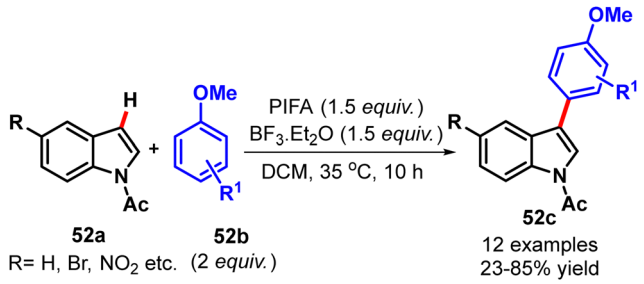

Scheme 52 PIFA mediated oxidative C-3 arylation of indole (Gu *et al.*[85]).

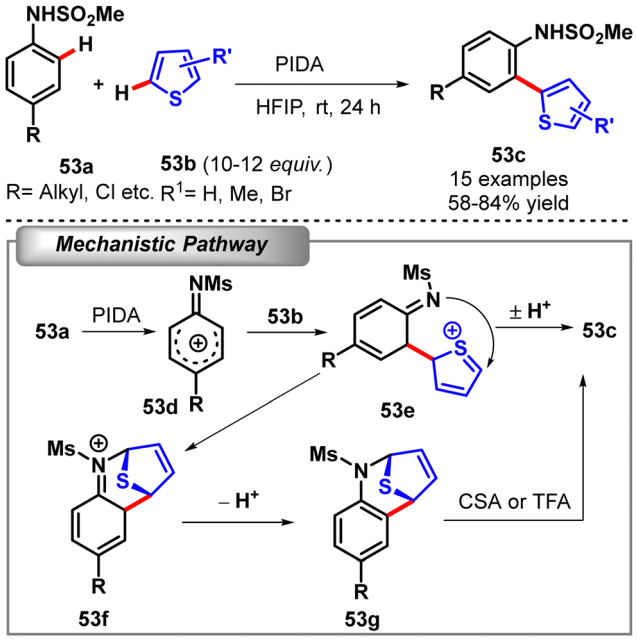

Scheme 53 PIDA mediated oxidative coupling of aniline derivatives (Jean *et al.*[86]).

(Scheme 53).[86] It is noteworthy that simple anilines were not able to produce the desired product, whereas excellent outcomes were obtained with *N*-aryl methanesulfonamides. However, along with the desired cross coupling product, a substantial amount of side product **53g** was generated through the formal [4+3] cycloaddition of the substrate with thiophene. A mechanistic hypothesis proposed that the addition of thiophene at the *o*-position of the cation radical **53d** generated from the aniline in the presence of PIDA furnished the sulfonium ion intermediate **53e**. The cation could directly convert to the product **53c** by proton exchange. In an alternative way, this sulfonium cation could nucleophilically intercept with the nitrogenous functionality to form the formal [4+3] cycloadduct **53g**, which could again be converted into the desired mixed biaryls under acidic conditions.

In 2013, Kita and co-workers developed a similar type of hypervalent iodine-mediated selective Csp^2–Csp^2 coupling of *N*-aryl methanesulfonamides with aromatic hydrocarbons (ArHs) (Scheme 54).[87] This was the first organocatalytic oxidative cross-biaryl coupling in combination with a catalytic amount of 2,2′-diiodobiphenyl derivative **54c** along with mCPBA as the terminal oxidant. Notably, these 2,2′- diiodobiphenyls are efficient precursors for the formation of highly reactive iodine(III) species in the presence of an oxidant. Moreover, the presence of the electron-donating methoxy groups in the catalyst **54c** seemed to accelerate the reoxidation with mCPBA for the regeneration of the active catalyst.

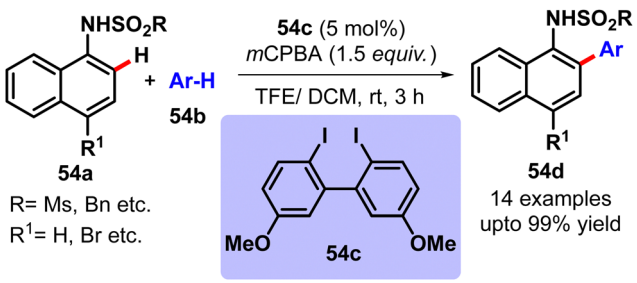

Scheme 54 Organocatalytic oxidative cross-biaryl coupling (Ito *et al.*[87]).

In 2013, Matcha *et al.* investigated a PIFA and $TMSN_3$ mediated direct acylation of N-heterocycles **55a** with a variety of alkyl and aryl aldehydes **55b** (35–94% yield) (Scheme 55).[88] Mainly various isoquinoline derivatives were tested for the oxidative acylation, although other heterocycles such as pyridine, quinoxaline, acridine, benzothiazole, carbazole and caffeine were smoothly functionalized under optimised conditions. The high KIE of 5.7 indicated the formation of the acyl radical as the rate determining step in the reaction. A plausible mechanism was suggested involving an initial ligand exchange between PIFA and $TMSN_3$ to generate the hypervalent iodine species **55d**, which underwent thermal homolytic cleavage to form an azide radical and an iodine centred radical. The azide radical then encountered the aldehyde **55b** to form an acyl radical **55f**, which promptly attacked the protonated N-heterocycle **55e** to form the coupled radical cation **55g** under thermodynamic control and finally converted into the product **55c** *via* oxidation followed by rearomatization.

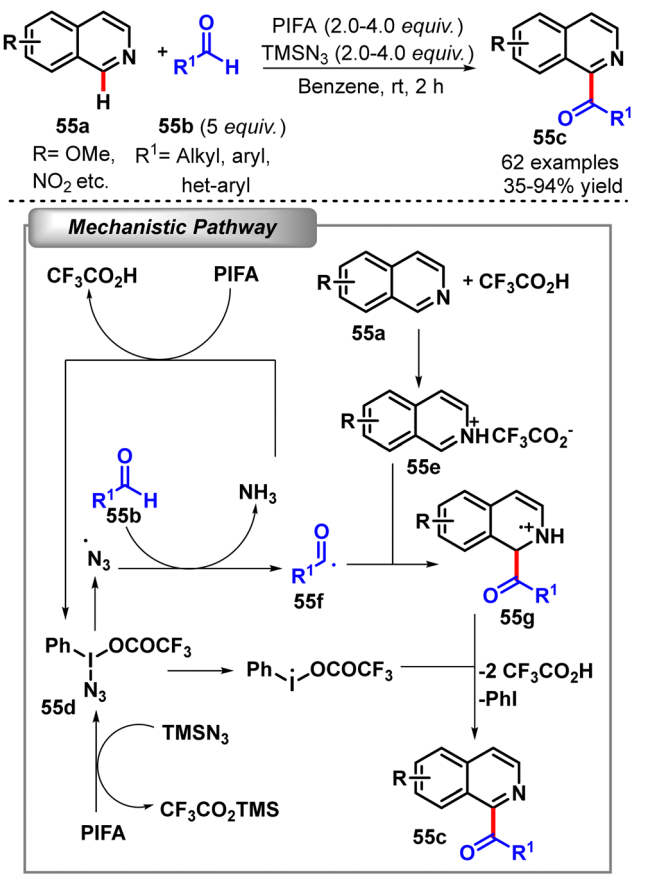

Scheme 55 Metal-free cross-dehydrogenative coupling of heterocycles with aldehydes (Matcha *et al.*[88]).

In 2016, Kita and co-workers reported a hypervalent iodine catalysed oxidative cross coupling reaction of phenols **56a** with a diverse range of arenes **56b** in HFIP solvent (40–90% yield) (Scheme 56).[89] In this reaction they had utilised 4-methoxy iodobenzene as a catalyst, oxone as a terminal oxidant in the presence of 18-crown-6 as a phase transfer catalyst and acetic acid as an additive to achieve the maximum yield of the cross coupling product. A tentative mechanism proposed the *in situ* generation of 4-OMe PIDA by the reaction of 4-methoxy iodobenzene, acetic acid and oxone. Now the phenol reacted with the hypervalent iodine species to form the phenoxyiodine(III) species **56d** and the subsequent addition of the other arene **56b** to this phenoxyiodine(III) afforded the desired cross coupling product **56c**.

In 2017, Lee *et al.* developed an iodosobenzene-promoted direct oxidative 3-arylation of quinoxalin-2(*H*)-ones **57a** with various aryl hydrazines **57b** for the synthesis of 3-arylquinoxalin-2(*H*)-one derivatives **57c** in moderate to good yields (40–86% yield) (Scheme 57).[90] A wide range of quinoxalines and aryl hydrazines were tested under optimal conditions to show the versatility of the method. A plausible reaction pathway depicted that the interaction of aryl hydrazine and PhIO produced the aryldiazene intermediate **57e**. This intermediate experienced a rapid aerobic oxidation followed by denitrogenation to afford the aryl radical **57g** and a subsequent addition of this radical to quinoxalin-2(*H*)-ones **57a** and oxidation gave the final product **57c**.

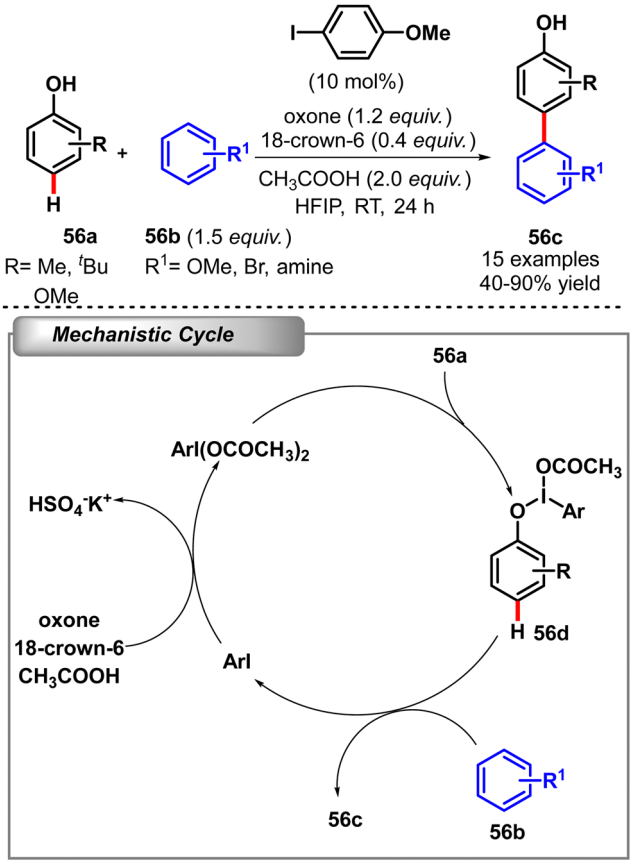

Scheme 56 HIR catalysed oxidative cross coupling of phenols with arenes (Morimoto *et al.*[89]).

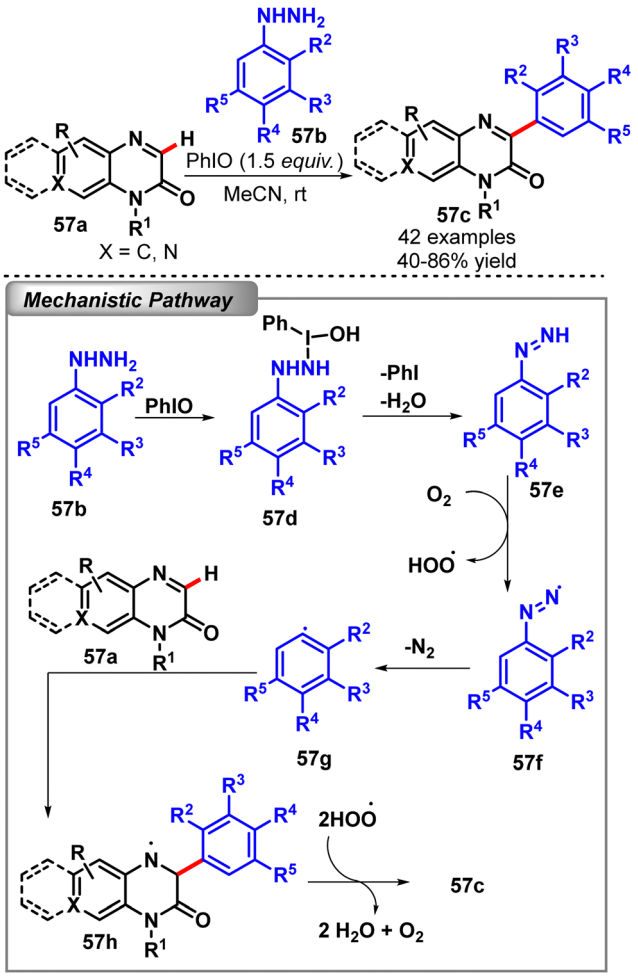

Scheme 57 Oxidative arylation of quinoxalin-2(*H*)-ones with various aryl hydrazines (Paul *et al.*[90]).

In 2018, the Waser group reported a new approach for the synthesis of mixed bi-(hetero)arenes **58c** by employing an electrophilic hypervalent benziodoxol(on)e iodine reagent (IndoleBX) **58b** (28–94% yield) (Scheme 58).[91] The oxidative coupling of C2-substituted IndoleBX with equimolar amounts of electron rich arenes **58a** such as indole, pyrrole and thiophene as nucleophiles selectively afforded the functionalized bi-indolyl heterocycles. It has to be mentioned that a Lewis acid such as TMSCl or TMSBr was required for the activation of the

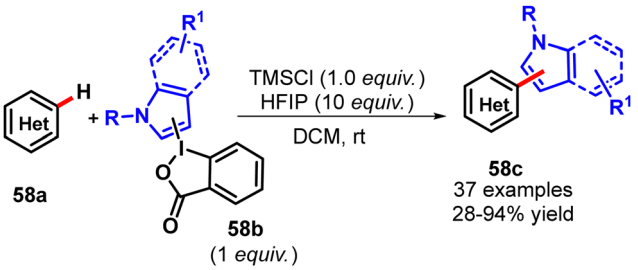

Scheme 58 Oxidative cross coupling of indoles with electron-rich (hetero)arenes (Du *et al.*[91]).

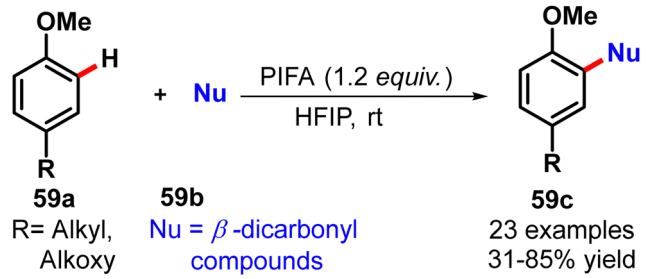

Scheme 59 Hypervalent iodine-induced intermolecular Csp^2–Csp^3 bond formation of *p*-substituted phenol ethers (Kita *et al.*[92]).

hypervalent iodine reagent to initiate the reaction and HFIP solvent for the stabilization of iodine(III) species. After rigorous screening, it was observed that the best results for the heteroarylation were obtained with *N*-Boc protected IndoleDBX reagents **58b** along with TMSBr as an activator.

4.1.4 Intermolecular direct Csp^2–Csp^3 bond formation. In 1994, Kita *et al.* introduced a PIFA induced nucleophilic addition of *p*-substituted phenol ethers **59a** in the presence of active methylene as a nucleophile (Scheme 59).[92] It was also observed that polar and low-nucleophilic protic solvents such as trifluoroethanol provided the best result. According to the UV and ESR spectroscopic studies, the researchers proposed that the reaction proceeded *via* cation radical species generated by the single-electron transfer (SET) from the charge-transfer (CT) complex of arene with PIFA followed by an immediate attack of the nucleophile to afford the desired product.

In 2013, the Boger group utilised this technique for the late-stage functionalisation of an indole alkaloid, vindoline **60a**, by PIFA promoted oxidative Csp^2–Csp^3 cross coupling with a wide variety of active methylene and active methylene like substrates such as β-ketoesters, β-diketones, β-ketoaldehydes, β-ketonitriles, malononitriles, and β-cyanoesters **60b** (Scheme 60).[93] This method provided an all-carbon quaternary centre with a prosperous avenue for the synthesis of vinblastine analogues (24–76% yield). The mechanism suggested that the reaction might proceed *via* the generation of the vindoline cation radical by the SET pathway followed by the attack of deprotonated active methylene and subsequent oxidation to afford the final product.

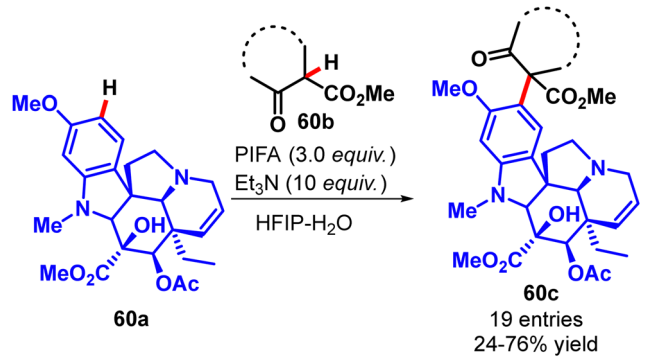

Scheme 60 Hypervalent iodine(III)-promoted intermolecular C–C coupling of vindoline with β-ketoesters (Turner *et al.*[93]).

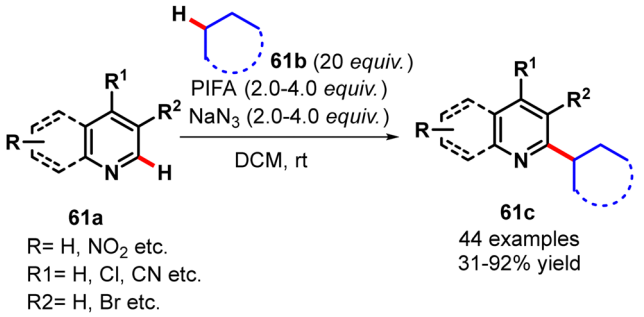

Scheme 61 Oxidative cross-coupling of alkanes with heteroarenes (Antonchick *et al.*[94]).

In 2013, Antonchick developed a PIFA and NaN_3 promoted oxidative cross-coupling of heteroarenes **61a** with unfunctionalized alkanes **61b** (Scheme 61).[94] It is noteworthy that the reaction preferred the tertiary alkanes and the bond formation selectively occurred at the electron-deficient position of arenes. The absence of the overoxidation product ensured the preferential activation of the stronger C–H bond in the presence of the weaker one. Moreover, a higher KIE of 7.6 indicated that the formation of the alkyl radical was the rate limiting step of the reaction. The reaction mechanism followed the usual pathway as the azide radical generated by the interaction of PIFA and NaN_3 selectively generated the alkyl radical from alkane which immediately reacted with the most electron poor centre of protonated heteroarene to form the radical cation. This radical cation was oxidised and a subsequent deprotonation provided the final product. The generality of this cross dehydrogenative coupling (CDC) reaction was explored by using a wide range of alkanes as well as heterocycles.

The same year, Himo and Olofsson studied unsymmetrical diaryliodonium salt **62b** mediated direct arylation of malonates **62a** (Scheme 62).[95] The reaction proceeded with the generation of a T-shaped intermediate (PhArI–Nu) by the reaction of the diaryliodonium salt and the nucleophile followed by the transposition of the nucleophile at the *ipso* position of the aryl group *via* the SET pathway. Notably, the migratory aptitude of the unsubstituted aryl moiety (Ph group) in the diaryliodonium salt increased as the number of ortho substitution of the dummy group increased and exhibited a clear "*anti-ortho* effect".

Later in 2014 the Antonchick group extended the oxidative cross-coupling methodology of chromones and thiochromones **63a** with simple nonfunctionalized cyclic as well as acyclic alkanes **63b** for the efficient synthesis of C-2 alkyl chromones

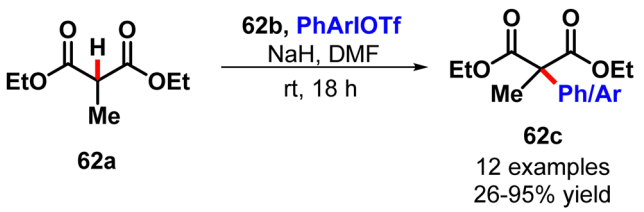

Scheme 62 Diaryliodonium salt mediated direct arylation of malonates (Malmgram *et al.*[95]).

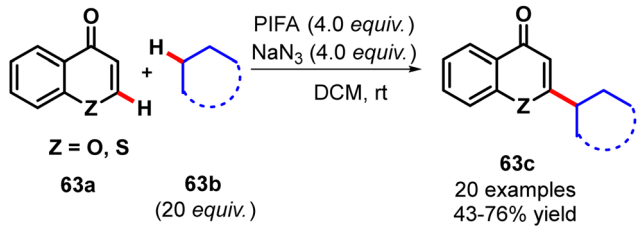

Scheme 63 HIR-mediated selective oxidative functionalisation of (thio)-chromones with alkanes (Narayan *et al.*[96]).

63c (43–76% yield) (Scheme 63).[96] Notably for the best yield, the batch-mode addition of 0.5 equiv. of PIFA and NaN_3 was found to be optimum.

In 2014, Shafir and co-workers described the α-arylation of β-dicarbonyls and α-cyano ketone **64a** where PIFA itself acted as the source of the 2-iodo aryl group (Scheme 64).[97] The mechanism proposed involved C–H α-arylation resulting from the [3,3]-sigmatropic shift from the *O*-enolate **64d**. Moreover, the presence of the iodoarene group proved this method to be more beneficial for late-stage functionalisation.

Recently in 2018, Sen *et al.* developed a PIDA mediated C2-alkylation of quinoline, isoquinoline and pyridine *N*-oxide derivatives **65a** by using *tert*- and sec-alkyl alcohol as the alkyl source (Scheme 65).[98] The alkylation reaction proceeded with the cleavage of the C–C bond of secondary and tertiary alcohols followed by the addition of that alkyl group to the heteroarene. A tentative mechanism was proposed involving the addition of PIDA with the alcohol **65b** to generate another hypervalent iodine intermediate **65d** which was promptly attacked by the quinolone N-oxide **65a**; a subsequent homolytic C–C bond cleavage *via* the SET pathway and rearomatisation afforded the C2-alkylated product **65c**.

In the same year, the Zhu group established a combination of PIFA and visible-light irradiation (100 W blue LEDs) for the alcohol-directed remote C(sp^3)–H heteroarylation (Scheme 66).[99] The reaction was initiated with the direct generation of alkoxy

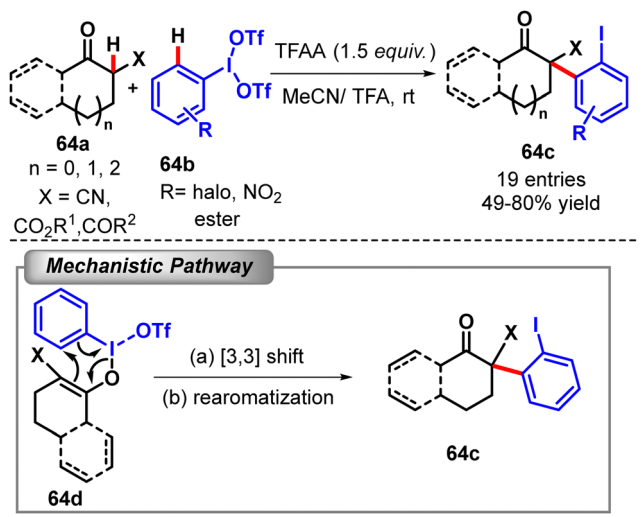

Scheme 64 An alternative approach to the classical α-arylation: the transfer of an intact 2-iodoaryl from HIR (Jia *et al.*[97]).

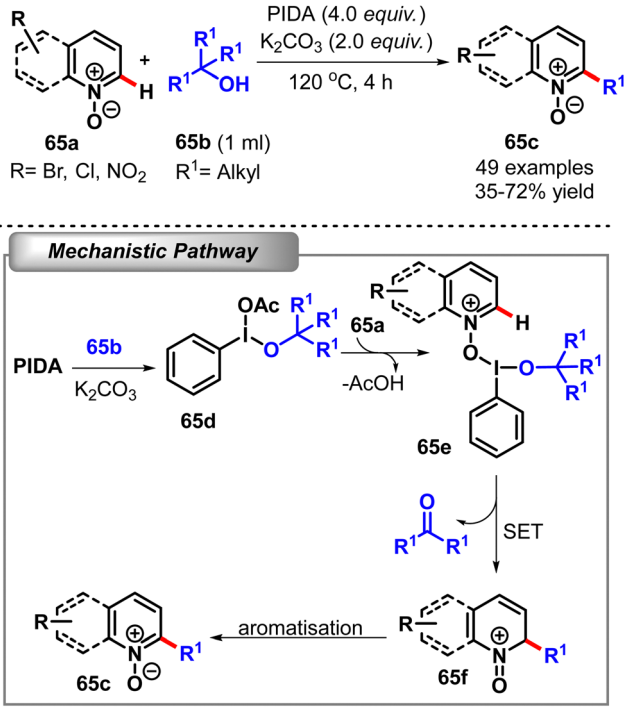

Scheme 65 PIDA mediated C2-alkylation of quinoline, isoquinoline and pyridine *N*-oxide derivatives (Sen *et al.*[98]).

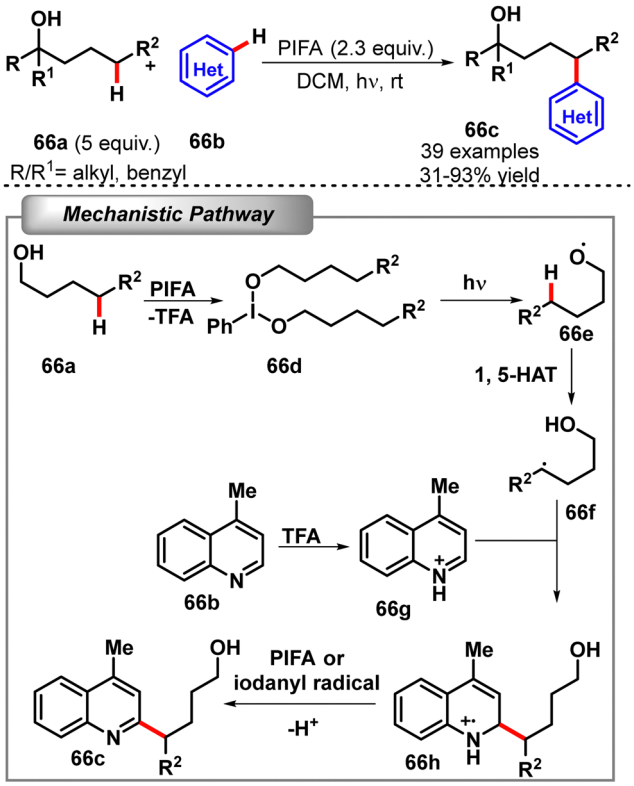

Scheme 66 PIFA mediated alcohol-directed remote C(sp^3)–H heteroarylation (Wu *et al.*[99]).

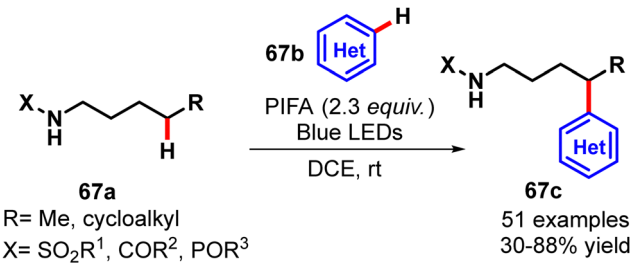

Scheme 67 PIFA mediated amide-directed remote C(sp^3)–H heteroarylation (Tang *et al.*[100])

radicals **66f** from free alcohols **66a** which triggered 1,5-HAT which in turn reacted with the heteroaryl for C–C bond formation. The reaction continued even in the absence of light, albeit at a lower yield, leading researchers to conclude that it was not a photocatalytic process. A wide number of heteroaryl derivatives irrespective of the electronic effect and even a few complex molecules such as voriconazole and eszopiclone were well tolerated under the optimised condition. Next a wide range of 1°, 2° and 3°-alcohols were also tested and 1,5-HAT was supposed to proceed *via* the more kinetically favourable six-membered cyclic transition state. The mechanism suggested the initial ligand exchange between PIFA and the alcohol **66a** to generate dialkoxyiodo benzene **66d**. Visible light induced homolysis of **66d** led to the formation of the alkoxy radical which triggered the subsequent 1,5-HAT to generate the alkyl radical **66f**. This alkyl radical underwent nucleophilic addition to the quinoline salt **66g** to furnish the radical cation **66h** and a subsequent SET oxidation by PIFA finally afforded the coupling product **66c**.

In 2019, they again reported the PIFA and visible light promoted regioselective heteroarylation of amides **67a** (30–88% yield) by the unactivated C(sp^3)–H bond functionalisation (Scheme 67).[100] This transformation was initiated with the generation of amidyl radicals directly from the amide N–H bond by visible-light irradiation which triggered 1,5-HAT to activate a remote C(sp^3)–H bond like the earlier case. On the other hand, PIFA acted as the initiator of the amidyl radical as well as an oxidant. Unlike the previous report, this reaction did not take place without the photo irradiation or under heating conditions in the dark. A wide variety of six membered nitrogen-containing heteroarenes with different functional groups were found to be suitable for the alkylation reaction at either *o*- or *p*-position. Similarly, a wide range of aliphatic amides such as carboxamides, sulfonamides, and phosphoramides were also tested for the remote C(sp^3)–H bond activation. The mechanism followed a similar path as described in the earlier case.

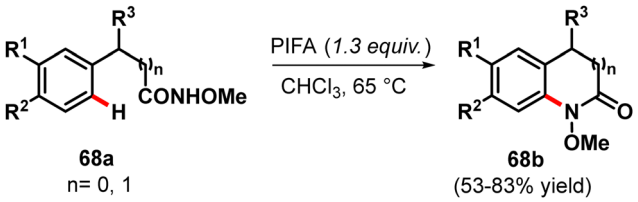

Scheme 68 Intramolecular oxidative C(sp^2)–N bond formation of *N*-methoxy amides (Yasuo *et al.*[101]).

4.2 C–N bond formation

4.2.1 Intramolecular direct C(sp^2)–N bond formation. In 1990, Kikugawa and Kawase reported a PIFA mediated intramolecular oxidative C(sp^2)–N bond formation of *N*-methoxy amides **68a** for the generation of *N*-aryl-*N*-methoxyamides **68b** (53–83% yield) (Scheme 68).[101] The proposed mechanism involved the initial formation of electron deficient nitrogen species by the interaction of *N*-methoxyamide with the hypervalent iodine reagent, the former being stabilised by a neighbouring methoxy group. Finally, the intramolecular attack of the aromatic group on the electron deficient nitrenium cation produced the product.

Later in 1996, Romero and his team also developed a similar kind of PIFA assisted oxidative amination of *N*-methoxy amides **69a** for the synthesis of *N*-substituted benzimidazolin-2-ones **69b** (26–79% yield) (Scheme 69).[102] A similar mechanism followed as well in this reaction. The authors had purposefully provided a route to remove the *N*-methoxy group by hydrogenation over Pd/C in ethanol.

In 2003, Kikugawa *et al.* introduced *N*-acylaminophthalimides **70a** as a new class of precursors for intramolecular C–H amination for the synthesis of benzoxazolone derivatives **70b** (30–70% yield) (Scheme 70).[103] Notably, they employed 4-chloro PIFA (4-Cl PIFA) as an oxidant in TFA solvent to avoid the *ipso*-cyclization that would give rise to the spiroannulated product.

Further in 2015, this same methodology was extended by the Fu group where they reported the PIDA mediated oxidative C–H amination of *N*,*N*′-diarylurea derivatives **71a** to obtain benzimidazol-2-one derivatives **71b** in moderate to good yields (33–88% yield) (Scheme 71).[104] Addition of Cs_2CO_3 as a base and HFIP as solvent increased the yield of the reaction. The mechanism

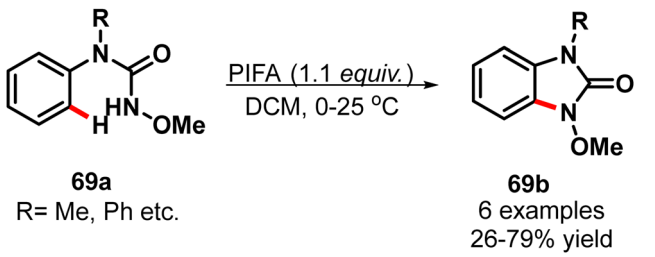

Scheme 69 PIFA assisted oxidative amination of N-methoxy amides (Romero *et al.*[102]).

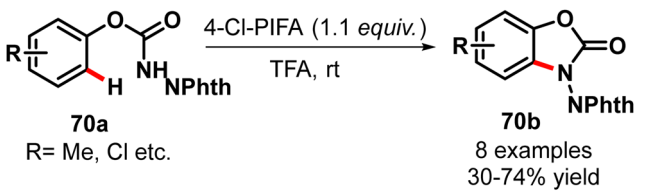

Scheme 70 PIFA assisted oxidative amination of *N*-methoxy amides (Kikugawa *et al.*[103]).

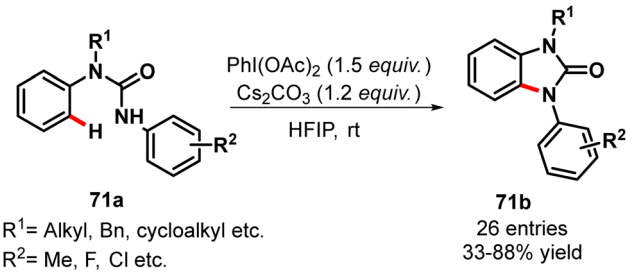

Scheme 71 Oxidative C–H amidation of *N,N′*-diarylureas with PIDA (Yu *et al.*[104]).

suggested the generation of the nitrogen centred cation by the treatment of PIDA followed by heterolysis of the N–I bond. An immediate intramolecular electrophilic addition to this cation and a subsequent rearomatization by deprotonation afforded the target product.

Due to the unique structural feature and a diverse range of applications in electronic devices like light-emitting diodes (LED), field-effect transistors (FET) and organic thin-film transistors (OTFT), carbazole has been recognised as one of the important moieties; unfortunately, its synthesis has eluded us despite extensive work. In this regard, the first metal free intramolecular oxidative coupling was reported by Chang *et al.* In 2011, they introduced a PIFA mediated oxidative C–N bond formation reaction of *N*-substituted amidobiphenyl derivatives **72a** for the synthesis of a wide range of *N*-substituted carbazoles **72b** (9–98% yield) (Scheme 72).[105] However, the yield of the carbazole product under this metal free condition was slightly lower than that of the complementary metal catalysed reaction. Moreover, the author suggested the possibilities for a radical or cationic radical mechanism for this transformation.

In the same year, Antonchick *et al.* developed an organocatalytic intramolecular oxidative C–N bond formation method for the synthesis of carbazoles (48–98% yield) (Scheme 73).[106] In this approach, they had used a catalytic amount of 2,2′-diiodo-4,4′,6,6′-tetramethylbi-phenyl **73b** along with peracetic acid for the *in situ* formation of the μ-oxo-bridged hypervalent iodine(III) catalyst which actually facilitated the amination reaction. Interaction of 2-phenylacetanilide **73a** with this catalyst by ligand substitution followed by oxidative fragmentation afforded the nitrenium ion and a subsequent nucleophilic attack by the adjacent arene unit provided the carbazole **73c.**

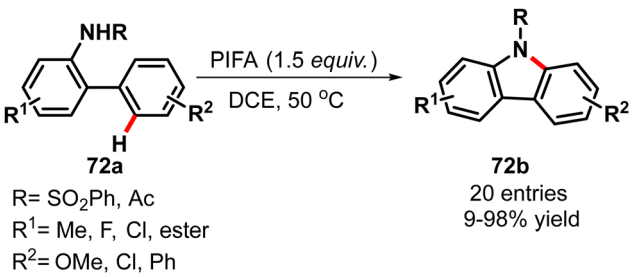

Scheme 72 PIFA mediated oxidative C–N bond formation reaction for the synthesis of carbazole (Cho *et al.*[105]).

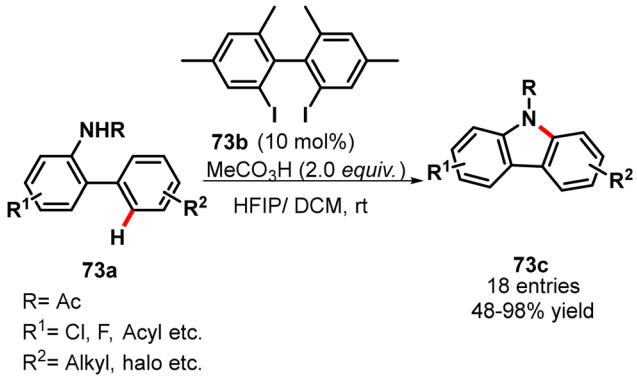

Scheme 73 Organocatalytic intramolecular oxidative C–N bond formation for the synthesis of carbazole (Antonchick *et al.*[106]).

Remarkably, the radical mechanism was ruled out as the reaction could not be impeded in the presence of a radical scavenger.

In the very next year, they again developed a PIDA mediated oxidative amination of 2,6-diarylated acetanilides for the synthesis of the hyellazole scaffold, *i.e.* 1-arylcarbazole moieties (52–88% yield) **74b.** A detailed mechanistic study suggested a 4π-electron–5-atom electrocyclization mechanism for this transformation (Scheme 74).[107]

In 2012, Wang and Du reported a PIFA mediated synthesis of carbazolone derivatives by the oxidative intramolecular amination of 2-aryl enaminones and *N*-substituted acyclic enaminones respectively (Scheme 75).[108] A plausible mechanism was proposed according to which the *N*-iodo intermediate **75c** generated through the interaction of enaminone **75a** and PIFA would undergo an electrophilic attack on the *N*-centre by the adjacent phenyl ring with the simultaneous release of iodobenzene and CF_3COOH to furnish the desired carbazolone **75b.**

Recently in 2018, Mal and co-workers developed hypervalent iodine reagent (HIR) mediated intramolecular oxidative C–N coupling reactions of *N*-(2′,4′,6′-trialkyl-[1,1′-biphenyl]-2-yl)methanesulfonamide **76a** *via* 1,2-alkyl migration followed by distal C–H bond functionalisation for the synthesis of 1,2,4-trialkyl-substituted carbazoles (35–98% yield) (Scheme 76).[109] The authors had used either a stoichiometric amount of PIDA or *in situ* generated hypervalent iodine(III) from a stoichiometric amount of iodobenzene (PhI) and mCPBA combination. A plausible mechanism was suggested

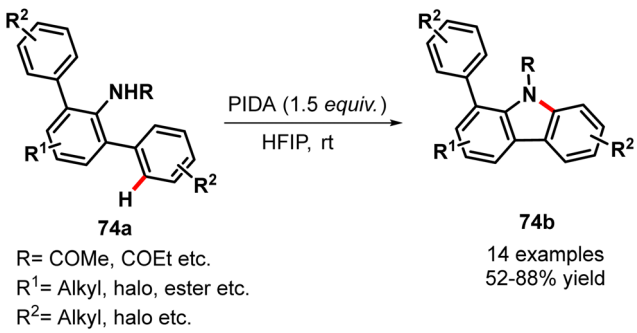

Scheme 74 PIDA mediated intramolecular oxidative C–N bond formation (Samanta *et al.*[107]).

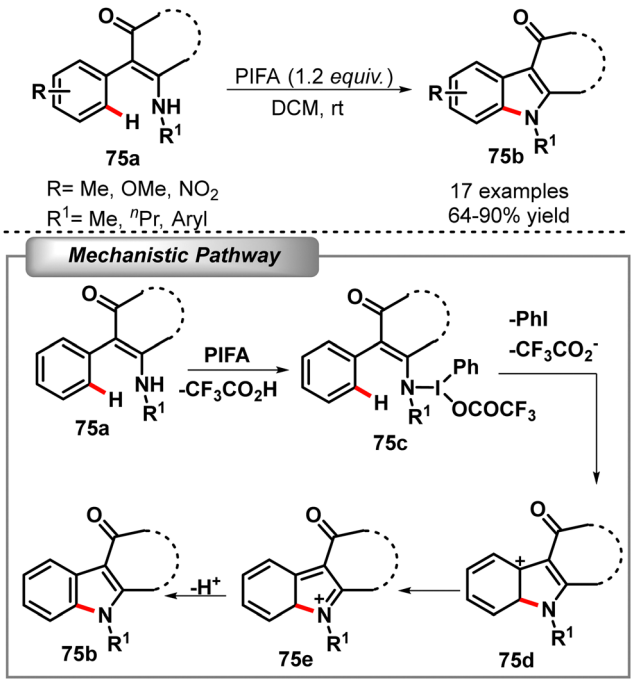

Scheme 75 PIFA mediated synthesis of carbazolone derivatives by the oxidative intramolecular amination (Ban *et al.*[108]).

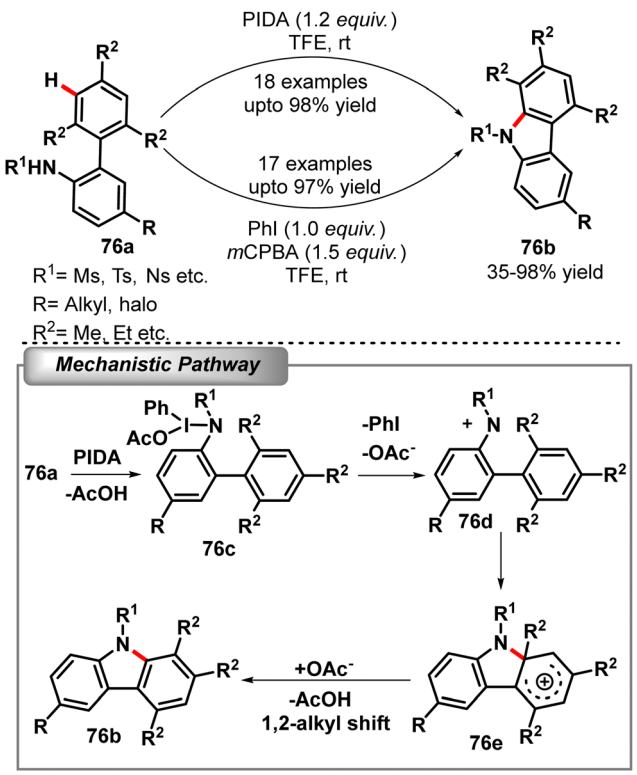

Scheme 76 HIR-mediated intramolecular oxidative C–N coupling reactions of sulfonamide (Bal *et al.*[109]).

which involved the generation of nitrenium intermediate **76d** by the interaction of sulfonamide **76a** and HIR. Then, electrophilic nitrogen species underwent nucleophilic reaction by the adjacent

Scheme 77 HIR-mediated access to 1,4-benzodiazepin-2-ones (Herrero *et al.*[110]).

trialkyl arene moiety to form the carbenium intermediate **76e** and a subsequent alkyl group migration to the next carbon followed by deprotonation afforded the desired carbazole **76b**.

During the early 2000, inspired by Kikugawa's pioneering work, Herrero *et al.* also described a PIFA mediated intramolecular oxidative amidation of methoxyamide derivatives **77a** for the construction of 1,4-benzodiazepin-2-one **77b** by utilising the ability of PIFA to generate *N*-acyl nitrenium ions from *N*-alkoxyamides (Scheme 77).[110]

The powerful potential of PIFA to generate the previously discussed *N*-acyl nitrenium ions from *N*-alkoxyamides was further expanded by the Dominguez group for the synthesis of optically active benzo-, naphtho-, and heterocycle-fused pyrrolo[2,1-*c*]-[1,4]-diazepin-5,11-dione derivatives **78b** starting from *L*-proline methoxy amides **78a** (Scheme 78).[111]

Malamidou-Xenikaki and co-workers utilised the PIFA mediated oxidative amidation of indenocarboxamide **79a** for the synthesis of indeno-1,4-diazepinones **79b** (14–75% yield) (Scheme 79).[112] A possible mechanistic explanation suggested the co-existence of two tautomers of indenocarboxamide in the solution, and its reaction with PIFA afforded the acylnitrenium ion *via* an

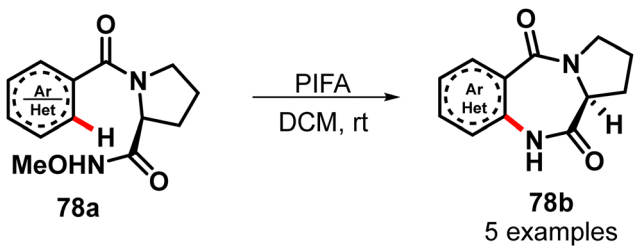

Scheme 78 HIR-mediated intramolecular oxidative C–N coupling for the synthesis of pyrrolo[2,1-*c*]-[1,4]-diazepin-5,11-dione derivatives (Correa *et al.*[111]).

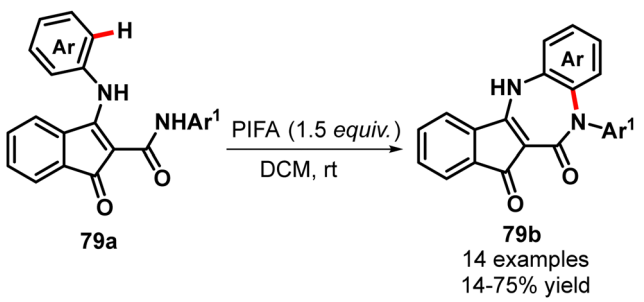

Scheme 79 HIR- mediated synthesis of fused indeno-1,4-diazepinones (Xenikaki *et al.*[112]).

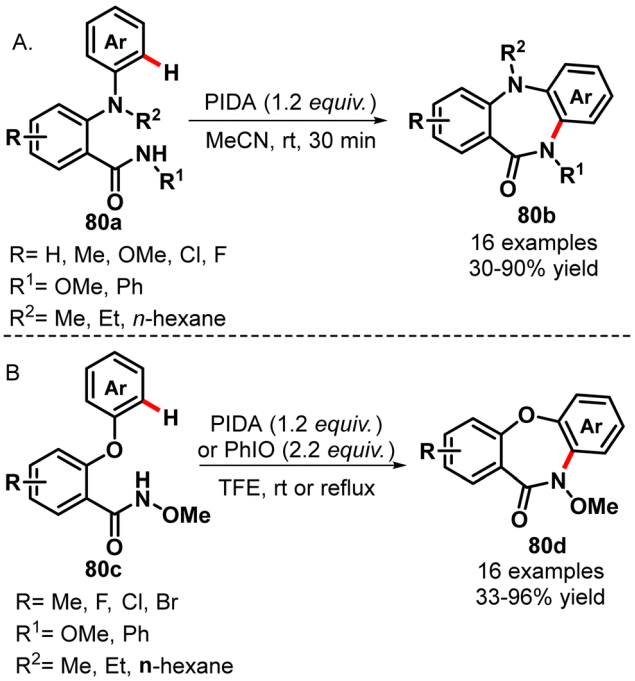

Scheme 80 PIDA promoted intramolecular oxidative amidation of benzamides (Guoa *et al.*,[113] Li *et al.*[114]).

oxidative process. The intramolecular attack of the nucleophilic aryl group on the acylnitrenium ion furnished the fused indenobenzodiazepinones.

In 2014, Du and Zhao reported a PIDA promoted intramolecular oxidative amidation of 2-(arylamino)benzamides **80a** *via* the formation of an acylnitrenium ion for the construction of 1,4-benzodiazepine skeleton **80b** (30–90% yield) (Scheme 80A).[113] It is worth mentioning that either the presence of the methyl group on the amide nitrogen instead of –OMe or a strong electron withdrawing group in the adjacent phenyl ring, to which the N-atom has to be attached, prevented the desired electrophilic cyclization reaction. Similarly they also synthesized the dibenzoxazepinone compounds **80d** from 2-(aryloxy)benzamides **80c** (33–96% yield) (Scheme 80B).[114] The coupling reaction with the unsubstituted or halogen substituted adjacent phenyl group was found to be successful with PIDA. However, for the electron-rich aryl, the desired cyclization was achieved in acceptable yield by using iodosobenzene (PhIO) in refluxing TFE.

The Du and Zhao group further extended the potential of hypervalent iodine(III) to generate the nitrenium ion from *N*-alkoxyamide or *N*-arylamide for the intramolecular oxidative C(sp^2)–H amidation to synthesize various important heterocycles. In 2013, they reported a PIDA mediated oxidative amination of *N*-methoxy enamide **81a** for the synthesis of indoloquinolinones **81b** in DCE solvent (75–94% yield) (Scheme 81A).[115] They had also utilised a similar method for the oxidative amination of 3-arylindole-2-carboxamide **81c** (63–91% yield) (Scheme 81B).[116]

In 2017, Zhang and his team presented a PIFA mediated intramolecular C(sp^2)-amidation of 2,2-disubstituted-2-benzoylacetamides **82a** for the synthesis of quinolinediones **82b** with 13–98%

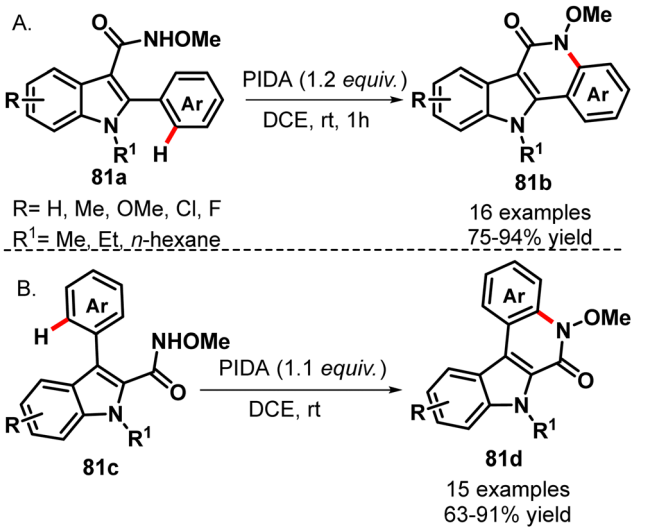

Scheme 81 Intramolecular oxidative C(sp^2)–H amidation to synthesize various important heterocycles (Zhang *et al.*,[115] Li *et al.*[116]).

yield (Scheme 82A).[117] Unfortunately, this oxidative cyclization is not fruitful with the aliphatic amides. The reaction was also envisaged to proceed *via* the generation of the *N*-acylnitrenium ion. Afterwards, they also synthesized spirocyclopropyl oxindoles **82d** from secondary cyclopropyl carboxamides **82c** using the same concept with 41–84% yield (Scheme 82B).[118] However, instead of PIFA, bis(*tert*butylcarbonyloxy)iodobenzene (PhI(OPiv)$_2$) in HFIP at 100 °C was found to be the best condition for this oxidative amination.

The very next year, they also synthesized quinolino[3,4-*b*]-quinoxalin-6(5*H*)-ones **83b** by the similar PIFA mediated oxidative C(sp^2)–H amidation of *N*-methoxy-3-phenylquinoxaline-2-carboxamide **83a** in good yield (up to 99%) (Scheme 83).[119]

Xue *et al.* established a hypervalent iodine(III) catalysed novel synthesis of phenanthridinones **84b** using an intramolecular

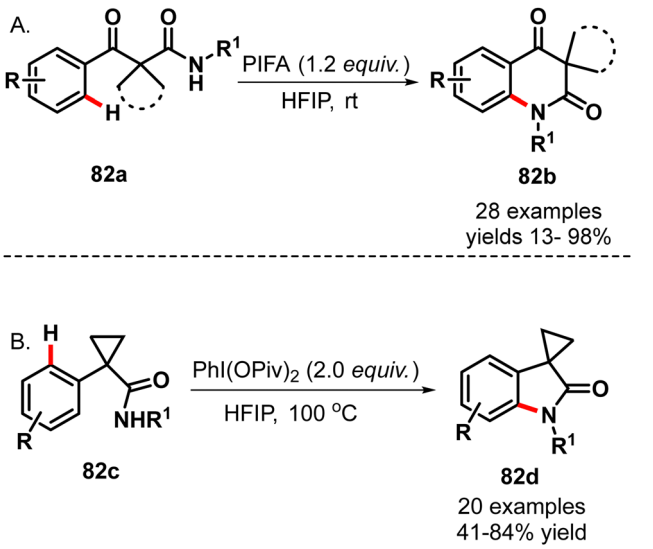

Scheme 82 Intramolecular oxidative C(sp^2)–H amidation of benzoylacetamides and cyclopropyl carboxamides (Zhang *et al.*[117,118]).

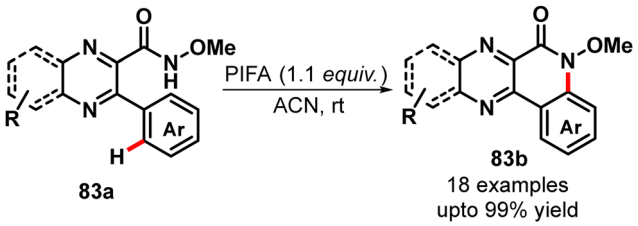

Scheme 83 Intramolecular oxidative C(sp^2)–H amidation for the synthesis of quinolino[3,4-*b*]quinoxalin-6(5*H*)-one (Hu *et al.*[119]).

oxidative C(sp^2)–H amidation reaction from *N*-methoxybenzamides **84a** (Scheme 84).[120] A catalytic amount of PhI along with mCPBA in HFIP solvent had been utilised as the optimised condition for this reaction. Depending on the substitution pattern on the adjacent aryl group with which coupling had taken place, a rearranged phenanthridinone (30–99% yield) was also formed along with the usual structure. The mechanism proposed the formation of *N*-methoxy-*N*-acylnitrenium ion **84d** by the interaction of HIR with methoxybenzamide **84a**. Electrophilic attack on the nitrenium ion by forming either an N–C(*ortho*-) bond (path a) or an N–C(*ipso*) bond (path b) provided the intermediates **84e** and **84g**, respectively. Intermediate **84e** afforded the desired phenanthridinone **84f** by proton abstraction. On the other hand, the double rearrangement of spiro carbocation followed by the elimination of a proton gave the rearranged product **84j**.

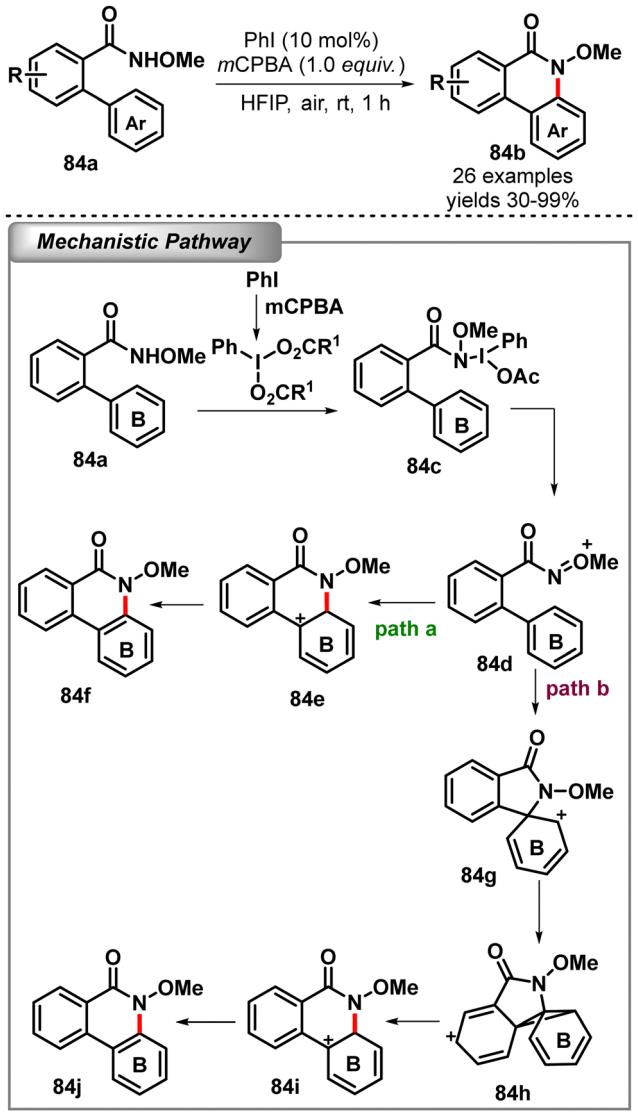

Scheme 84 Intramolecular oxidative C(sp^2)–H amidation for the synthesis of phenanthridinones (Liang *et al.*[120]).

Next, they again disclosed a sequential one-pot iodine-mediated amidation/bromination reaction of *N*-methoxybenzamides **85a** for the synthesis of 2-bromo phenanthridinones **85b** with moderate to excellent yield (42–89%) (Scheme 85).[121] For this transformation, they used PhI as a catalyst, peracetic acid as an oxidant and TBAB as a bromide source. They also repeated the reaction with 2.5 equiv. of PIDA instead of the catalytic system where they found a small improvement in yields. The product 2-bromo phenanthridone was very useful for the late-stage functionalisation.

In 2019, Bera *et al.* disclosed a PIFA mediated synthesis of phenanthridine derivatives **86b** *via* the intramolecular oxidative C–N coupling reaction of benzimidazoles **86a** (yield 82–98%) (Scheme 86).[122] The authors demonstrated that the reaction proceeded with the anti-aromatic ($4n\pi$) endocyclic nitrenium ion intermediate that was directly generated from the interaction of benzimidazole with PIFA.

This benzimidazole is a ubiquitous structural motif routinely found in a vast range of natural products and bioactive synthetic molecules. In 2012, Huang *et al.* investigated the PIDA promoted oxidative C(sp^2)–H bond imidation of *N*-aryl benzamidine **87a** for the synthesis of 2-arylbenzimidazole **87b** (Scheme 87).[123]

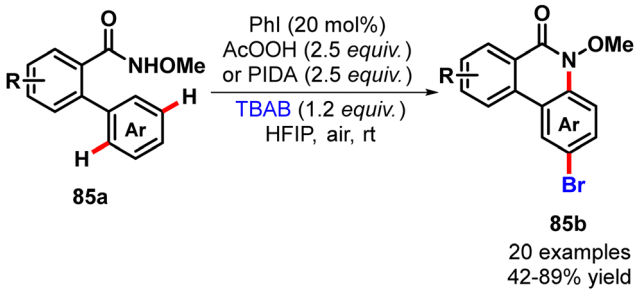

Scheme 85 Intramolecular oxidative C(sp^2)–H amidation for the synthesis of 2-bromo phenanthridinones (Liang *et al.*[121]).

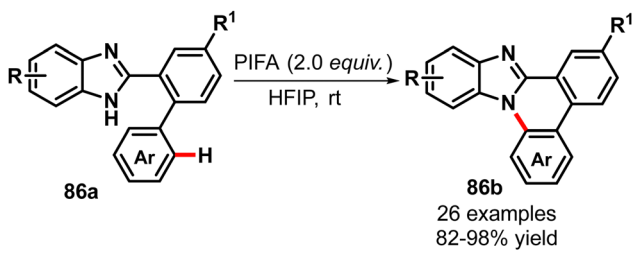

Scheme 86 Intramolecular oxidative C(sp^2)–N coupling reaction for the synthesis of benzimidazoles (Bera *et al.*[122]).

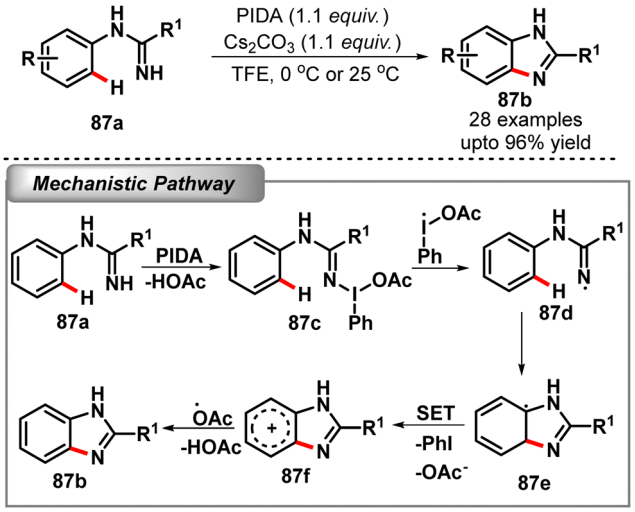

Scheme 87 PIDA promoted oxidative C(sp^2)–H bond imidation of *N*-aryl benzamidine (Huang *et al.*[123]).

This method was also suitable for the synthesis of 2-alkyl-benzimidazoles. Furthermore, the inhibition of the reaction in the presence of a radical scavenger suggested the involvement of radical species during the reaction. A possible mechanism was proposed which involved the generation of *N*-centred radical intermediate **87d** by the interaction of PIDA and amidine **87a**. The addition of the tethered aromatic ring to this radical generated the cyclohexadienyl radical **87e** which upon oxidation and proton abstraction yielded the benzimidazole **87b**.

The very next year, they again synthesized pyrido[1,2-α]benzimidazoles **88b** by a hypervalent iodine(III) catalysed oxidative C–N bond formation of *N*-aryl-2-aminopyridines **88a** (Scheme 88).[124] A catalytic amount (10 mol%) of PhI and a stoichiometric amount of peracetic acid in HFIP were found to be suitable for this transformation to give the desired product with 67–99% yield. The mechanism suggested the nucleophilic attack of the aniline nitrogen on the iodine(III) center which was *in situ* generated

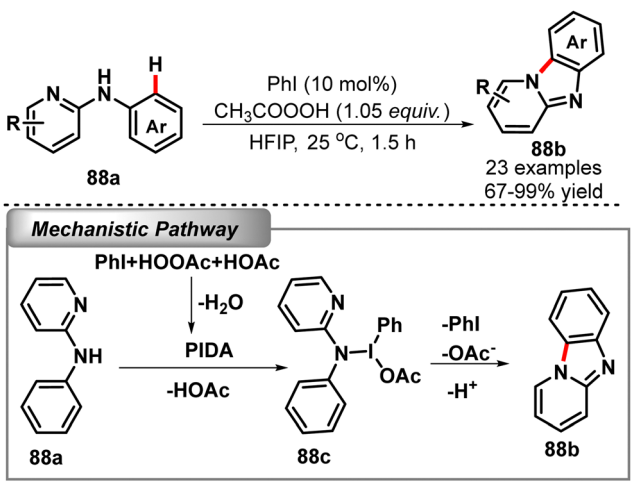

Scheme 88 HIR promoted synthesis of pyrido[1,2-α]benzimidazoles (He *et al.*[124]).

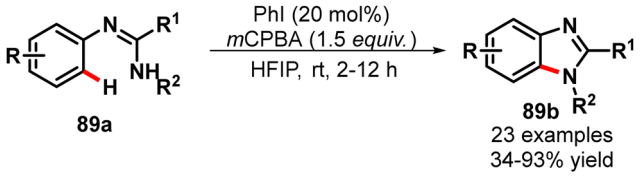

Scheme 89 HIR catalysed oxidative C–H amination of amidines (Alla *et al.*[125]).

from the catalytic PhI and peracetic acid. Subsequent nucleophilic attack of the pyridine nitrogen on the aniline of intermediate **88c** containing an electrophilic *N*-iodo moiety and concurrent deprotonation rearomatization finally furnished the desired product **88b**. The released PhI during this process again entered the catalytic cycle by oxidation.

In the same year, the Punniyamurthy group reported a similar hypervalent iodine catalysed oxidative C–H amination of sulfonyl/aryl amidines **89a** for the synthesis of 1,2-disubstituted benzimidazoles **89b** (34–93% yield) (Scheme 89).[125] This reaction was performed in the presence of 20 mol% of PhI and a stoichiometric amount of terminal oxidant *m*CPBA in HFIP solvent. The reaction also proceeded *via* the formation of the nitrenium ion intermediate in the presence of *in situ* generated HIR.

In 2014, Long and colleagues conducted a PIDA mediated intramolecular oxidative C(sp^2)–H amination of *N*-alkyl-*N*′-arylamidine **90a** to generate the benzimidazole **90b** in polar solvent acetonitrile with an excellent yield of up to 99% (Scheme 90).[126] The polar solvent actually stabilised the cationic nitrenium intermediate through the solvation stabilization.

In the same year, Nageswar Rao *et al.* developed a HIR catalysed oxidative C–N bond formation of *N*-aryl-2-amino-N-heterocycles **91a** for the synthesis of benzimidazole-fused heterocycles **91b** with 72–99% yield in water under ambient conditions (Scheme 91).[127] The reaction was actually promoted by the *in situ* generated Koser's reagent (PhI(OH)(OTs)) by using PIDA (0.2 equiv.) as an iodine source along with PTSA.H_2O and *m*CPBA

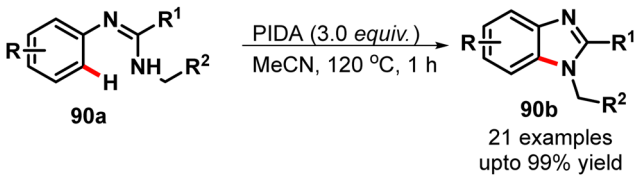

Scheme 90 HIR mediated C(sp^2)–H amination of *N*-alkyl-*N*′-arylamidine (Lin *et al.*[126]).

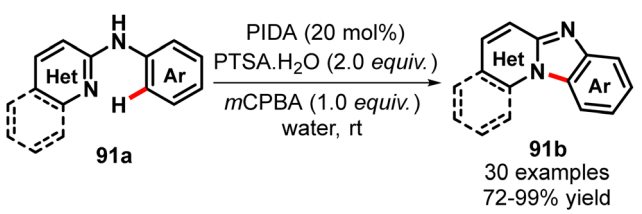

Scheme 91 HIR mediated C(sp^2)–N bond formation for the synthesis of benzimidazole-fused heterocycles (Rao *et al.*[127]).

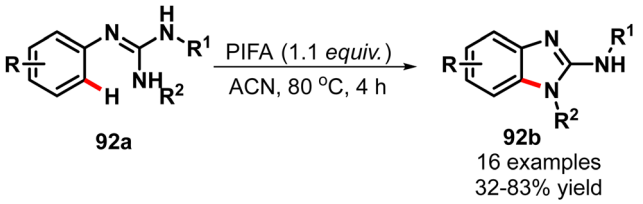

Scheme 92 PIFA-mediated intramolecular oxidative C(sp^2)–H amination of various guanidine derivatives (Chi *et al.*[128]).

as an oxidant in water. A plausible mechanism for the amination was suggested, namely, the usual formation of electrophilic *N*-iodo species and a subsequent nucleophilic attack of the adjacent benzene ring on the pyridine nitrogen and deprotonation to provide the benzimidazole derivatives.

The Zhang group synthesized PIFA mediated 2-aminobenzimidazoles **92b** by the intramolecular oxidative C(sp^2)–H amination of various guanidine **92a** (32–83% yield) (Scheme 92).[128] A tentative mechanism was suggested involving the initial oxidation of one N–H bond in guanidine by PIFA and the subsequent attack of the attached arene on this electron deficient nitrogen and rearomatization to furnish 2-aminobenzimidazole.

In 2015, Maiti *et al.* reported a PIDA promoted C(sp^2)–H amidation of (2-benzylidene)aminophenyl-4-methylbenzenesulfonamide for the synthesis of 1,2-disubstituted multifunctional benzimidazole derivatives **93b** in good to excellent yield (33% to >98%) (Scheme 93).[129]

Xu *et al.* reported a PIFA promoted intramolecular C–H bond cycloamination reaction of pyrimidyl arylamines or enamines **94a** for the synthesis of imidazo[1,2-α]pyrimidine derivatives **94b** (46–97% yield) (Scheme 94).[130] The mechanism suggested the usual formation of the nitrenium ion by the nucleophilic attack of aniline nitrogen on the HIR. Now the product could be obtained either by a stepwise bond formation or by a direct

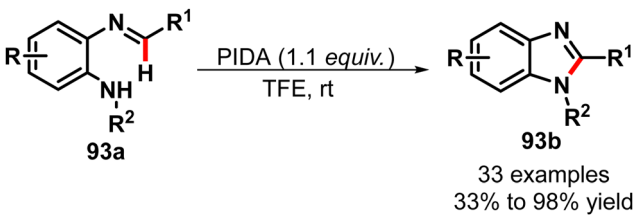

Scheme 93 PIDA-mediated intramolecular C(sp^2)–H amidation for the synthesis of 1,2-disubstituted benzimidazole (Maiti *et al.*[129]).

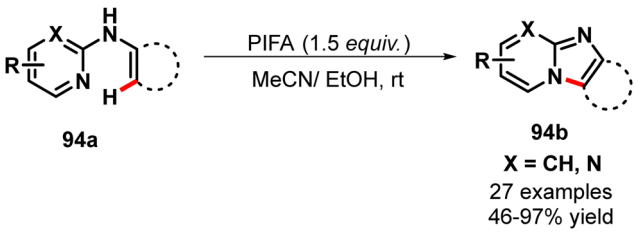

Scheme 94 PIFA promoted intramolecular C–H bond cycloamination reaction of pyrimidyl arylamines (Qian *et al.*[130]).

cycloaddition by the pyrimidyl nitrogen atom on the aniline ring.

In 2015, Subba Reddy developed a HIR catalysed oxidative C(sp^2)–H amination of aryl hydrazine dicarboxylates **95a** for the synthesis of benzo[*c*]cinnoline derivatives **95b** with moderate to excellent yield (55–85%) (Scheme 95).[131] These are considered as privileged scaffolds in medicinal chemistry due to their promising anticancer properties. The reaction was performed in the presence of 30 mol% of PhI and 2 equiv. of oxone in TFE solvent. The reaction was supposed to proceed *via* one pot sequential amination, ester hydrolysis, and decarboxylation.

The construction of the indole skeleton has been a topic of great interest because of the widespread prevalence of the indole moiety in many natural products and designed medicinal agents. In 2006, the Zhao group first reported a PIFA mediated intramolecular oxidative C–N bond formation of 2-aryl-3-arylamino-2-alkenenitriles **96a** for the synthesis of various *N*-aryl or alkyl indole derivatives **96b** (41–94% yield) (Scheme 96A).[132] The authors suggested a radical cyclisation pathway by the homolytic cleavage of the N–I bond for this transformation. After this report there was hardly any approach for the metal free oxidative indole synthesis until Muniz *et al.*'s work in 2014. Here they disclosed a modified Koser's reagent employed oxidative cyclization of 2-amino styrene **96c** to indole **96e** (32–92% yield) (Scheme 96B).[133] This reaction provided the optimum yield with the combination of PhIO and 2,4,5-tris-isopropylbenzenesulfonic acid **96d** by the *in situ* generation of modified Koser's reagent. Due to the acidic conditions, the Boc group was beyond the scope of the present transformation. The authors proposed a tentative reaction mechanism which involved the interaction of modified Koser's reagent and the alkene group to form the 1,2-iodooxygenated intermediate **96f**. This intermediate was stabilised by the neighbouring phenyl group *via* the formation of cyclopropyl phenonium ion **96h**. Now the opening of the cyclopropyl group by amine functionality could be possible in two different ways; attack at the methylene carbon afforded the indole through the **96i** intermediate or the attack at the tertiary carbon atom provided the indole alternatively *via* the elimination of the aryl sulfonic acid **96j**.

In 2018, Mo and co-workers synthesized 3-substituted and 2,3-disubstituted indoles **97c** by 3,5-dimethyl PIDA (**97b**) mediated intramolecular amination of 2-alkenylanilines **97a** with comfortable yield (28–87%) (Scheme 97).[134] The mechanism

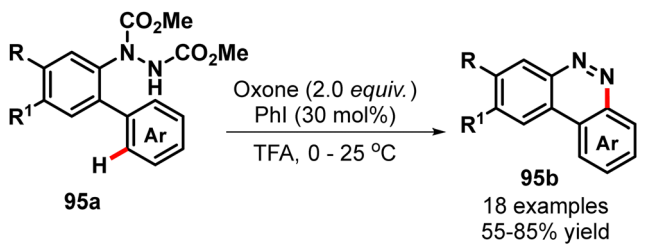

Scheme 95 HIR catalysed oxidative C(sp^2)–H amination of aryl hydrazine dicarboxylates for the synthesis of benzo[c]cinnoline derivatives (Subba Reddy *et al.*[131]).

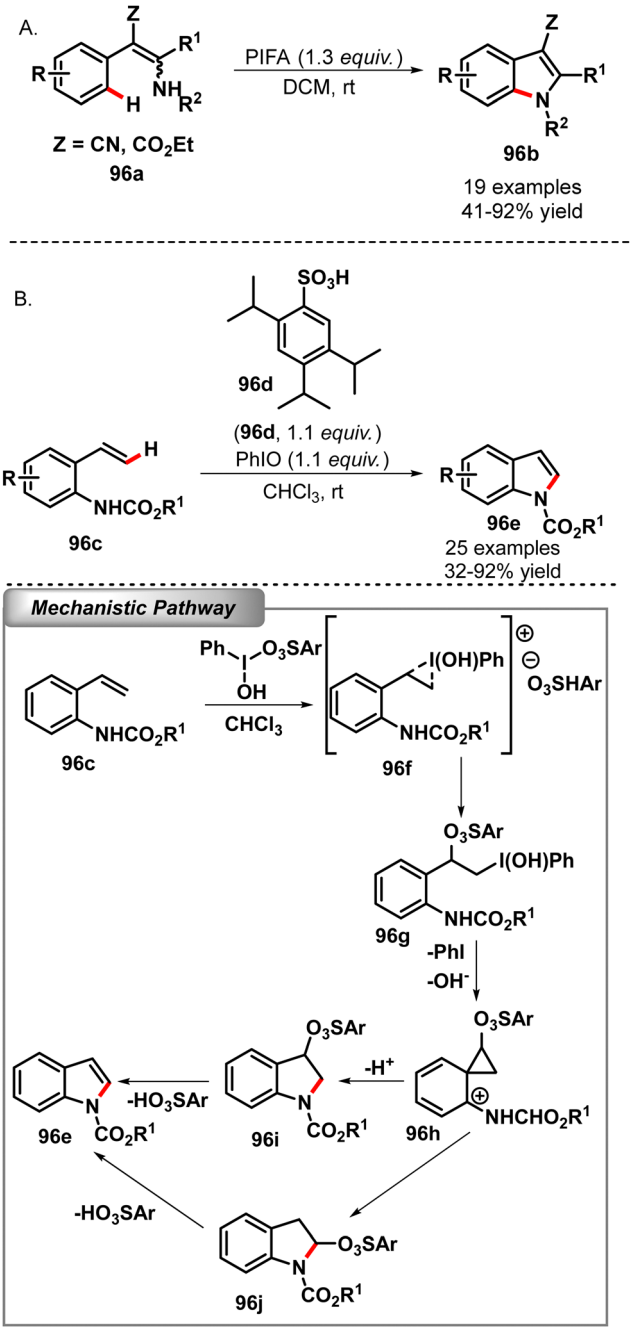

Scheme 96 HIR-mediated intramolecular oxidative C–N bond formation for the synthesis of indole derivatives (Du *et al.*,[132] Fra *et al.*[133]).

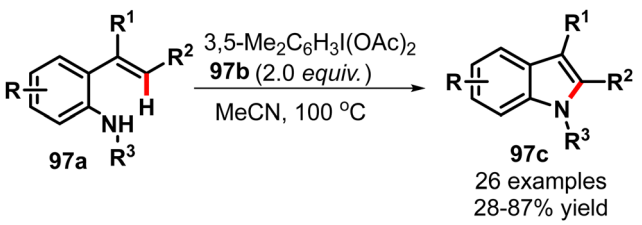

Scheme 97 HIR-mediated intramolecular oxidative C–N bond formation for the synthesis of substituted indole derivatives (Zhao *et al.*[134]).

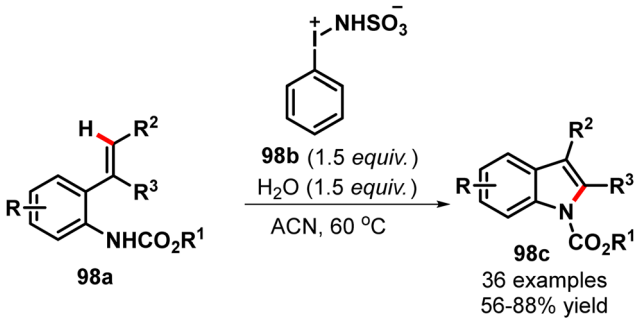

Scheme 98 HIR-mediated intramolecular oxidative C–H amination for the synthesis of various indole derivatives (Xia *et al.*[135]).

suggested that the desired indole was derived through the E1 elimination of 3-acetoxy indoline.

Later, the Zhang group developed a new bench-stable water-soluble hypervalent iodine(III) reagent (phenyliodonio)sulfamate **98b** mediated C–H amination of 2-alkenylanilines **98a** involving an aryl migration/intramolecular cyclization cascade reaction for the synthesis of various indoles **98c** (56–88% yield) (Scheme 98).[135] The reaction mechanism also followed Muniz's cyclopropyl phenonium ion pathway.

In 2015, Zhu *et al.* demonstrated a PIDA mediated oxidative C–H cycloamination of vinyl hydrazones **99a** for the synthesis of a wide variety of pyrazoles **99b** (23–98% yield) (Scheme 99).[136] The reaction followed the usual nitrenium ion pathway.

4.2.2 Intramolecular direct C(sp^3)–N bond formation. Unactivated C(sp^3)–H bond functionalisation is always considered as a vital transformation in organic synthesis. In this regard, the Hofmann–Loffler–Freytag (HLF) reaction is the most popular as well as valuable method for the formation of non-activated C(sp^3)–N bonds.

An interesting finding in this field was first reported by Fan *et al.* as a δ sp^3 C–H bond activation for the intramolecular amination of C(sp^3)–H bonds with PIDA/I_2 for the synthesis of pyrrolidine derivatives with excellent yield (5–87%) (Scheme 100).[137] Notably, a strong electron-withdrawing group like sulfonamide was essential for this intramolecular amination; however, benzamide and trifluoroacetamide were inefficient for this transformation. A tentative mechanism was suggested involving the initial formation of acetyl hypoiodite from the reaction between PIDA and I_2, which led to the formation of sulfonamidyl radical **100d** from the corresponding sulfonamide **100a**. This sulfonamidyl radical then underwent a 1,5-H shift to form δ-carbon radical **100e**, which would be further oxidized and provide the pyrrolidine **100b** by cyclization.

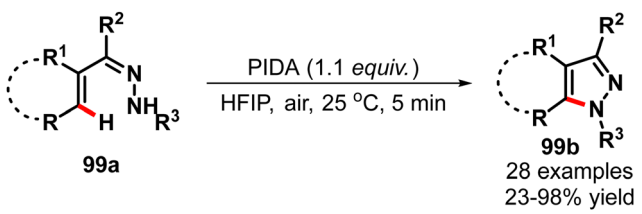

Scheme 99 PIDA-mediated intramolecular oxidative C–H cycloamination for the synthesis of various pyrazole derivatives (Liang *et al.*[136]).

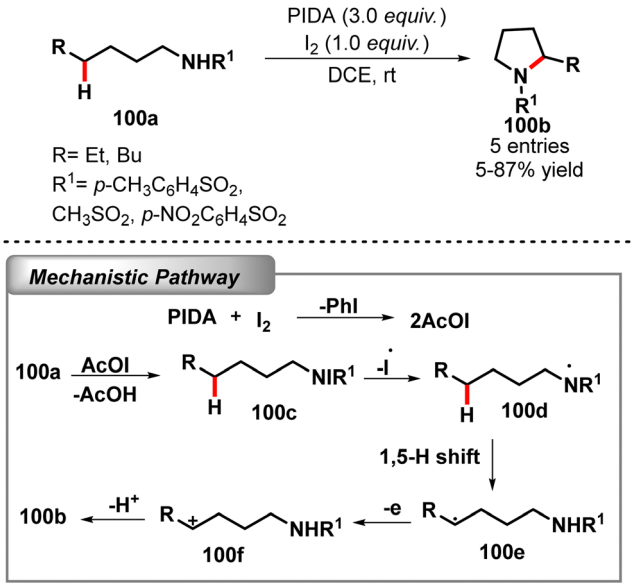

Scheme 100 δ C(sp^3)–H bond activation with PIDA/I_2 for the synthesis of pyrrolidine derivatives (Fan *et al.*[137]).

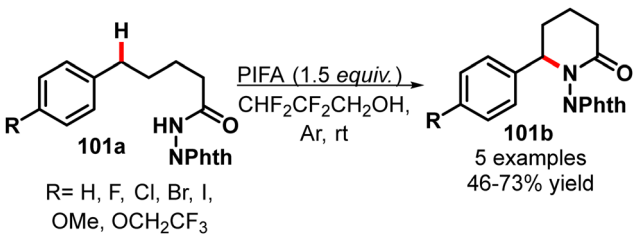

Scheme 101 PIFA mediated oxidative intramolecular C(sp^3)–H amination (Nagasima *et al.* [138]).

During the same time, Kikugawa and co-workers reported a PIFA mediated oxidative intramolecular C(sp3)–H amination of *N*-(5-arylpentanamido)phthalimide **101a** for the synthesis of 5-aryl-*N*-phthalimido-δ-lactam **101b** (Scheme 101).[138] The cyclization occurred at the benzylic position to provide δ-lactams with the aryl group at the α-position to the ring nitrogen in 2,2,3,3-tetrafluoro-1-propanol.

Later in 2010, the Fan group again reported a PhIO/Bu_4NI mediated stereoselective synthesis of highly functionalized azetidines **102b** from a Michael adduct of 2-aminomalonates and chalcones **102a** (Scheme 102A).[139] The mechanism suggested the generation of a new type of HIR by the interaction of iodosobenzene and Bu_4NI with which the Michael adduct reacted either through the amide functionality or with the active methylene carbon to finally afford the desired azetidine. They had again delineated a PhIO/Bu_4NI mediated oxidative cyclization of amidoalkylation adducts of activated methylene compounds **102c** for the synthesis of *N*-benzoyl aziridines **102d** (Scheme 102B).[140] The aziridination was only successful when the active methylene compound was bearing an ester (–CO_2Et or –CO_2Me) group. The mechanism suggested a [1, 3] intramolecular nucleophilic attack by the nitrogen atom on the C–I bond to furnish the corresponding *N*-benzoyl aziridine.

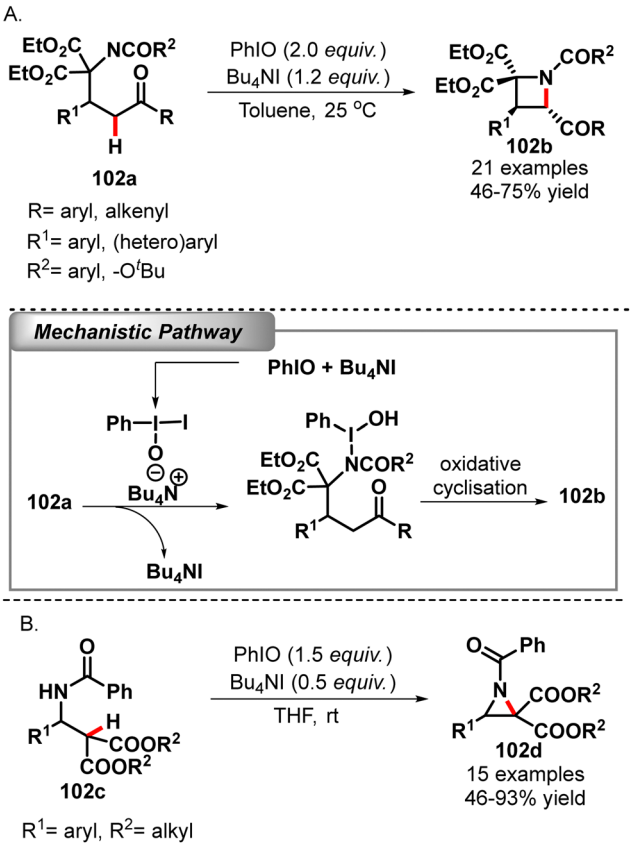

Scheme 102 HIR-mediated oxidative intramolecular C(sp^3)–H amination for the synthesis of azetidine and aziridine (Ye *et al.*,[139] Fan *et al.*[140]).

In 2013, Mao *et al.* developed a $PhI(OPiv)_2$ mediated intramolecular C(sp^3)–H bond amination of 1-acetyl *N*-aryl cyclopropane carboxamide **103a** for the efficient synthesis of tetramic acid derivatives **103b** (Scheme 103).[141] The transformation was optimised with 3.0 equiv. of $PhI(OPiv)_2$ and 15.0 equiv. of propionic acid as a Brønsted acid additive in nitromethane solvent.

In 2015, Shi developed an *in situ* generated hypervalent iodine(III) catalysed intramolecular *tert*iary C(sp^3)–H amination of 2-alkyl-*N*-methoxybenzamide **104a** for the synthesis of γ-lactams **104c** (Scheme 104).[142] The maximum yield was obtained with 20 mol% of 2-iodo biphenyl **104b** and 1.5 equiv. of *m*CPBA as an oxidant in HFIP solvent. Furthermore, the stereospecific tertiary C–H aminations enhanced the value of this protocol in the field of asymmetric synthesis.

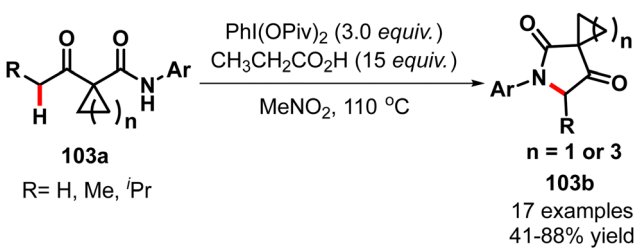

Scheme 103 HIR-mediated oxidative intramolecular C(sp^3)–H amination for the synthesis of tetramic acid derivatives (Mao *et al.*[141]).

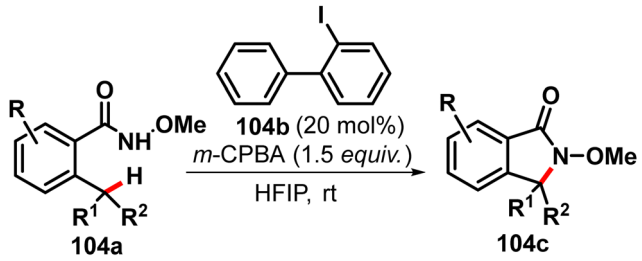

Scheme 104 HIR-catalysed intramolecular tertiary C(sp^3)–H amination of 2-alkyl-*N*-methoxybenzamide for the synthesis of γ-lactams (Zhu *et al.*[142]).

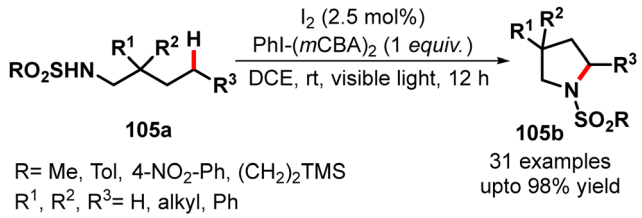

Scheme 105 HIR-catalysed intramolecular oxidative amination of sulphonamides of saturated hydrocarbons (Martinez *et al.*[143]).

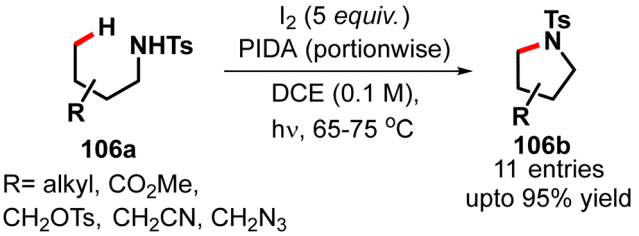

Scheme 106 HIR-catalysed intramolecular oxidative amination for the synthesis of pyrrolidine (Paz *et al.*[144]).

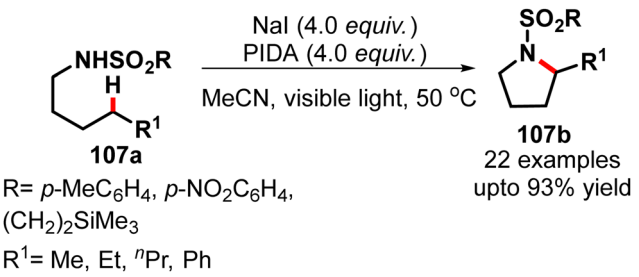

Scheme 107 HIR-mediated δ C–H amination of unactivated secondary C(sp^3)–H for the synthesis of pyrrolidine (Wappes *et al.*[145]).

In the same year, the Muniz group presented a unique iodine-catalyzed intramolecular oxidative amination of sulphonamides **105a** of saturated hydrocarbons for the synthesis of a wide variety of nitrogen heterocycles **105b** (Scheme 105).[143] The oxidative intramolecular C–H amination reaction was performed in the presence of active catalyst I(mCBA) generated by the interaction between molecular iodine (2.5 mol%) and the hypervalent iodine(III) reagent PhI(*m*CBA)$_2$ (1 equiv.) along with the combination of radical chain reaction in the presence of external visible light. The radical chain pathway initiated the rate-limiting step of the transformation, which was demonstrated by the hydrogen abstraction at δ-carbon by the nitrogen centred radical.

In 2015, another strategy was presented by Herrera and co-workers for the synthesis of pyrrolidine **106b** by iodine mediated light induced primary C(sp^3)–H amination by the single hydrogen atom transfer (SHAT) mechanism (Scheme 106).[144] This reaction involved the use of an excess of molecular iodine in more concentrated conditions (0.1 M in DCE) and a portion wise addition of PIDA with irradiation (80 W tungsten lamp) in a sealed tube.

In 2016, Wappes *et al.* reported a NaI/PIDA mediated and visible light promoted (23 W CFL) δ(C–H) amination of unactivated secondary C(sp^3)–H bonds for the formation of a broad range of functionalized pyrrolidines **107b** (Scheme 107).[145] Notably, this method manifested an exclusive δ-selectivity even in the presence of weaker C(sp^3)–H bonds. The transformation proceeded in the presence of the triiodide (I_3) based system, which was generated *in situ* from the oxidation of NaI with PIDA.

Later in 2017, Bolm and his team developed an I_2/PIDA mediated and visible light initiated HLF type reaction of *S*-arylsulfoximines **108a** for the synthesis of dihydroisothiazole oxides **108b** (Scheme 108).[146] A tentative mechanism was suggested which involved the formation of the N–I bond from the starting material upon light irradiation of PIDA and I_2. Again, under the influence of light, the N–I bond was cleaved to generate the N-centred radical and a subsequent 1,5 HAT provided the C-centred radical. The C-centred radical was oxidised to form a C-centred cation and ring closure by sulfoximine by deprotonation afforded the final product as shown in Scheme 100.

Recently, Kumar *et al.* also reported a similar NaI/PIDA mediated and visible light (blue LED) initiated intramolecular γ-C(sp^3)–H bond amidation of alkyl imidated **109a** for the formation of functionalized dihydropyrrole derivatives **109b** (Scheme 109).[147] This protocol also enabled the formation of intermolecular C–I bonds under the reaction condition, which could be further functionalized.

4.2.3 Intermolecular direct C(sp^2)–N bond formation. In 2009, the Chang group reported a PIDA mediated amination of

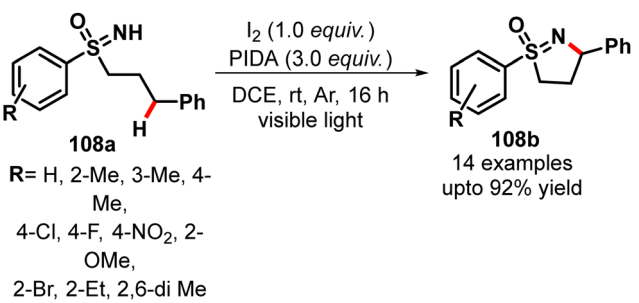

Scheme 108 HIR-mediated HLF type reaction for the synthesis of dihydroisothiazole oxides (Zhang *et al.*[146]).

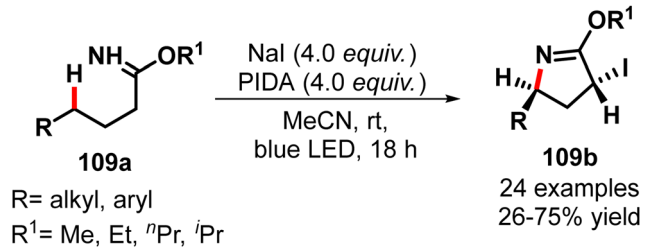

Scheme 109 NaI/PIDA mediated and visible light (blue LED) initiated intramolecular γ-C(sp^3)–H bond amidation (Kumar *et al.*[147]).

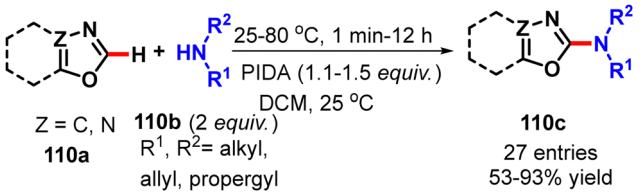

Scheme 110 PIDA mediated intermolecular amination of azoles with secondary amines (Joseph *et al.*[148]).

azoles **110a** with various secondary amines **110b** (Scheme 110).[148] This reaction could not be labelled as a classical C–H functionalisation reaction since the cleavage of the C–H bond α to the amidine nitrogen was not involved in the rate determining step (KIE = 1.0). However this was the first report of metal free intermolecular C–N bond formation reaction.

In 2011, they again developed a PIDA mediated new synthetic strategy for the intermolecular oxidative C–N bond formation of arenes (Scheme 111).[149] Depending on the choice of the nitrogen source, they had a complete control of chemoselectivity between aryl sp^2 and benzylic sp^3 C–H bond imidation. Consequently, phthalimide derivatives **111b** were found to be suitable for the C(sp^2)–N bond formation under the reaction condition to form compound **111c**, whereas dibenzenesulfonimide **111d** afforded benzylic sp^3 C–H bond imidation product **111e**.

Simultaneously, the DeBoef group also established a similar PIDA mediated intermolecular oxidative C–N bond formation

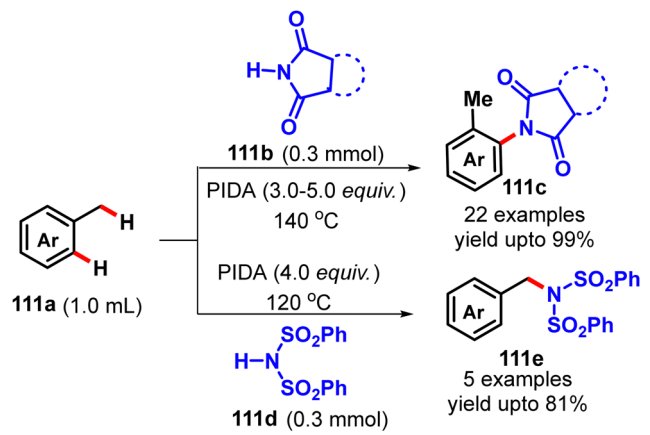

Scheme 111 PIDA mediated intermolecular oxidative C–N bond formation of arenes (Kim *et al.*[149]).

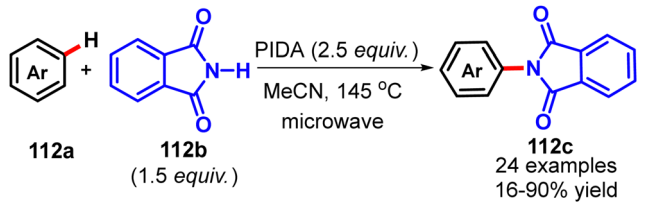

Scheme 112 PIDA mediated intermolecular oxidative C–N bond formation of arenes under microwave irradiation (Kantak *et al.*[150]).

between arene **112a** and phthalimide **112b** under microwave heating (Scheme 112).[150] Notably, sterically hindered arenes and those that contain electron-withdrawing substituents afforded the product in reduced yields. However, the KIE value around 1.0 suggested that neither C–H nor N–H bond cleavage was the rate limiting step, rather a SET mechanism was proved to be operating in this reaction pathway which was further confirmed by the complete inhibition of the reaction by TEMPO.

In 2012, Antonchick and co-workers developed a 4-Me PIDA mediated intermolecular direct oxidative functionalisation of anilides (**113b**) by simple arenes for the synthesis of N1, C4-bis aryl aniline (**113c**) *via* a cascade C–C and C–N bond formation (Scheme 113).[151] The proposed mechanism involved the HIR mediated oxidation of *N*-phenylacetamides **113b** to the nitrenium ion **113d** which was stabilized by charge delocalization to the carbenium ion **113e**, and a subsequent double nucleophilic arylation on both C and N centred ion afforded the desired product **113c**.

Again, they developed an *in situ* generated hypervalent iodine catalysed intermolecular oxidative process for the

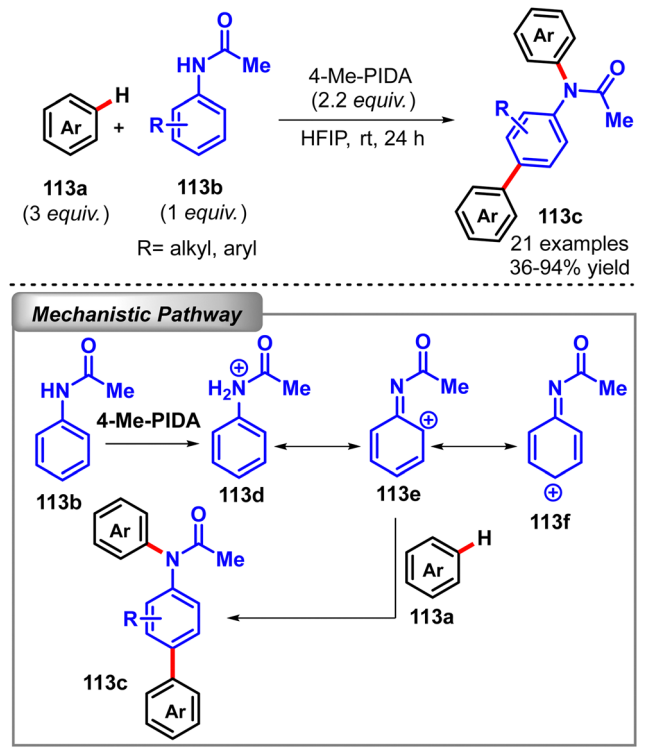

Scheme 113 HIR-mediated intermolecular direct oxidative functionalisation of anilides (Samanta *et al.*[151]).

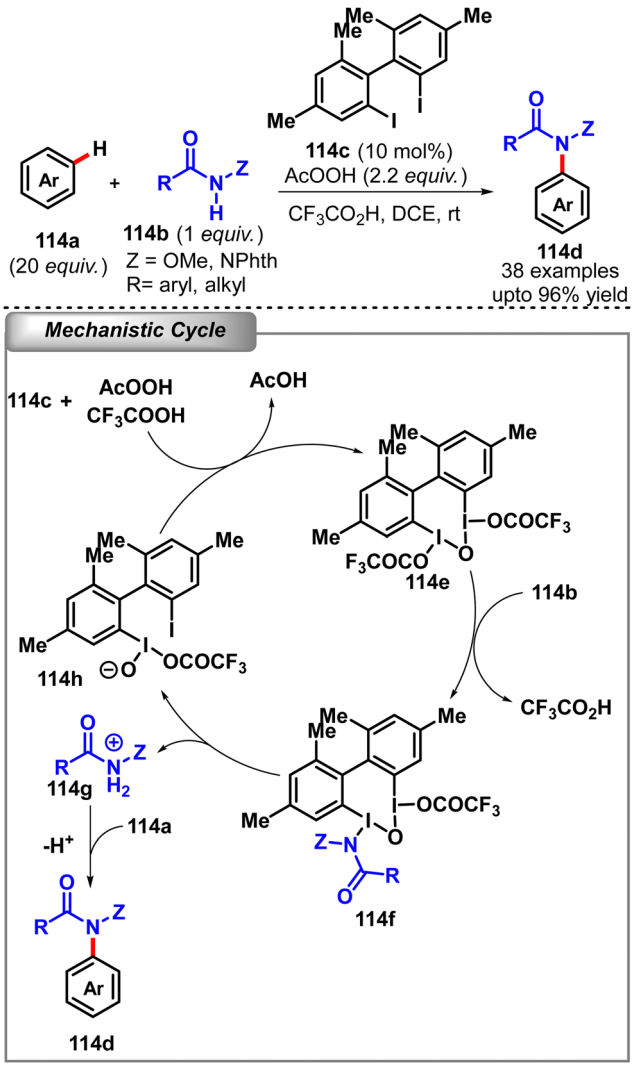

Scheme 114 HIR-catalysed intermolecular direct oxidative amination and hydrazination of non-prefunctionalized arenes (Samanta *et al.*[152]).

amination and hydrazination of non-prefunctionalized arenes **114a** (Scheme 114).[152] For this transformation, they had used 4,4′,6,6′-tetramethyl 2,2′-diiodo biphenyl **114c** as a catalyst (10 mol%), peracetic acid as an oxidant (2.2 equiv.), and TFA as an additive (5 equiv.) in DCE. A tentative mechanism was suggested involving the initial formation of μ-oxo-bridged active hypervalent iodine(III) **114e** by the interaction between aryl iodide and peracetic acid followed by the formation of nitrenium ion **114g** from the corresponding amine or hydrazine **114b** through the **114f** intermediate. Then the arene **114a** attacked the electron-deficient nitrenium ion to provide the desired products **114d**.

In 2015, the Antonchick group again established a PIDA mediated oxidative intermolecular amination of nonfunctionalized electron rich arenes **115a** with the amino derivatives of different heterocycles such as pyridines, pyrimidine, isoquinoline, and benzothiazole **115b** for the synthesis of disubstituted amine **115c** in HFIP solvent (Scheme 115).[153] The reaction also proceeded through usual formation of the nitrenium ion followed by the nucleophilic attack of arene.

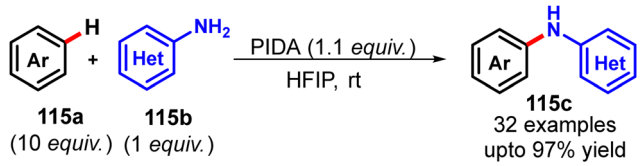

Scheme 115 PIDA mediated oxidative intermolecular amination of non-functionalized electron rich arenes (Manna *et al.*[153]).

In the same year, Zhang and Li reported a $PhI(OPiv)_2$ mediated intermolecular oxidative C–H amination of 8-acylaminoquinolines **116a** with *N*-fluorobenzenesulfonimide (NFSI) for the synthesis of C5-aminated quinolines **116b** (Scheme 116A).[154] A tentative mechanism was suggested with the generation of a radical cation intermediate **116c** by the interaction of 8-acylaminoquinolines **116a** with $PhI(OPiv)_2$ through the SET pathway. At the same time a nitrogen radical **116d** was also generated from NFSI with the iodine radical which was immediately coupled with the cation radical at the *p*-position and a subsequent deprotonation furnished the desired product **116b**. Later, Xu and Zhu also developed

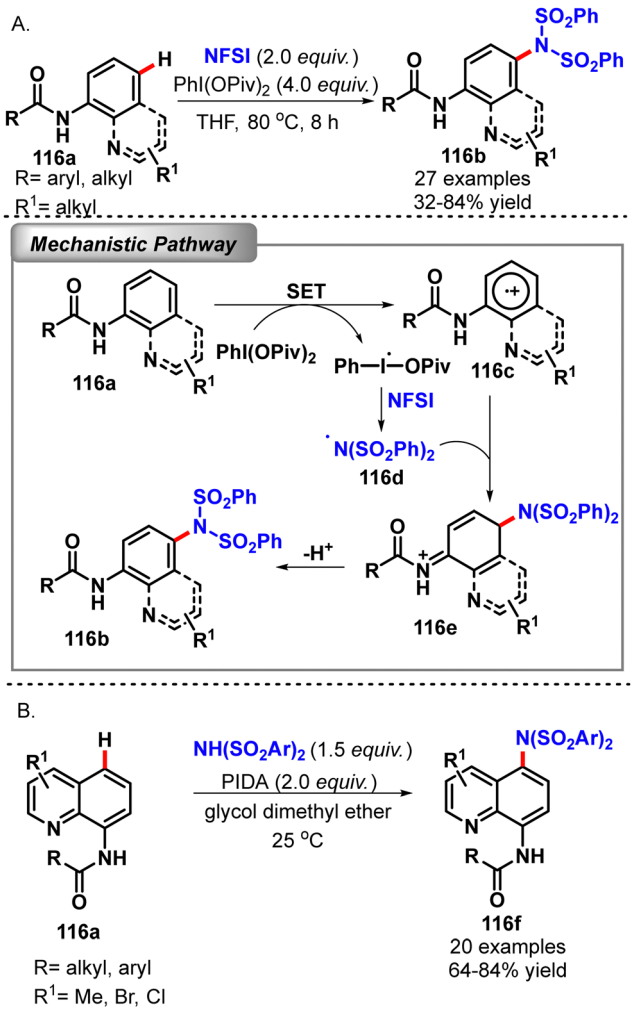

Scheme 116 $PhI(OPiv)_2$ mediated intermolecular oxidative C–H amination of 8-acylaminoquinolines (Wang *et al.*,[154] Ji *et al.*[155]).

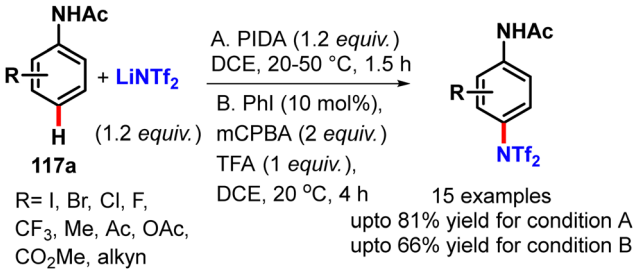

Scheme 117 Intermolecular direct *p*-selective C–H imidation of acetanilides (Pialat *et al.*[156]).

a PIDA mediated intermolecular oxidative remote C–H bond amidation at the C5 position of diversely substituted 8-aminoquinoline scaffolds with dibenzenesulfonimides in glycol dimethyl ether solvent (Scheme 116B).[155]

In 2015, Taillefer and his team also developed a mild, direct, nucleophilic imidation of a wide range of acetanilide derivatives **117a** by employing either a stoichiometric amount of PIDA or a catalytic amount of iodobenzene along with *m*CPBA as an oxidant (Scheme 117).[156] In this transformation, they exploited $LiNTf_2$ as a nucleophilic nitrogen source which exhibited exclusive *p*-selectivity and an excellent tolerance for a variety of functional groups at both ortho and meta positions.

Later in 2017, Sun and his team reported a PIFA-mediated intermolecular C–N bond formation between diversely substituted quinolines **118a** and a secondary amine, mainly saccharin, to afford 2-aminoquinolines **118c** *via* a nitrogen centered radical process (Scheme 118).[157] Apart from quinolines, other nitrogen heterocycles such as isoquinoline, quinoxaline, quinazoline, pyridine and pyrrole were also tested which produced the respective 2-aminoheteroarenes in good yield. The reaction seemed to follow a catalytic cycle involving nitrogen-centred radical species.

Contemporarily the Hajra group also demonstrated a PIDA-mediated direct oxidative C–H amination between imidazopyridines **119a** and secondary alicyclic amines **119b** to synthesise 3-amino substituted imidazopyridines **119c** in 1,4-dioxane at ambient temperature (Scheme 119A).[158] Experimental outcomes suggested the radical pathway for the transformation. Again in 2018, they developed a PIDA-mediated regioselective imidation of imidazoheterocycles **119a** using commercially available NFSI as an imidating agent in toluene solvent (Scheme 119B).[159]

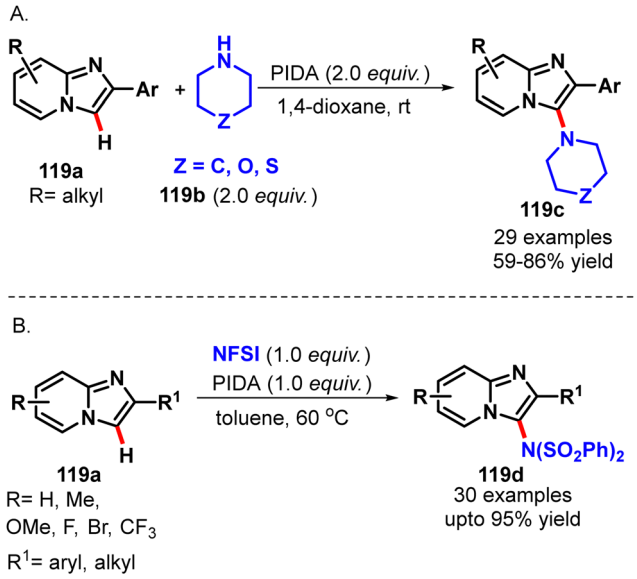

Scheme 119 PIDA-mediated direct oxidative C–H amination of imidazopyridines (Mondal *et al.*,[158] Singsardar *et al.*[159]).

Other heterocycles such as imidazo[2,1-*b*]thiazole, benzo[*d*]-imidazo[2,1-b]thiazoles, *N*-substituted indole and indolizine derivatives also underwent smooth regioselective imidation under optimised reaction conditions. The transformation probably proceeded with PIDA-mediated oxidation of imidazopyridine to the respective radical cation through the SET pathway.

Recently, Wu and co-workers also disclosed a PIDA mediated direct intermolecular oxidative C–N bond coupling of unactivated imidazo[1,2-*a*]pyridines with NH-sulfoximines for the synthesis of a large variety of C-3 sulfoximidoyl-functionalized imidazo[1,2-a]-pyridines in DMSO solvent (Scheme 120).[160] Notably, the electron-withdrawing groups on the benzene ring of imidazo[1,2-*a*]pyridines exhibited better yield than the corresponding electron-donating groups. Several control experiments suggested a radical pathway for the transformation.

Back in 1991, Kita *et al.* first reported a PIFA mediated intermolecular oxidative azidation of aromatic molecules using $TMSN_3$ as a nucleophile in HFIP solvent (Scheme 121).[161] While the aromatic hydrocarbons bearing high electron donating

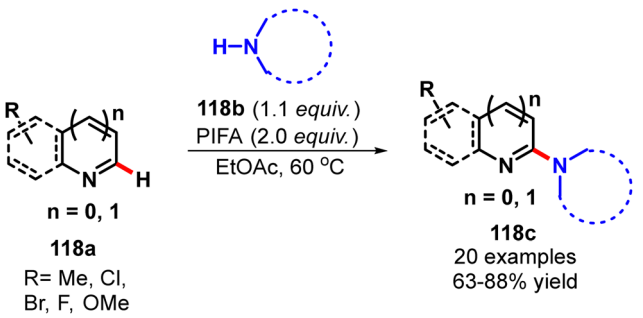

Scheme 118 PIFA-mediated intermolecular C–N bond formation between substituted quinolines and secondary amines (Zhao *et al.*[157]).

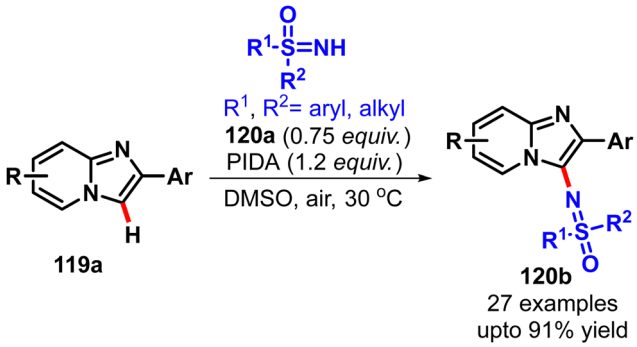

Scheme 120 PIDA mediated direct intermolecular oxidative C–N bond coupling of unactivated imidazo[1,2-*a*]pyridines (Luan *et al.*[160]).

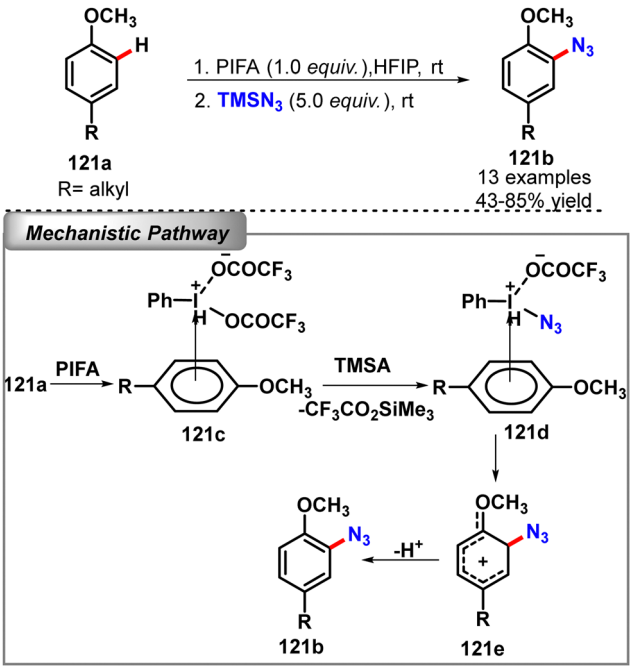

Scheme 121 PIFA mediated intermolecular oxidative azidation of aromatic molecules (Kita *et al.*[161]).

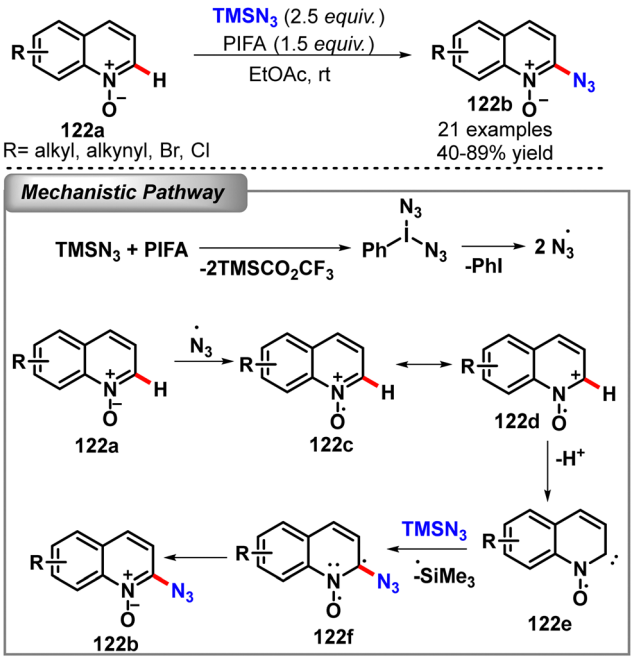

Scheme 122 PIFA mediated oxidative C2–H azidation of quinoline *N*-oxides with $TMSN_3$ (Li *et al.*[162]).

groups reacted smoothly with PIFA, electron deficient groups could not provide the azido compounds under the same conditions. A probable mechanism was suggested involving the formation of π-complex **121c** of PIFA with the arene moiety. The ligand exchange of PIFA with azide generated another π-complex **121d** intermediate which was finally transformed into a σ-complex **121e** with the reductive elimination of iodobenzene and a subsequent rearomatization by deprotonation finally furnished the aromatic azide **121b**.

Recently in 2015, the Li group reported a PIFA mediated oxidative C2–H azidation of quinoline *N*-oxides with $TMSN_3$ *via* the polarity reversal strategy (Scheme 122).[162] Through EPR studies the authors suggested a mechanism which was initiated with the double ligand exchange between PIFA and $TMSN_3$ to afford $PhI(N_3)_2$, which further generated the azide radical by thermal homolysis. Now this azide radical could help the quinoline *N*-oxide **122a** to undergo SET oxidation to generate the radical cation **122c** or **122d**, which could transform into the carbene-stabilized N–O radical **122e** by deprotonation. The immediate single electron transfer (SET) from carbene to $TMSN_3$ finally afforded the product **122b** with the removal of the TMS radical, which was witnessed by the EPR trapping.

4.2.4 Intermolecular direct C(sp^3)–N bond formation. In 2009, Fan *et al.* described an intermolecular benzylic amidation of alkyl arene with sulfonamides by combining PIDA with molecular iodine under the solvent-free condition (Scheme 123).[163] A tentative mechanism was suggested according to which the PIDA/I_2-mediated amidation reaction proceeded with the generation of a sulfonamidyl radical.

In 2011, the Qu group developed a similar PIDA and trace amount of molecular iodine combination for the synthesis of

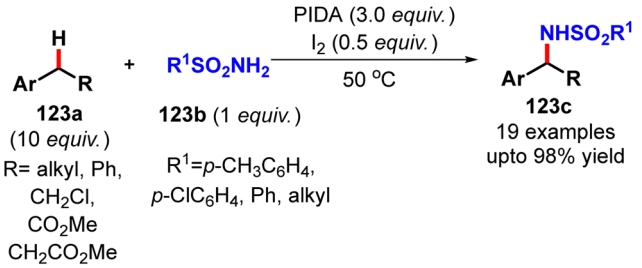

Scheme 123 HIR-mediated intermolecular benzylic amidation of alkyl arene with sulfonamides (Fan *et al.*[163]).

N-9 alkylated purine nucleoside analogues by the intermolecular CDC between the sp^3 N–H of purine bases and the sp^3 C–H of a series of ethers (Scheme 124).[164] To gain better results with diverse ethers the reaction was further irradiated with a 200 W tungsten filament lamp.

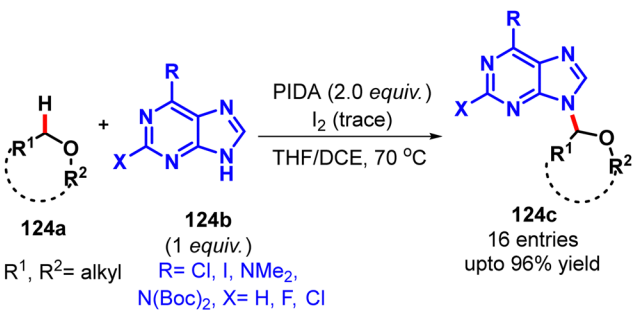

Scheme 124 HIR-mediated synthesis of N-9 alkylated purine nucleoside analogues (Guo *et al.*[164]).

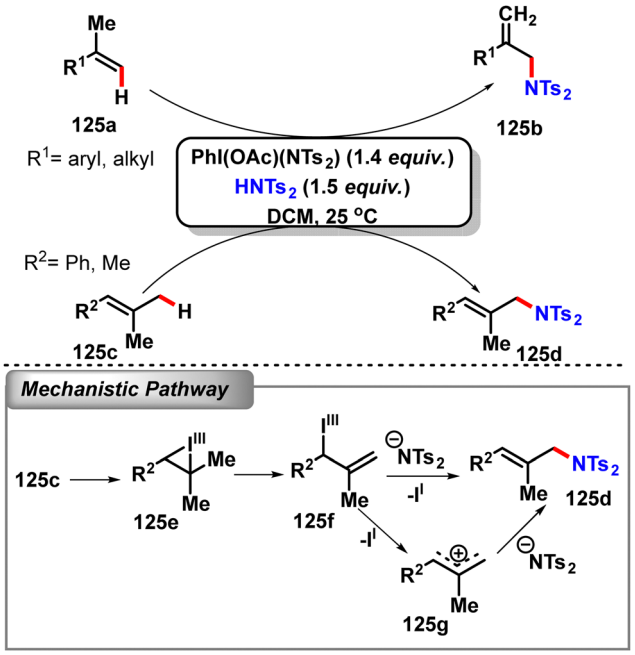

Scheme 125 HIR-mediated intermolecular allylic amination of α-methyl styrene derivatives (Souto *et al.*[165]).

In 2012, the Muniz group developed a PhI(OAc)(NTs_2)-mediated direct intermolecular allylic amination of α-methyl styrene derivatives by using bistosylimide as a nitrogen source (Scheme 125).[165] A plausible mechanism was suggested namely the formation of an iodo(III)cyclopropane **125e** from the styrene derivative **125c** followed by regioselective opening at the less hindered terminal methylene position. A subsequent elimination of the electrophilic iodine(III) by the deprotonation of the primary methyl group afforded the desired product. Furthermore, a strong KIE (5.0) also corroborated the C–H bond cleavage as the rate determining step.

In 2014, Buslov and Hu demonstrated a Ph_2IPF_6-mediated direct intermolecular C–H bond amination of cyclic and acyclic alkyl ethers **126a** with a wide range of alkyl or aryl substituted sulfonamides, amides, imide, and secondary amines **126b** (Scheme 126).[166] 1 equiv. of NaH base was essentially required for the transformation. A significant value of KIE (4.6) suggested the involvement of the α-C–H bond cleavage of the ether as the rate determining step.

Recently in 2018, Li and co-workers developed a $PhI(OCOPh)_2$ mediated remote oxidative benzylic C–H amination of 4-methylanilides **127a** with NFSI in 2-Me THF solvent (Scheme 127).[167]

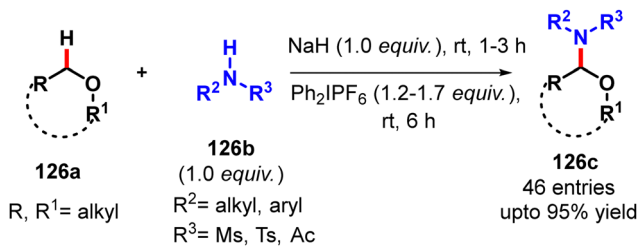

Scheme 126 HIR-mediated intermolecular C–H bond amination of cyclic and acyclic alkyl ethers (Buslov *et al.*[166]).

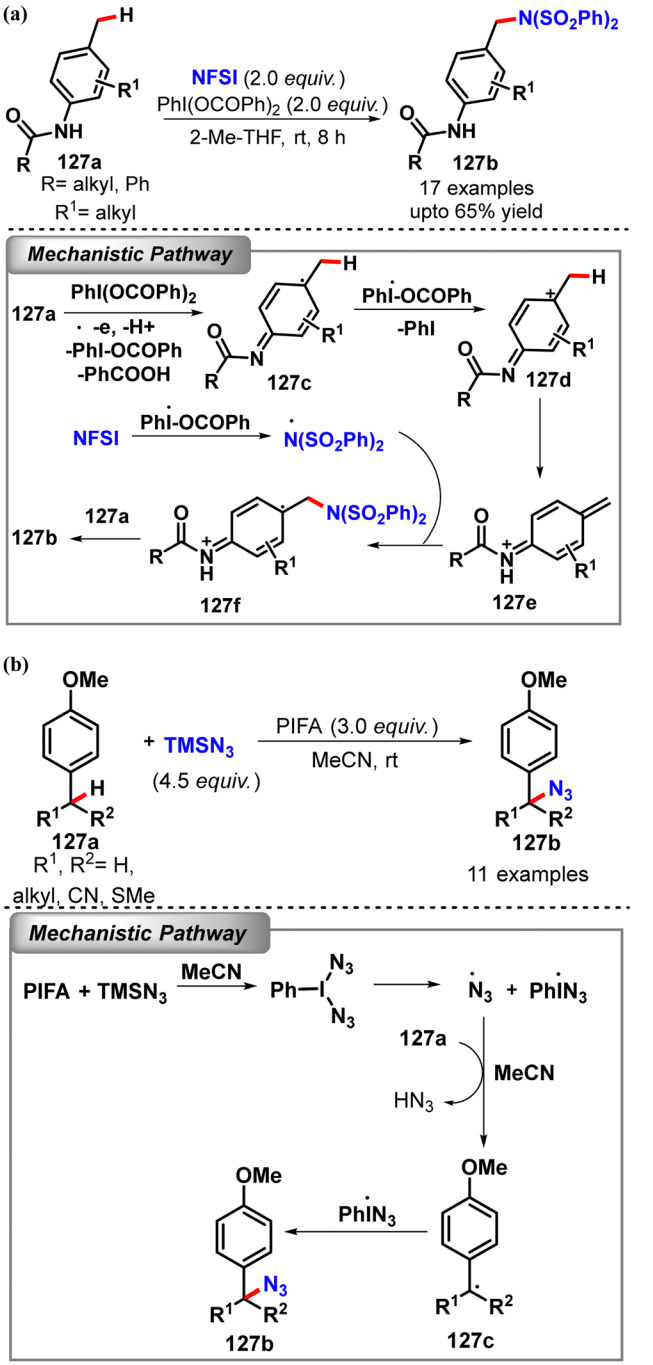

Scheme 127 (a) HIR-mediated remote oxidative benzylic C–H amination of 4-ethylanilides (Yang *et al.*[167]). (b) PIFA mediated direct alkylic azidation at the benzylic position (Kita *et al.*[168]).

For multiple substitution on the arene unit, only *p*-C(sp^3)–H amination occurred, and no amination was observed at the ortho or meta-methyl group of the anilides. A plausible mechanism for this remote oxidative benzylic C–H amination was proposed involving the initial oxidation of 4-methylanilide **127a** by the HIR to generate a radical intermediate **127c**. A single electron transfer of this radical intermediate generated the cation **127d** which might isomerize to a dienamine intermediate

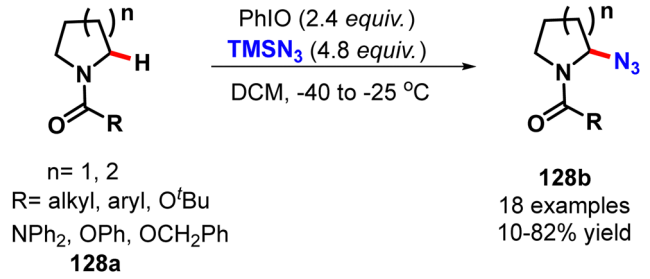

Scheme 128 PIFA mediated α-azidation of amides (Magnus *et al.*[169]).

127e. Simultaneously, NFSI was converted to a nitrogen radical which promptly reacted with the dienamine intermediate **127e** and a subsequent reduction furnished the product **127b**.

In 1994, the Kita group first reported a PIFA mediated direct alkylic azidation at the benzylic position of *p*-alkyl anisole using $TMSN_3$ as the azide source in MeCN solvent (Scheme 128).[168] The mechanism suggested the initial generation of $PhI(N_3)_2$ as the new HIR by the interaction of PIFA and $TMSN_3$ in MeCN solvent which was not sufficiently strong to form the CT-complex of the arene unit. Rather $PhI(N_3)_2$ dissociated into azide and iodine centred radicals. This azide radical abstracted the benzylic proton to form a benzyl radical and the subsequent interaction with the $PhIN_3$ radical afforded the alkylic azide.

Contemporarily, Magnus *et al.* developed a direct α-azidation procedure for amides, carbamates and ureas with hypervalent iodine(III) reagent PhIO in the presence of $TMSN_3$ as the azide source (Scheme 128).[169]

Later in 1998, the Kita group also developed an iodosylbenzene (PhIO)-mediated α-azidation of cyclic sulfides **129a** in the presence of $TMSN_3$ in MeCN solvent (Scheme 129).[170] A tentative mechanism was suggested wherein a nucleophilic attack of sulfide on PhIO in the presence of $TMSN_3$ provided an

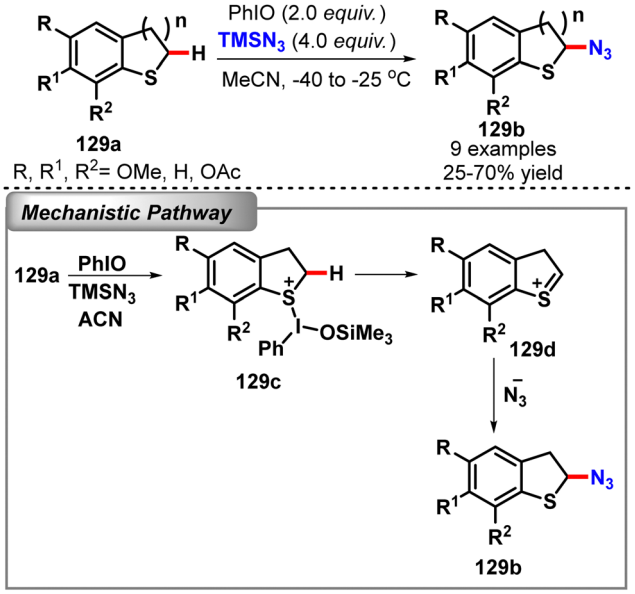

Scheme 129 PhIO-mediated α-azidation of cyclic sulfides (Tohma *et al.*[170]).

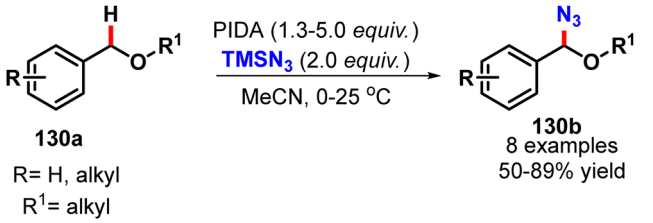

Scheme 130 PIDA-promoted C(sp^3)–H azidation of ethers at the benzylic position (Pedersen *et al.*[171]).

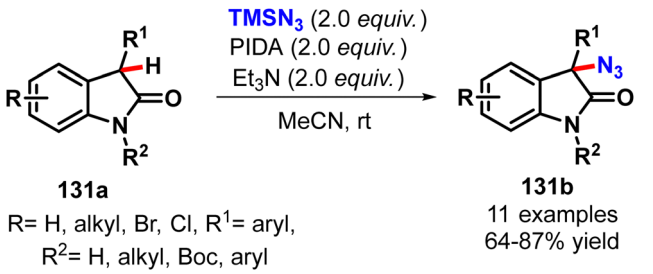

Scheme 131 PIDA-promoted C(sp^3)–H azidation of 2-oxindoles (Chen *et al.*[172]).

iodosulfonium cation **129c** which was deprotonated to give sulfonium cation intermediate **129d**, and a successive azide anion attack on the α-position afforded the product **129b**.

Later in 2005, Bols and co-workers also reported a PIDA-promoted C(sp^3)–H azidation of ethers **130a** at the benzylic position using $TMSN_3$ as an azide source in acetonitrile solvent (Scheme 130). The reaction also followed the usual radical pathway.[171]

Recently in 2018, Wei and his team designed a PIDA mediated direct C(sp^3)–H azidation of 2-oxindoles **131a** with the azide reagents at room temperature (Scheme 131).[172] $TMSN_3$ was found to be the best azide source and Et_3N the best additive for maximum yields.

4.3 C–O bond formation

4.3.1 Intramolecular direct C(sp^2)–O bond formation. In 2004, the Kita group developed a PIFA-mediated intramolecular oxidative nucleophilic substitution reaction of electron-rich aryl alkyl alcohols for the synthesis of chroman derivatives (Scheme 132).[173] The addition of montmorillonite K10 (MK10) as a solid acid additive afforded the maximum yield. The reaction proceeded *via* the formation of spiro-dienone-type intermediate **132e** through the radical cation **132d** generation followed by the migration reaction of the spiroether in the presence of MK10 in HFIP to provide the C-migrated chroman derivatives **132b**.

In 2010, Gu and Xue reported a PIFA and $BF_3{\cdot}OEt_2$-mediated direct intramolecular oxidative cyclization of electron-neutral or electron-deficient 3-arylpropionic acids **133a** for the efficient synthesis of 3,4-dihydrocoumarins **133b** in good yield at 30 °C (Scheme 133).[174]

In 2013, Du and Zhao also constructed functionalized coumarins by PIDA/I_2-mediated and irradiation-promoted

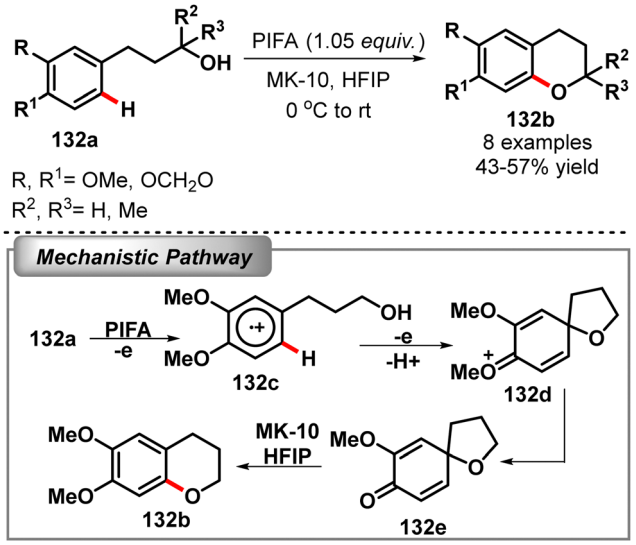

Scheme 132 PIFA-mediated intramolecular oxidative nucleophilic substitution reaction of electron-rich aryl alkyl alcohols (Hamamoto *et al.*[173]).

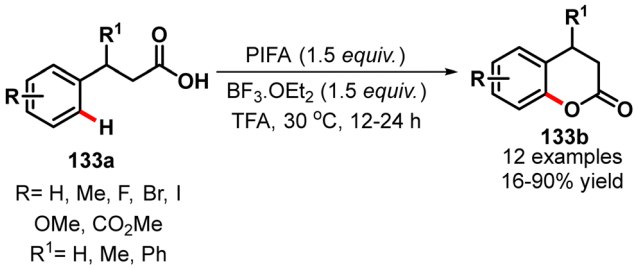

Scheme 133 PIFA-mediated intramolecular oxidative cyclization of 3-arylpropionic acids (Gu *et al.*[174]).

(200 W tungsten lamp) intramolecular oxidative coupling of phenylacrylic acid between the sp^2-carbon of the phenyl ring and the oxygen atom of the pendant carboxylic acid moiety (Scheme 134).[175] Notably, the presence of any electron-withdrawing substituent on the phenyl ring disfavoured the reaction. A plausible mechanism was suggested, namely, the initial formation of hypoiodite **134d** by the interaction of phenyl acrylic acid **134a** with PIDA followed by concurrent release of PhI. Next, photolytic cleavage of hypoiodite generated the oxygen centred radical **134e** which immediately cyclized with the adjacent phenyl ring to form aryl radical **134f**. A PIDA promoted subsequent SET oxidation converted this radical to cation intermediate **134g**. Finally, the proton abstraction from this cation intermediate afforded the product **134b**.

In 2014, Martin and co-workers reported a hypervalent iodine catalysed intramolecular C(sp^2)–O bond formation of 2-aryl benzoic acid derivatives **135a** for the efficient synthesis of benzolactones **135c** (Scheme 135).[176] It was found that 20 mol% of 4-Me iodobenzene **135b** along with 2.2 equiv. of peracetic acid as an external oxidant in HFIP was the most suitable condition for this transformation.

Lupton and Hutt presented an *in situ* generated hypervalent iodine catalysed intramolecular oxidative cyclisation of

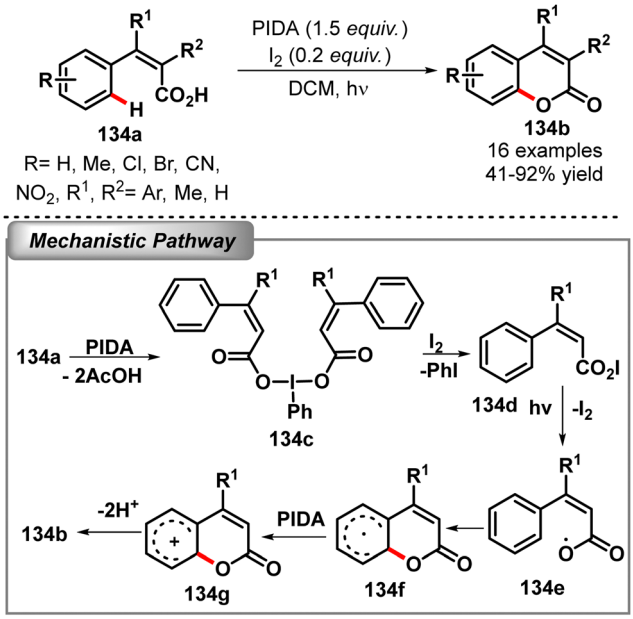

Scheme 134 HIR-mediated intramolecular oxidative coupling of phenylacrylic acid for the synthesis of coumarin derivatives (Li *et al.*[175]).

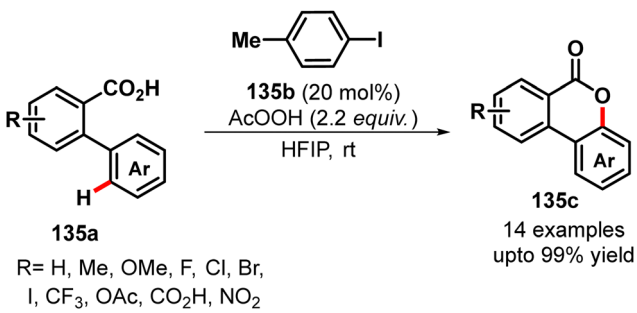

Scheme 135 HIR-catalysed intramolecular C(sp^2)–O bond formation of 2-aryl benzoic acid derivatives (Wang *et al.*[176]).

vinylogous esters bearing the *m*-methoxy benzyl group **136a** for the synthesis of benzopyran containing heterocycles **136b** (Scheme 136).[177] The reaction required 20 mol% of PhI and 1.5 equiv. of *m*CPBA as an external oxidant to allow the benzopyrans to be accessed in good yields. Interestingly, the

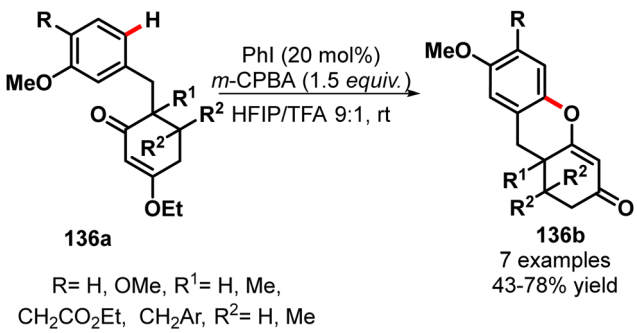

Scheme 136 HIR-catalysed intramolecular oxidative cyclisation of vinylogous esters (Ngatimin *et al.*[177]).

presence of the *p*-methoxy benzyl group afforded the spirofuran derivatives instead of benzopyran. However, with a substrate containing both *m*- and *p*-dimethoxy benzyl groups, a preferential synthesis of benzopyran was observed.

Benzofuran scaffolds, a unique structural motif possessing interesting pharmacological and cytotoxic properties, are frequently found in numerous naturally occurring bio-active molecules. In 2012, the Wirth group described the synthesis of 2-arylbenzofurans and 2-arylnaphthofurans **137b** by a PIDA-promoted intramolecular oxidative cyclization of ortho-hydroxystilbenes **137a** in MeCN (Scheme 137).[178] A tentative mechanism was proposed which involved the formation of a three-membered iodonium intermediate **137c** by the interaction of stilbene and PIDA. This iodonium intermediate underwent intramolecular cyclization with the phenolic oxygen atom, and a subsequent elimination of the hypervalent iodine provided the title compound **137b**.

In 2012, Yu and his team achieved a PIFA mediated intramolecular oxidative C–O coupling of *N*-(4-alkoxy-phenyl) and *N*-(4-acetamido-phenyl) benzamides **143a** for the synthesis of benzoxazoles **138b** (Scheme 138).[179] This reaction required additional 2 equiv. of TMSOTf as a Lewis acid in MeCN under dilute conditions (0.01 M) for the maximum yield of the desired benzoxazoles. However, the drawback of the method was that only electron-rich 4-alkoxy-substituted substrates along with the strong nucleophilicity of the amide oxygen were necessary for this transformation. The authors suggested that the reaction might follow either a cationic or a radical pathway.

In 2012, Zhao and Du reported a PIDA-mediated intramolecular cyclization of enamides for the synthesis of various functionalized oxazoles **139b** through the C–O bond formation (Scheme 139).[180] This reaction required 2.0 equiv. of $BF_3{\cdot}OEt_2$ as an additive for the maximum yield. A possible mechanistic pathway suggested the formation of iodo-intermediate **139d** by

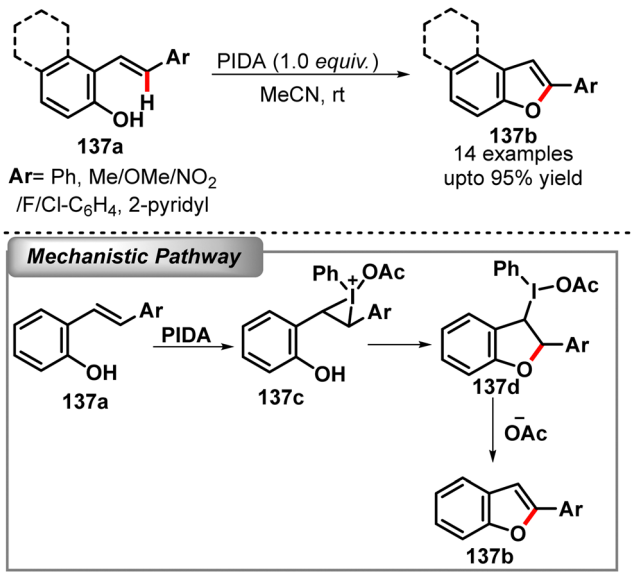

Scheme 137 PIDA-promoted intramolecular oxidative cyclization of *ortho*-hydroxystilbenes for the synthesis of benzofuran derivatives (Singh *et al.*[178]).

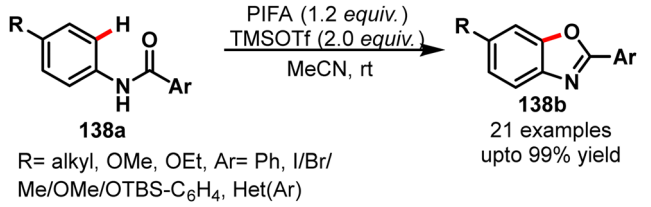

Scheme 138 PIFA mediated intramolecular oxidative C–O coupling for the synthesis of benzoxazole derivatives (Yu *et al.*[179]).

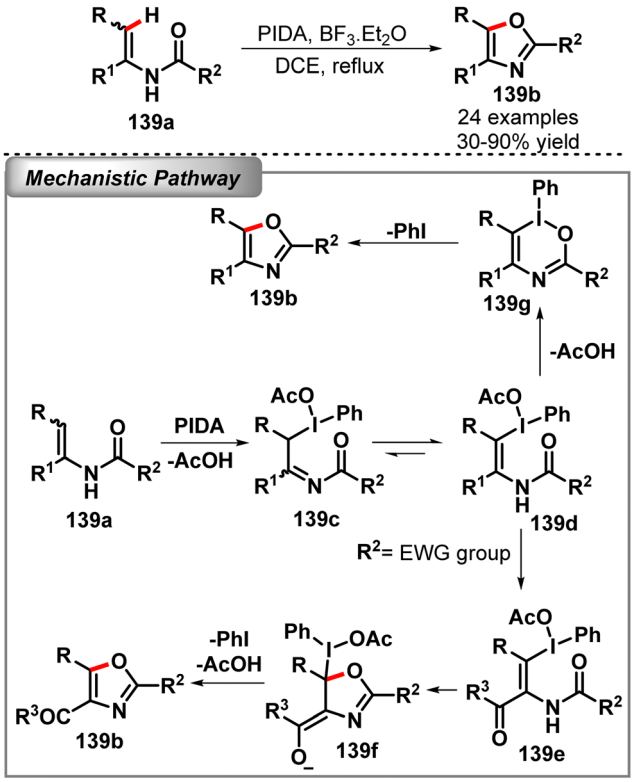

Scheme 139 PIDA-mediated intramolecular cyclization of enamides for the synthesis of functionalized oxazoles (Zheng *et al.*[180]).

the interaction of enamide **139a** with PIDA followed by imine-enamine isomerization. If the substituent *R*2 represents an electron-withdrawing group, a five-membered oxazole product was formed by the nucleophilic attack of the carbonyl oxygen atom on the sp^2 carbon bonded to the hypervalent iodine atom followed by subsequent reductive elimination of PhI and AcOH. Alternatively, if R^2 represents a non-electron withdrawing group such as –Me or –H, intermediate **139d** might experience an intramolecular cyclization by the attack of the carbonyl oxygen atom on the iodine centre followed by the reductive elimination of PhI through bond migration to furnish the title oxazole compound **139b**.

In 2016, Radha Krishna *et al.* accomplished the synthesis of unexpected oxazolines **140c** and oxazines **140d** by the PIDA-mediated intramolecular cyclization of *N*-allylamides **140a** and *N*-alkenylamides **140b** respectively (Scheme 140).[181] This reaction required 10 equiv. of HF.py as an additive for maximum

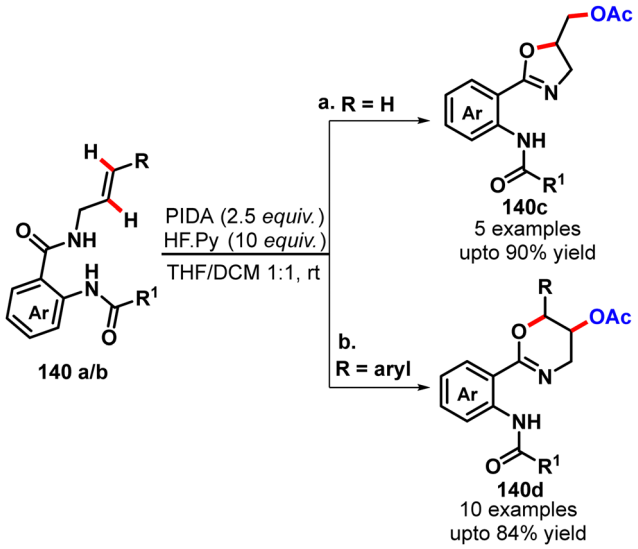

Scheme 140 PIDA-mediated intramolecular cyclization of *N*-allylamides for the synthesis of oxazolines and oxazines (Ranjith *et al.*[181]).

yield; however, no fluorinated product was obtained. The reaction mechanism was suggested to be the usual formation of a cyclic iodonium ion by the interaction of PIDA and allylamides with the influence of HF·py. The amide oxygen attacked this cyclic iodonium ion in either an *exo*- or *endo*-fashion. The *exo*-fashion attack led to the formation of five membered oxazolines, whereas the *endo*-fashion attack provided the oxazine derivatives.

Recently in 2019, the Jiang group investigated a bench stable fluorobenziodoxole (**141b**)-mediated intramolecular cyclization of *N*-acetyl enamines **141a** for the efficient synthesis of a wide range of oxazoles **141c** (Scheme 141).[182] With 10 mol% of $BF_3{\cdot}OEt_2$ as an additive and 4 Å molecular sieves they achieved the maximum yield of the oxazoles in acetonitrile solvent. A tentative mechanism was suggested wherein the initial activation of the fluoroiodane **141b** by a Lewis acid and a subsequent addition to the alkene afforded the intermediate **141d**. An intramolecular nucleophilic attack by the carbonyl oxygen atom on the carbon atom bearing the iodine formed a five-membered ring intermediate **141e** with the release of the iodine **141f** followed by deprotonation and elimination of HF to furnish the oxazole **141c**.

At the same time, Ding *et al*. also developed a similar type of PIDA-mediated intramolecular cyclization with the migration of an aryl group for the synthesis of 2,5-disubstituted oxazoles **142b** from allylic amides **142a** (Scheme 142).[183] This reaction was optimised with the use of 10 mol% of $BF_3{\cdot}OEt_2$ as an additive in THF with a variety of well tolerated functional groups.

4.3.2 Intramolecular direct C(sp^3)–O bond formation. In 2009, Fan *et al.* investigated the PIDA/TBAI-mediated intramolecular oxidative cyclization of *o*-acyl phenols for the convenient synthesis of α-acetoxy benzofuranones (Scheme 143).[184] The success of the reaction was very much dependent on the use of TBAI and NaOAc; as the tetrabutylammonium cation is crucial to the reaction and the latter actually quenched the generated acid by-product. A tentative mechanism was suggested which involved an initial formation of HIR, $PhI_2(OAc)$ and Bu_4NOAc

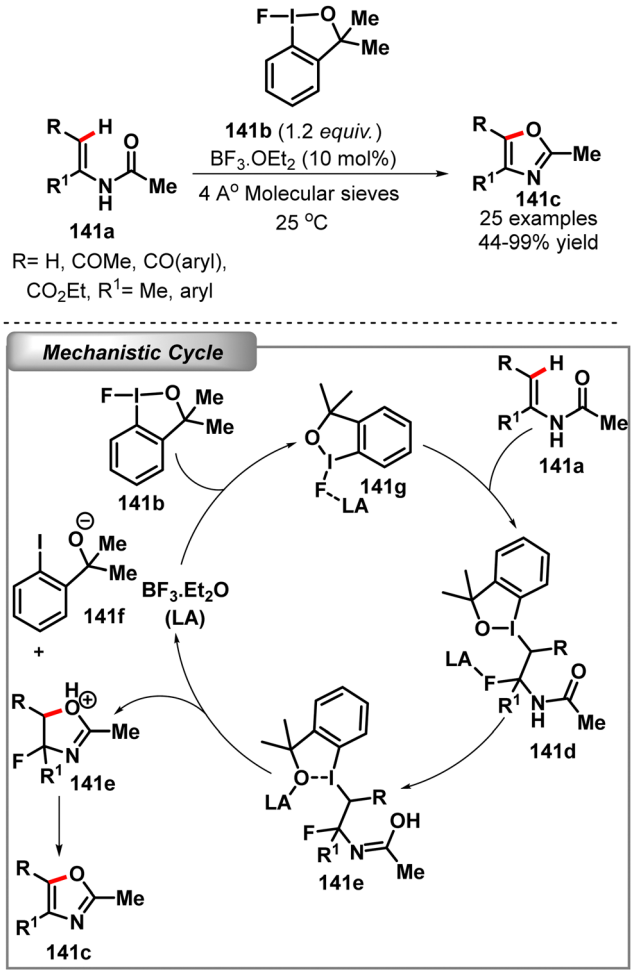

Scheme 141 HIR-mediated intramolecular cyclization of *N*-acetyl enamines for the synthesis of oxazoles (Xu *et al.*[182]).

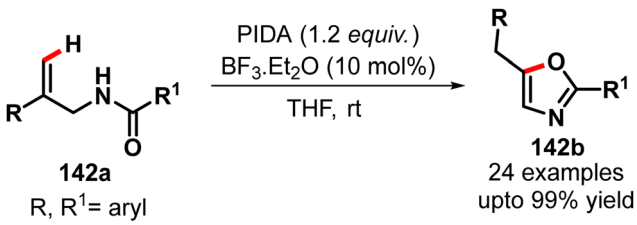

Scheme 142 PIDA-mediated intramolecular cyclization for the synthesis of oxazoles from allylic amides (Xu *et al.*[183]).

by the reaction between PIDA and TBAI. This Bu_4NOAc acted as a base to generate the enolate anion of *o*-propionylphenol which immediately interacted with the newly generated HIR and underwent a ligand exchange to form the acetoxylated intermediate. This intermediate again reacted with another equivalent of $PhI_2(OAc)$ in the presence of Bu_4NOAc and a subsequent intramolecular nucleophilic displacement by the oxygen finally afforded the title product. During the reaction, HI and AcOH were generated as by-products and the additive NaOAc quenched these acids.

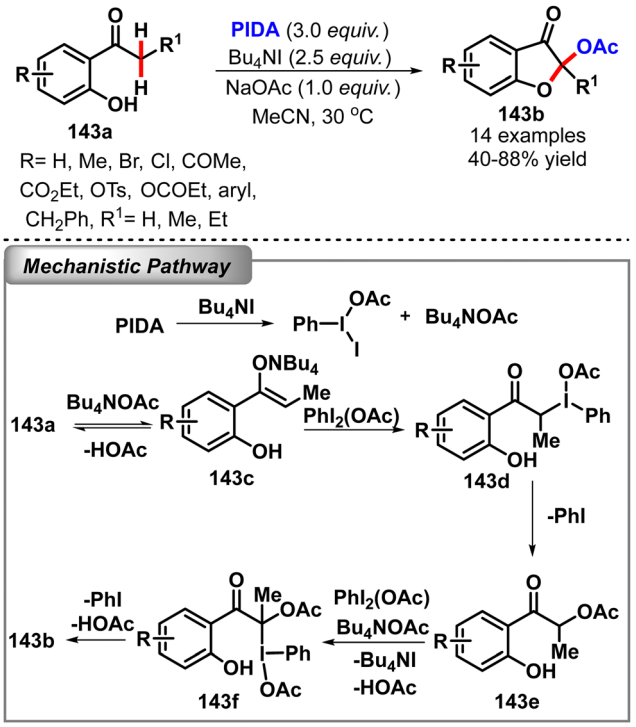

Scheme 143 PIDA-mediated intramolecular oxidative cyclization of *o*-acyl phenols for the convenient synthesis of α-acetoxy benzofuranones (Fan *et al.*[184]).

In 2016, Du and co-workers reported chiral aryliodine-mediated cascade C–O and C–C bond formations of alkyl 3-oxo-pentanedioate monoamide derivatives for the enantioselective organocatalytic oxidative spirocyclization leading to the formation of diverse spirofurooxindoles with high enantioselectivity (Scheme 144).[185] The reaction proceeded *via* oxidative C–O bond formation followed by oxidative C–C bond formation, with the latter being the enantioselectivity-determining step.

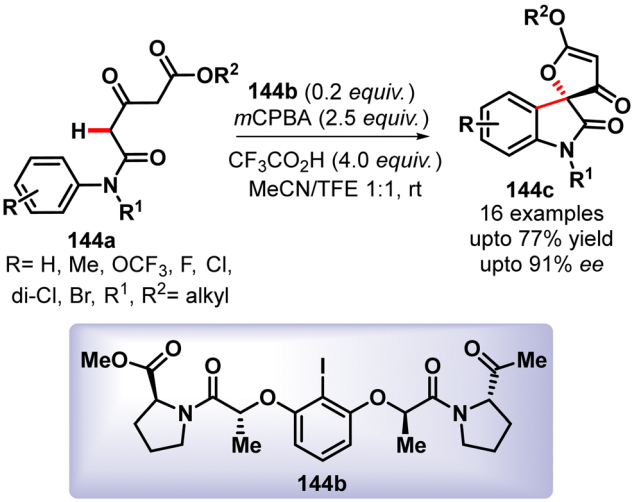

Scheme 144 Chiral aryliodine-mediated cascade C–O and C–C bond formations of alkyl 3-oxopentanedioate monoamide derivatives (Cao *et al.*[185]).

In 2018, the same group developed a PIFA-mediated cascade intramolecular oxidative cyclisation of 3-(2-hydroxyphenyl)-*N*-methyl-3-oxo-*N*-phenylpropanamide and its derivatives for the synthesis of a unique class of spirofurooxindoles that involved the formation of a C(sp^3)–O bond prior to that of the C(sp^3)–C(sp^2) bond (Scheme 145).[186] The plausible mechanism depicted the initial interaction of the tautomerized enol form **145c** with PIFA and a subsequent intramolecular cyclization by the phenolic oxygen atom to afford the benzofuranone **145e**. This benzofuranone again equilibrated into its enol form which reacted with another equivalent of PIFA. This intermediate **145g** then experienced an intramolecular electrophilic aromatic substitution reaction by the aniline ring, resulting in a new C–C

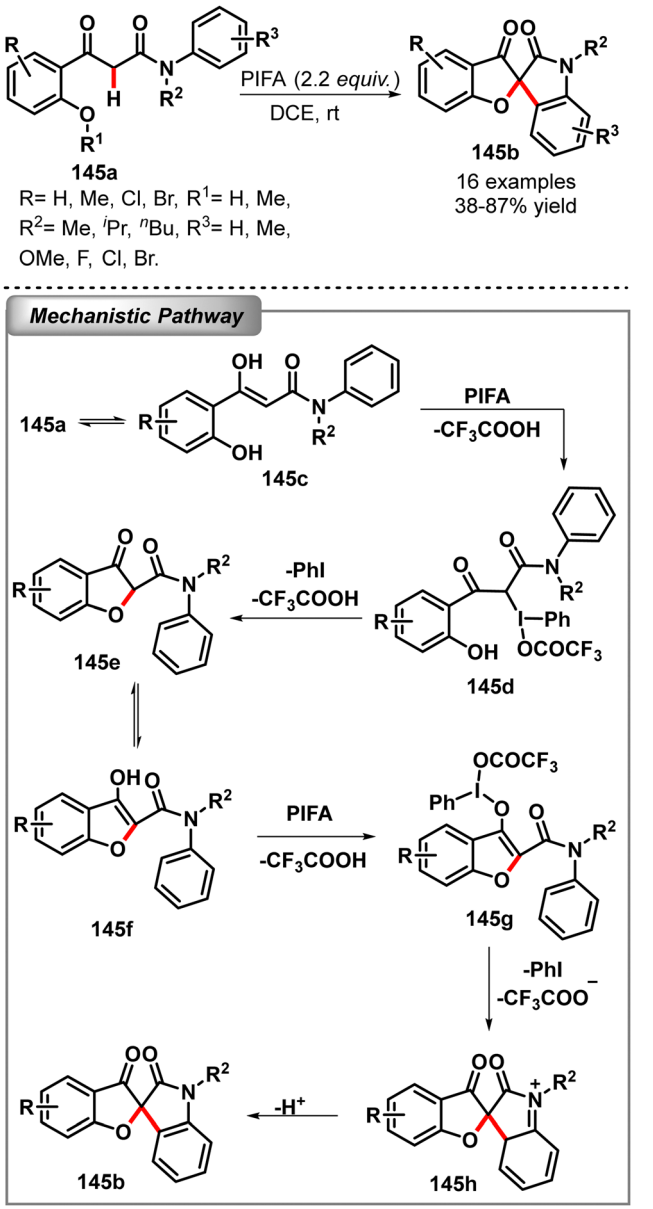

Scheme 145 PIFA mediated cascade intramolecular oxidative cyclisation of 3-(2-hydroxyphenyl)-*N*-methyl-3-oxo-*N*-phenylpropanamide (Sun *et al.*[186]).

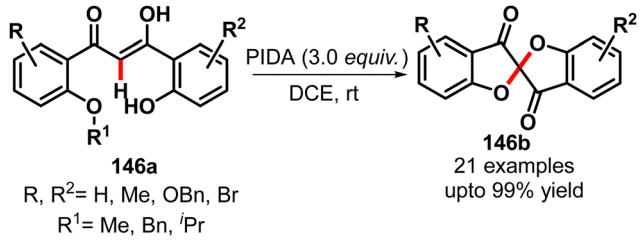

Scheme 146 PIDA-mediated intramolecular dual oxidative C–O bond formation for the synthesis of spiro-benzo[β]furan-3-one derivatives (Xing *et al.*[187]).

bond. Finally, with the removal of a proton, the title spirofurooxindole compound **145b** was obtained.

Recently in 2019, the same group reported a PIDA-mediated intramolecular dual oxidative C–O bond formation of protected 3-hydroxy-1,3-bis(2-hydroxyaryl)pro*p*-2-*en*-1-ones **146a** for the efficient synthesis of spiro-benzo[*b*]furan-3-one derivatives **146b** in good to excellent yield (Scheme 146).[187] A wide variety of substrates bearing either electron-donating groups or electron-withdrawing groups were well tolerated under this reaction condition.

In 2010, Dominguez *et al.* presented a PIFA-mediated intramolecular allylic oxycarbonylation reaction of 5-carbamoyl dihydropyrimidines **147a** for the synthesis of furo[3,4-*d*]pyrimidinone derivatives **147b** (Scheme 147).[188] A probable mechanism was suggested according to which the HIR-mediated formation of nitrenium intermediate **147c** from the amide followed by 1,5-hydride shift and a subsequent intramolecular nucleophilic attack of the amide group rendered compound **147e**. Aqueous hydrolysis of this intermediate **147e** afforded the title compound **147b**.

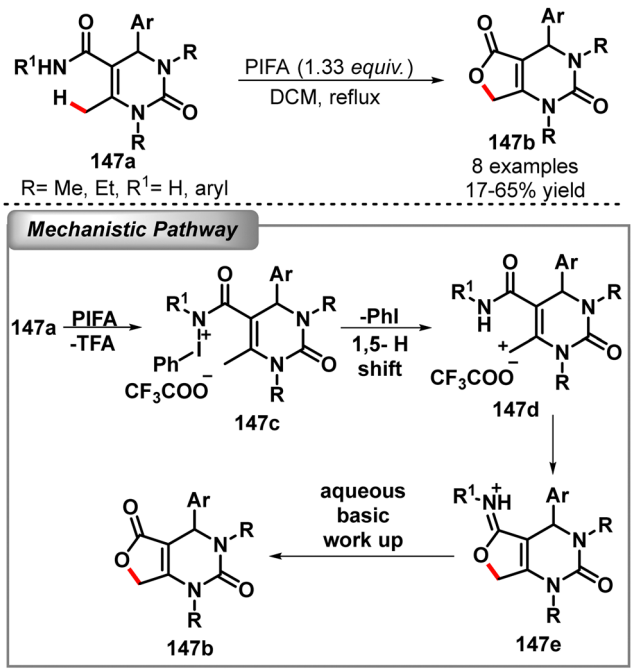

Scheme 147 PIFA-mediated intramolecular allylic oxycarbonylation reaction (Couto *et al.*[188]).

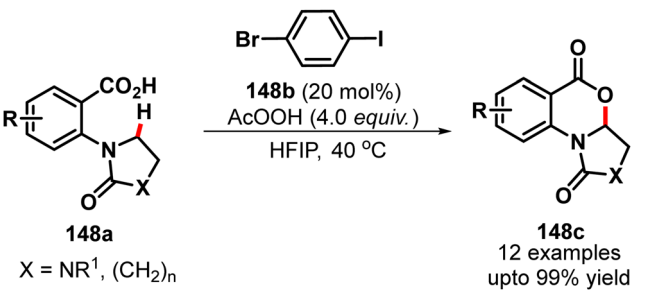

Scheme 148 HIR-catalysed intramolecular C(sp^3)–O bond formation of 2-(2-oxopyrrolidin-1-yl)benzoic acid derivatives (Wang *et al.*[189]).

In 2014, Martin and co-workers reported a hypervalent iodine catalysed intramolecular C(sp^3)–O bond formation of 2-(2-oxopyrrolidin-1-yl)benzoic acid derivatives for the efficient synthesis of 5H-pyrrolo[1,2-*a*] [3,1]benzoxazinones (Scheme 148).[189] It was found that 20 mol% of 4-Br iodobenzene **148b** along with 4.0 equiv. of peracetic acid as an external oxidant in HFIP was the most suitable condition for this transformation.

In 2014, Du and Zhao discovered a PIDA/NaN_3-mediated oxygenation of the C(sp^3)–H bond adjacent to the nitrogen of *N*,*N*-diaryl tertiary amine **149a** for the direct intramolecular C(sp^3)–O bond formation in good to excellent yield (Scheme 149).[190] Furthermore, it was found that the two diaryl substituents on the tertiary amine were very much crucial for this transformation. The mechanism suggested the *in situ* formation of $PhI(N_3)OAc$ by the interaction of PIDA and NaN_3 followed by direct nucleophilic

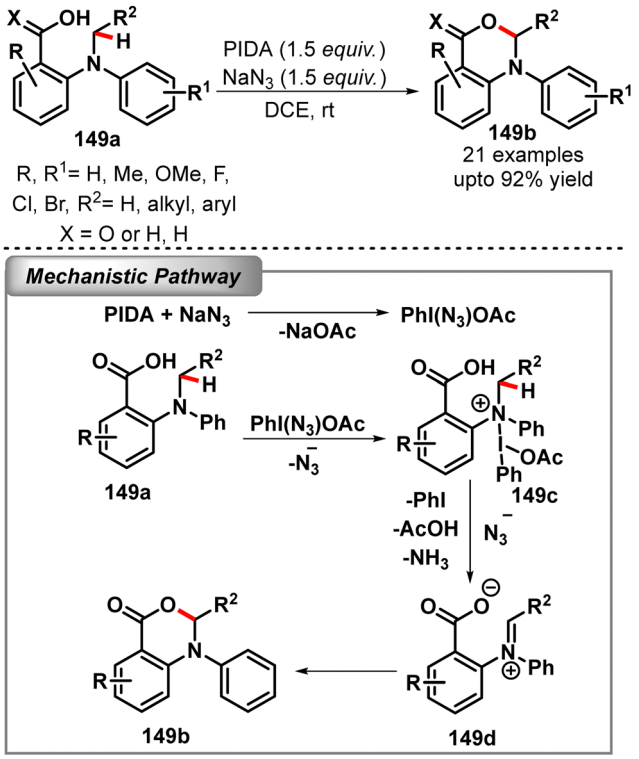

Scheme 149 HIR-mediated direct intramolecular C(sp^3)–O bond formation (Zhang *et al.*[190]).

attack of the N-center of tertiary amine on the iodine centre to generate the ammonium ion intermediate **149c**. This intermediate was converted into iminium salt **149d** by N_3 and a subsequent intramolecular nucleophilic cyclization by the carboxylic acid group furnished the final product **149b**.

4.3.3 Intermolecular direct C(sp^2)–O bond formation. In 2002, the Kikugawa group described the reaction of anilides with HIR. When the acyl group of the anilide was electron rich, the incorporation of the hydroxy group at the *p*-position of the anilide was observed in the presence of PIFA in TFA (Scheme 150A).[191] Not only anilides, but also benzannulated lactams experienced a similar hydroxylation. The trifluoroacetoxy group was transferred to the *p*-position of the anilide aromatic ring which was hydrolyzed during the workup procedure to furnish the corresponding phenol. The same concept was recently utilised by the Mal group where they used MeOD or TFE instead of TFA solvent to afford the C-alkoxylation reaction of anilides (Scheme 150B).[192] In 2011, Gu and co-workers also reported the PIFA/$BF_3{\cdot}OEt_2$-combination mediated *p*-acetoxylation and *p*-etherification of anilides by using AcOH and alcohols as the solvent respectively (Scheme 150C).[193] Later using $TsOH.3H_2O$ as an additive they also obtained the *p*-tosyloxylated products with high regioselectivity (Scheme 150D).[194]

In 2014, Pan *et al.* reported a PIDA mediated *p*-acetoxylation reaction of *N*-aryl-arylsulfonamides by the selective functionalisation of the *N*-aryl C(sp^2)–H bond (Scheme 151).[195] Interestingly, *p*-substituted sulfonamides afforded the selective mono-acetoxylation with *o*-selectivity. A plausible mechanism was suggested involving the formation of nitrenium cation intermediate **151d** by the interaction of arylsulfonamides **151a** and PIDA. Subsequently, this nitrenium cation underwent delocalization to form more stable cation **151e**, which readily reacted with AcOH to provide *p*-acetoxylated arylsulfonamides (**151b**). For the *p*-substituted arylsulfonamide, the charge delocalization of the nitrenium ion generated the cationic intermediate at the *o*-position which reacted with acetic acid to furnish *o*-acetoxylated arylsulfonamides.

Simultaneously Guo and co-workers investigated a PIDA-mediated 3 component reaction between aniline **152a**, a range of aldehydes **152b** and alcohol to produce *p*-alkoxyl-substituted *N*-arylimines **152c** (Scheme 152).[196] The preliminary control experiments revealed that the C=N double bond is essential for the reaction. The possible mechanism thus suggested the initial reaction between the PIDA and the C=N double bond of imine **152d** to generate a π-complex type intermediate **152e** which was oxidized to generate carbon cation intermediate **152f** at the *p*-position of the aryl imine and a subsequent nucleophilic attack of alcohol followed by deprotonation afforded the title compound **152c**.

In 2010, Huang *et al.* described a PIDA mediated acetoxylation of indole **153a** for the synthesis of 1H-indol-3-yl acetate **153b** in moderate to good yield in MeCN solvent (Scheme 153A).[197] The reaction required KOH as an additional base to quench the acid by-product. Unfortunately, *N*-protected indole could not exhibit the product formation. Later the Punji group also developed a PIDA-mediated regioselective C-3 acetoxylation of *N*-substituted indoles **153c** in the AcOH/Ac_2O (7 : 3) mixture (Scheme 153B).[198] This study suggested that a π-electron-deficient (hetero)arene substituent on the nitrogen atom of indole greatly enhanced the selectivity of the C3-acetoxylation reaction. The control experiments showed that the transformation proceeded through the formation of 2,3-diacetoxylated indoline as an active intermediate

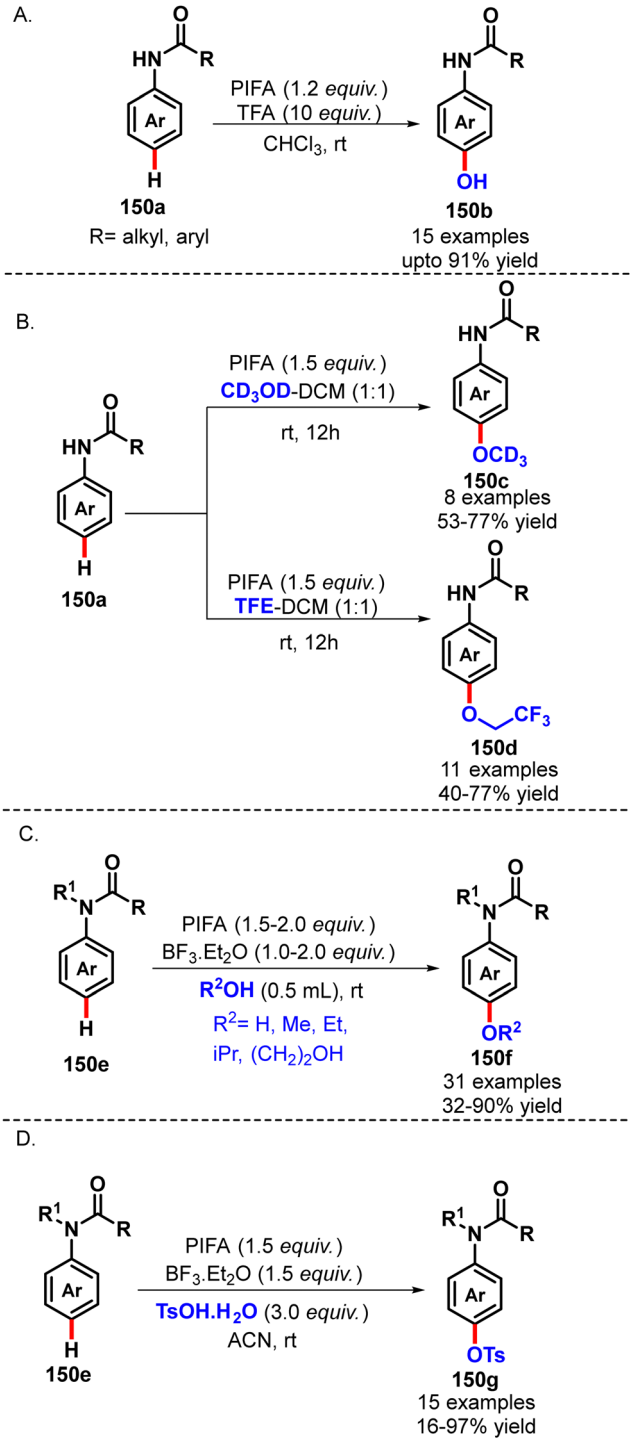

Scheme 150 HIR-mediated intermolecular C(sp^2)–O bond formation of anilides (Itoh *et al.*,[119] Maiti *et al.*,[192] Liu *et al.*[193,194]).

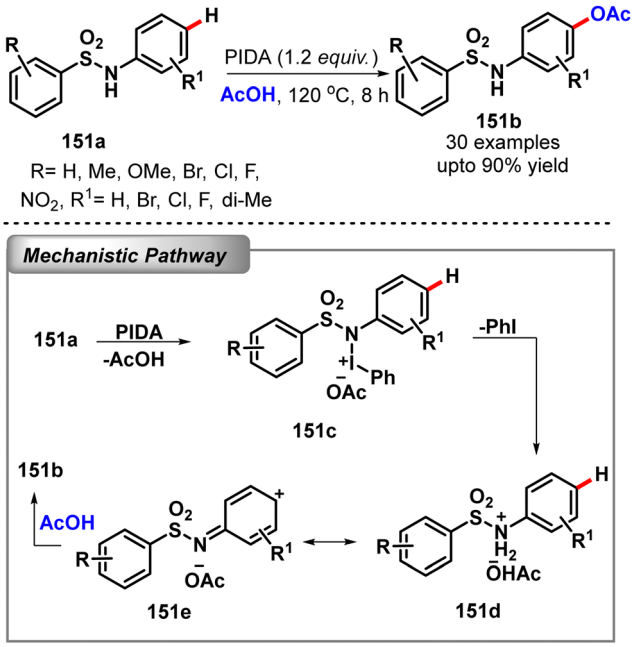

Scheme 151 PIDA-mediated *p*-acetoxylation of *N*-aryl-arylsulfonamides (Wang *et al.*[195]).

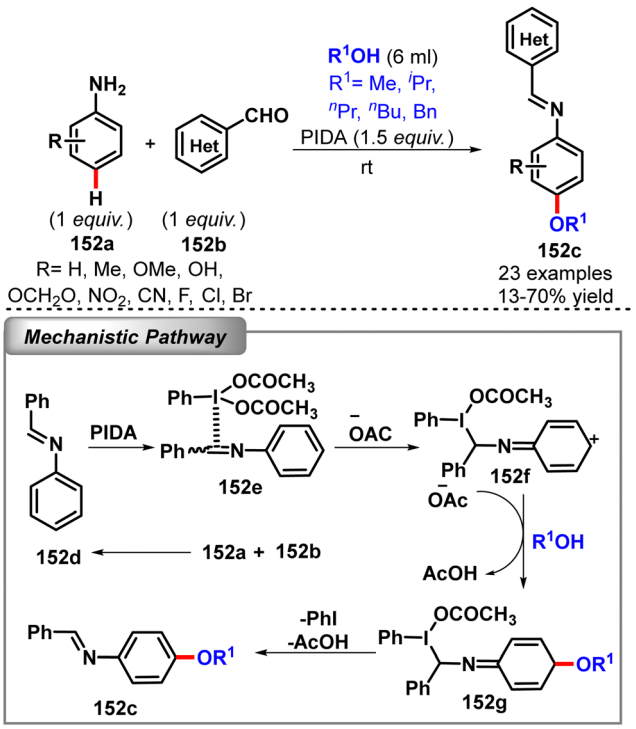

Scheme 152 PIDA-mediated *p*-alkoxylation of *N*-arylimines (Jiang *et al.*[196]).

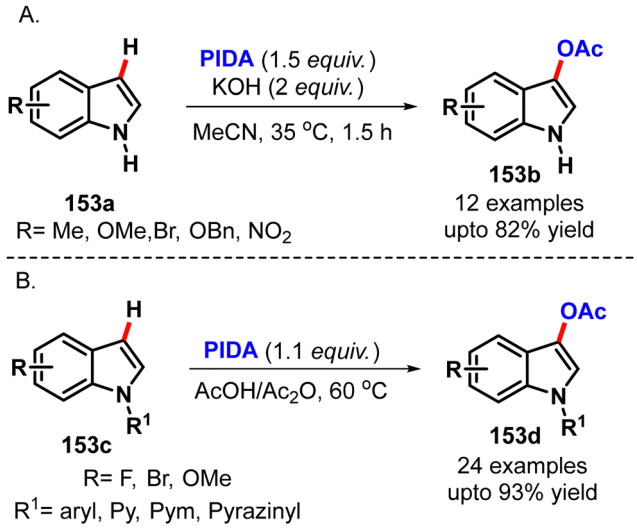

Scheme 153 PIDA-mediated C3-acetoxylation of indole (Liu *et al.*,[197] Soni *et al.*[198]).

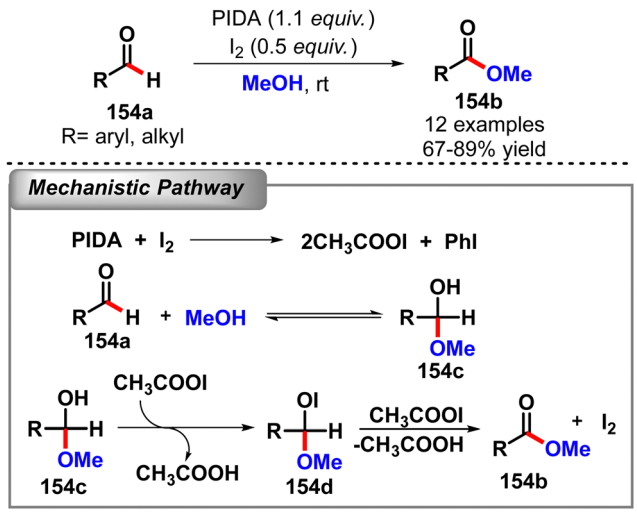

Scheme 154 PIDA/I_2-mediated direct oxidative esterification of aldehydes (Karade *et al.*[199]).

and the dehydroacetoxylation was facilitated in the presence of a π-deficient arene substituent on the *N*-atom of indoles.

In 2006, the Karade group first reported a PIDA/I_2-combination for the direct oxidative esterification of aldehydes **154a** in methanol solvent. Not only aromatic aldehydes, but also long chain aliphatic aldehydes also exhibited this methyl esterification in good yield (Scheme 154).[199] A tentative mechanism was suggested involving the initial formation of acetyl hypoiodite by the chemical oxidation of molecular iodine with PIDA. Next the *in situ* generated methyl hemiacetal **154c** from the aldehyde in MeOH solvent was oxidized by the acetyl hypoiodite to afford the corresponding hemiacetal hypoiodite **154d**. Another equivalent of acetyl hypoiodite then promoted the concomitant oxidation of hemiacetal hypoiodite to afford the methyl ester **154b**.

At the same time, Liang *et al.* also developed the PIDA-mediated transformation of primary alcohols and aldehydes to *N*-hydroxysuccinimide esters **155c** (Scheme 155).[200] Here the *N*-hydroxy succinimide (NHS) **155b** not only acted as an esterification agent but also as an activator of PIDA in this transformation. The plausible reaction mechanism also depicted an

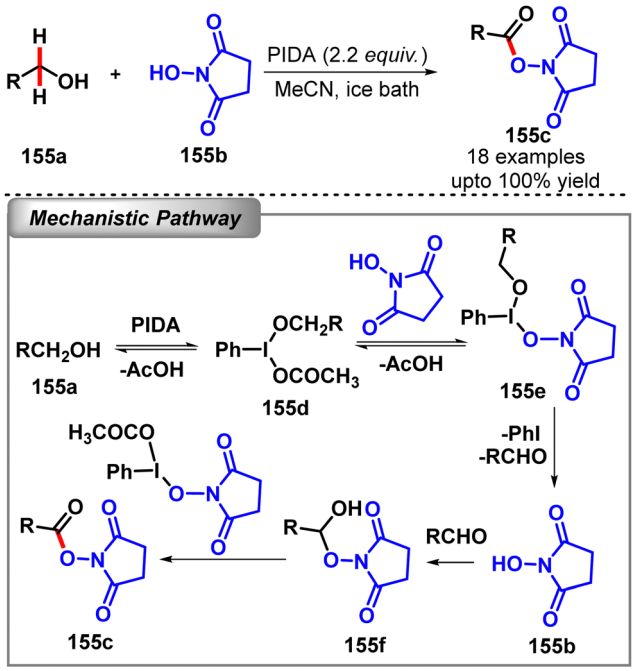

Scheme 155 PIDA-mediated transformation of primary alcohols to N-hydroxysuccinimide esters (Naiwei *et al.*[200]).

initial ligand exchange reaction between PIDA and primary alcohol **155a** and the primary alcohol was oxidised to the corresponding aldehyde in the presence of NHS. This aldehyde again reacted with NHS to form NHS-hemiacetal **155f** which was further oxidised in the presence of the active NHS-PIDA complex.

In 2011, Du and Zhao established a PIFA-mediated transformation of the β-monosubstituted enamines **156a** to a variety of 4,5-disubstituted 2-(trifluoromethyl)oxazoles **156b** *via* the oxidative β-trifluoroacetoxylation of the enamine followed by subsequent intramolecular cyclization (Scheme 156).[201] A proposed mechanistic pathway suggested the initial formation of β-iodo iminium salt **156c** by the interaction of β-monosubstituted enamines with PIFA. Next, the expelled trifluoroacetate anion attacked the C–I centre to generate β-trifluoroacyloxy iminium intermediate **156d**. The proton transfer from the iminium center to the carbonyl oxygen of the trifluoroacetate moiety followed by an intramolecular attack on the electron-positive carbonyl group by the amino group afforded the oxazole derivative **156b** with a subsequent elimination of water.

In 2012, they again developed a PhIO-promoted direct intermolecular oxidative C(sp^2)–O bond formation between enamines **157a** and various carboxylic acids to furnish a wide variety of β-acyloxy enamines **157b** (Scheme 157).[202] They utilised this method by converting β-acyloxy enamines into various oxazole compounds **157c** *via* intramolecular condensation in AcOH. A tentative mechanism was suggested involving the *in situ* generation of $PhI(OCOR)_2$ from the reaction of PhIO and carboxylic acid (RCO_2H) followed by subsequent β-acyloxylation of enamines as reported earlier.

Recently in 2018, the Loh group developed a PIDA mediated highly site-selective acyloxylation of stable enamines **158a** for

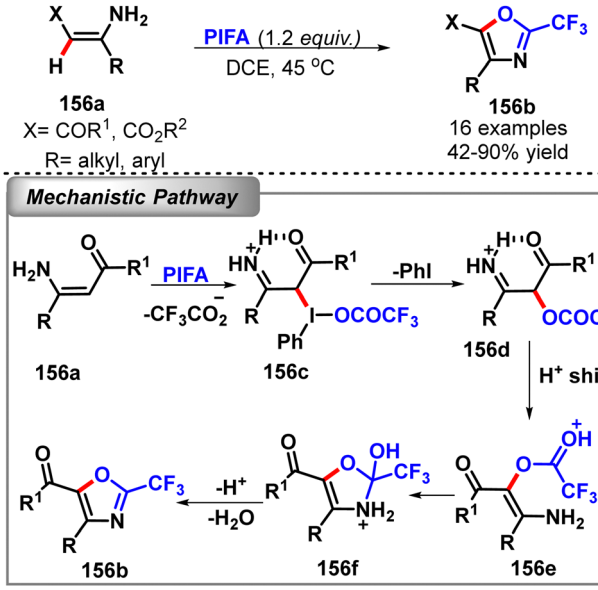

Scheme 156 PIFA-mediated transformation of the β-monosubstituted enamines to oxazoles (Zhao *et al.*[201]).

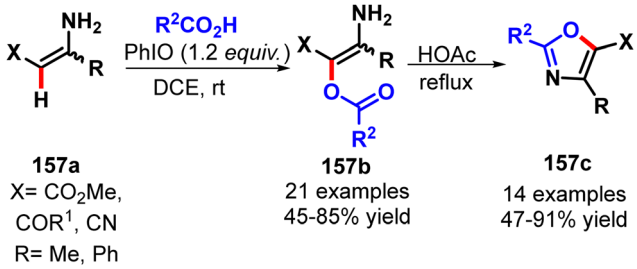

Scheme 157 PhIO-promoted direct intermolecular oxidative C(sp^2)–O bond formation of enamines (Liu *et al.*[202]).

the synthesis of (*E*)-vinyl acetate derivatives **158b** and **158c** (Scheme 158).[203] Interestingly, in TFE solvent, β-site-selective product **158b** was obtained using 1.3 equiv. of PIDA. However, α-site-selective product **158c** was also achieved in MeCN solvent with the use of 2.0 equiv. of PIDA and 2.0 equiv. of water. However, the α-site-selective product was rearranged to the amide compound under the reaction condition. The reaction mechanism suggested the usual formation of iodonium intermediate **158d** by the interaction of enaminone **158a** with PIDA. β-Acyloxylation product **158b** was explained by the nucleophilic attack of the –OAc anion at the β-site of the iminium intermediate with the release of iodobenzene followed by deprotonation. Alternatively, if –OAc attacked at the α-site of the iminium ion with a subsequent elimination of iodobenzene the α-acyloxy enamine intermediate **158c** was obtained. This intermediate underwent protonation and rearrangement to furnish the amide compound.

4.3.4 Intermolecular direct C(sp^3)–O bond formation. In 2009, Liang and co-workers studied the PIDA mediated direct α- and β-C(sp^3)–H *cis* diacetoxylation of piperidine adjacent to the nitrogen atom (Scheme 159).[204] The mechanism suggested

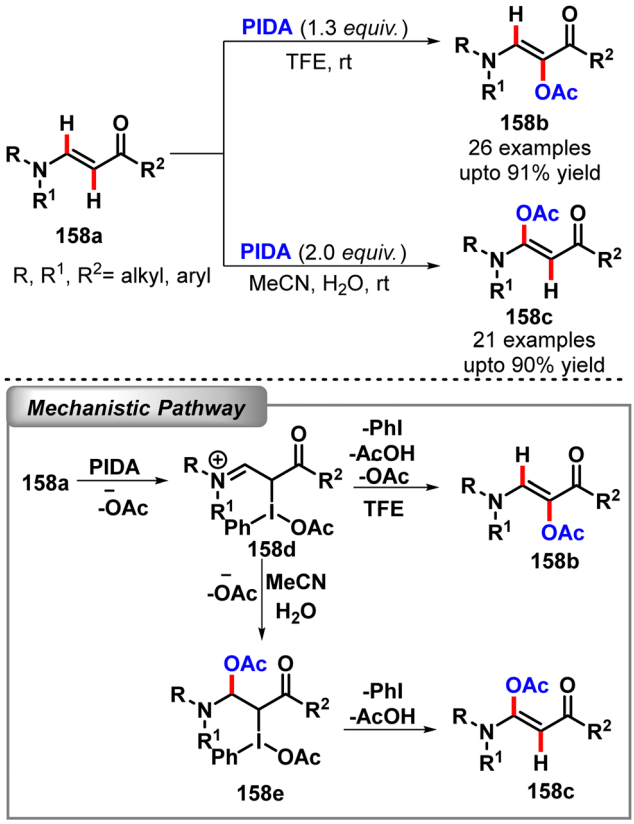

Scheme 158 PIDA mediated highly site-selective acyloxylation of stable enamines (Wang *et al.*[203]).

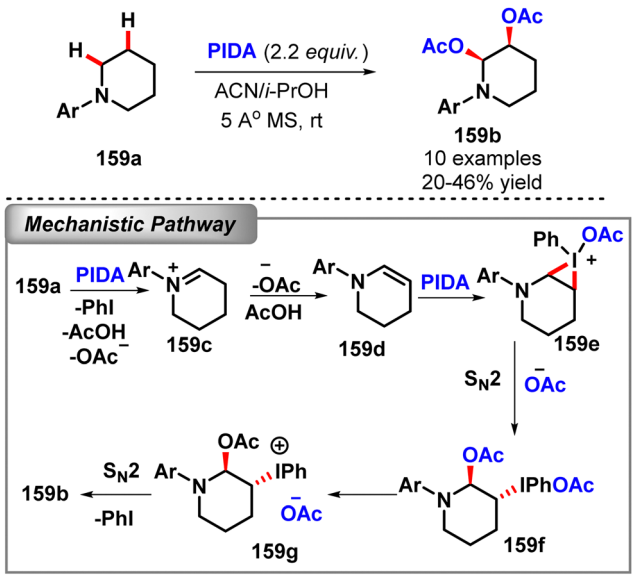

Scheme 159 PIDA mediated direct *cis* diacetoxylation of the piperidine derivative (Shu *et al.*[204]).

the formation of iminium ion **159c** by the reaction of piperidine derivative **159a** and PIDA. β-Hydrogen elimination afforded the enamine **159d**, which underwent an electrophilic addition of PIDA to form a three membered iodonium species. Acetate

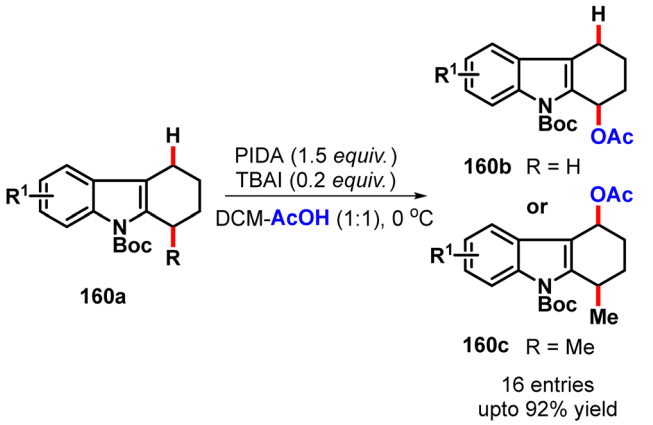

Scheme 160 PIDA-mediated regioselective acetoxylation of 2,3-disubstituted indoles (Zaimoku *et al.*[205]).

attack on this iodonium intermediate **159e** and a subsequent elimination of iodobenzene *via* S_N2 type nucleophilic substitution afforded the *cis*-2,3-diacetoxylated product **159b**.

Later Taniguchi and co-workers developed a PIDA/TBAI-mediated direct α-acetoxylation of 2,3-disubstituted indoles (Scheme 160).[205] In general, 2α-acetoxylation **160b** was achieved usually; however the regioselectivity was switched to 3α-position **160c** when 2α-position was blocked by another alkyl group. Moreover, the high KIE value of 5.7 clearly indicated that the rate of deprotonation at the α-position of indole was the rate determining step.

In 2016, the Su and Mo group performed a PIDA mediated β-acetoxylation of tertiary alcohol **161a** for the synthesis of β-acetoxy alcohols **161b** in good yield with excellent diastereoselectivity (Scheme 161).[206] This reaction afforded the best results in acetic acid solvent at 100–130 °C. The transformation was found to be good for diarylalkyl alcohol; however replacement of the aryl group by the alkyl group eventually decreased the yield and no transformation was observed for trialkyl alcohol. Furthermore, when there were two types of β-positions in the alcohol, the β-acetoxylation at the methyl group occurred more preferably than that at the methylene group. Not only linear alcohols, but also cyclic alcohols were verified for successful transformation.

In 2018, Studer *et al.* developed a PIDA mediated intermolecular acetoxyaminoalkylation of α-diazo amides **162a** with tertiary aryl amines **162b** in methanol solvent (Scheme 162).[207] A tentative mechanism was suggested according to which the three-component reaction started with the formation of iminium ion

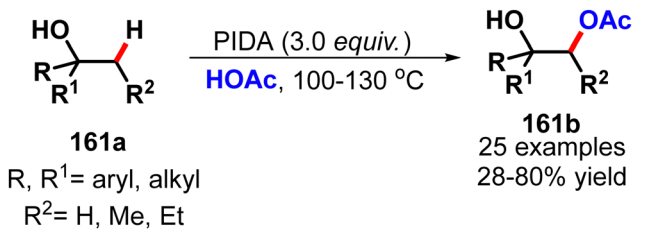

Scheme 161 PIDA-mediated β-acetoxylation of tertiary alcohols (Zhao *et al.*[206]).

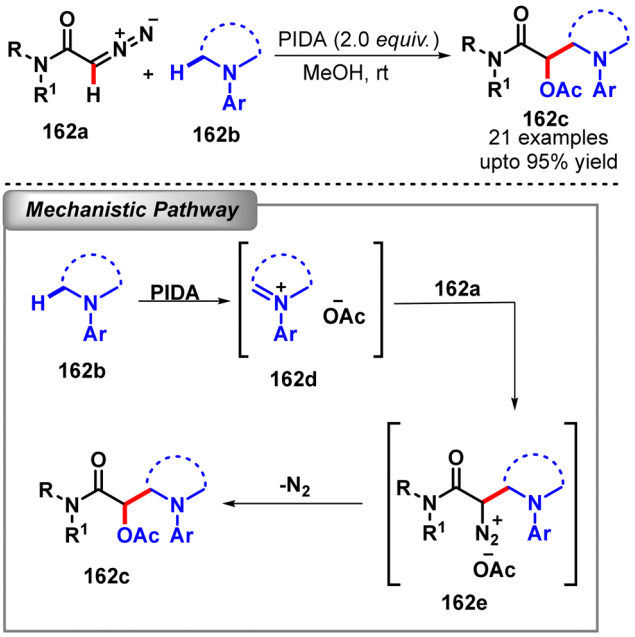

Scheme 162 PIDA mediated intermolecular acetoxyaminoalkylation of α-diazo amides (Doben *et al.*[207]).

162d by the PIDA mediated oxidation of the corresponding amine followed by its reaction with α-diazo compound **162a** and subsequent nucleophilic attack by the acetate anion to afford the title compound **162c** with the loss of nitrogen.

Very recently, the Wang group introduced a PIDA-mediated radical cyclization of *o*-(allyloxy)arylaldehydes **163a** and *N*-hydroxyphthalimide (NHPI) **163b** for the synthesis of substituted chroman-4-ones **163c** in DCM solvent by intermolecular C(sp^3)–O bond formation followed by intramolecular C–C bond formation (Scheme 163).[208] No isolation of the desired product in the presence of a radical scavenger recommended the radical mechanism for the reaction. The reaction mechanism thus suggested the formation of the PINO radical by the reaction of NHPI with PIDA. Then this PINO radical was added to the terminal side of the double bond of 2-(allyloxy)benzaldehyde **163a** and a subsequent radical cyclization with this newly generated radical with aldehyde afforded the O-centred radical **163e**. A hydrogen atom transfer (HAT) reaction of this O-centred radical then afforded the C-centred radical **169f** which underwent a SET oxidation by PIDA followed by deprotonation to afford the title product 163.

4.4 C-Halogen bond formation

4.4.1 Fluorination reaction. Fluorine chemistry has become a major multidisciplinary area of research. The refinement of drug pharmacodynamics and pharmacokinetics, as well as applications in agrochemical and materials science, has benefited greatly from the use of fluorinated molecules, which have their own unique chemical, physical, and biological properties.[209] The presence of at least one fluorine atom in the structure of 20% of the marketed drugs and even 30–40% of the agrochemicals validates the significant influence of fluorinated compounds.[210]

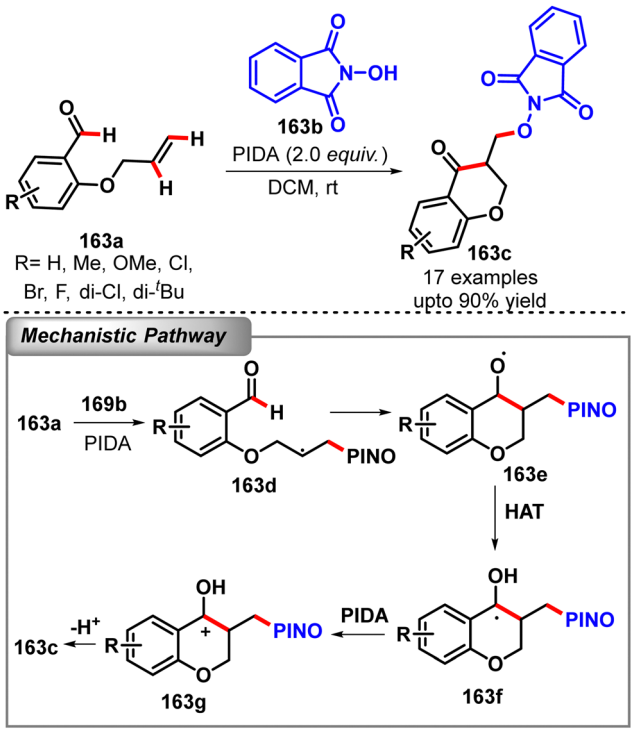

Scheme 163 PIDA-mediated radical cyclization of *o*-(allyloxy)arylaldehydes for the synthesis of substituted chroman-4-ones (Chen *et al.*[208]).

Moreover, the radioactive ^{18}F radionuclide dependent positron emission tomography (PET) widens the utility of the fluorinated compounds in the field of medicine and radiochemistry as well.[211] Herein, we intend to showcase the up to date studies on the hypervalentiodine(III)-mediated fluorination reactions. Moreover, fluorinated λ^3-iodanes have also been developed like difluoroiodoarene, Togni reagent or fluorobenziodoxole over the past few years.

4.4.1.1 Direct C(sp^2)–F bond formation. In 2011, the Miyamoto group first reported a hypervalent phenyl-λ^3-iodane-mediated *p*-selective aromatic fluorination of 3-phenylpropyl ethers **164a** for the synthesis of 3-(4-fluorophenyl)propyl ethers **164b** in good yields (Scheme 164).[212] They had used an activated iodosylbenzene monomer18-crown-6 complex [PhI(OH)BF_4.18C6] as the HIR in the

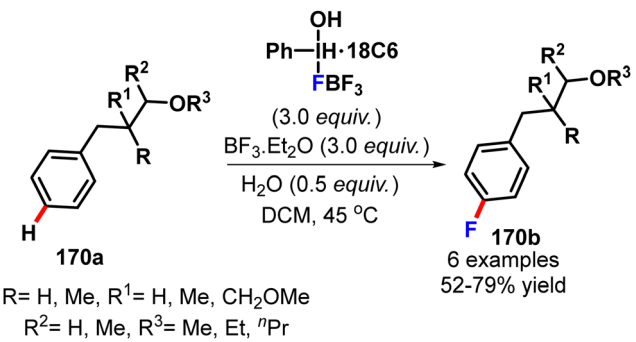

Scheme 164 HIR-mediated *p*-selective aromatic fluorination of 3-phenylpropyl ethers (Saito *et al.*[212]).

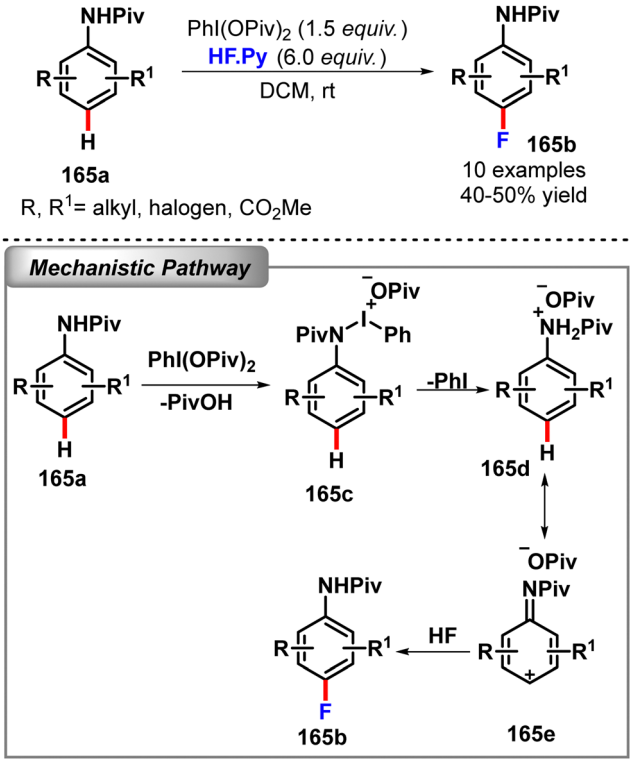

Scheme 165 HIR-mediated regioselective *p*-fluorination of anilides (Tian *et el.*[213]).

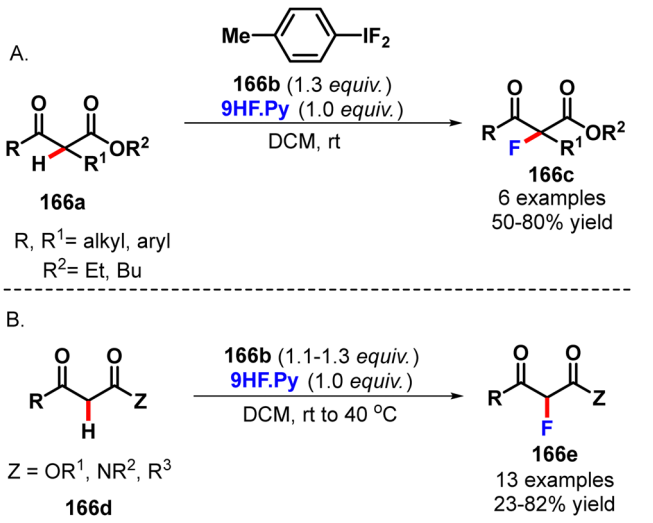

Scheme 166 HIR-mediated selective α-fluorination of β-dicarbonyl compounds (Hara *et al.*,[214] Yoshida *et al.*[215]).

presence of $BF_3{\cdot}Et_2O$ and water. It was further found that the presence of the etheric oxygen atom in the substrate seemed to be essential for this unique *p*-selective fluorination because of the neighbouring group participation.

In 2013, Meng and Li developed a $PhI(OPiv)_2$-promoted straightforward regioselective *p*-fluorination of anilides **165a** using HF.Py as a nucleophilic fluoride source (Scheme 165).[213] By thorough screening, it was found that pivaloyl protected aniline afforded the highest yield in this reaction. Anilides containing electron donating groups provided good yield whereas substrates with electron-withdrawing groups required a prolonged reaction time and furnished moderate yields which demonstrated the impact of electronegativity of the anilide substituent on the reaction. The mechanism suggested that the initial nucleophilic attack of anilide **165a** on $PhI(OPiv)_2$ followed by the cleavage of the N–I bond furnished nitrenium ion intermediate **165d**. This intermediate was stabilised by the charge delocalization of the phenyl ring, and the trapping of the fluoride anion at the para position finally gave the title product **165b**.

4.4.1.2 Direct C(sp^3)–F bond formation. In 1996, the Hara group first reported the *p*-iodotoluene difluoride **166b**-mediated selective α-fluorination of β-ketoesters **166a** in the presence of Olah's reagent (Pyr.9HF) (Scheme 166A).[214] Also the α-substituted ketoesters underwent the fluorination reaction but with relatively less yield than the unsubstituted ones. Later in 2003, the same group developed the *p*-iodotoluene difluoride-mediated selective α-fluorination of β-dicarbonyl compounds **166d** such as β-ketoesters, ketoamides, and diketones under neutral conditions (Scheme 166B).[215] They performed the reaction in CH_2Cl_2 at 40 °C without Pyr.HF but the reactions were slow compared to the previous method under acidic conditions.

In 2011, Kitamura *et al.* again achieved the α-fluorination of 1,3-dicarbonyl compounds **167a** by utilising the combination of iodosylbenzene (PhIO) and aqueous hydrofluoric acid (Scheme 167A).[216] Here the aqueous HF played two important roles: (a) a reagent for the *in situ* generation of $PhIF_2$ and (b) an activating agent of $PhIF_2$ for the transformation. The reaction proceeded through the enol form **167c** of the 1,3-dicarbonyl compound followed by the interaction with $PhIF_2$. The resulting intermediate **167d** then readily underwent nucleophilic displacement by a fluoride ion to afford the α-fluoro β-dicarbonyl compounds **167b**.

In 2013, the Stuart group developed an air and moisture stable cyclic hypervalent iodine(III) reagent **167e** for the electrophilic fluorination of 1,3-dicarbonyl compounds **167a** (Scheme 167B).[217] This reaction could afford difluorination along with monofluorination depending upon the concentration of fluoroiodane, temperature and the reactivity profile of β-dicarbonyl compounds. With the more reactive β-diketone substrate, a mixture of mono and difluorinated products were obtained, and at high temperature with 3 equiv. of fluoroiodane, difluorinated 1,3-diketone **167f** was observed exclusively. In the next year, Kita and Shibata reported an *in situ* generated hypervalent iodine catalysed nucleophilic fluorination of β-dicarbonyl compounds **167g** to afford α-fluorinated β-ketoesters, β-ketosulfones and β-ketoamides **167h** in good to excellent yields (Scheme 167C).[218] They had used a catalytic amount of *p*-iodotoluene (15 mol%) as the iodoarene, 1.3 equiv. of *m*CPBA as an external oxidant and Pyr.HF as the fluoride source which eventually generated the $ArIF_2$ catalyst as the key player behind the success of the transformation. Finally, they had also introduced the chiral iodoarene catalysts derived from (*R*)-binaphthyl diiodide for the asymmetric transformation.

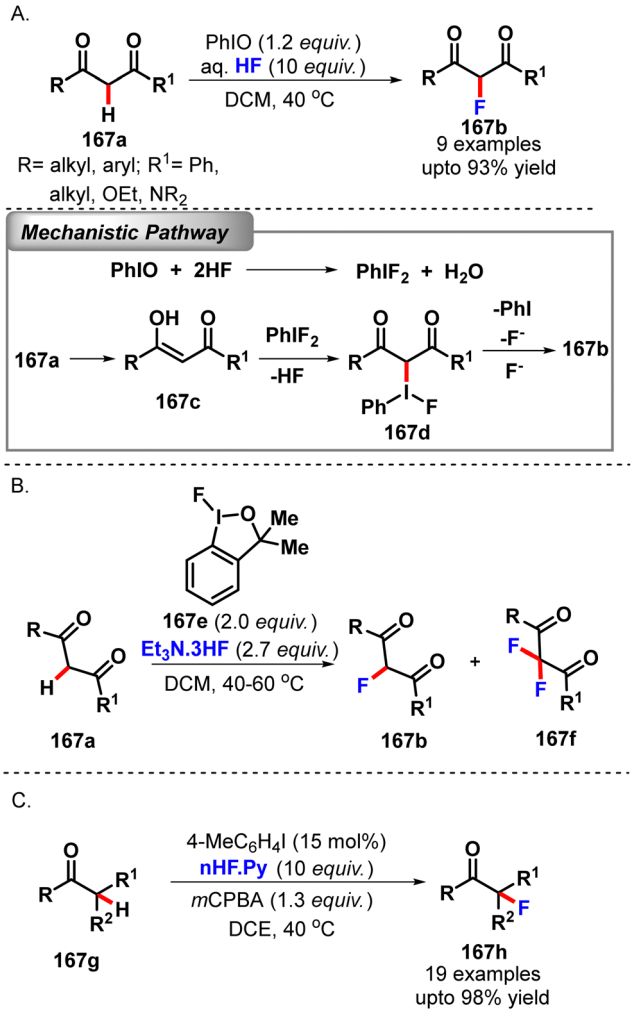

Scheme 167 HIR-promoted selective mono- and di-fluorination of 1,3-dicarbonyl compounds (Kitamura *et al.*,[216] Geary *et al.*,[217] Suzuki *et al.*[218]).

In 2014, Kitamura *et al.* conducted a ArIO promoted direct α-fluorination of acetophenone derivatives **168a** using a TEA·5HF complex as a fluorine source instead of aqueous hydrofluoric acid (Scheme 168A).[219] It was found that PhIO and *p*-substituent of iodosylarenes afforded the desired product in comparable yield. Not only unsubstituted acetophenone, but also the α-substituted acetophenone derivatives were also tested for this reaction which also furnished the desired α-fluorinated products **168b** in good yield. After the success, they also reported the direct α-fluorination of malonic esters **168c** with the combination of PhIO and $Et_3N{\cdot}5HF$ to access the corresponding 2-fluoromalonic esters **168d** in good to high yields (Scheme 168B).[220] For the substituted malonate ester, the fluorinated product was formed only at a low yield due to steric reason. Recently Wang and Kitamura introduced a non-basic HF·THF (5 : 1)/*p*-iodosyltoluene combination for the catalytic α-fluorination of 1,3-dicarbonyl compounds **168e** (Scheme 168C).[221] It was observed that the reaction with PhIO/5 HF·TEA afforded the highest yield of the corresponding fluorinated compounds **168f.**

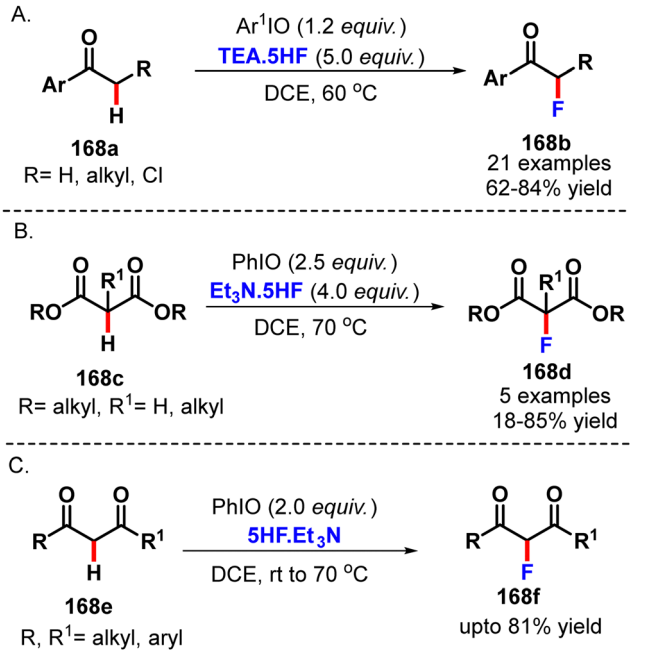

Scheme 168 ArIO-mediated direct α-fluorination of acetophenone derivatives, malonic esters and 1,3-dicarbonyl compounds (Kitamura *et al.*,[219,220] Wang *et al.*[221]).

In 2005, Wirth *et al.* reported a $PhIF_2$-mediated α-fluorination of α-seleno amide/ester/nitrile **169a** by the seleno-Pummerer reaction in moderate yield (Scheme 169).[222] The mechanism suggested that initial interaction of the hypervalent iodine with the selenium atom generated the cationic seleno-iodonium intermediate **169c.** This intermediate experienced a proton elimination and a subsequent fluorination afforded the monofluorinated selenides **169b.**

4.4.2 Other halogenation reactions. In 2018, Guangming Li and co-workers developed a general sterically controlled strategy for accessing various *p*-substituted aniline derivatives using *in situ* generated bulky hypervalent iodinium reagents (Scheme 170).[223] The protocol employed readily available reagents in an environmentally friendly manner using environmentally less hazardous

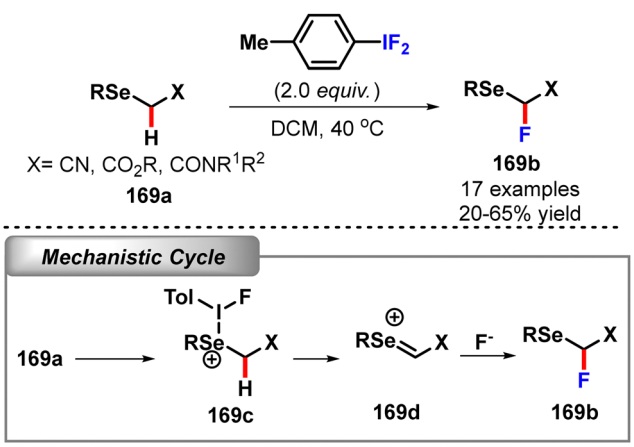

Scheme 169 HIR-mediated direct α-fluorination of α-seleno amide/ester/nitrile (Arrica *et al.*[222]).

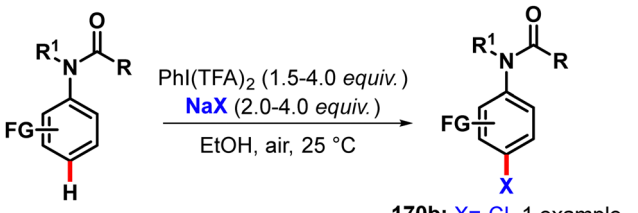

Scheme 170 HIR-mediated *p*-C–H halogenation of aniline derivatives (Xu *et al.*[223]).

solvents and proceeded without the use of transition metals. Initially, a ligand exchange between $PhI(TFA)_2$ and sodium salts was operative, affording the *in situ* generated bulky hypervalent iodinium reagent. Owing to the large steric demand of the HIR and the electronic nature of anilides, chlorination, bromination and iodination would selectively occur at the *p*-position *via* an incipient halide radical generation.

5. Metal free photo induced C–H functionalisation

Scientists draw much of their creativity and motivation from nature, which is also our greatest teacher. Synthetic chemists strive to reach the pinnacle of sustainable chemical reactivity, which is represented by photosynthesis. The most recent breakthroughs in photochemical methods, and in particular photoredox catalysis, have opened the door in this direction.[224] Already mentioned is the fact that in the last two decades, transition metal catalysed elegant C–H bond activation has gone from being a pipe dream to a commonplace reaction in both academia and industry. Photoredox-initiated reactions, catalysed by transition metal complexes or organic photoredox catalysts, represent an additional paradigm shift within the study of C–H activation. While the transition metal-based photoredox-catalysts typically comprised of metal–polypyridyl complexes offer metal–ligand charge transfer properties, the metal free organic dyes or large organic molecules such as eosin, rhodamine, 9-fluorenone, Rose Bengal, acridinium salts, *etc.* can absorb the light in the visible or near-visible region and offer the desired green alternative.[225] We believe that the organo-photoredox catalysts are just the beginning of what we promise will be a sustainable area of research for many years to come, even though most of the reported visible light induced catalytic C–H functionalisation methods still rely on the excellent reactivity of transition metal-based photoredox-catalyst complexes. Today, not only do we have photocatalyst-free methods for C–H functionalization, but also smart techniques where only visible light irradiation is required.

5.1 Organo-photoredox catalyst promoted C–H functionalisation

The organic chromophores have been recognized in organic synthesis for their ability to participate in photoinduced electron transfer (PET) processes. As we have already depicted there are a growing number of publications on C–H bond functionalisation *via* transition metal based photoredox catalysis, but the catalytic use of organic dyes in organic synthesis is somewhat less familiar. In particular, we wish to draw attention to organic photoredox catalysts, which not only provide "metal-free green" alternatives to the existing transition metal catalysed examples, but also boast a diversity of reactivities that promise to be useful in the discovery and optimization of new synthetic methodologies. There are several classes of organic photoredox catalysts which are used rigorously, namely, cyanoarenes such as DCB and DCN, benzophenones, quinones such as DDQ, pyrylliums, acridines, xanthenes such as Eosin Y, Rose Bengal, and rhodamine 6G, thiazines and so on.

5.1.1 C(sp^2)–H bond functionalisation

5.1.1.1 Arylation/heteroarylation. In 2012, the König group developed the eosin Y (1 mol%) catalysed C(sp^2)–H bond arylation of heteroarenes **171a** with aryl diazonium salts **171b** with visible light (green light) irradiation for the first time (Scheme 171).[226] It has to be noted that for the direct arylation of furan, electron-withdrawing or neutral group substituted diazonium salts were proved to be more efficient than the electron donating group containing ones. Not only furan, but also other heteroarenes such as pyrrole and thiophene also exhibited the transformation in good to moderate yield. However, the inhibition of the reaction in the presence of radical quencher TEMPO and the detection of TEMPO-adduct assured the radical mechanism for this reaction. The mechanism suggested the initial photoexcitation of Eosin Y by

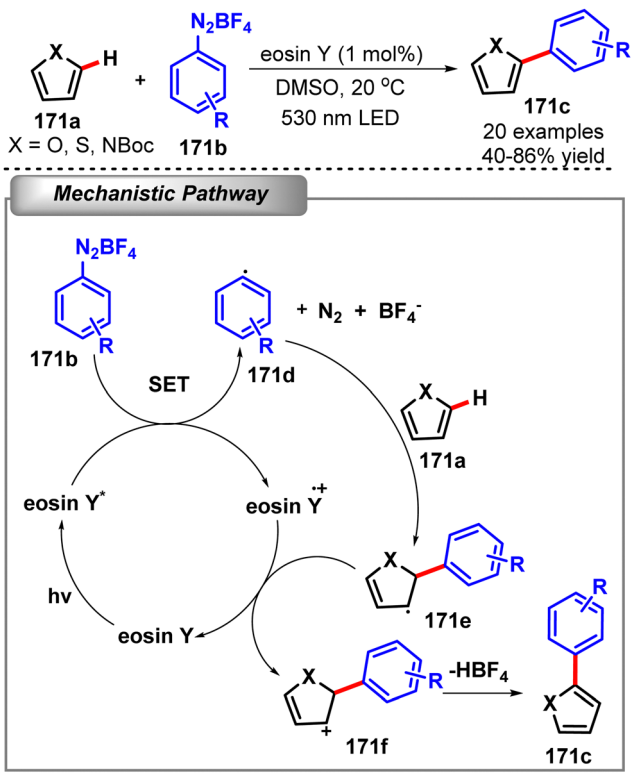

Scheme 171 Eosin Y catalysed C(sp^2)–H bond arylation of heteroarenes (Hari *et al.*[226]).

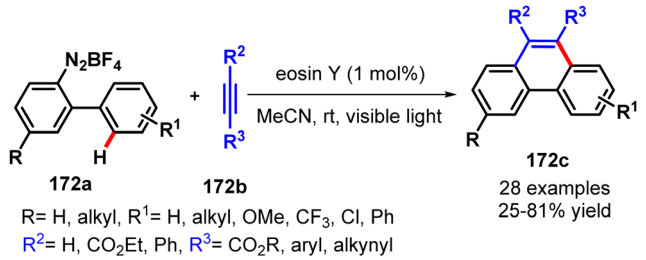

Scheme 172 Eosin Y catalysed C(sp^2)–H bond functionalisation for the synthesis of phenanthrene derivatives (Xiao *et al.*[227]).

visible light irradiation followed by the formation of aryl radical **171d** from the aryl diazonium salt **171b** by the SET pathway from the excited state of eosin Y. Addition of this aryl radical to heteroarene followed by oxidation afforded the carbocation intermediate **171f**. This oxidation might be facilitated by either the eosin Y radical cation or the radical chain transfer mechanism from the aryl diazonium salt. Finally, deprotonation of the carbocation intermediate furnished the desired coupling product **171c**.

In the same year Zhou and co-workers synthesized phenanthrene derivatives by the eosin Y catalysed, visible light (24 W fluorescent bulb) promoted [4+2]-benzannulation of biaryl diazonium salts **172a** and alkynes **172b** (Scheme 172).[227] A wide range of functional groups on bi-phenyldiazonium salts and alkynes were well tolerated in this transformation.

In 2013, the Zhao group used iodo-Bodipy **173c** or styryl-iodo-Bodipy **173d** as an organic photoredox catalyst for the arylation of furan and thiophene under the irradiation of a 35 W Xenon lamp ($\lambda > 385$ nm) (Scheme 173).[228] The reaction time was shorter (1 h) than the previously reported reaction by eosin Y by the König group. This was due to the stronger photocatalytic ability of Bodipy with higher reduction potential of the triplet excited state.

In 2014, the Konig group also developed the perylene diimide (PDI) photocatalysed direct arylation of heterocyclic pyrroles **174a** with aryl halides **174b** especially aryl chloride under visible light irradiation (455 nm blue LED) (Scheme 174).[229] The reaction required Et_3N as a reducing agent to form the coloured

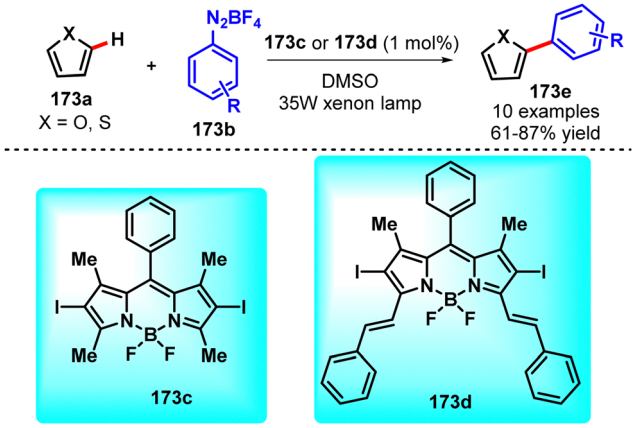

Scheme 173 Bodipy catalysed C(sp^2)–H bond arylation of heteroarenes (Huang *et al.*[228]).

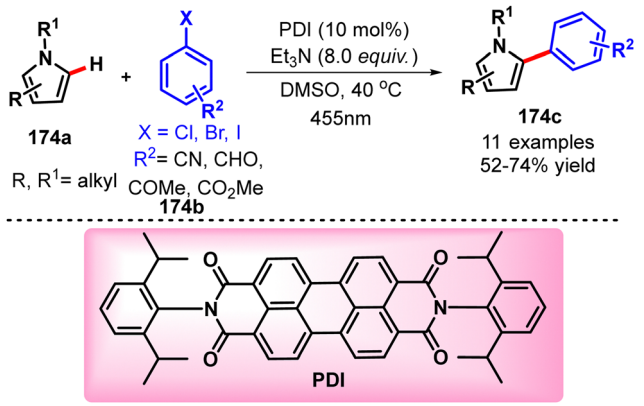

Scheme 174 PDI catalysed C(sp^2)–H bond arylation of heteroarenes (Ghosh *et al.*[229]).

PDI radical anion upon irradiation which was further confirmed by spectroscopic investigations. This PDI radical anion could again be excited by visible light, and in the absence of oxygen, this radical anion was very stable. Importantly, the reducing power of the excited state of the PDI radical anion at least reached or exceeded the reduction potential of aryl chlorides which was indeed tough to achieve. Two consecutive visible light-induced electron transfer processes of perylene diimide dyes resembled a minimalistic chemical model of the Z scheme in biological photosynthesis and thus extended the scope of visible light photocatalysis to aryl chlorides.

Later in 2015, Maity *et al.* achieved the eosin Y catalysed C–H arylation/heteroarylation of heteroarenes by blue LED-irradiation utilising *in situ* diazotization of heteroaryl amines **175b** by *t*BuONO (Scheme 175).[230] Several heteroarenes **175a** such as furan, pyrrole, and thiophene were tested for this C–H arylation with different amines such as heteroaryl amines, 2-ethynylanilines and substituted anilines. The complete inhibition of the transformation in the presence of TEMPO suggested the radical mechanism. The mechanism proceeded through the initial diazotization of aryl/heteroarylamine with ^{t}BuONO.

In 2016, Read de Alaniz and his team developed the ability to tune the reduction potential of a new phenothiazine (PTH) scaffold-based photoredox catalyst for the chemoselective C–C bond formation reactions using aryl halides (Scheme 176).[231] They found that the less reducing catalyst, tris-acetyl-PTH **176c**, could selectively activate C–I bonds, while both C–I and C–Br bonds could be activated by the highly reducing PTH catalyst **176e**. They not only achieved intermolecular coupling, but also the intramolecular version of this coupling reaction.

Scheme 175 Eosin Y catalysed C(sp^2)–H bond arylation of heteroarenes *via in situ* diazotization of heteroaryl amines (Maity *et al.*[230]).

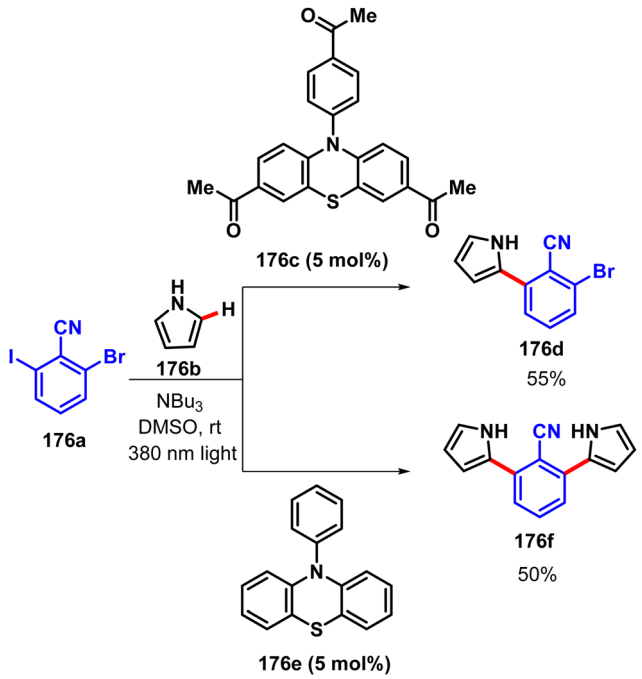

Scheme 176 PTH catalysed chemoselective C–C bond formation (Poelma *et al.*[231]).

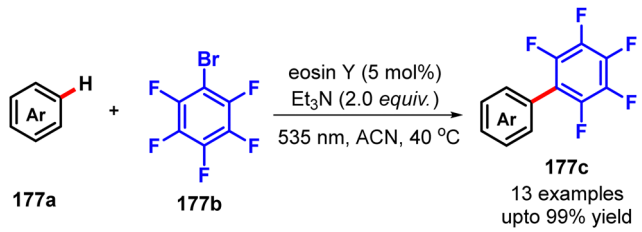

Scheme 177 Eosin Y catalysed direct arylation of simple arenes with fluorinated aryl bromides (Meyer *et al.*[232]).

In 2016, the Konig group again developed the eosin Y photocatalysed direct arylation of simple arenes **177a** with fluorinated aryl bromides **177b** under visible light irradiation (535 nm green LED) (Scheme 177).[232] This reaction required Et_3N as a sacrificial electron donor as well as an acid quencher during the catalytic cycle. The reactions with benzene, toluene and benzothiazole led to the single isomers, whereas other monosubstituted arenes gave the mixtures of *o*-:*m*-:*p*-isomers.

Afterwards, they again reported a photo-excited rhodamine 6G radical anion catalysed coupling of heteroaryl bromides and pyrrole derivatives for the synthesis of heteroaromatic biaryls (Scheme 178A).[233] In this transformation, along with the photocatalyst they utilised DIPEA as a sacrificial electron donor and acetonitrile as the optimised solvent under blue light irradiation at room temperature. This reaction was very much substrate specific as the other heterocycles such as (benzo)-furan and (benzo)-thiophene did not exhibit any transformation. The tentative mechanism suggested the initial photoexcitation of Rh-6G with blue LEDs followed by acceptance of an electron from the sacrificial electron donor (DIPEA) to yield the radical anion of Rh-6G. This radical anion again absorbed a second photon (upon blue light irradiation) to reach its excited state which has a higher reduction potential. Now the excited radical anion was able to reduce the heteroaryl bromides **178a** to the heteroaryl radical **178d** and returned to its ground state. The heteroaryl radical **178d** was trapped by pyrrole derivatives **178b** to provide bis heteroaryl radical **178e** which upon oxidation and rearomatisation gave the final product **178c**. A substantial amount of dehalogenated reduced by-product was formed by hydrogen atom transfer from the radical cation of DIPEA or from the solvent. They further extended this consecutive photoinduced electron transfer process (conPET) concept for the photocatalytic arylation or heteroarylation of chloro-substituted heterocycles **178f** and a variety of arenes and heteroarenes (178B).[234]

In the next year, Konig and Gryko also showed the electron-poor tetra(pentafluorophenyl)porphyrin **179c** catalysed direct C–H arylation of heteroarenes **179a** such as furan and thiophene with diazonium salts under visible light irradiation (blue LED, 455 nm) (Scheme 179).[235] This photochemical arylation was also effective for other compounds like coumarin. However, the

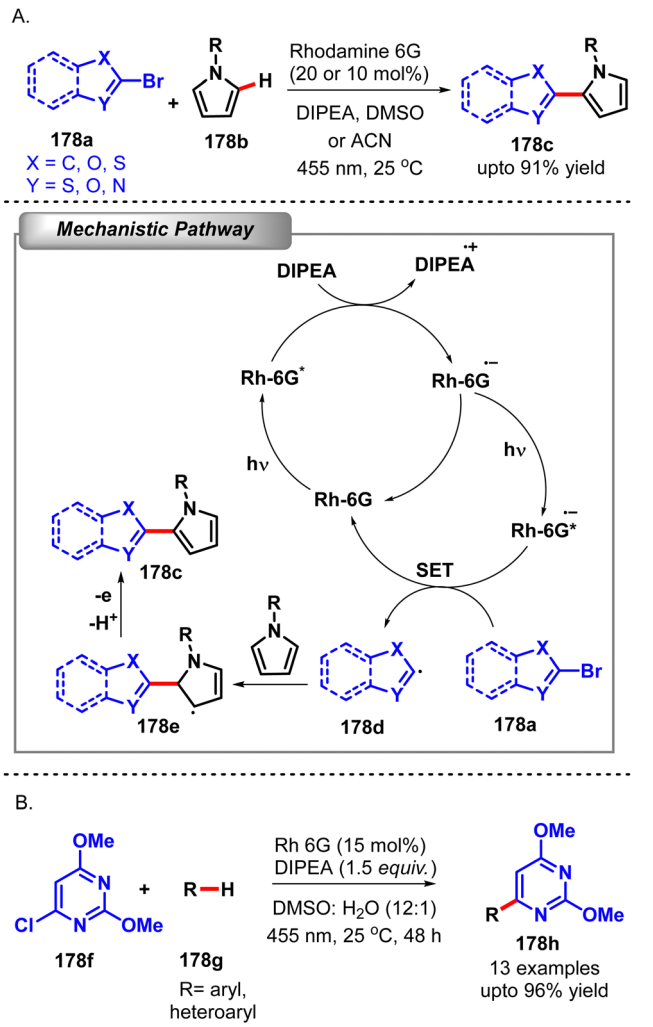

Scheme 178 Rhodamine 6G catalysed direct arylation of simple arenes and heteroarenes (Marzo *et al.*,[233] Graml *et al.*[234]).

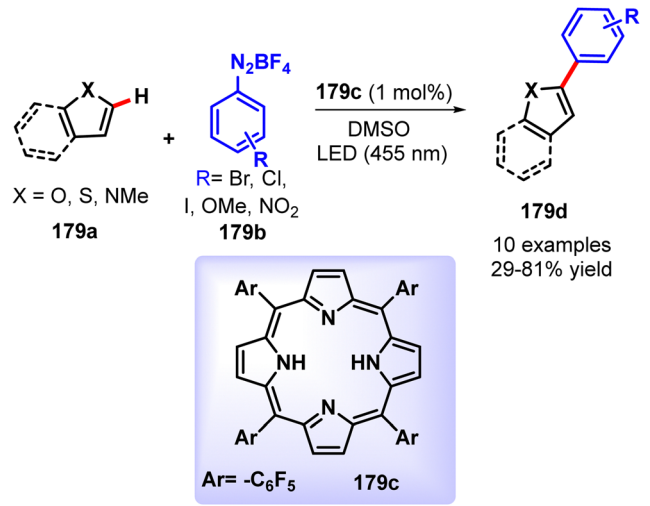

Scheme 179 Porphyrin catalysed direct C–H arylation of heteroarenes (Rybicka-Jasińska *et al.*[235]).

arylation of pyrrole and indole derivatives was proved to be difficult since they effectively quenched the luminescence of the porphyrin.

In the same year, Xu *et al.* presented a 9,10-dihydro-10-methylacridine ($AcrH_2$) **180b** catalysed direct C–H arylation of (hetero)-arenes **180a** likely with aryl diazonium salts under visible light irradiation (3 W blue LEDs) (Scheme 180).[236] Under optimum conditions, the desired coupling product was provided by not only heteroarenes like thiophene, furan, and pyrrole, but also by unactivated benzene derivatives. Furthermore, the complete inhibition of the reaction in the presence of radical quencher TEMPO suggested the radical pathway for the transformation.

In 2019, Jiao and co-workers described a self-promoted direct α-arylation of boron dipyrromethene dyes (BODIPYs) **181a** with aryl diazonium salts under the illumination of visible light (Scheme 181).[237] Interestingly, with 1.2 equiv. of ArN_2BF_4, the monoarylated BODIPY **181b** was isolated as the major product under a 1 W LED (λ_{max} = 450 nm), while the α-diarylated product **181c** was formed exclusively with 4.0 equiv. of ArN_2BF_4 under the irradiation of a 10 W 450 nm LED.

In the same year, Yadav and his team reported the eosin Y catalysed direct C(sp^2)–H arylation of anilines **182a** with aryl

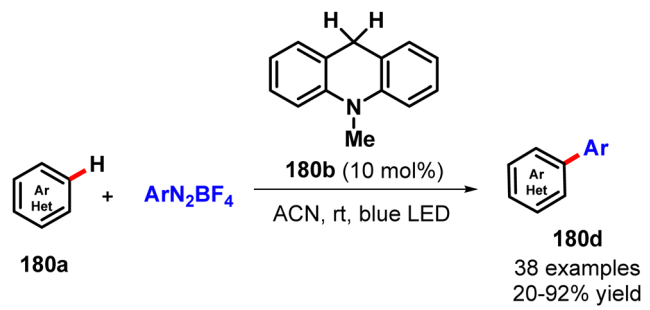

Scheme 180 9,10-Dihydro-10-methylacridine catalysed direct C–H arylation of heteroarenes (Feng *et al.*[236]).

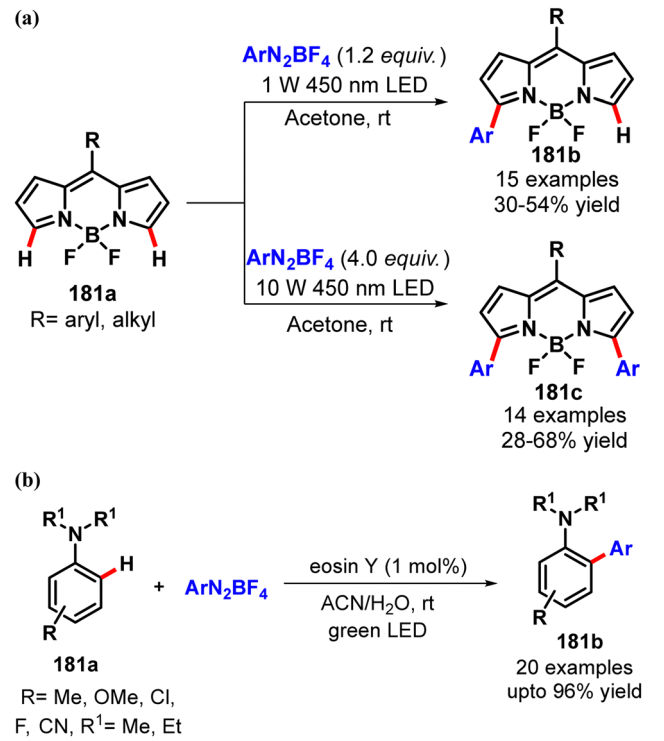

Scheme 181 (a) Self-promoted direct α-arylation of the BODIPY dye (Wang *et al.*[237]). (b) Eosin Y catalysed direct C(sp^2)–H arylation of anilines (Kapoor *et al.*[238]).

diazonium for the synthesis of 2-aminobiphenyls **182b** under irradiation with visible light (green LEDs) (Scheme 182).[238] While alkyl and methoxy substituents on the aromatic ring of anilines afforded the corresponding biaryls in high yields, other substitutions such as Cl, F and CN groups were compatible to furnish only moderate yield. Usually, the arylation was observed at the *o*- and *p*-positions with respect to the amino substituent. Notably, *N*,*N*-dialkylated anilines had been used as substrates because mono-alkylated and simple anilines quickly transformed into triazenes under the reaction conditions.

Very recently, Procter and co-workers established a one-pot formal cross dehydrogenative coupling of non-prefunctionalised arene partners with various heteroarenes and arenes through the marriage of interrupted Pummerer activation and organophotocatalysis (Scheme 182).[239] The blueprint of the transformation was commenced with sulfoxide activation of the nucleophilic arene by the interrupted Pummerer reaction using dibenzothiophene S-oxide (DBTSO) **182b** to generate the corresponding aryldibenzothiophenium salt (Ar–DBT+) followed by single-electron transfer (SET) from the photoexcited (34 W blue LED) catalyst PTH **182e** resulting in the formation of an aryl radical species which further reacted with heteroarenes **182c**. A wide range of arenes **182a** likely electron rich arenes, phenol and aniline derivatives and the arenes containing sensible halogen, triflate, mesyl, keto, amido, ester, trifluoromethyl and cyano groups provided the desired heterobiaryls with complete chemoselectivity. Similarly, a range of substituted pyrroles, thiophenes, furans, benzofuran and indole were successfully employed as the trapping hetero(arenes) in the coupling reaction.

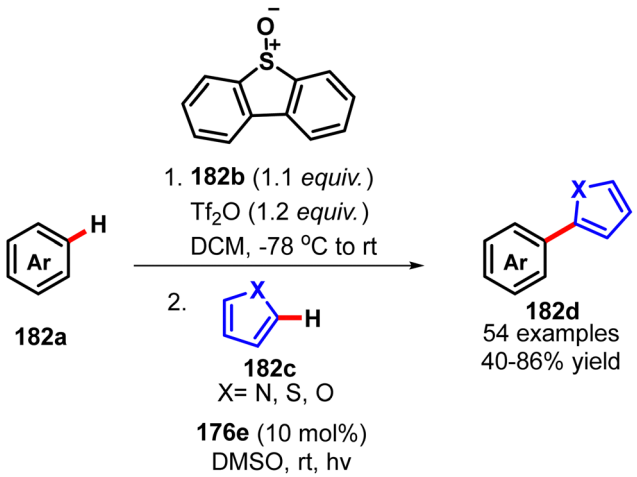

Scheme 182 Cross dehydrogenative coupling of non-prefunctionalized arene partners with various heteroarenes *via* the interrupted Pummerer reaction (Auckland *et al.*[239]).

Scheme 183 Eosin Y catalysed C–H arylation of anthranils (Adak *et al.*[240]).

Recently Hashmi *et al.* reported the Eosin Y disodium salt-catalysed C–H bond arylation at the C-3 position of anthranils **183a** with aryl diazonium salts under the irradiation of blue LEDs (Scheme 183).[240] Here again the electron-rich substituted aryl diazonium salt delivered a relatively low yield than the electron withdrawing group substituted ones.

5.1.1.2 Allylation. In 2019, Aleman and coworkers reported a chromoselective photocatalytic approach for the allylation reaction of a variety of heteroarenes **184b** like pyrroles (react through the C2 position) and indoles (react through the C3 centre) with allyl acetate derivatives **184a** (Scheme 184).[241] Notably, under UV-light irradiation (355 nm) *Z*-allylated products **184c** were obtained almost exclusively (up to >98:2) with the 10-phenyl-10H-phenothiazine (PTH) photocatalyst, while the *E*-isomer **184e** (up to >2:98) was procured by changing the light source to visible light (420 nm) and the catalytic system to phenoxazine catalyst **184d**. Based on the extensive mechanistic and photochemical proofs, laser flash photolysis studies and DFT calculations, the author suggested a nucleophilic attack of heteroarenes to an allyl-cation intermediate **184g**. Furthermore, according to theoretical calculations, photosensitization and subsequent isomerization of *E*-allyl acetate by the photocatalyst were feasible, while photosensitization and subsequent isomerization of *Z*-allyl acetate were not possible.

5.1.1.3 Formylation/acylation. In 2014, the Li group developed an aerobic Rose Bengal photoredox catalysed visible-light-promoted (14 W fluorescent lamp) indole C-3 formylation using TMEDA

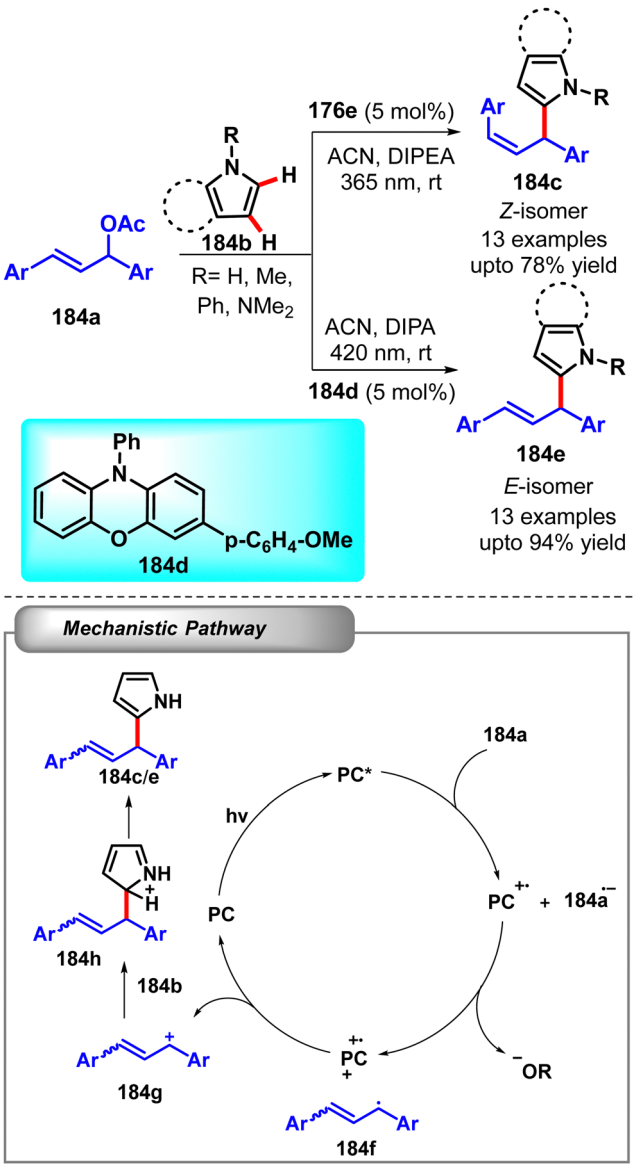

Scheme 184 Chromoselective allylation of heteroarenes (Martínez-Gualda *et al.*[241])

185b as the formyl carbon source (Scheme 185).[242] This transformation required molecular oxygen as an external oxidant and KI as an additive for better yield. A wide variety of indoles **185a** were found to be compatible under the reaction condition. However, the indole moiety with strong electron-withdrawing *N*-protecting groups afforded lower yield due to the lowering of electron density of the indole ring. Similarly, electron withdrawing substituents on the indole ring also shut down the reaction. Different control experiments suggested the superoxide radical anion pathway for the transformation. A tentative mechanism was proposed according to which the initial oxidative quenching of the visible-light promoted Rose Bengal (RB*) by TMEDA resulted in the formation of the Rose Bengal radical anion and TMEDA radical cation **185d**. Rose Bengal was regenerated by transferring an electron to O_2 to form the superoxide radical anion. At the same time, the TMEDA radical cation

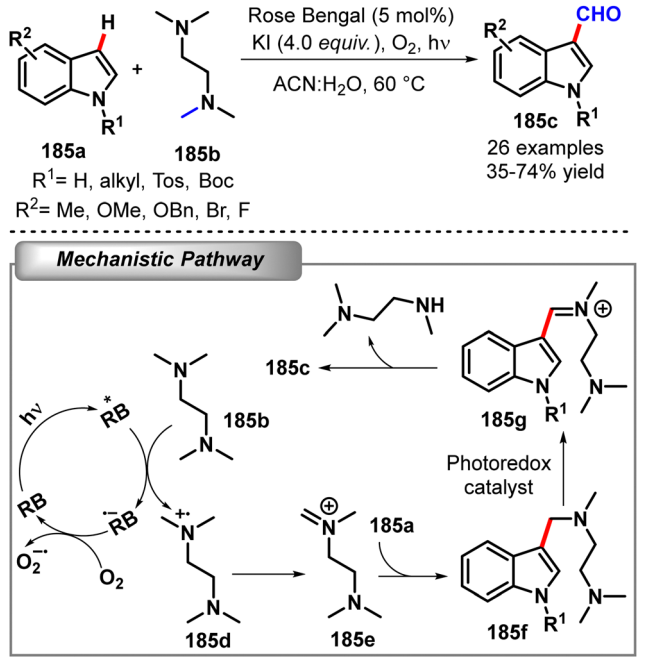

Scheme 185 Rose Bengal catalysed C-3 formylation of indole (Li *et al.*[242]).

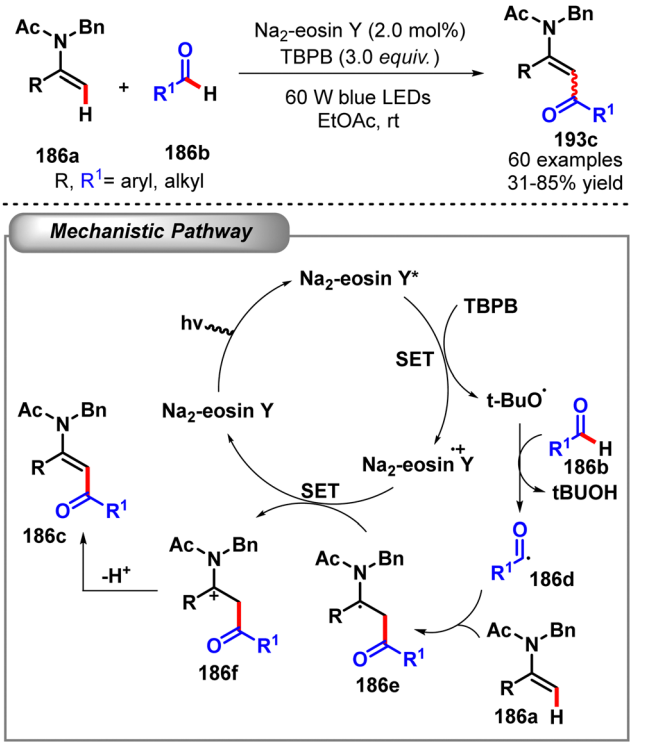

Scheme 186 Na_2-eosin Y catalysed C(sp^2)–H acylation of enamides (Zhao *et al.*[243]).

released a hydrogen atom to afford iminium ion **185e**. Now, a nucleophilic attack of indole to the iminium ion **185e** followed by deprotonation furnished C-3-substituted indole intermediate **185f**. Afterwards, a second visible-light photoredox cycle occurred and generated the iminium ion **185g** which underwent hydrolysis to provide 3-formyl-indole **185c**.

Recently Loh and co-workers demonstrated the Na_2-eosin Y catalysed efficient C(sp^2)–H acylation of enamides **186a** with aldehydes **186b** for the synthesis of a diverse range of synthetically crucial geometrically defined *E*-configured β-acylated enamides **186c** under the irradiation of 60 W blue LEDs (Scheme 186).[243] A wide variety of α-arylated enamides were well compatible with this reaction. Interestingly, the acylation of α-alkylated enamides with aldehyde preferentially furnished Z-configured products. Simultaneously, a broad array of aromatic and aliphatic aldehydes were proved to be efficacious coupling partners, affording the *E*-configured β-acylated enamides in moderate to good yield. A plausible mechanism was suggested involving an initial photo-excitation of Na_2-eosin Y followed by a single electron transfer to *tert*-butyl peroxybenzoate to generate the *tert*-butyloxy radical. Next, the *tert*-butyloxy radical reacted with aldehyde **186b** to form an acyl radical species **186d** which was then intercepted by enamide **186a** to forge radical intermediate **186e**. Subsequently, a single electron oxidation of the intermediate A by the Na_2-eosin radical cation furnished a carbon cationic species **186f** which finally produced the desired β-acylated enamides **186c** by deprotonation. To minimize the allylic strain between the newly installed acyl group and the bulky group on the nitrogen atom, *E*-acylated enamides were preferentially formed.

5.1.1.4 Alkylation. In 2013, the Itoh group showed that the anthraquinone-2-carboxylic acid could act as an organic photoredox catalyst for the visible-light-induced desulfonative trifluoromethylation of arenes and heteroarenes **187a** employing sodium trifluoromethanesulfinate (Scheme 187).[244] A tentative mechanism was suggested wherein the photoinduced downhill electron transfer from the CF_3SO_2 anion to the excited state of the photocatalyst for the generation of $CF_3SO_2^{\bullet}$ and the facile release of SO_2 not only generated $CF_3^{\bullet}$ but also regenerated the ground state of AQN. The addition of this $CF_3^{\bullet}$ to the electron-rich

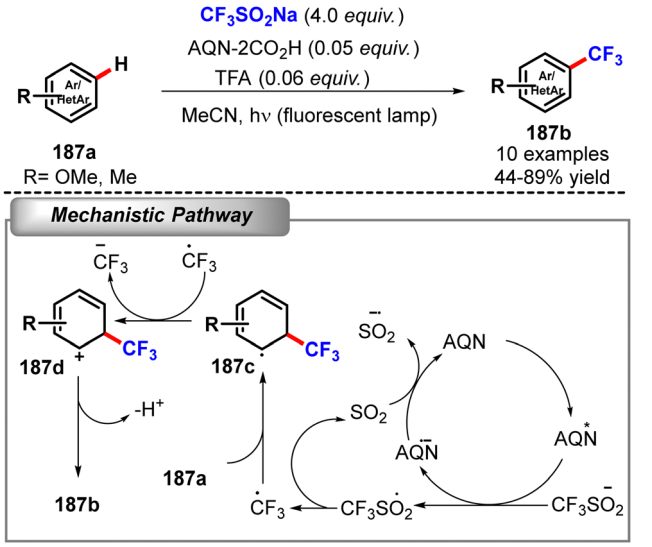

Scheme 187 Desulfonative trifluoromethylation of arenes and heteroarenes (Cui *et al.*[244]).

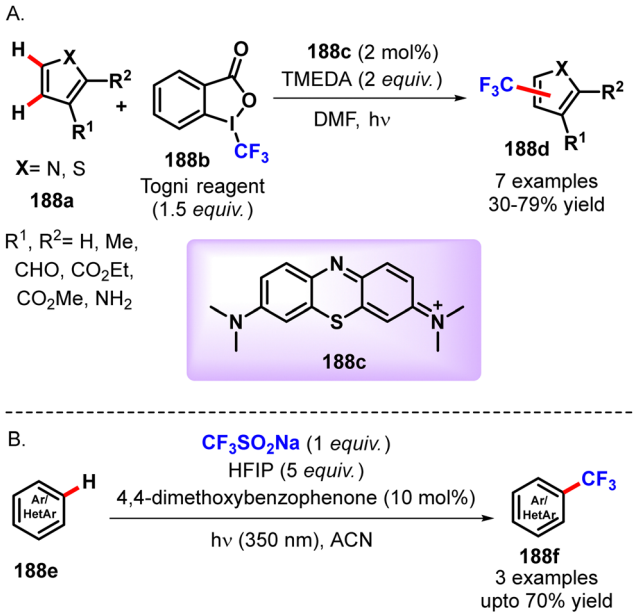

Scheme 188 Organophotoredox catalysed trifluoromethylation of heteroarenes and arenes (Pitre *et al.*,[245] Lefebvre *et al.*[246]).

position of the aromatic ring **187a** was followed by oxidation and deprotonation to afford the fluoroalkylated arenes **187b**.

During this period, the Scaiano group also demonstrated the methylene blue photosensitizer **188c** catalysed trifluoromethylation of electron-rich heterocycles **188a** by employing Togni's reagent **188b** (Scheme 188A).[245] Later, a similar type of trifluoromethylation of arene and heteroarenes **188e** was also reported by Rueping *et al.* by introducing 4,4′-dimethoxybenzophenone as an organic photoredox catalyst (Scheme 188B).[246]

In 2015, Postigo and colleagues developed an inexpensive organic dye, Rose Bengal, that catalysed the radical homolytic aromatic substitution (HAS) reaction of aniline derivatives with perfluoroalkyl halides for the synthesis of perfluoroalkylated anilines at *p*- and *o*-positions through irradiation at ambient temperature with a household fluorescent light bulb (visible light) or under exposure to solar light (Scheme 189).[247] This reaction required Cs_2CO_3 as an additive to regenerate the catalyst as well as the alkylated aniline products.

The radical alkylation strategy has received tremendous attention now-a-days for the easy late-stage derivatization. In this regard, the photoredox Minisci type radical alkylation reaction of heteroarenes defined a delicate route. In 2017,

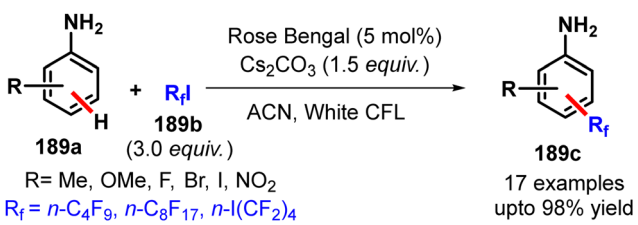

Scheme 189 Rose Bengal catalysed perfluoroalkylation of aniline derivatives (Vallejo *et al.*[247]).

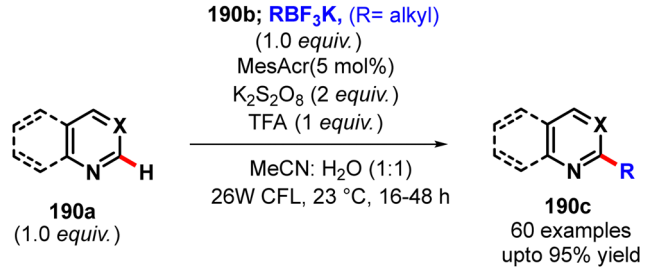

Scheme 190 MesAcr catalysed Minisci type radical alkylation of heteroarenes (Matsui *et al.*[248]).

Molander and co-workers first envisioned a potentially synchronized organophotocatalysed (mesitylacridinium perchlorate) marriage between alkyltrifluoroborate reagents **190b** and the heteroarenes **190a** like quinolone cores, quinoxaline, indazole, and isoquinoline for the synthesis of several unprecedented, complex alkylated heteroarene molecules **190c** (Scheme 190).[248] As an appended application, the synthesis of bipyridine-type ligands as well as the late-stage functionalisation of medicinally relevant molecules has been portrayed.

In the same year, Molander and Matsui again reported a similar mesitylacridinium (MesAcr) perchlorate (1 mol%) catalysed Minisci type coupling between 2-trifluoroborato-4-chromanones and various heteroarenes for the synthesis of heteroaromatic flavanones under visible light irradiation (26 W CFL) (Scheme 191).[249] Not only lepidine, but also other heteroarenes such as isoquinoline, quinoxalin, caffeine, and pyridine successfully furnished the coupling product in moderate to good yield. This group basically utilised the 2-trifluoroborato-4-chromanones **191a**, which generated the alkyl radical under photo redox catalysed conditions.

In the same year, the Bolm group outlined about Eosin Y photocatalysed perfluoroalkylation of terminal alkenes **192a** *via* an atom transfer radical addition elimination (ATRE) reaction (Scheme 192).[250] This transformation was well tolerated with various functional groups on the alkene and the process had been utilized for late stage perfluoroalkenylation of complex and diversely substituted molecules. A plausible mechanism for the visible light promoted ATRE reaction was proposed according to which the oxidative quenching of the photocatalyst by the perfluoroalkyl halide **192b** led to the generation of perfluoroalkyl radical **192d** which was intercepted immediately

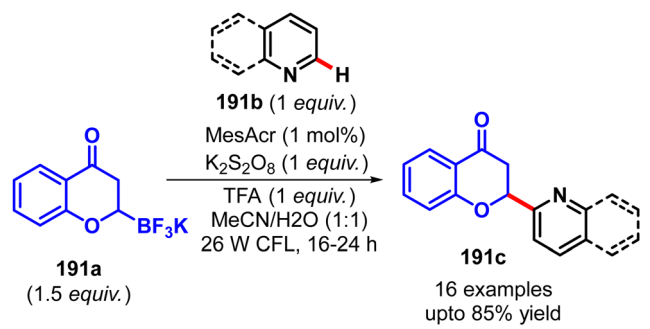

Scheme 191 MesAcr catalysed direct C–H alkylation of heteroarenes (Matsui *et al.*[249]).

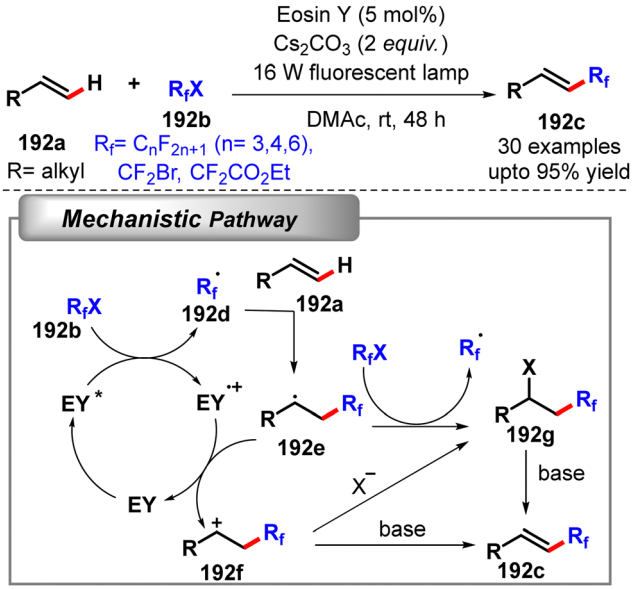

Scheme 192 Eosin Y catalysed perfluoroalkylation of terminal alkenes *via* ATRE reaction (Tiwari *et al.*[250]).

with the alkene **192a** to form radical **192e**. Now this radical could either oxidize to give carbocationic intermediate **192f** or it could react with another equivalent of perfluoroalkyl halide to generate the halide intermediate **192g**. The carbocationic intermediate **192f** either formed the intermediate **192g** *via* the addition of halide anion or it could directly afford the alkene **192c** by deprotonation with base. The halide intermediate **192g** could experience dehydrohalogenation to afford the alkene **192c**. This pathway seemed to be more relevant since the independent experiment also afforded the same product.

The same year Nicewicz and co-workers disclosed the acridinium photoredox catalysed synthesis of aromatic nitriles **193b** *via* direct C–H functionalisation using trimethylsilyl cyanide under an aerobic atmosphere which was proved to be compatible with a variety of electron donating and withdrawing groups, halogens, nitrogen, and oxygen-containing heterocycles as well as aromatic-containing pharmaceutical agents (Scheme 193).[251] In this transformation, TMSCN was proved to be the optimal cyanation reagent due to its controlled release of cyanide over the course of the reaction maintaining the low effective concentration of the free cyanide anion during the reaction along with the use of phosphate buffers (pH 9.0) as the co-solvent. A plausible mechanism was proposed involving the oxidation of arene **193a** to the corresponding cyclohexadienyl radical cation **193c** by the photo-excited acridinium under blue LED irradiation. Cyanide then encountered the radical cation either *o*- or *p*- to the electron donating substituent followed by oxidation by molecular oxygen to afford the desired benzonitrile product **193b**. However, the unselective product formation could not fully support the pathway. But the observed *o*-, *p*- regioselectivity could be better explained by the location of partial charges on the intermediate.

In 2018, Weng *et al.* reported a Rose Bengal photocatalysed Friedel–Crafts C3-alkylation reaction of indole derivatives **194a** using *N*,*N*-dimethylanilines **194b** under visible light irradiation

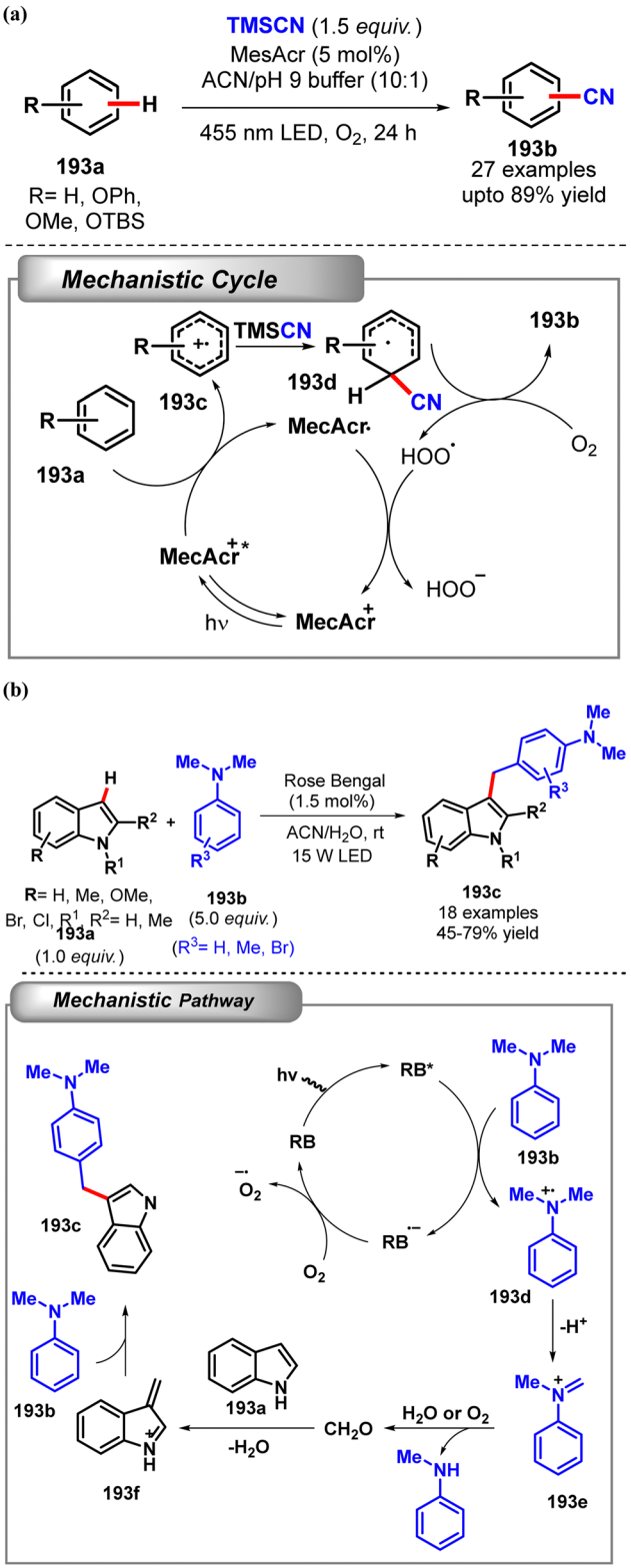

Scheme 193 (a) MesAcr catalysed direct C(sp^2)–H cyanation of arenes (McManus *et al.*[251]). (b) Rose Bengal catalysed Friedel–Crafts C3-alkylation of indole (Dai *et al.*[252]).

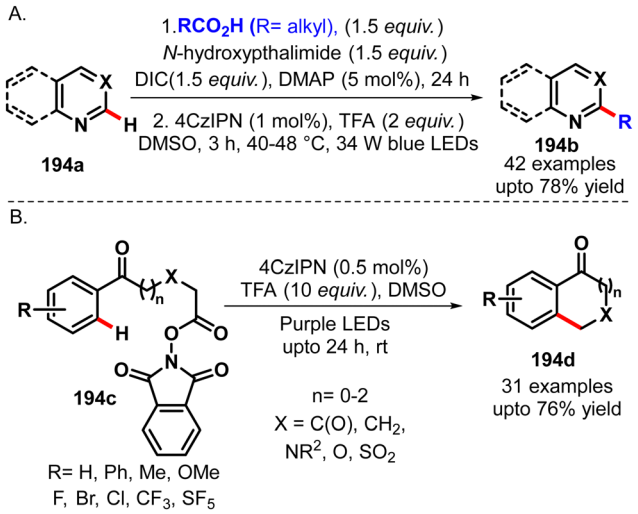

Scheme 194 CzIPN catalysed inter- and intramolecular Minisci reaction (Sherwood *et al.*[253,254]).

(Scheme 194).[252] This transformation was compatible with various functional groups on both indoles and anilines. A probable mechanism was suggested according to which the reductive quenching of photoexcited RB by *N*,*N*-dimethylaniline **194b** resulted in the formation of an aniline cation radical **194d**. The photoredox cycle was continued by the oxidation of the RB anion radical to the ground state Rose Bengal by molecular oxygen. On the other hand, the aniline radical cation **194d** deprotonated presumably by the superoxide radical anion to generate iminium ion **194e**. Then the iminium ion was oxidized or hydrolyzed to afford formaldehyde and *N*-methylaniline. Now, a three-component reaction of indole, formaldehyde and *N*,*N*-dimethylaniline took place through the involvement of 3-methylidene-3*H*-indolium cation intermediate **194f** to afford the final product **194c**.

In the same year, Sherwood and co-workers developed a visible light promoted organic photoredox (4CZIPN) catalysed one-pot Minisci reaction employing carboxylic acids as radical precursors *via* the *in situ*-generated *N*-(acyloxy)phthalimides (NAP) in the presence of DMAP and *N*,*N*′-diisopropylcarbodiimide (DIC) in DMSO (Scheme 194A).[253] This transformation displayed a wide substrate scope and more importantly was found to be beneficial for the late-stage functionalisation of nucleosides and marketed drug scaffolds. In the following year, the same group reported the decarboxylative intramolecular arene alkylation utilizing NAP as radical precursors using the same 4CzIPN as an organic photocatalyst and visible light (purple LED; 427 nm) (Scheme 194B).[254]

In 2019, Natarajan and coworkers developed the Rose Bengal catalysed intramolecular cyclization reaction of *N*-biarylglycine esters **195a** to phenanthridine-6-carboxylates **195b** in water under visible-light (34 W blue LED) irradiation in an open air atmosphere (Scheme 195).[255] During the generalization, it was found that the substrates bearing electron donating groups on the aromatic ring of glycine ester afforded phenanthridine-6-carboxylates in higher yields than those bearing electron-deficient groups. A tentative mechanism was suggested involving the single electron reduction of photoexcited Rose Bengal by

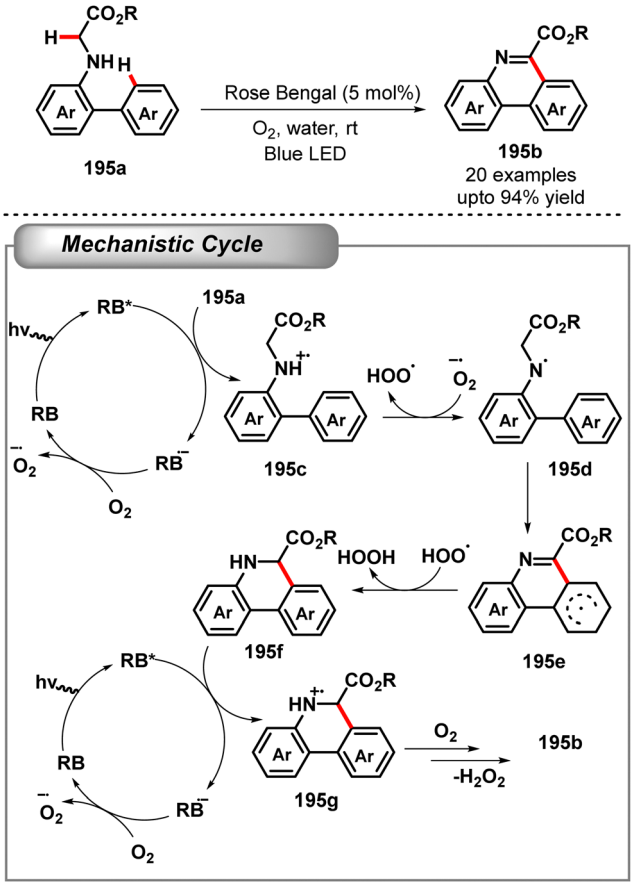

Scheme 195 Rose Bengal catalysed intramolecular cyclization reaction of *N*-biarylglycine esters (Natarajan *et al.*[255]).

glycine ester **195a** to generate the Rose Bengal anion radical and amine radical cation **195c**. Afterwards, the RB anion radical was oxidized by molecular oxygen to afford the superoxide anion radical which deprotonated the amine radical cation to furnish biarylglycine ester radical **195d** and the hydroperoxyl radical. Now the biarylglycine ester radical immediately underwent an intramolecular C–H aromatic coupling to form a new radical intermediate which further experienced oxidation followed by deprotonation to give methyl-5,6-dihydrophenanthridine-6-carboxylate **195f** and H_2O_2. Next, a second similar photoredox catalytic cycle was operated again to furnish the title product **195b**.

Recently, the Meng group developed the Rose Bengal photosensitizer catalysed visible light (21 W white LED) promoted alkylation of indoles **196b** with nitroalkenes **196a** in water for the efficient synthesis of 3-(2-nitroalkyl)indoles **196c** in moderate to good yields (Scheme 196).[256] Diverse functional groups on nitroethenylbenzene as well as on the indole ring were well tolerated under the reaction condition.

5.1.2 C(sp^3)–H bond functionalisation. In the recent few years, the photoinduced electron transfer (PET) strategy has been successfully utilized as a mild and efficient alternative to the use of classical oxidising agents. One of such examples is the formation of iminium cation species from the corresponding amine which upon interaction with potent nucleophiles afforded important structural skeletons.

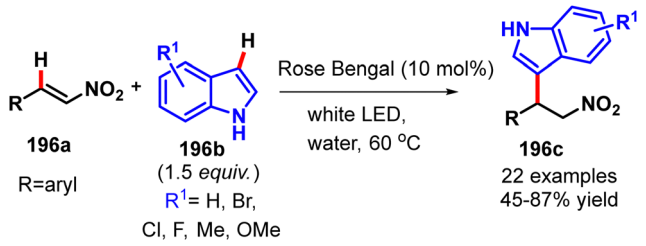

Scheme 196 Rose Bengal catalysed alkylation of indoles with nitroalkenes (Yu *et al.*[256]).

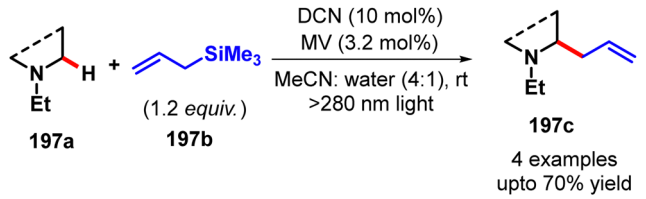

Scheme 197 Organophotoredox catalysed C–H functionalisation at the α-position of *tertiary* amine derivatives (Pandey *et al.*[257]).

In 1992, Pandey and his group utilised 1,4-dicyanonaphthalene (DCN) as a PET catalyst owing to its high photooxidative ability for the C–H functionalisation at the α-position of tertiary amine derivatives with allylsilanes as nucleophiles (Scheme 197).[257] In these transformations, methyl viologen (MV^{2+}) was employed as the electron relay reagent to match the potential of oxygen and cyanoarenes.

In 2000, Cocquet and co-workers utilised a catalytic amount of methylene blue (MB) as the photosensitizer for the visible light induced photooxidation of various *N*-arylaminopiperidines or *N*-arylaminopyrrolidines **198a** for the synthesis of corresponding α-cyano compounds **198b** in the presence of trimethylsilyl cyanide (Scheme 198).[258] Further in the presence of water, cyanation products were transformed into the corresponding lactams.

Later in 2011, Konig and Hari reported Eosin Y catalysed visible light mediated coupling of sp^3 C–H bonds α- to the nitrogen atom of tetrahydroisoquinolines **199a** with nitroalkanes, dialkyl malonates, and malononitrile in good yield (Scheme 199A).[259] A tentative mechanism was proposed: a single electron transfer from tetrahydroisoquinoline **199a** to the excited state of eosin Y afforded an aminyl cation radical **199d** which then lost a hydrogen atom to generate the iminium ion **199e**. A subsequent trapping of **199e** with pronucleophiles thus resulted in the desired product **199c**.

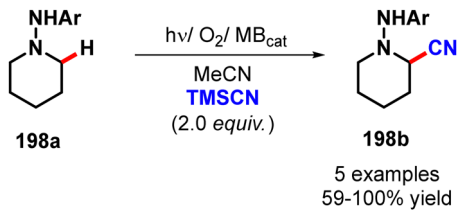

Scheme 198 Organophotoredox catalysed C–H cyanation at the α-position of N-arylaminopiperidine derivatives (Cocquet *et al.*[258]).

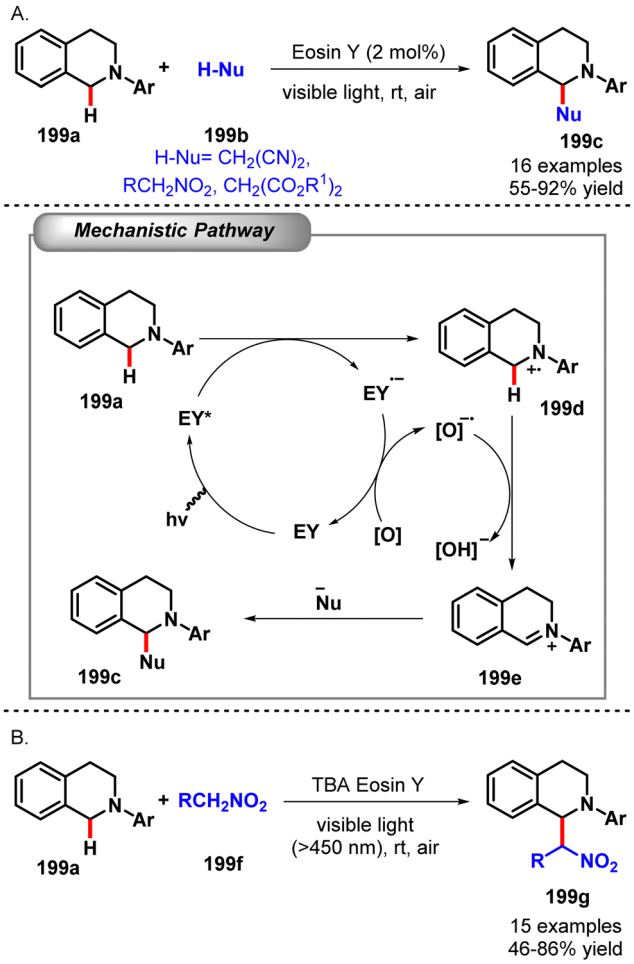

Scheme 199 Organophotoredox catalysed sp^3 C–H bond functionalisation of tetrahydroisoquinoline derivatives (Hari *et al.*,[259] Liu *et al.*[260]).

Later, the Wu group also reported a similar type of reaction employing organosoluble eosin Y bis(tetrabutylammonium salt) (TBA-eosin Y) as a photocatalyst in dilute solution (Scheme 199B).[260] Both the reactions required molecular oxygen for the success of the reactions.

In 2013, Rueping and his team developed a Rose Bengal photoredox catalysed continuous flow process for the efficient synthesis of α-functionalized tertiary amines **199c** (Scheme 200A).[261] Nitroalkanes, TMSCN, and dialkyl malonates **199b** were reacted with various *N*-aryl tetrahydroisoquinolines **199a** to provide the corresponding α-functionalized products in moderate to excellent yields. Advantageously, shorter reaction times were required than the previously reported batch conditions. Moreover, a multicomponent Ugi reaction was also performed with *N*,*N*-dimethylanilines **200a** with different isocyanides to obtain highly valuable α-amino amides **200c** in good yields (Scheme 200B).

Later in 2015, Raston and Stubbs reported a similar type of α-functionalisation of tertiary amines by using a microfluidic vortex fluidic device (VFD) operating in either confined or continuous mode involving Rose Bengal as the organic photoredox catalyst (Scheme 200C).[262] They also showed that the process significantly minimized the processing time compared to batch processing with comparable or improved yields.

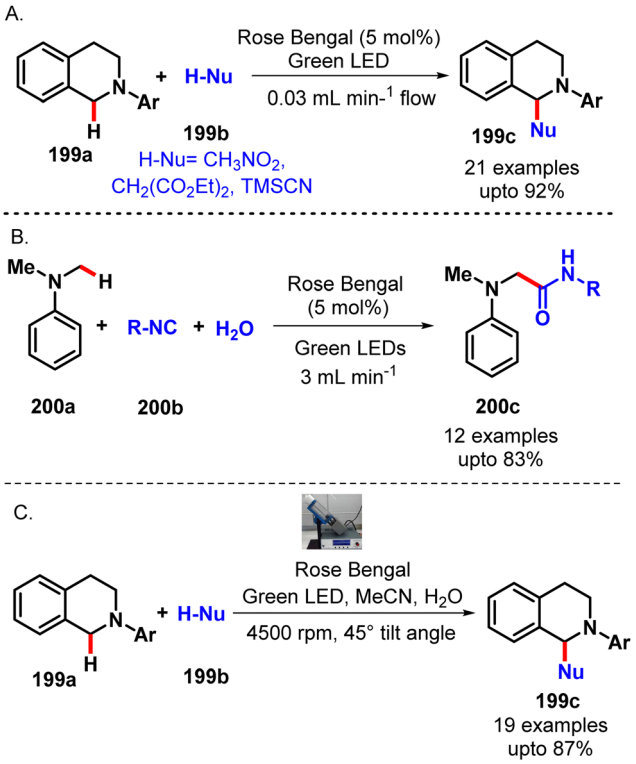

Scheme 200 Organophotoredox catalysed sp^3 C–H bond functionalisation of tertiary amine derivatives under a continuous flow process (Rueping *et al.*,[261] Gandy *et al.*[262]).

In the following year, Jiang and co-workers developed a dicyanopyrazine-derived (DPZ) push–pull chromophore **201b** as a new kind of organic photoredox catalyst where the electron-donating 2-methoxythienyl moiety provided a broad absorption range up to 500 nm along with excellent redox properties (Scheme 201).[263] Then this catalyst was successfully applied in the CDC reaction of *N*-aryltetrahydroisoquinolines **201a** with various nucleophiles mainly nitromethane. The major benefits of this catalyst were the lowest possible catalyst loading (0.1 mol% and even 0.01 mol%) and the requirement of a low power light source.

Later, in the very next year, they demonstrated a similar dicyanopyrazine-derived chromophore (DPZ) **201b** as a photoredox catalyst for the controllable selective syntheses of four

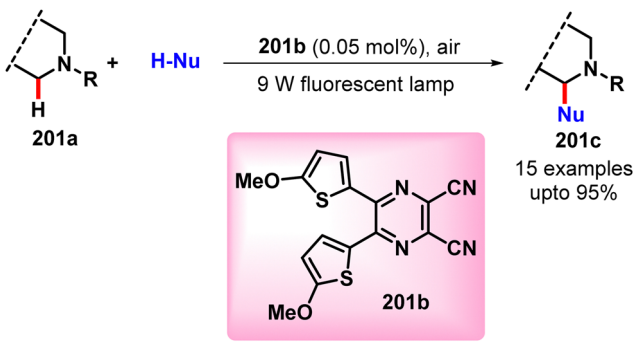

Scheme 201 DPZ catalysed sp^3 C–H bond functionalisation of *tertiary* amine derivatives (Zhao *et al.*[263]).

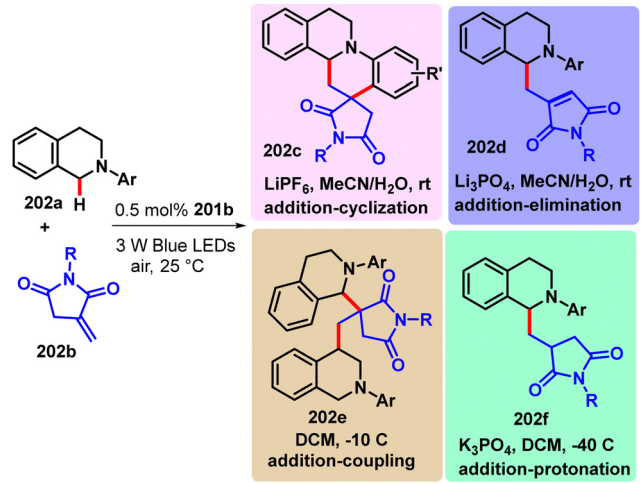

Scheme 202 DPZ catalysed controllable selective product formation between *N*-tetrahydroisoquinolines and *N*-itaconimides (Liu *et al.*[264]).

distinct products from common starting materials, namely, *N*-tetrahydroisoquinolines (THIQs) **202a** and *N*-itaconimides **202b**, through four different pathways including addition-cyclization **202c**, addition-elimination **202d**, addition-coupling **202e** and addition-protonation **202f** (Scheme 202).[264] The electronic properties suggested that the HOMO–LUMO gap of DPZ (E_g = 2.82 eV) facilitated the generation of the α-amino radical by single-electron transfer (SET). The planar and polarizable π-system of DPZ would help to stabilize the radical anion through delocalization and should be instrumental in postponing its subsequent oxidation by oxygen and finally detained the formation of an iminium ion from the α-amino radical which reacted with *N*-itaconimide as an electrophile.

In 2016, they again disclosed a cooperative photoredox and asymmetric catalysis for the enantioselective aerobic oxidative C(sp^3)–H olefination of *N*-tetrahydro-β-carbolines (THCs) **203a** as well as aryltetrahydroisoquinolines (THIQs) **203b** (Scheme 203).[265]

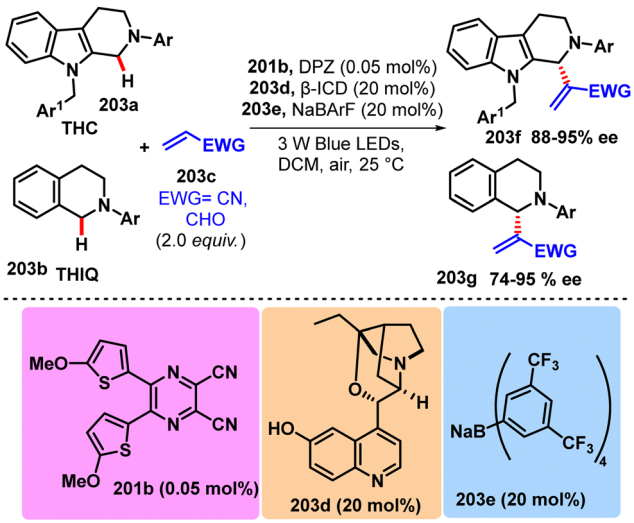

Scheme 203 Cooperative photoredox and asymmetric catalysis enabled enantioselective C(sp^3)–H olefination of THCs and THIQs (Wei *et al.*[265]).

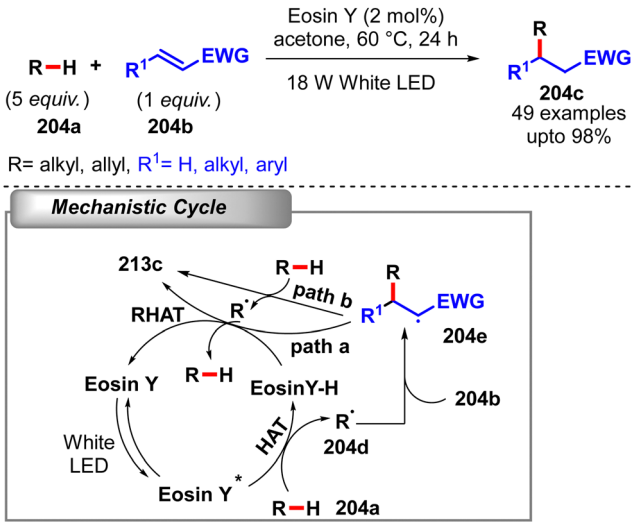

Scheme 204 Eosin Y catalysed direct C(sp^3)–H alkylation (Fan *et al.*[266]).

This method significantly featured a triple-catalyst strategy, involving a dicyanopyrazine derived chromophore (DPZ) **201b** as an organic photoredox catalyst, β-isocupreidine (β-ICD) **203d** as a chiral Lewis base catalyst and NaBArF **203e** as an inorganic salt cocatalyst for the straightforward access of a series of valuable α-substituted THCs **203f** and THIQs **203g** in high yield with excellent regio- and enantioselectivity (up to 95% ee).

Apart from the single-electron transfer (SET), hydrogen atom transfer (HAT) has also been frequently involved in photocatalysis, which can not only activate substrates without the limitation of redox potentials but can also offer enormous opportunities for C–H activation. In this context, Jie Wu and his group demonstrated that Eosin Y can behave as an effective direct hydrogen atom transfer catalyst for C–H activation reaction (Scheme 204).[266] With this concept, they reported the alkylation of C–H bonds with electron-deficient alkenes as a model study with a wide substrate scope. Based on the series of experiments, a plausible mechanism was suggested involving the initial formation of a carbon cantered radical **204d** by visible-light-activated *eosin Y through a HAT process which was subsequently trapped by an electron-deficient alkene **204b** to selectively form radical adduct **204e**. Finally the reaction took place either by RHAT between eosin Y–H and radical **204e** (path a) or through another THF molecule and radical **204e** (path b) thereby delivered the desired alkylation product **204c**, followed by RHAT between THF radical and eosin Y–H (19.9 kcal mol^{-1}) to regenerate the ground state eosin Y catalyst.

Recently, Sureshkumar *et al.* reported an organophotocatalysed direct multiple α-C(sp^3)–H alkylation of phosphoramides with electron deficient alkenes for the selective synthesis of mono-, di- and tri-alkylated products (Scheme 205).[267] While Eosin-Y was used as a HAT photocatalyst for mono-α-C(sp^3)–H alkylation **205c** of phosphoramide derivatives, the acridinium photocatalyst was found to be suitable for di- and tri-C(sp^3)–H alkylation **205d** and **205e** of phosphoramides.

Recently, Hashmi and colleagues employed diaryl ketone as a photoredox catalyst for the efficient visible light-promoted chemo- and regioselective hydroalkylation of chloroalkynes *via*

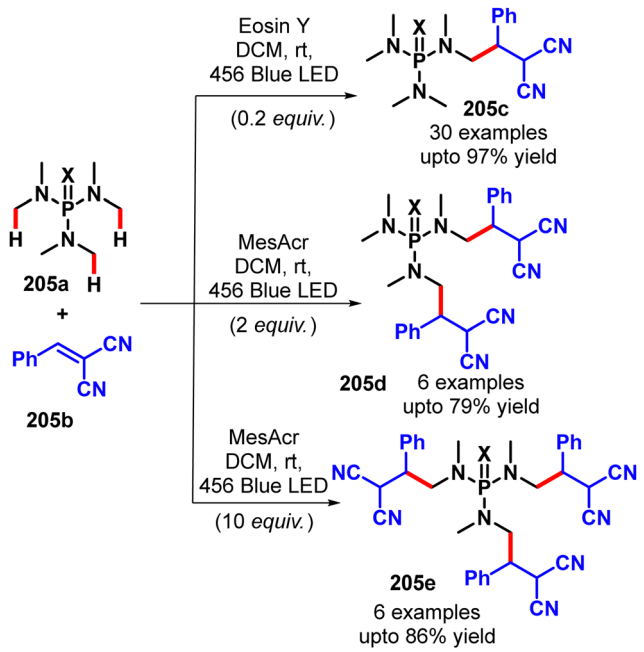

Scheme 205 Organophotocatalysed direct multiple α-C(sp^3)–H alkylation of phosphoramides (Ghosh *et al.*[267]).

direct sp^3 C–H functionalisation of ethers, amides, alcohols and even unactivated hydrocarbons (Scheme 206).[268] However, when bromoalkyne **206d** was used instead of chloroalkyne **206c**, a chemoselectivity switch to sp^3 C–H alkynylation **206f** was observed instead of vinyl halide.

Very recently, Xu and co-workers designed a novel naphthalimide based organic photocatalyst (Cz-NI) for the direct C(sp^3)–H carbamoylation of saturated aza-heterocycles **207a** by oxidative Ugi reaction under mild conditions (Scheme 207).[269] A high primary kinetic isotope effect (k_H/k_D= 3.3) indicated that the C(sp^3)–H bond cleavage was the rate limiting step of this carbamoylation reaction. After thorough experiments, it was also confirmed that the oxygen atom of the carbonyl group in the amide product came from the water generated by the photocatalytic process from pentafluoro nitrobenzene (PFNB).

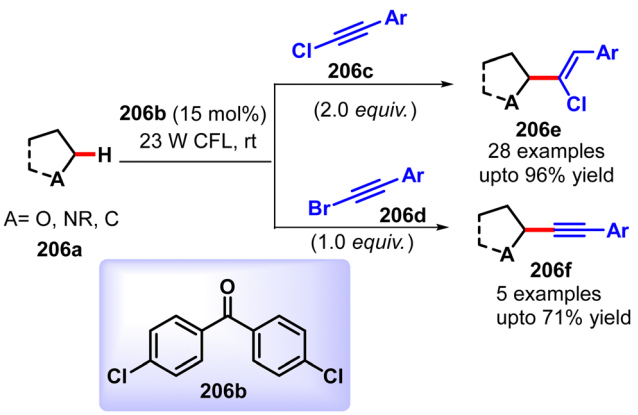

Scheme 206 Chemoselective sp^3–C–H functionalisation with chloro- and bromoalkynes (Adak *et al.*[268]).

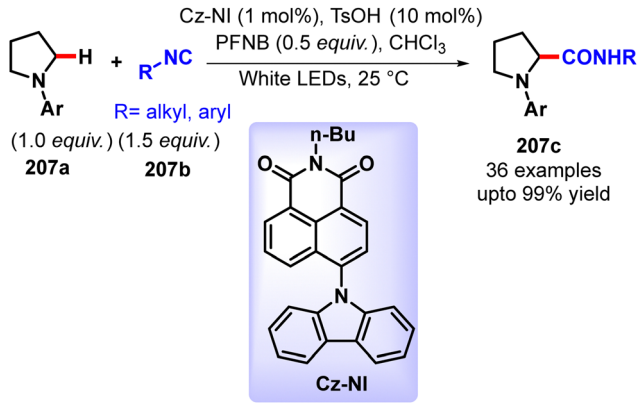

Scheme 207 Cz-NI catalysed direct C(sp^3)–H carbamoylation of saturated aza-heterocycles (Yi *et al.*[269]).

5.1.3 C–Heteroatom bond formation

5.1.3.1 C–N bond formation. Among other heteroatoms, the development of efficient methods to fabricate C–N bonds often portrays an important and appealing goal in modern day synthetic chemistry. Over the last two decades, C–H functionalisation involving a radical process has emerged as an ideal, cost effective, greener approach to construct C–N bonds and in this direction organo-photocatalysis offers a worthwhile access to generate the radical species.

The intermolecular C–N coupling reaction is always challenging from unactivated precursors due to the inert nature of N–H bonds. In 2017, Xia *et al.* successfully developed a CDC method through merging organic photoredox catalyst **208c** with persulfate as an oxidant to enable the direct cross-coupling reaction between phenols **208a** and acyclic diarylamines **217b** to produce triarylamines **208d** (Scheme 208).[270] In this transformation, they used 2,4,6-triphenylpyrylium salt as the organo photoredox catalyst **208c** and $(NH4)_2S_2O_8$ as an oxidant as the best optimised condition. However, the efficiency of this reaction was closely related to the electronic effects of the substituent on the diaryl amines. The amines bearing electron-donating groups, *i.e.*, methyl and *tert*-butyl, afforded the product more readily with moderate to good yield. The Stern–Volmer quenching experiments and the EPR experiments suggested that the diarylamine was able to quench the excited state of the photocatalyst much more efficiently than phenol. Based on the experiments, a mechanism was proposed as the SET pathway by the excited photocatalyst by abstracting an electron from amine **208b** to produce PC anion radical and amine cation radical **208e**. The ground state of PC was then regenerated from $PC^{\bullet -}$ by donating an electron to $SO_4^{\bullet -}$. On the other hand, phenol **208a** became oxidised by the amine cation radical **208e** to phenoxonium radical **208f** and regenerated the amine through radical chain propagation. Afterward, the *N*-centered radical cation **208e** released a proton and coupled with phenoxonium radical **217g** to furnish the final product **208d**.

However, the direct C–H/N–H amination with aliphatic amines remains an unmet challenge since many methods for their functionalisation lead to C–C bond formation α- to the

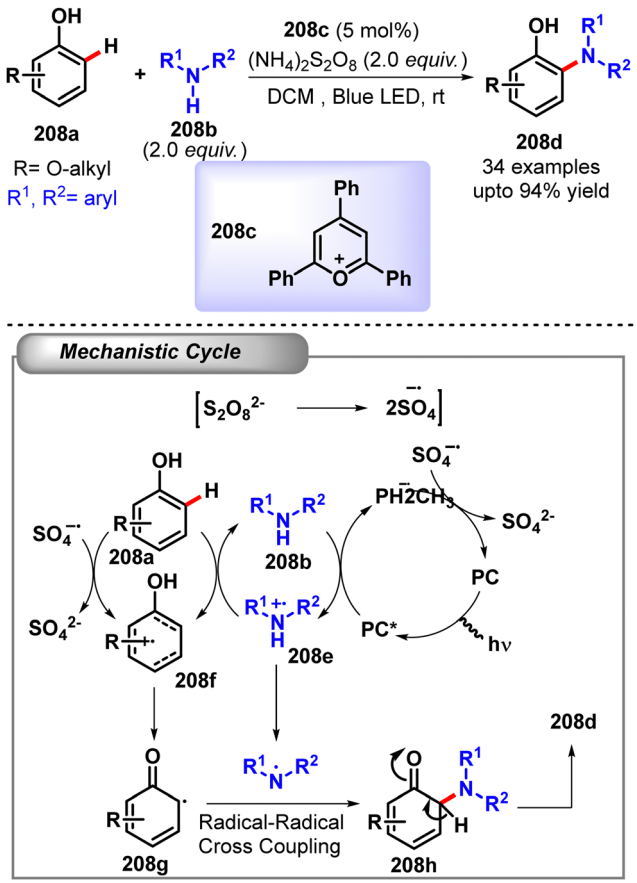

Scheme 208 Organophotoredox catalysed cross-dehydrogenative amination between phenol and diarylamine (Zhao *et al.*[270]).

nitrogen atom. Although organometallic cross-coupling chemistry has evolved as one of the most reliable approaches to assemble complex aromatic compounds, only a few mild metal free photocatalytic aminations have been reported so far.

Among these, Nicewicz's group demonstrated an excellent prototype for site-selective aryl C(sp^2)–H amination of a variety of simple and complex aromatics **209a** with pharmaceutically valuable heteroaromatic azoles **209b** through an organic photoredox catalyst system consisting of an acridinium catalyst **209c** and a nitroxyl radical co-catalyst (Scheme 209).[271] In most cases of aromatic substrates, good selectivity for the *p*-regioisomer over the *o*-regioisomer was obtained, and for some aromatic heterocycles and disubstituted benzenes, only a single product was detected. In addition, they explored this catalytic sequence for the direct synthesis of aniline using ammonium carbamate. A probable mechanism was delineated as the initial photoexcitation of Mes-Acr+ followed by reduction of it to the acridine radical Mes-Acr$^{\bullet}$ and aryl cation radical **209e**. This cation radical then interacted with azole **209b** and a subsequent deprotonation would generate the adduct radical **209g**. Next TEMPO took part in the reaction to aromatize radical intermediate **209g** directly by H-atom abstraction to afford the product **209d**.

In this direction, a couple of years later, the Nicewicz group again developed an acridinium photo-redox catalysed direct

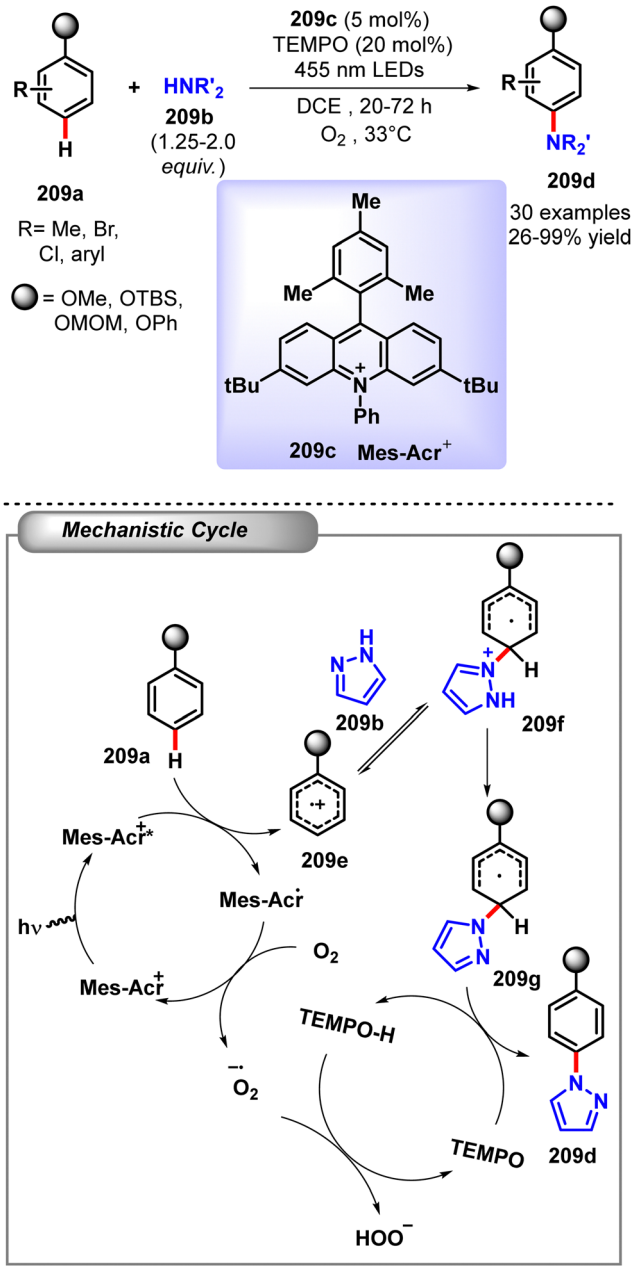

Scheme 209 Organophotoredox catalysed site-selective arene C–H amination (Romero *et al.*[271]).

C–H functionalisation of various electron-rich aromatics and heteroaromatics **210a** for the construction of C–N bonds employing primary amines **210b** under an aerobic atmosphere (Scheme 210).[272] A broad variety of primary amines such as amino acids, more complex amines along with the electron rich aromatics including biologically active arenes were the competent coupling partners in this reaction. A plausible mechanism was proposed which involved the initial photo excitation of Mes-Acr$^+$ to Mes-Acr^{+}* followed by subsequent oxidation of amine **210b** to generate the amine radical cation **210d**. The addition of the arene **210a** to the amine radical cation formed the cyclohexadienyl radical intermediate **210e** which could be rearomatized using molecular oxygen.

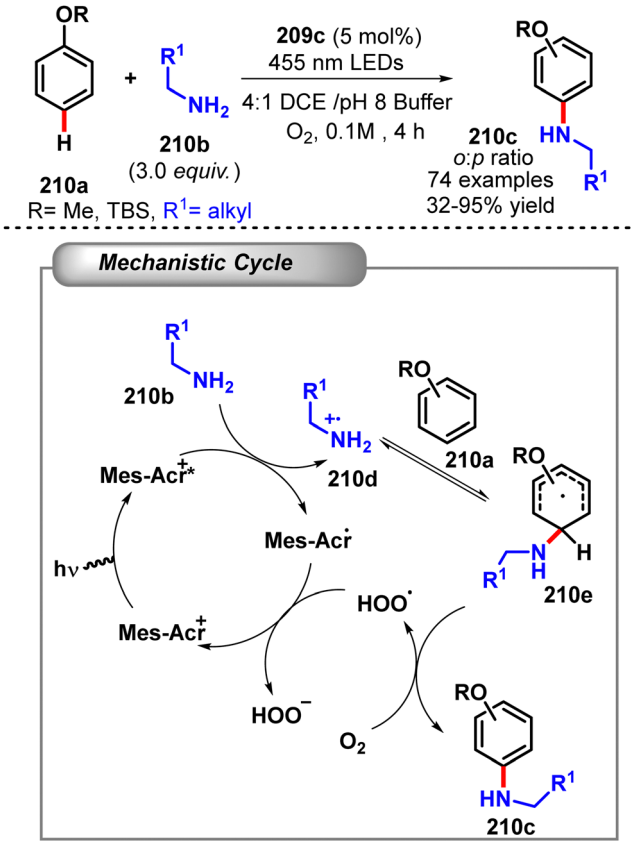

Scheme 210 Organophotoredox catalysed site-selective arene C–H amination with primary amines (Margrey *et al.*[272]).

The next year, they developed a similar acridinium-based photocatalytic methodology for the visible light mediated C(sp^3)–H azidation of aliphatic compounds **211a** using sulfonyl azide **211b** as the azide source in combination with K_3PO_4 as a key additive in HFIP as the solvent (Scheme 211).[273] This method was applicable for a wide range of cyclic as well as acyclic hydrocarbons and drug molecules with moderate to good yield. Most strikingly in contrast to previous reports, the excited state photocatalyst (Mes-Acr + *) was not directly involved in the alkane C–H activation step; rather it would be able to oxidize the phosphate to the corresponding oxygen centred radical which was then able to abstract a hydrogen radical from the hydrocarbon **211a** to form the aliphatic radical intermediate **211e**. This aliphatic radical was then trapped by the sulfonyl azide **211b** to provide the final product **211c**. The ground state of the catalyst was regenerated by a back-electron transfer to the sulfonyl radical.

Afterwards, Wei and Zhao reported an Eosin Y catalyzed visible-light-induced direct C(sp^2)–H/N–H CDC-amination of quinoxalin-2(1*H*)-one **212a** with both aliphatic primary and secondary amines **212b** leading to 3-aminoquinoxalin-2(1*H*)-ones **212c** (Scheme 212).[274] Based on control experiments, a tentative mechanism was proposed as the SET pathway by the excited Eosin Y* affording the Eosin Y$^{\bullet-}$ radical anion and amine nitrogen radical cation **212d**. Subsequently, the oxidation of Eosin Y$^{\bullet-}$ by dioxygen (air) generated the ground state Eosin

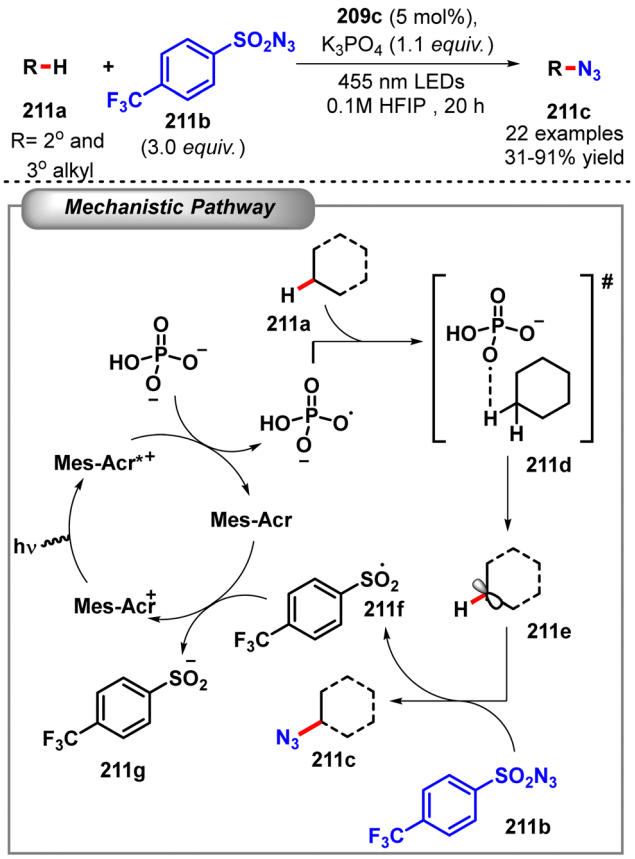

Scheme 211 Organophotoredox catalysed aliphatic C–H azidation (Margrey *et al.*[273]).

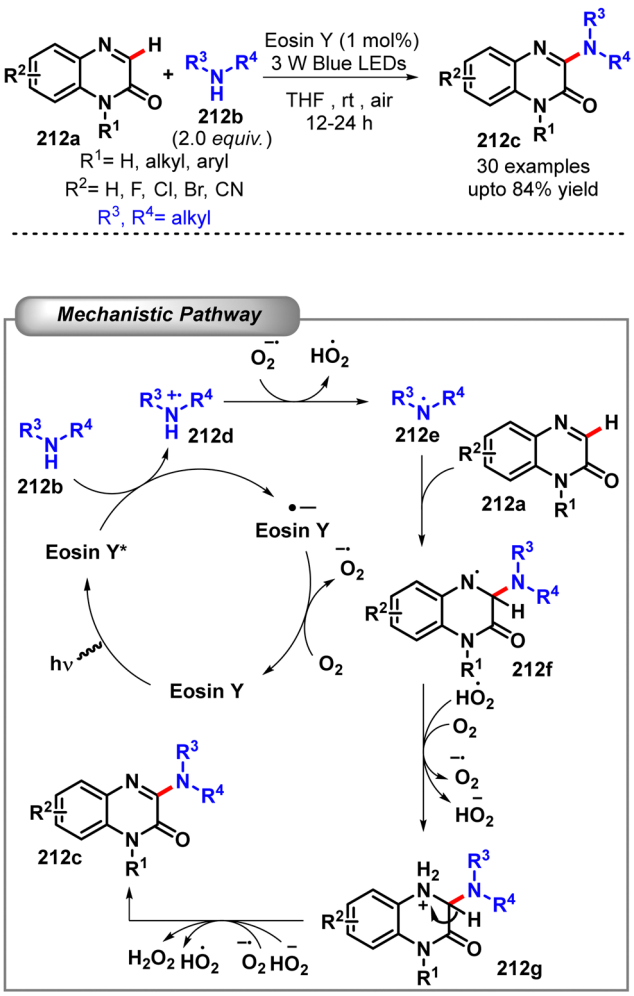

Scheme 212 Organophotoredox catalysed cross-dehydrogenative coupling of quinoxalinones with aliphatic amines (Wei *et al.*[274]).

Y and $O2^{\bullet-}$. Next the nitrogen radical intermediate **212e** was formed by the deprotonation of the nitrogen radical cation **212d** by $O_2^{\bullet-}$ which then encountered quinoxalin-2(1*H*)-one **212a** followed by oxidation through the SET process and deprotonation to finally afford the desired C–N coupled compound **212c.**

Guan and co-workers utilised Rose Bengal as a metal-free organic photocatalyst for alkene C–H amination at the benzylic position upon visible-light irradiation in open air for the efficient synthesis of a series of *N*-vinylazole derivatives **213c** (Scheme 213).[275] A plausible reaction mechanism was proposed involving the initial photoexcitation of the photocatalyst RB followed by a single-electron oxidation of benzotriazole **213a** by RB* to generate the cation radical **213d** along with RB(–). RB(–) was then oxidized to regenerate the ground state of RB by O_2 through the generation of a superoxide anion radical. Further, the deprotonation of the cation radical **213d** resulted in the formation of azole radical **213e** which subsequently reacted with 2-benzylidenepropanedinitrile **213a** to produce the radical intermediate **213f.** Then, **213f** underwent another single-electron transfer (SET) oxidation and deprotonation to deliver the desired product **213c.** During this process, the superoxide radical anion accepts two protons and one electron to form H_2O_2.

In 2019, Rafique and Braga disclosed an Na_2 eosin-Y catalyzed C–N bond formation reaction through the C(sp^2)–H azo coupling of imidazo-heteroarene **214a** with aryl diazonium salts, under acid free conditions in good to excellent yields (Scheme 214).[276] This reaction is complementary to Konig's C–C bond formation reactions. Based on the thorough control experiments, the reaction might be operating *via* two possible mechanisms, *i.e.* radical and ionic pathways.

In 2019, Konig and his team developed the idea of semiconductor photoredox catalysis (SPC) through the visible-light-responsive hexagonal boron carbon nitride (h-BCN) photocatalyst for C–H/N–H coupling of arenes **215a** with azoles **215b** (Scheme 215).[277] It was observed that O_2 and visible light were indispensable elements for this amination reaction. In contrast to the homogeneous photosensitizer, this catalyst exhibited remarkable performance for the selective arene C(sp^2)–H functionalisation (yields up to 95%) as well as good stability (6 recycles). The method was suitable for a wide range of substrates with satisfactory site selectivity. The probable mechanism suggested that the semiconductor was photoexcited to give electrons and holes. Afterwards, the carbon cationic radical **215d** was generated upon SET from the arene **215a** to the catalyst. Subsequently a nucleophilic substitution/deprotonation/oxidative aromatization occurred to generate the desired product **215c.**

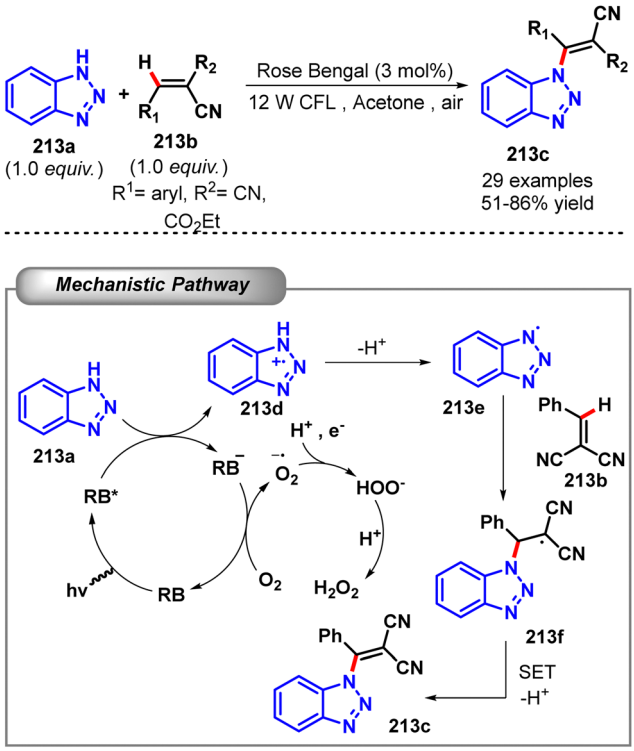

Scheme 213 Organophotoredox catalysed aerobic oxidative direct C–H amination of electron deficient alkenes (Xin *et al.*[275]).

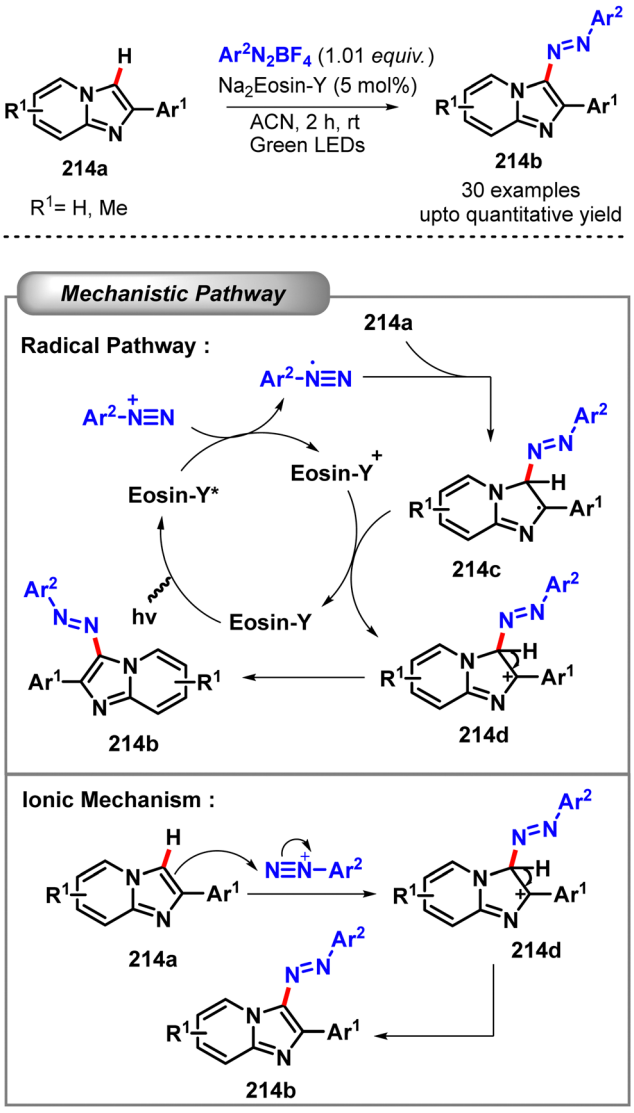

Scheme 214 Organophotoredox catalysed direct C(sp^2)–H bond azo coupling of imidazo heteroarene (Saba *et al.*[276]).

Earlier in 2015, Lijser and co-workers developed a novel visible light-photocatalyzed oxidative cyclization of 2′-arylbenzaldehyde oxime ethers **216a** in the presence of 9,10-dicyanoanthracene (DCA) as a photosensitizer in acetonitrile for the synthesis of phenanthridines **216b** (Scheme 216).[278] This oxidative cyclization exhibited high functional group tolerance and a broad substrate scope. The mechanism involved the initial oxidation of the oxime ether **216a** to the corresponding radical cation intermediate **216c** followed by the nucleophilic attack by the aromatic ring onto the nitrogen of the oxime ether radical cation leading to the formation of a Wheland-type cation **216e** and an α-amino radical. This α-amino radical presumably underwent a rapid N–O bond homolysis, and a subsequent deprotonation of the cyclized cation intermediate **216f** finally afforded the phenanthridine product **216b**.

5.1.3.2 C–O bond formation. The wide occurrence of the C–O bond in numerous biologically active molecules and natural products has earned much attention from the synthetic organic chemists to develop an efficient method for the construction of the C–O bond. Herein we particularly focus on the metal-free photoredox catalysed C–H functionalisation for the synthesis of the C–O bond.

In 2017, Hajra and co-workers developed direct C-3 alkoxylation of imidazopyridines **217a** by employing Rose Bengal as an inexpensive and nontoxic organic dye under visible light photoredox catalysis at ambient temperature (Scheme 217).[279] The beauty of the method was the usage of air as the sole green oxidant. This method was well explored through a wide range of substrate scopes and functional group tolerance.

Successively, the group also delivered an efficient visible-light-promoted regioselective route for the acyloxylation of C(sp^3)–H of aryl-2*H*-azirines **218a** using PIDA by utilising the same organic dye (Scheme 218).[280] The most striking feature of this reaction was the selective C(sp^3)–H functionalisation over the easy ring opening of the strained azirine ring. By comparing the redox potential of RB, azirine as well as PIDA, the authors had reasonably suggested that the excited state of rose bengal (RB*) has been oxidized by PIDA and generated the acetoxy radical ($CH_3COO^{\bullet}$) and the acetate anion (CH_3COO^-), along with an RB radical cation ($RB^{+\bullet}$). A successive HAT from **218a** by the acetoxy radical followed by a single electron transfer to the RB+ led to the formation of intermediate azirine carbocation **218d** and regenerated the ground state of the photocatalyst (RB). Finally, the nucleophilic attack by the acetate anion on the newly generated carbocation **218d** afforded the desired acetoxylated product **218b**.

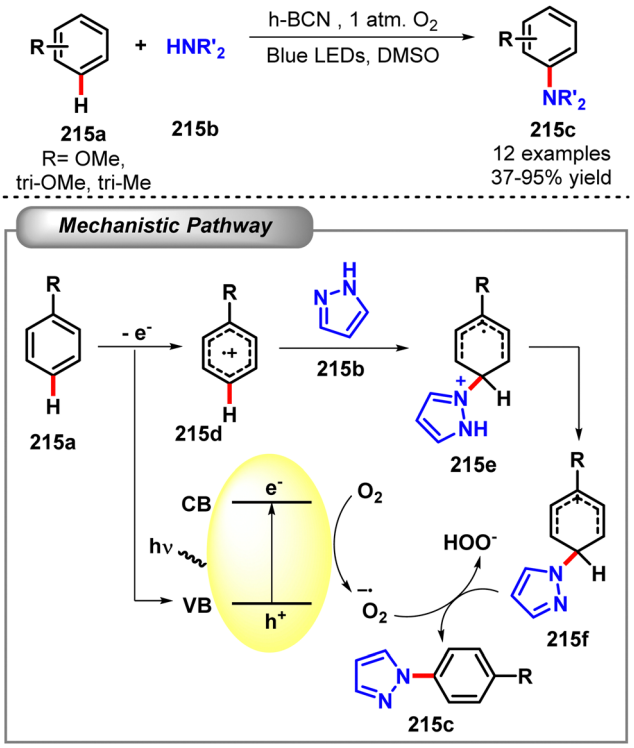

Scheme 215 Semiconductor photocatalysis for C(sp^2)–H functionalisation (Zheng *et al.*[277]).

Later, in 2019 Li and his group also reported mesityl acridinum catalysed visible light induced alkoxylation of quinoxalin-2(1*H*)-ones **219a** with various primary and secondary alcohols under ambient conditions to render the corresponding 3-alkoxylated quinoxalin-2(1H)-ones **219b** in good yields (Scheme 219A).[281] Here also, the atmospheric oxygen acted as the sole oxidant like the earlier one. Recently, the Hao group also reported a similar visible light induced C3–H fluoroalkoxylation of quinoxalin-2(1*H*)-ones **219a** with readily available fluoroalkyl alcohols by employing Eosin-Y as the organic photoredox catalyst (Scheme 219B).[282] As usual, the control experiments suggested a radical pathway for this reaction.

5.1.3.3 C–P bond formation. Phosphorus containing aromatic compounds play a crucial role in regulating the physical, chemical, and biological properties of the adjacent arenes, making them useful in organic synthesis, materials science, and inorganic chemistry. Therefore, transition-metal-catalyzed strategies of C–P bond formation are sufficiently described in the literature, but naturally, we are most interested in the metal-free synthesis of the same. In 2016, the Wu group first reported the eosin B catalysed visible light promoted first direct C–H phosphorylation of thiazole derivatives **229a** with diaryl/dialkyl phosphine oxides **220b** (Scheme 220A).[283] A wide variety of thiazole derivatives as well as different phosphine oxides were examined in this cross dehydrogenative coupling reaction. While the electron withdrawing group on the thiazole or benzothiazole increased the reactivity and the yield, the electron donating substituent afforded moderate yield. Meanwhile H_2 was the only bi-product in this transformation which was further determined by the generation of D_2 while employing the deuterium versions of the starting materials. Shortly after this report, a similar type of Na_2 Eosin Y catalysed visible light-promoted C–H phosphorization of benzothiazoles for the construction of arylphosphonates was also showcased by the Lei group (Scheme 220B).[284] In this transformation, oxygen was used as the sole green oxidant and the EPR study clearly revealed the formation of the phosphonyl radical intermediate during the process.

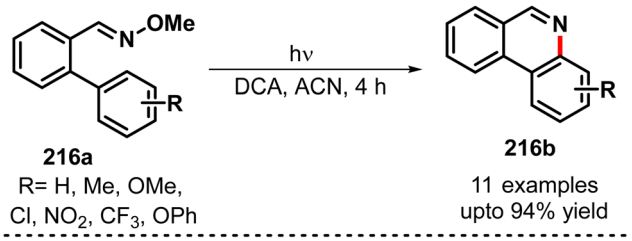

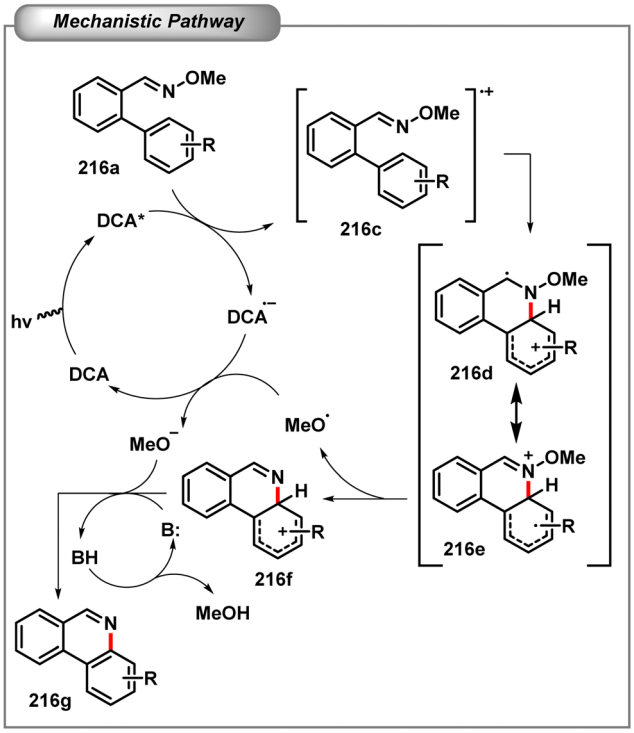

Scheme 216 Catalytic oxidative cyclization of 2′-arylbenzaldehyde oxime ethers (Hofstra *et al.*[278]).

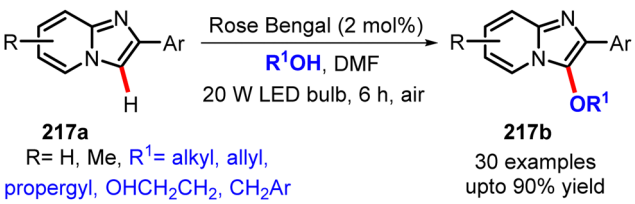

Scheme 217 Organophotocatalysed direct C-3 alkoxylation of imidazopyridines (Kibriya *et al.*[279]).

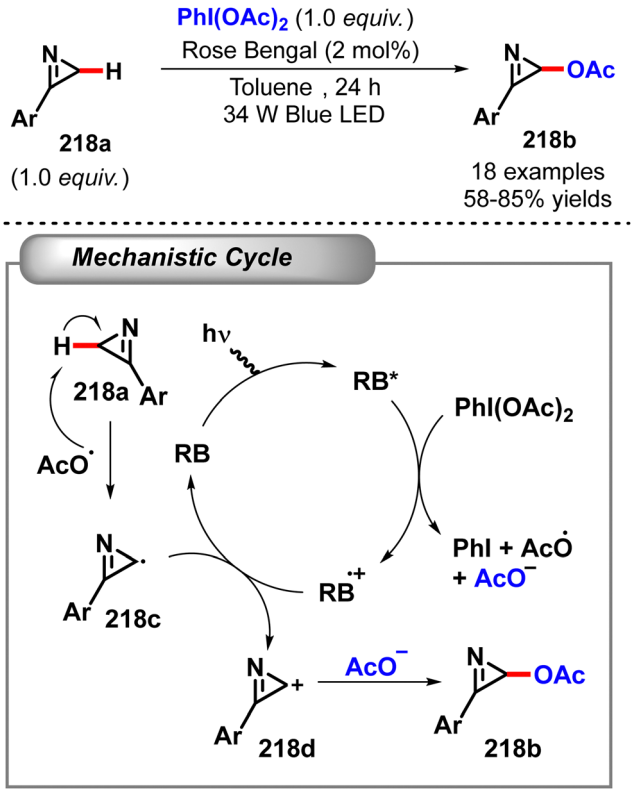

Scheme 218 Organophotocatalysed regioselective C(sp^3)–H acyloxylation of aryl-2H-azirines (De *et al.*[280]).

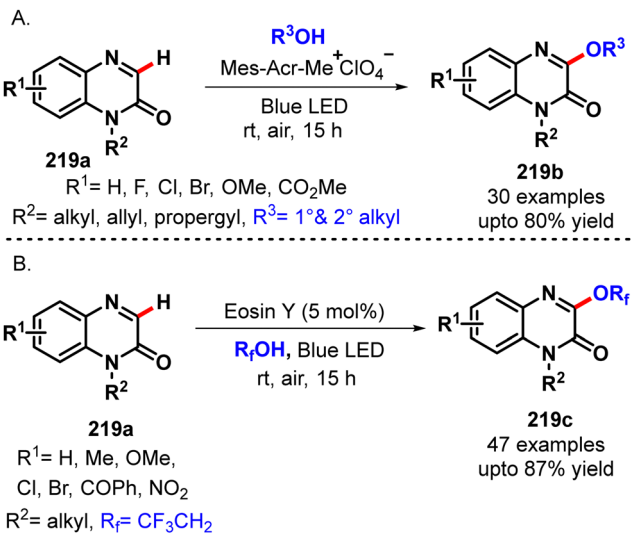

Scheme 219 Organophotocatalysed alkoxylation of quinoxalin-2(1*H*)-ones (Zhao *et al.*,[281] Xu *et al.*[282]).

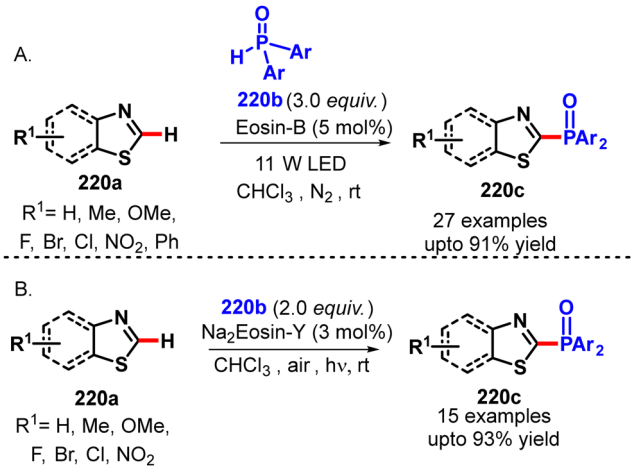

Scheme 220 Organophotocatalysed C(sp^2)–H phosphorization of benzothiazole (Luo *et al.*,[283] Peng *et al.*[284]).

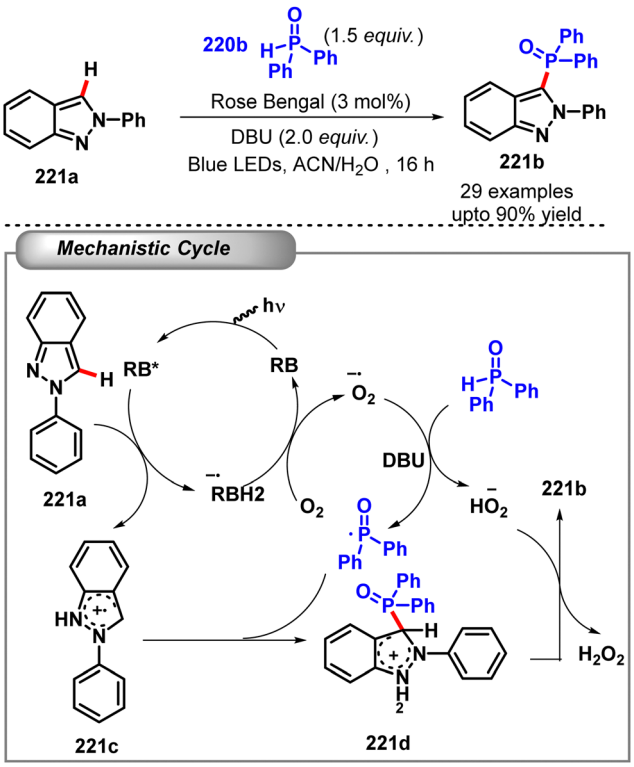

Scheme 221 Organophotocatalysed aerobic radical C(sp^2)–H phosphonylation of 2H-indazoles (Singsardar *et al.*[285]).

Two years later, Hajra and co-workers developed a visible-light-induced phosphonylation of 2H-indazoles **221a** with diphenylphosphine oxide using Rose Bengal as an organophotoredox catalyst under ambient air at room temperature (Scheme 221).[285] Based on the control experiments, a plausible mechanism was suggested involving the initial oxidation of indazole **221a** to indazole radical cation **221c** along with $RB^{\bullet -}$. The photocatalyst was regenerated by reducing O_2 to the superoxide radical anion ($O_2^{\bullet -}$) which acted as a HAT catalyst to generate the P-centered diphenylphosphinoyl radical in the presence of DBU. Thereafter, the intermolecular coupling between indazole radical cation **221c** and the diphenylphosphinoyl radical generated cation intermediate **221d**. Finally, the deprotonation by HO_2^- from intermediate **221d** afforded the phosphonylation product **221b**.

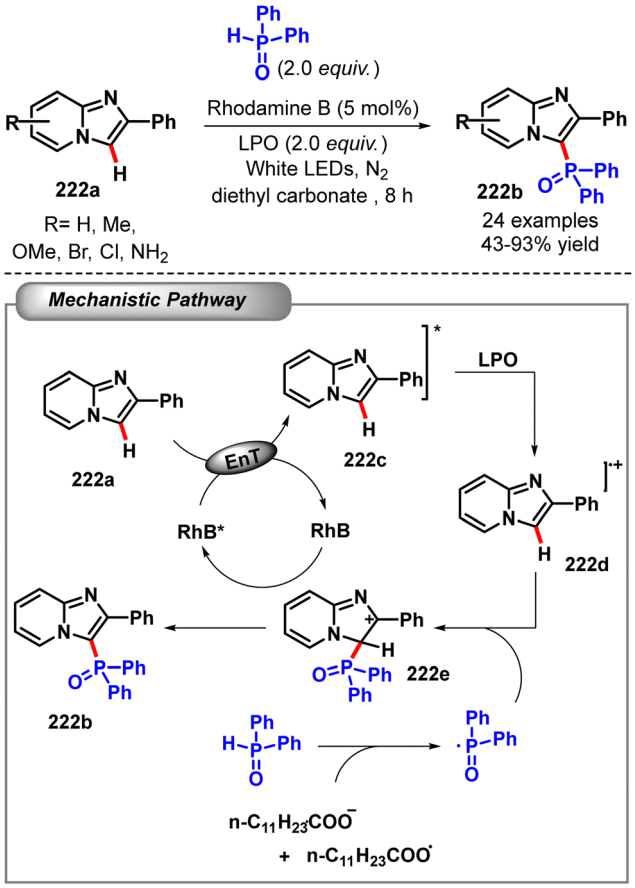

Scheme 222 Organophotocatalysed phosphorylation of imidazo-fused heterocycles (Gao *et al.*[286]).

Recently, the Yu group disclosed a metal and base-free procedure for the Rhodamine B catalysed visible light promoted phosphorylation of imidazo[1,2-*a*] pyridines **222a** with phosphine oxides at room temperature (Scheme 222).[286] On the basis of the results of control experiments, a plausible mechanism was proposed for this visible-light-promoted reaction. Considering the oxidation potential of imidazo pyridine **222a** [+1.68 V (*vs.* SCE)] and the redox potential of RhB* [+1.26 V (*vs.* SCE)], the SET process between **222a** and RhB* could be ruled out. However, an energy transfer (EnT) process should be involved between **222a** (S0) and RhB*, providing the triplet state **222a** (T) along with the regeneration of RhB. Subsequently, the reaction between **222c** (T) and LPO generated the radical cation **222d** along with the anion and radical from LPO, which could react with phosphine oxides *via* the HAT process to produce the phosphoryl radical. Finally, the coupling of intermediates **222d** and the phosphoryl radical delivered the corresponding cation **222e**, which was then converted into the desired product **222b** *via* deprotonation.

5.1.3.4 C–Halogen bond formation. Since organohalides are essential substrates for both classic organic chemistry and metal-mediated cross-coupling reactions, the ability to introduce a halogen atom into a molecule is of great importance in the study of synthetic organic chemistry.

5.2 Fluorination reaction

In 2013, the Chen group reported an organophotoredox catalysed, operationally simple method for the direct conversion of benzylic C–H groups **223a** to C–F (Scheme 223).[287] However, the choice of the catalyst could provide the selective formation of mono- and difluorination products. In that aspect, 9-fluorenone catalyzed the benzylic C–H monofluorination **223b**, while the xanthone catalyst promoted benzylic C–H difluorination **223c**. Here, selectfluor (I and II) had been used for the fluorine donor for such transformation respectively. A probable mechanism suggested that an intermolecular benzylic C–H abstraction by a photoexcited ketone would give benzylic radical **223d** and a subsequent atom transfer from an electrophilic fluorinating agent would provide benzylic fluoride **223b**. Furthermore, the modest primary KIE value (1.9) indicated that a non-metal radical C–H abstraction was involved in the rate-determining step.

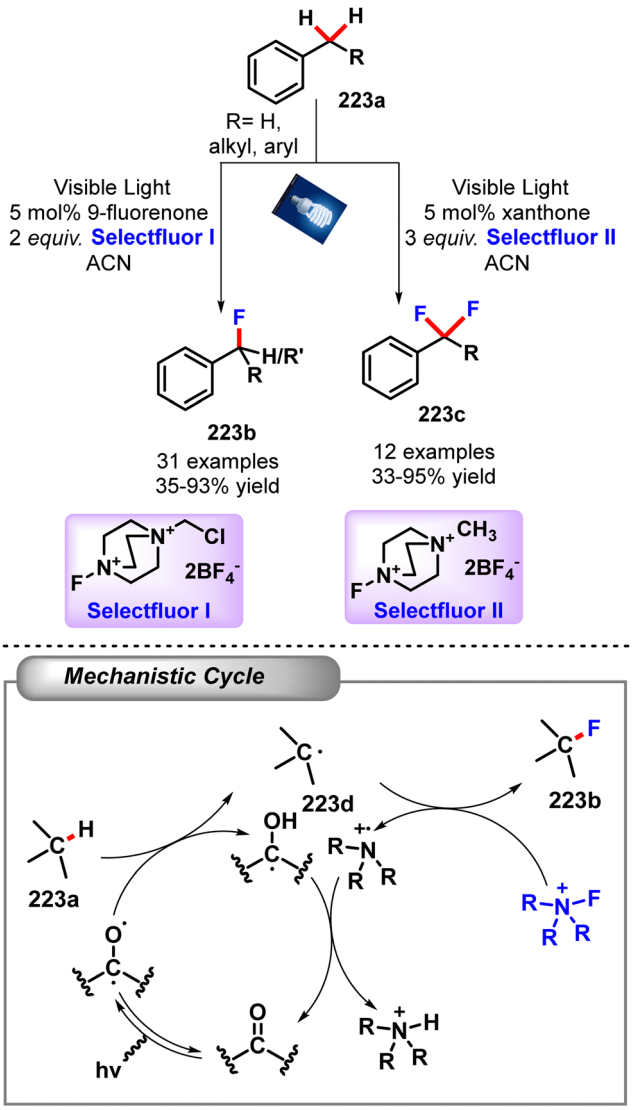

Scheme 223 Visible light promoted organophotocatalysed selective benzylic mono- and difluorination (Xia *et al.*[287]).

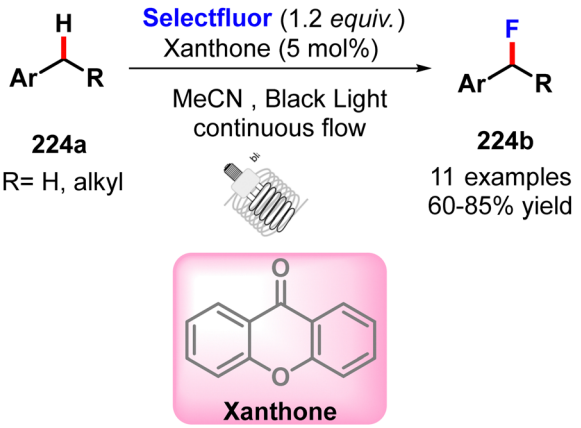

Scheme 224 Visible light promoted organophotocatalysed continuous-flow process for benzylic fluorinations (Cantillo *et al.*[288]).

The very next year, Cantillo *et al.* demonstrated a similar light induced benzylic C–H fluorination **224b** through a continuous-flow protocol in less than 30 min reaction time (Scheme 224).[288] They also utilised selectfluor as the fluorine source and xanthone as an organo-photoredox catalyst. In contrast to the earlier one, they only obtained the monofluorination product **224b** by using xanthone. It is worth mentioning that the flow photoreactor is based on transparent fluorinated ethylene propylene tubing and a household compact fluorescent lamp. The combination of xanthone with black-light irradiation resulted in very efficient fluorination.

5.2.1 Photocatalyst free only light promoted C–H bond functionalisation. It has been noted that functionalizing a C–H bond under visible light conditions does not always necessitate the use of an exogenous photocatalyst. Either the substrates can form a charge transfer complex when exposed to visible light, or they can absorb light and become excited at the specified frequency. These properties lead to the sustainability of the photo induced reactions.

In this regard, in 2019, Jin and Zhao utilised selectfluor **225c** as a HAT reagent under visible light irradiation for the direct arylation of unactivated C(sp^3)–H bonds **225b** with heteroarenes **225a** (Scheme 225).[289] Initially, selectfluor **225c** was activated by visible light irradiation to generate *N*-radical cation **225e** which can abstract a hydrogen atom from alkane **225b** to provide alkyl radical **225g** which was then intercepted by protonated electron-deficient heteroarene **225a'** to furnish aminyl radical cation **225h**. Deprotonation followed by SET to the selectfluor furnished the desired alkyl-aryl coupling product **225d**. In this method, they demonstrated a diverse range of chemical feedstocks, such as alkanes, ketones, esters, and ethers, and complex molecules that readily undergo intermolecular C(sp^3)–C(sp^2) bond formation with a broad array of heteroarenes.

In the same year, Kumar and co-workers reported a unique exogenous photocatalyst free visible light induced method for the organochalcogenylation of the sp^2 C–H bond of indoles **226a** using diaryl dichalcogenides **226b** (S, Se, and Te) (Scheme 226).[290] Various functionalities on either indoles or aryl dichalcogenides exhibited amenability to this developed reaction. The mechanistic

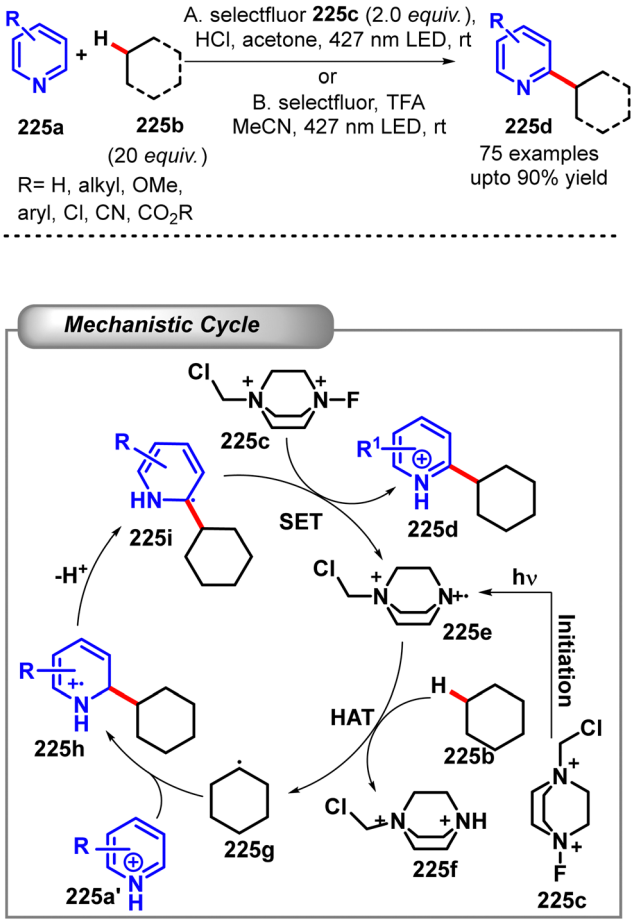

Scheme 225 Visible light promoted aliphatic C–H arylation (Zhao *et al.*[289]).

studies suggested the initial formation of indole radical cation **226d** upon visible light irradiation and simultaneous reaction with molecular oxygen. This radical cation **226d** could be stabilized by resonance to indolyl radical **226d'** which in turn reacted with diaryl dichalcogenide, forming an arylchalcogenylated indole cation **226e**. The anion radical of $O2^{\bullet -}$ generated by visible light irradiation would abstract a proton from cation **226e**, and thus would facilitate the formation of desired unsymmetrical selenide **226c** and perhydroxyl radical $HO_2^{\bullet}$. In the second cycle, this perhydroxyl radical was converted to hydrogen peroxide which was confirmed by ^{1}H NMR.

Nevertheless, Melchiorre *et al.* developed a visible light-mediated C–H hydroxyalkylation of quinolines and isoquinolines **227b** by exploiting the excited-state reactivity of 4-acyl-1,4-dihydropyridines **227a**, which can readily generate acyl radicals **227d** upon blue light absorption without the assistance of an external photocatalyst or oxidant (Scheme 227).[291] A plausible mechanism was suggested wherein the photoexcited acyl-DHP **227a*** was oxidized by the pyridinium ion to form an unstable acyl-DHP radical cation which generated the acyl radical **227d** by homolytic cleavage. This acyl radical **227d** then reacted with the protonated heteroarene **227e** to form radical cation intermediate **227f**. Furthermore, a proton-transfer and spin-centre-shift followed by a SET process afforded the final product **227c**. The method

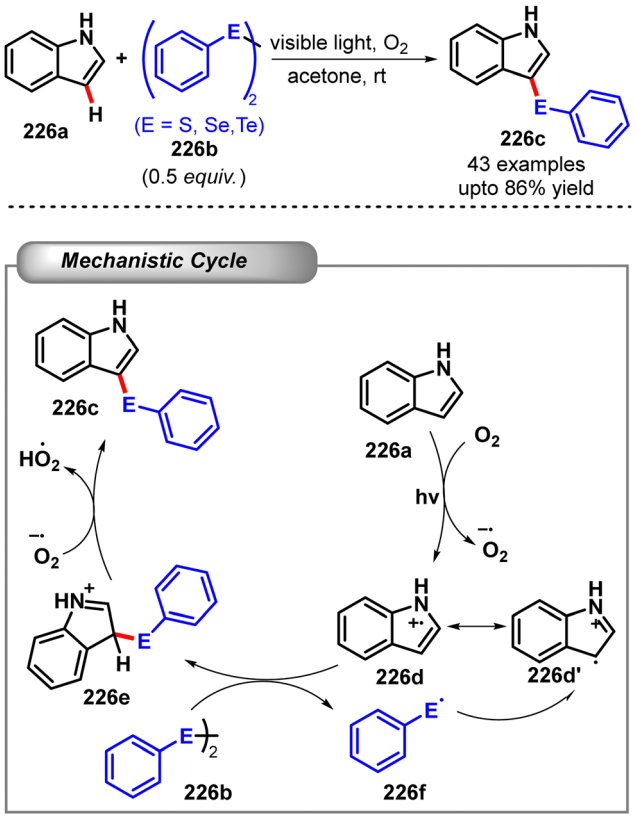

Scheme 226 Visible-light induced reagent free C-3 chalcogenation of indoles (Rathore *et al.*[290]).

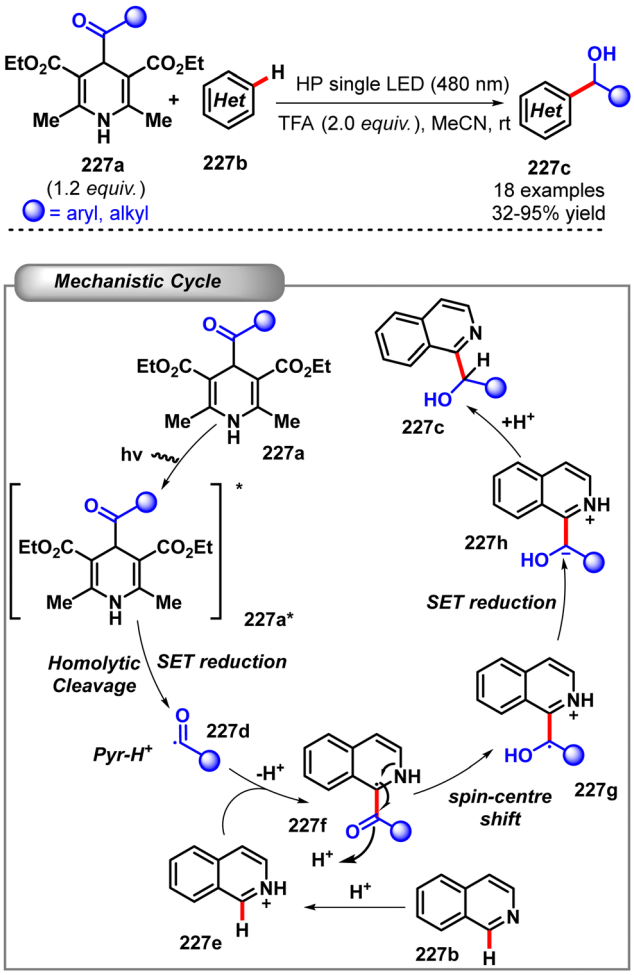

Scheme 227 Photochemical C–H hydroxylation of heteroarenes (Bieszczad *et al.*[291]).

showcased high functional group tolerance which was accounted for the late-stage functionalisation of active pharmaceutical ingredients and natural products.

5.2.2 Electron donor–acceptor (EDA) complexes. Electron donor–acceptor (EDA) complexes are the aggregates of electron rich and electron deficient compounds. These complexes can controllably generate radicals under mild conditions through selective photoexcitation events. Recently, Stephenson and his team have come up with a similar idea where they manifested the visible light-driven sp^2 C–H trifluoromethylation and Minisci alkylation reactions by employing 2-methoxynaphthalene **228c** as a donor and acylated ethyl isonicotinate *N*-oxide **228e** as an acceptor that undergo a fast N–O bond fragmentation upon photoexcitation (Scheme 228).[292] In this reaction they showed the rare example of EDA photochemistry in a catalytic regime by regenerating the donor species during the reaction.

Earlier in 2019, Glorious and co-workers described the alkylation of heteroarenes or enamines through the photoexcitation of EDA complexes between traceless pyridinium salt acceptors **229b** and heteroarene or enamine donors **229a** (Scheme 229).[293] However, the addition of morpholine **229c** as base dramatically improved the yield of the alkylation reaction which suggested that there was a chance to form 1:1 complexes of indole **229a** and morpholine **229c** along with indole **229a** and [PyN]-AlaOMe **229b**. Their molar extinction coefficients suggested that complex **229b** was the most photochemically active species. The detailed mechanistic study suggested that the photoexcited charge transfer from indole **229a** to pyrilium salt **229b** helped to generate alkyl radical **229g** by fragmentation from pyrilium radical **229e**. This radical was further added to indole **229a** to form radical intermediate **229h**. Another SET process between radical intermediate **229h** and the complex of pyridinium salts **229b** and morpholine **229c** afforded the alkylation product **229d** and regenerated pyridinyl radical **229e**.

In 2020, de Oliveira and co-workers described a visible-light induced C–H arylation of diazines **230a** with aryldiazonium salts **230b** by the generation of an EDA complex between diazines and aryldiazonium salt (Scheme 230).[294] The crucial step involved the formation of an aryl radical **230d** through a SET process in the excited state of a photoactive EDA complex. It is worth mentioning that the DMSO solvent played an important role in forming the EDA complex.

Contemporarily, Xu and co-workers also disclosed a visible-light-promoted deaminative C(sp^3)–H alkylation of glycine and peptides **231a** using Katritzky salts **231b** as alkylation reagents (Scheme 231).[295] Mechanistic studies suggested the formation of a colored EDA complex in the presence of **231a** and **231b** (a ternary EDA complex might form in the presence of DBU). Under violet LED (395–400 nm) irradiation, a SET process was

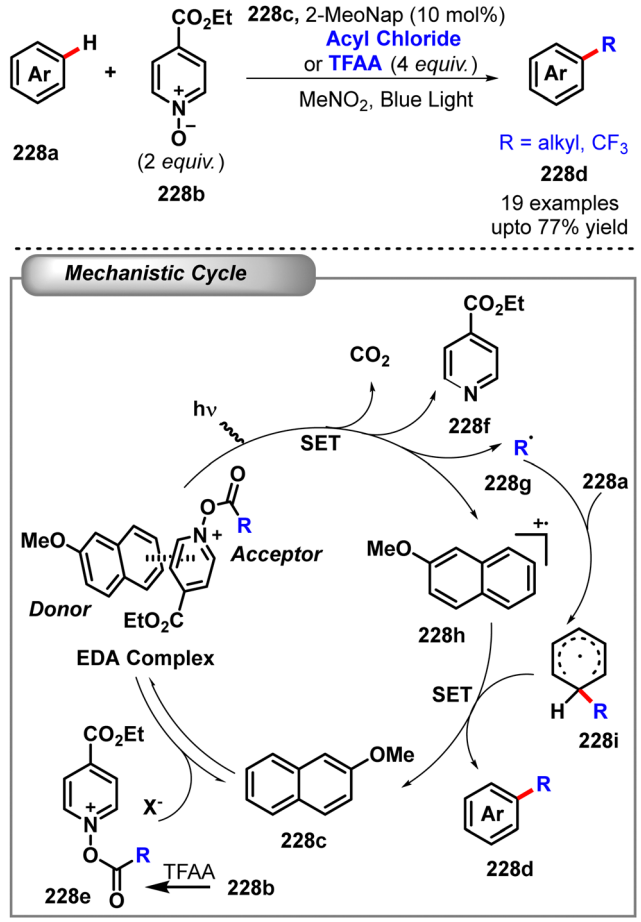

Scheme 228 Catalytic electron donor–acceptor complex platform for radical trifluoromethylation and alkylation of arene (McClain *et al.*[292]).

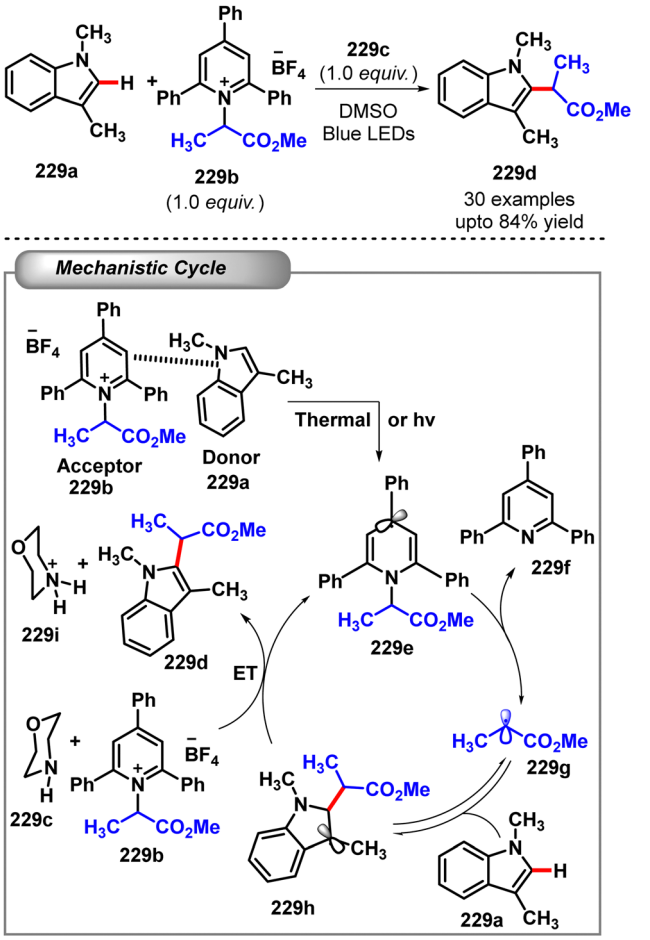

Scheme 229 Visible light mediated charge transfer enables C–C bond formation (James *et al.*[293]).

realized between **231a** and **231b** to generate radical **231d** which was fragmented to form 2,4,6-triphenylpyridine and an alkyl radical **231f**. Simultaneously, radical cation **231e** was deprotonated under basic conditions to provide a stable α-carbon radical **231g**. Finally, the radical–radical cross coupling between **231f** and **231g** gave the desired alkylated product **231c**.

6 Metal free C–H activation

6.1 FLP catalysed C(sp^3)–H activation

During the past few years, frustrated Lewis pairs (FLPs) have been considered as an effective alternative strategy to transition metal catalysts for C–H functionalisation reactions.[21] They are basically metal free catalysts where the cooperative reactivity is observed due to the combination of Lewis acid (LA) and Lewis base (LB) which act as an electron acceptor and donor respectively.

In this regard, Fontaine and colleagues described the first activation of a Csp^3–H bond by simple ansa-aminoboranes **232a** to form novel heterocycles **232b:** a N/B frustrated Lewis pair (FLP) ruptured a Csp^3–H bond (Scheme 232).[296] A significant C–H bond activation activity of 1-BR_2-2-NR_2-C_6H_4 *ansa*-aminoboranes paved an ideal beginning point for the study. In an age where metal catalysis is in high demand, FLP mediated C–H functionalisation opened the door to the ever-growing pharmaceutical, agrochemical as well as organic electronics industries. Under mild heating, the ambiphilic molecule (2-NMe_2-C_6H_4)$_2$BH activates the C–H bond of a methyl group attached with the nitrogen atom, resulting in the formation of an unprecedented N–B heterocycle. Using quantum mechanical simulations, the mechanistic specifics of these alterations are examined. Calculations indicate that concurrent H_2 release through an FLP-type mechanism is thermodynamically favourable, even when the reaction products are slightly thermodynamically uphill.

6.2 FLP catalysed C(sp^2)–H activation

In 2015, Fontaine and colleagues reported their design for an FLP catalyst capable of splitting and functionalizing Csp^2–H bonds (Scheme 233).[297] In this method, the electron density of the Csp^2–H bond is transferred to a Lewis acidic borane, while a Lewis basic amine is believed to extract a proton. This study employed the borane (1-TMP-2-BH_2-C_6H_4)$_2$ (TMP, 2,2,6,6-tetramethylpiperidine) **233c** as a synthetically simple catalyst. Not only did the heterocyclic substrate's nucleophilic carbon have direct access to the Lewis acidic BH_2 moiety, but the bulky

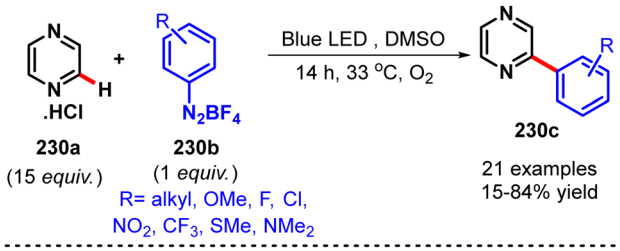

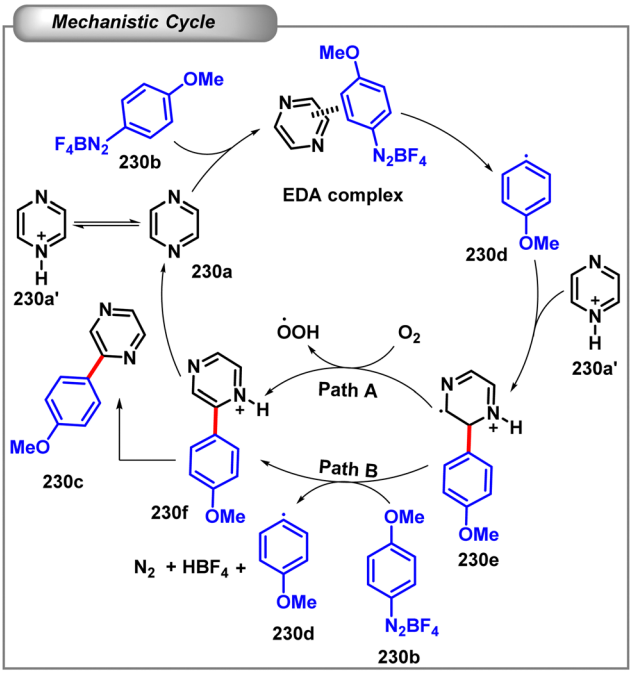

Scheme 230 Visible-light induced C–H arylation of diazines with aryldiazonium salts (Silva *et al.*[294]).

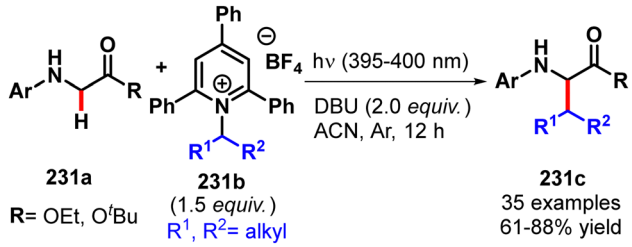

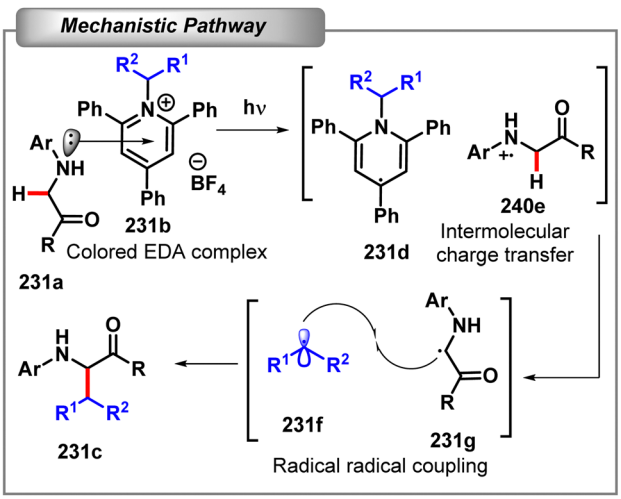

Scheme 231 Visible light promoted C(sp^3)–H alkylation by intermolecular charge transfer (Wang *et al.*[295]).

amine moiety also promoted proton abstraction from Csp^2 while preventing head-to-tail dimerization. In addition to catalysing the borylation of furans, pyrroles, and electron-dense thiophenes, it could also activate the C–H bonds of heteroarenes. The reported selectivity was in addition to that observed for most transition metal catalysts utilised in this process.

Later in 2018, Zhang *et al.* demonstrated the disproportionation aspect of the $B(C_6F_5)_3$-catalyzed C–H borylation by synthesising a range of C3-selective borylated indoles **234c** and transfer hydrogenated indoline derivatives **234d** at room temperature without the need of any additive or the release of small molecules (Scheme 234).[298] This catalyst system exhibited outstanding catalytic performance for real-world applications, including easy scalability in solvent-free settings and a high catalytic lifetime across 10 repeated additions of starting materials. By choosing appropriate substrates and adjusting the amount of catechol borane, the formation of by-products could be inhibited. It is noteworthy that the convergent disproportionation reaction of indole was achieved by heating at 120 °C, which allowed the continuous conversion of indoline products back to indoles, followed by the disproportionation reaction to produce C3-borylated indole and indoline for the next catalytic cycle, and thus achieving C3-borylated indoles in up to 98% excellent yield.

In the next year, Rochette *et al.* reported the first transfer borylation between aryl boronic esters (2-furylBcat) **235b** and arenes **235a** using commercially available 2-mercaptopyridine **235c** as a metal-free catalyst (Scheme 235).[299] This synthetic process outperformed other contemporary methods in terms of C–H borylation reaction cost cutting, enabling better group tolerance, a wider catalyst landscape, and the exploitation of more favourable working conditions. Lewis basic (pyridine) and Brønsted acid sites are present on the ambiphilic molecule 2-mercaptopyridine. A plausible mechanism was proposed as follows: while the acidic proton can be transferred to the aryl group to generate furan **235f**, the Lewis base can react with the electrophilic boron atom of the arylboronate **235b**. The aromatization of pyridine as a result of C–H activation is the desired driving force of the cycle. After the formation of the B–C bond, the heteroaryl boronate **235d** could be released, regenerating the catalyst **235c**.

6.3 Other metal free directed C–H borylation

In 2019, the Shi group demonstrated a comprehensive technique for the directed C–H borylation of arenes and heteroarenes without the need of metal catalysts, accommodating the efficient formation of a range of C-heteroatom bonds (Scheme 236A).[300] Unlike earlier methods, this technique to C–H borylation was feasible, cost-effective, and environmentally friendly. It is

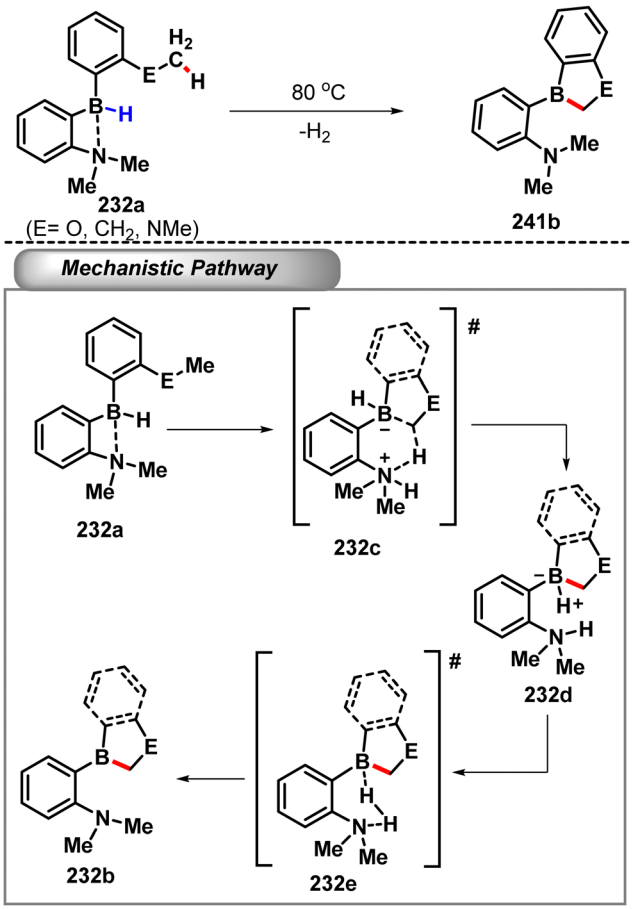

Scheme 232 Frustrated Lewis pair mediated Csp^3–H activation (Rochette *et al.*[296]).

possible to synthesise C7- and C4-borylated indoles **236c** and **236f** respectively using a process that is mild and compatible with a wide variety of functional groups. Calculations based on the density functional theory indicated the mechanism, which involves BBr_3 functioning as both a reagent and a catalyst. Here the pivaloyl group acted as the directing group which offered the ortho C–H electrophilic borylation **236b** and **236e** by utilising the BBr_3 reagent where the central B atom was tetrahedral and was chelated by O. The corresponding borylated products were *in situ* converted to pinacol boronate ester **236c** and **236f**. The conversion of produced boron species into natural products and pharmaceutical scaffolds demonstrates the potential value of the strategy.

At the same time, using commercial BBr_3 solutions, Ingleson and co-workers also showed the similar C7-borylation of indoles **236a** and ortho borylation of anilines **236g** in the presence of an efficient and easily removable *N*-pivaloyl directing group (Scheme 236B).[301] Due to the tolerability of C6-substituted indoles with BBr_3, this technique complemented both directed lithiation methods and borylation with FLP and iridium-catalysis. In a few instances, pinacol was required to isomerize the original borylated regioisomer in order to generate the desired products comprising C5-B and C7-B units. Moreover, carbazoles and

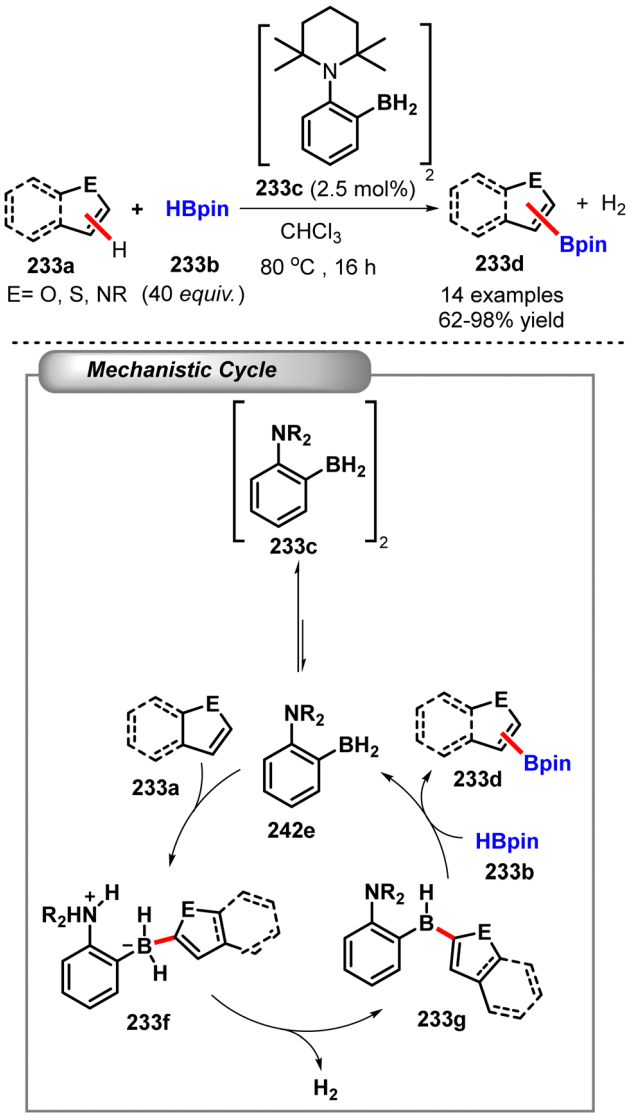

Scheme 233 FLP catalysed $C(sp^2)$–H bond activation and borylation of heteroarenes (Légaré *et al.*[297]).

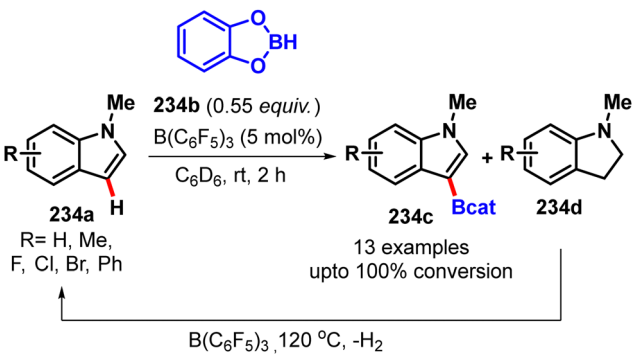

Scheme 234 $B(C_6F_5)_3$-catalyzed C3-borylation of indoles (Zhang *et al.*[298]).

anilines were also amenable to acyl-directed electrophilic borylation with a high degree of ortho selectivity. More precisely, under moderate heating condition at 60 °C, the pivaloyl group could

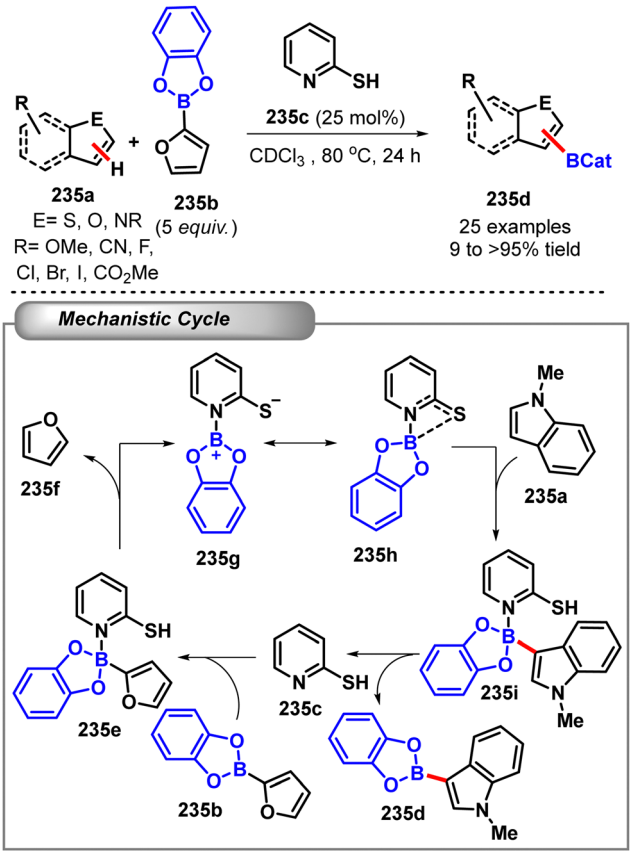

Scheme 235 Isodesmic C–H borylation of heteroarenes (Rochette *et al.*[299]).

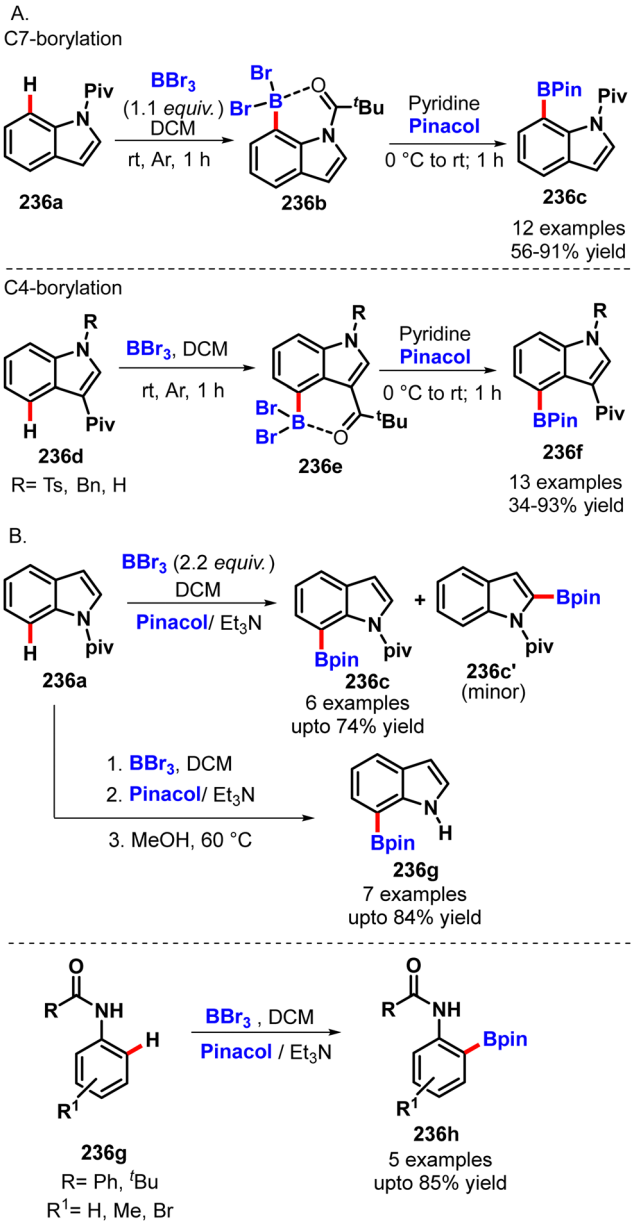

Scheme 236 Metal-free directed sp^2 C–H borylation of indole and aniline (Lv *et al.*,[300] Iqbal *et al.*[301]).

also be cleaved and directly afforded the NH-free borylated indole derivatives. Therefore, because of the prevalence of heterocycles with N–H groups, this borylation strategy with BBr_3 could be used as a versatile method.

6.4 Metal free C–H silylation

In 2015, Grubbs and colleagues described an earth abundant water soluble KO^{t}Bu catalysed heteroaromatic C–H silylation reaction by the cross-dehydrogenative coupling between arenes and silane reagents (Scheme 237).[302] Especially, sp^2 and few sp^3 C–H silylation processes were materialized under the optimised conditions. This concept provided a competitive advantage over previous procedures, which were usually hampered by functional group incompatibility, a limited application field, high catalyst prices and scarcity, and unclear scaling. This silylation proceeded under mild conditions without hydrogen acceptors, ligands, or additives and could be scaled up to more than 100 grams under optional solvent-free conditions. This transformation was applicable for an array of privileged heteroaromatic scaffolds and to several carbocyclic aromatic moieties. For the indole substrates, this silylation occurred regioselectively at the C2 position. On difficult-to-activate substrate classes with precious metal catalysts, silylation occurs with great yield and regioselectivity. Moreover, the direct silylation of active medicinal components had manifested the late-stage functionalisation.

7 Miscellaneous metal free C–H activation and functionalisation

7.1 Metal free C–H functionalisation of alkanes

In 2017, Davies and co-workers reported a thermally induced C–H functionalisation of alkanes **238b** by metal-free donor–acceptor aryldiazoacetates **238a** (Scheme 238).[303] A variety of C–H insertion products were obtained with moderate to good yield and, in some instances, with good site selectivity, favouring the functionalisation of the C–H bond with the highest degree of substitution. In addition, the study reveals that background thermal reactions must be considered in metal-catalysed C–H insertion reactions of donor/acceptor diazo compounds conducted at elevated temperatures.

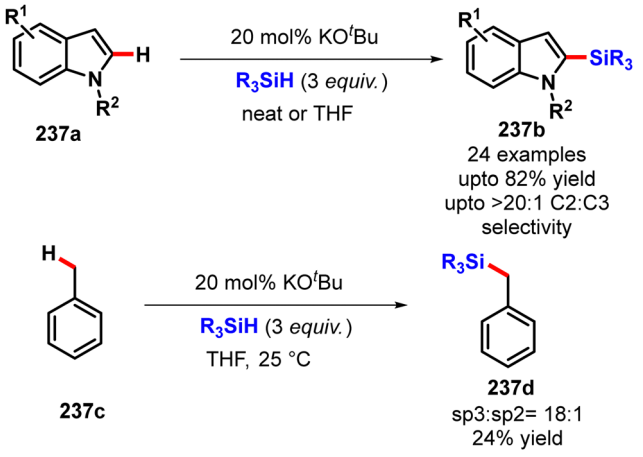

Scheme 237 Silylation of C–H bonds in aromatic heterocycles (Toutov *et al.*[302]).

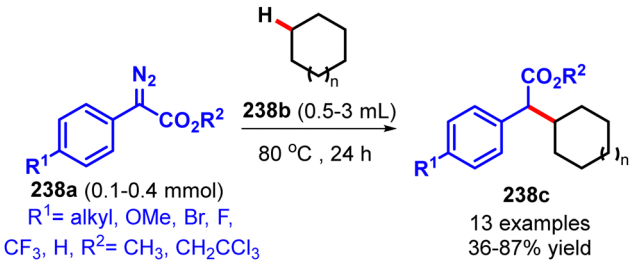

Scheme 238 Metal free C–H functionalisation of alkanes by aryldiazoacetates (Tortoreto *et al.*[303]).

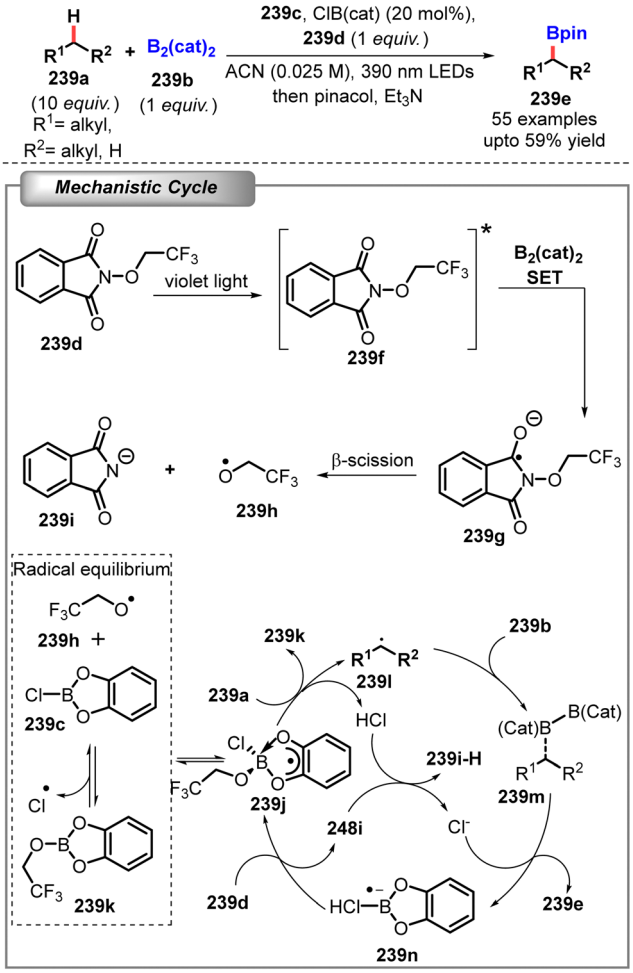

Scheme 239 Metal-free photoinduced C(sp^3)–H borylation of alkanes (Shu *et al.*[304]).

Recently, Aggarwal and colleagues reported a metal-free photoinduced borylation of non-activated C(sp^3)–H bonds **239a** using chloride as hydrogen atom transfer catalyst. For the successful C–H borylation, they selected *N*-(2,2,2-trifluoroethoxy)phthalimide **239d** which indeed generated the electrophilic 2,2,2-trifluoroethoxy radical **239h** which was stable and allowed the borylation of strong C(sp^3)–H bonds (Scheme 239).[304] After thorough experiments, they proposed a plausible mechanism in which an initial photoexcitation of *N*-alkoxyphthalimides **239d** to **239f** followed by reductive quenching by B_2Cat_2 and subsequent β-scission of radical anion **239g** afforded the trifluoroethoxy radical **239h**. Subsequently, a chlorine radical was formed through the reaction of **239h** with ClB(cat) **239c** *via* radical 'ate' complex **239j**. HAT from **239a** generated hydrochloric acid and alkyl radical **239l**. Borylation of **239l** with $B_2(cat)_2$ proceeded *via* radical complex **239m**, with cleavage of the B–B bond affording the C–H borylated product **239c** and the generation of **239n**. This **239n** could regenerate **239j** through SET between chloride-stabilized boryl radical **239n** and **239d**.

7.2 Metal free C–H functionalisation of alkenes or arenes

In 2018, Wang *et al.* reported a metal-free, direct alkene C(sp^2)–H cyanation of a diverse range of alkenes **240a** by the combination of TMSCN and a HIR [bis(trifluoroacetoxy)iodo]arene **240b** (Scheme 240).[305] The reaction actually proceeded through the *in situ* generated aryl(biscyano)iodine(III) reagent **240d** in the presence of TMSOTf. The mechanism involved an electrophilic activation of alkene **240a** with **240d**, which was further assisted by interaction with TMSOTf, followed by the generation of cyclic iodonium intermediate **240e**. Then the regioselective ring-opening of **240e** by the cyanide anion provided the intermediate **240f** and the subsequent diastereoselective deprotonation eventually provided the title compound **240c**.

Recently this year, Shu and co-workers developed a metal-free photocatalytic regioselective C–H alkylation method for electron-rich arenes **241a** that employs both activated and unactivated alkenes **241b** (Scheme 241).[306] The reaction tolerated both terminal and internal alkenes, as well as activated and unactivated alkenes, such as styrene derivatives, unsaturated alkenes, enols, acyl enamines, alkenyl borates, alkenyl halides, and aliphatic alkenes, providing direct access to linear alkylated electron-rich arenes. On the other hand, the reaction is permissive of a broad range of aromatic rings with various substitution patterns, and alkynes can be employed to generate C–H vinylation of electron-rich arenes.

Recently, in 2019 Proctor and colleagues reported the production of benzothiophenes **242c** from non-prefunctionalised arenes **242a** and allyl sulfoxides *via* direct twofold vicinal C–H

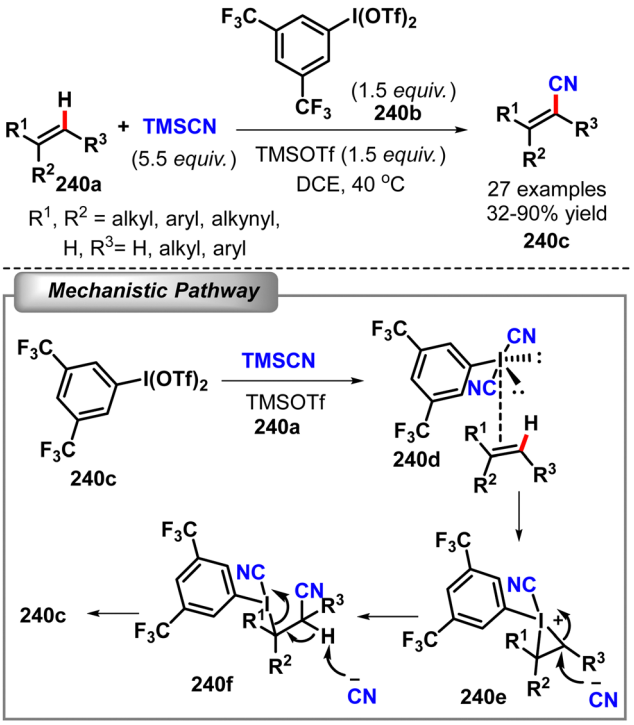

Scheme 240 Metal free direct C–H cyanation of alkenes (Wang *et al.*[305]).

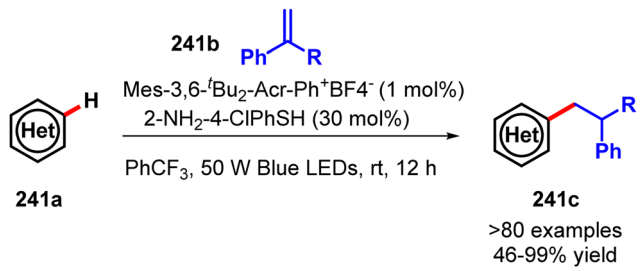

Scheme 241 Organophotocatalytic regioselective C–H alkylation of electron-rich arenes (Chen *et al.*[306]).

functionalisation of arenes (Scheme 242).[307] This one-pot annulation exploited an interrupted Pummerer reaction/[3,3]-sigmatropic rearrangement/cyclization sequence to create a variety of benzothiophene compounds.

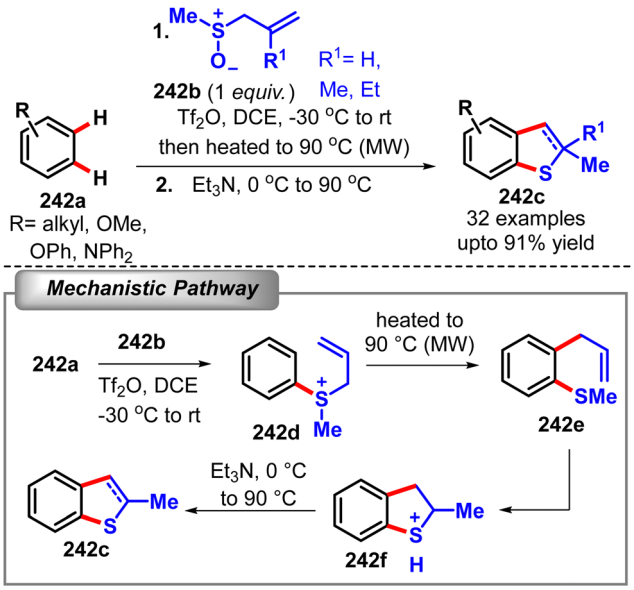

Scheme 242 Twofold C–H functionalisation of arene for the synthesis of benzothiophene (Yan *et al.*[307]).

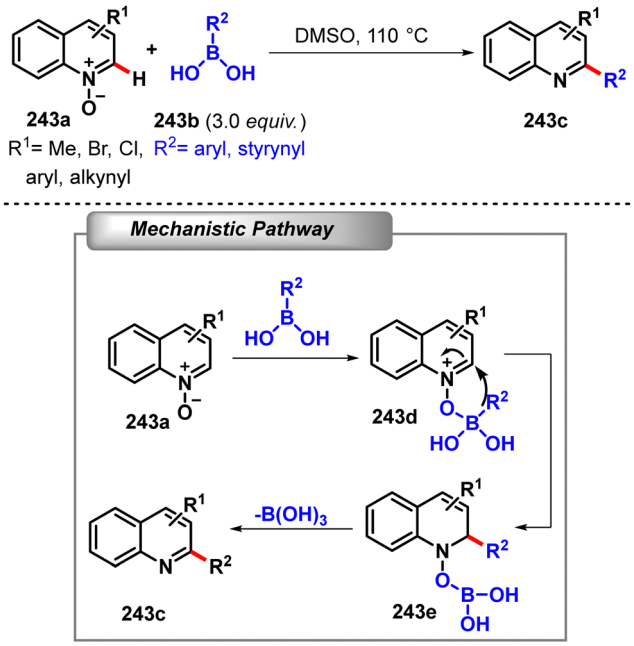

Scheme 243 Metal free cross coupling by C–H functionalisation of quinoline *N*-oxide (Bering *et al.*[308]).

7.3 Metal free quinoline functionalisation

Quinoline derivatives are significantly prevalent building blocks in synthetic organic chemistry due to their wide applications in pharmaceutical, agrochemical, and dye industries. Consequently, the construction of different quinoline derivatives from readily available precursors under metal free conditions is a predominant research goal, especially in the pharmaceutical industry.

In this regard, in 2015, Antonchick *et al.* developed a one-step C–H bond functionalisation of quinoline *N*-oxides by the Petasis type regioselective cross-coupling reaction with boronic acids (Scheme 243).[308] A broad range of 2-substituted quinolines **243c** were synthesised by this methodology with excellent yield. A probable mechanism hinted about the initial coordination of boronic acid **243b** with quinoline *N*-oxides **243a** followed by Petasis type aryl migration reaction *via* a nucleophilic attack at the C2 position.

In the early 2016, Sharma and his group reported a convenient catalyst and solvent-free method for the synthesis of quinoline substituted α-hydroxy carboxylic derivatives **244c** by hydroxy-heteroarylation of olefins **244b** with quinoline *N*-oxides **253a** under neat conditions (Scheme 244).[309] A wide range of quinoline *N*-oxide derivatives were studied under this condition.

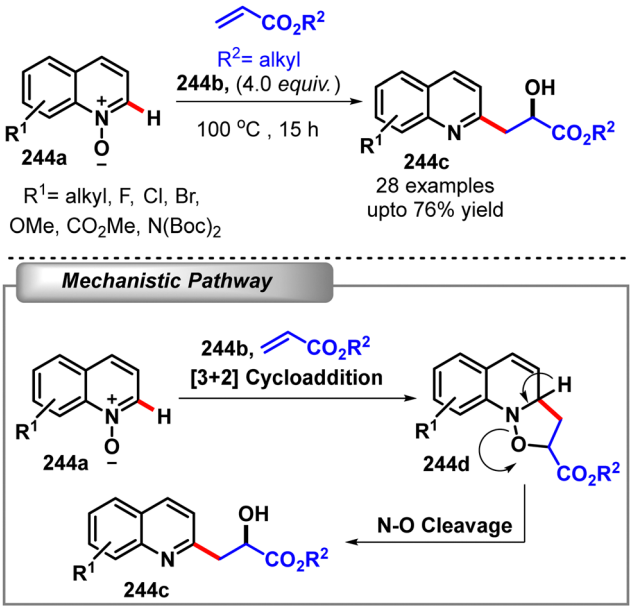

Scheme 244 Metal free alkylation of quinoline *N*-oxides with olefins (Kumar *et al.*[309]).

A plausible mechanism was suggested according to which the reaction might proceed through the 1,3-dipolar cycloaddition followed by cleavage of the N–O bond to furnish the final product.

The same year, Wang and his comrades developed a convenient route for the regioselective syntheses of 2-alkenylquinolines **245c** by reductive olefination of quinoline *N*-oxides **245a** under mild Brønsted acid (AcOH) conditions (Scheme 245A).[310] Not only a wide range of quinoline *N*-oxides but also a diverse range of activated olefins and styrenes underwent smooth reaction under this developed protocol. The reaction proceeded *via* 1,3-dipolar cycloaddition of quinoline *N*-oxide with ethyl acrylate to form the five-membered isoxazolidine intermediate **245d** followed by acid-assisted cleavage of the N–O bond and further dehydration. Contemporarily, Bower and co-workers delineated a simple Brønsted acid (TsOH) catalysed coupling of quinoline *N*-oxides **245a** with alkenes **245g** for the easy access of C2-alkenylated products **254h** (Scheme 245B).[311] A wide range of heteroarenes and alkenes were well tolerated under this condition. This transformation also proceeded through the similar thermally promoted [3+2]-dearomative cycloaddition between the quinoline *N*-oxide and alkene followed by Brønsted acid catalysed N–O cleavage and dehydration.

Recently in 2018, Xiao and his team developed an efficient and atom economic methodology of a Brønsted acid (TsOH·H2O) promoted *N*-amidation of quinoline *N*-oxides **246a** by exploiting inexpensive and commercially available nitriles **246b** as the amidation reagents for the synthesis of various *N*-(quinolin-2-yl)amides **246c** (Scheme 246A).[312] A large set of aromatic and aliphatic nitriles were efficiently coupled with quinoline *N*-oxide to regioselectively render the desired products under optimized conditions. A high KIE (2.2) value suggested that the cleavage of the C–H bond of quinoline *N*-oxide might be involved in the

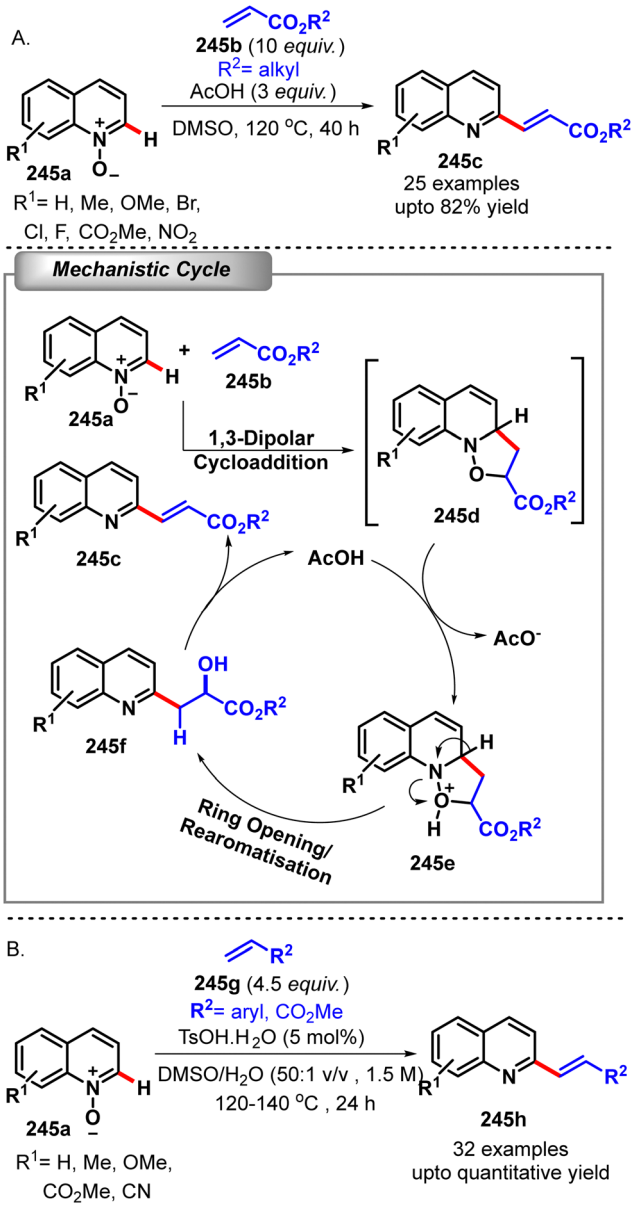

Scheme 245 Metal free reductive olefination of quinoline *N*-oxides for the synthesis of 2-alkenylquinoline (Xia *et al.*,[310] Crisenza *et al.*[311]).

rate-determining step of this reaction. A probable mechanism suggested was proposed which involved an initial 1,3-dipolar cycloaddition of quinoline *N*-oxide with nitrilium ions **246d** to form the five-membered oxadiazolidine intermediate **246e** followed by ring-opening reaction and deprotonation/aromatization to furnish the target product **246c**. Simultaneously, He and co-workers reported a deoxygenative 2-amidation of quinoline *N*-oxides **246a** by employing readily available nitriles as the amide source and methyl carbazate as both the radical activating reagent and oxygen source. Furthermore, selectfluor was required for the oxidation of methyl carbazate to generate the radical (Scheme 246B).[313] Based on the detailed experimental results a possible reaction mechanism was presumed involving the initial oxidation of the methyl carbazate by selectfluor *via*

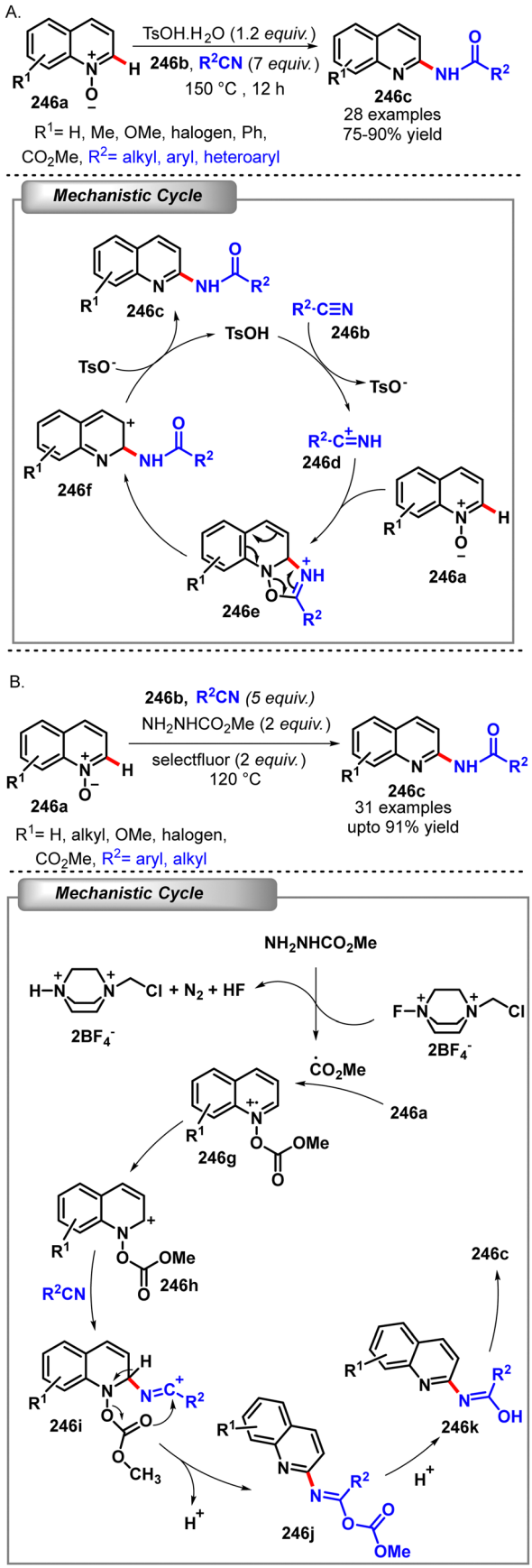

Scheme 246 Metal free *N*-amidation of quinoline *N*-oxides for the synthesis of N-(quinolin-2-yl)amides (Chen *et al.*,[312] Xie *et al.*[313]).

SET to generate a carbon-centered ester radical and its subsequent coupling with quinoline *N*-oxide **246a** followed by oxidation to render quinolinium intermediate **246h.** Next, the nucleophilic attack of nitrile to cationic α-carbon of intermediate **246h** generated an intermediate **246i,** which underwent dehydro-aromatization to form an intermediate **246j** which was finally decomposed to a benzimidic acid **246k** followed by rapid tautomerization to produce the target product. This is the first report on the ester-radical-activated highly regioselective addition of nitriles to quinoline *N*-oxides.

In 2019, Sharma *et al.* established a microwave-assisted, catalyst-free synthesis of various 2-anilinoquinolines **247c** by combining three components like quinoline *N*-oxides **247a** and aryldiazonium salts **247b** in acetonitrile (Scheme 247).[314] A wide range of quinoline *N*-oxide derivatives underwent smooth regioselective aminoarylation under this protocol. A plausible reaction mechanism was proposed involving the initial formation of intermediate **247d** from aryldiazonium tetrafluoroborate **247b** and acetonitrile under microwave heating followed by [3+2] cycloaddition of intermediate **247d** with quinoline *N*-oxide **247a** to provide another intermediate **247e.** Subsequent proton abstraction from intermediate **247e,** rearomatisation and hydrolysis finally afforded the desired product **247c.**

In the same year, Das and his group demonstrated a regioselective C2-cyanation of quinoline *N*-oxides using trimethylsilyl cyanide **248b** without the requirement of any external activator, metal, base or even solvent (Scheme 248).[315] The reaction proceeded smoothly under conventional heating as well as microwave irradiation within a short period of time.

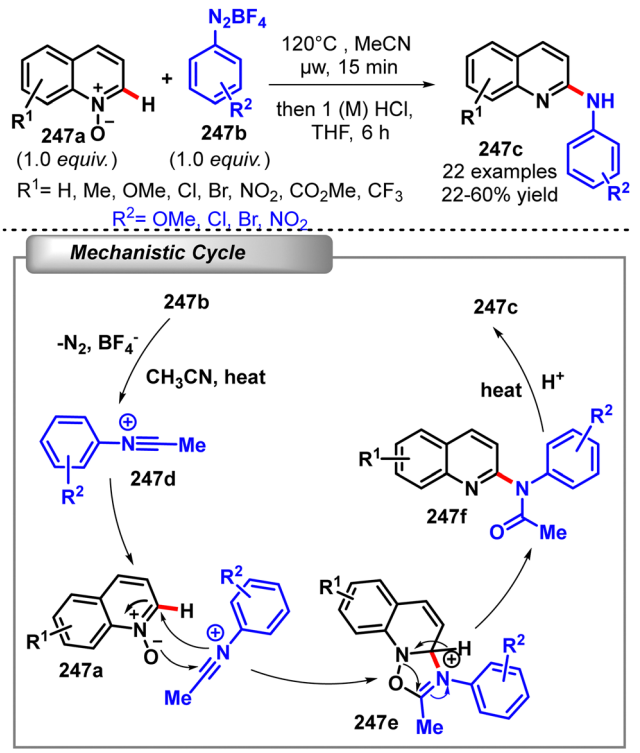

Scheme 247 Catalyst-free synthesis of 2-anilinoquinolines (Dhiman *et al.*[314]).

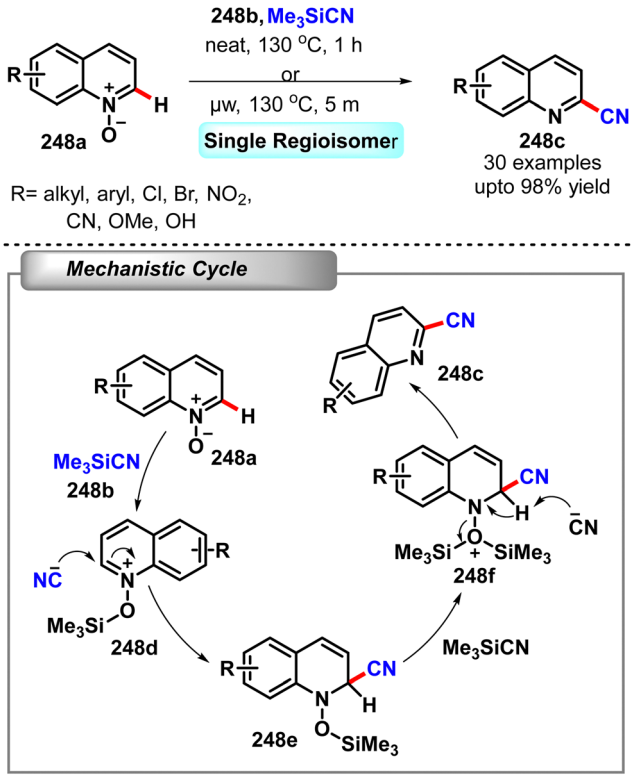

Scheme 248 Metal free regioselective C2-cyanation of quinoline *N*-oxide (Sharmah *et al.*[315]).

A plausible reaction mechanism was proposed involving the initial activation of quinoline *N*-oxide **248a** by trimethylsilyl cyanide **248b** followed by nucleophilic addition of the cyanide anion at the C-2 position of the activated ring to afford the dearomatized intermediate **248e.** This intermediate was further activated by an additional equivalent of trimethylsilyl cyanide and a subsequent rearomatisation led to the desired C2-cyanation of quinoline *N*-oxides with the concomitant release of hexamethyldisiloxane [$(Me_3Si)_2O$] as the by-product which was detected in GC-MS and confirmed by ^{29}Si NMR spectroscopy.

Recently they again displayed an operationally simple method of synthesizing 2-amino azines **249c** *via* [3+2] dipolar cycloaddition of azine *N*-oxide with carbodiimide under simple heating conditions without any transition metal catalyst, activator, base, and solvent (Scheme 249).[316]

7.4 Metal free allyic C–H functionalisation

In 2008, Cheng and Bao reported a DDQ mediated highly efficient allylic alkylation by the oxidative-coupling reaction between diarylallylic sp^3 C–H **250a** and active methylene **250b** sp^3 C–H bonds (Scheme 250).[317] A wide range of 1,3 dicarbonyl compounds were tested along with several diaryl alkenes.

In the same year, Floreancig and coworkers also reported the DDQ mediated allylic C–H activation of 1,2-disubstituted allylic ether **251a** for the synthesis of pyrone derivatives **251b** (Scheme 251).[318] It is noteworthy that (*E*)-1,2-disubstituted allylic ether reacted smoothly than the corresponding *Z*-isomer due to the heightened steric interactions that destabilized the oxocarbenium ion.

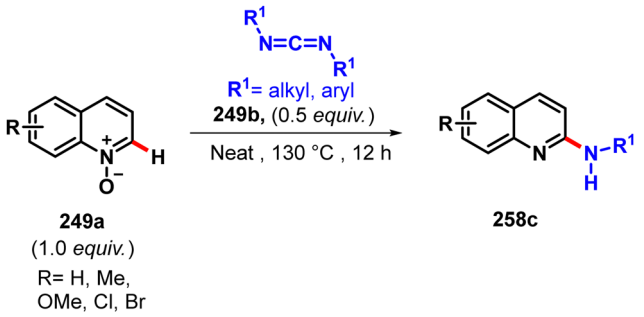

Scheme 249 Synthesis of 2-amino azines *via* [3+2] dipolar cycloaddition of azine *N*-oxide with carbodiimide (Sharmah *et al.*[316]).

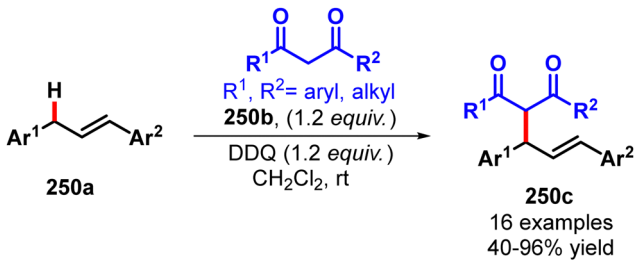

Scheme 250 DDQ mediated highly efficient allylic alkylation (Cheng *et al.*[317]).

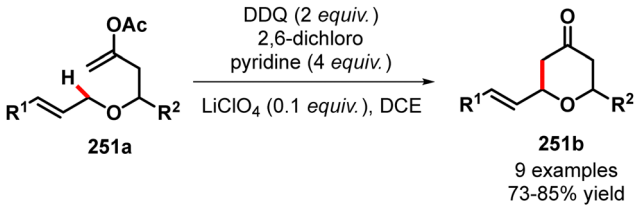

Scheme 251 DDQ mediated allylic C–H activation of 1,2-disubstituted allylic ether (Tu *et al.*[318]).

Recently in 2017, Zhou *et al.* reported a visible light mediated alkylation of unactivated allylic/benzylic sp^3 C–H bonds by employing an organo-photoredox catalyst (Scheme 252).[319] MesAcr was found to be the best in this business which seamlessly provided the allylic or benzylic radical through photoredox-induced alkene/arene radical cation deprotonation followed by the immediate interception of the resulting radical with electron deficient olefins to afford the alkylated product. A wide range of

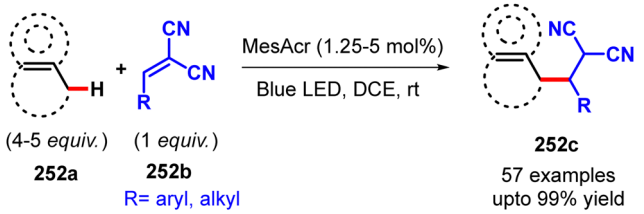

Scheme 252 Visible light mediated alkylation of unactivated allylic sp^3 C–H bonds (Zhao *et al.*[319]).

cyclic or acyclic olefins **252a** were readily involved along with a variety of trisubstituted alkenes **252b**. Moreover, the synthetic utility of this methodology was demonstrated by the scale-up reaction in both batch reactors and continuous-flow reactors.

7.5 Metal free radical C–H functionalisation

In 2012, Inoue and co-workers developed a chemoselective C(sp^3)–H amination of benzylic, propargylic, and aliphatic C–H bonds **253a** by utilising catalytic N-hydroxyphthalimide (NHPI) **253c** as the radical precursor and stoichiometric dialkyl azodicarboxylate **253b** as the aminating source (Scheme 253).[320] A plausible mechanism was suggested involving one electron oxidation of NHPI with dialkyl azodicarboxylate to generate the electron deficient phthalimide *N*-oxyl radical (PINO) **253e** which then regioselectively abstracted hydrogen from the electron-rich C(sp^3)–H bond to form carbon radical **253f**. This electron-rich carbon radical **253f** reacted with dialkyl azodicarboxylate **253b** to render amidyl radical **253g** which further abstracted the hydrogen of NHPI to regenerate PINO and provide the final hydrazinated product **253d**. A wide variety of substrates had responded well under this method.

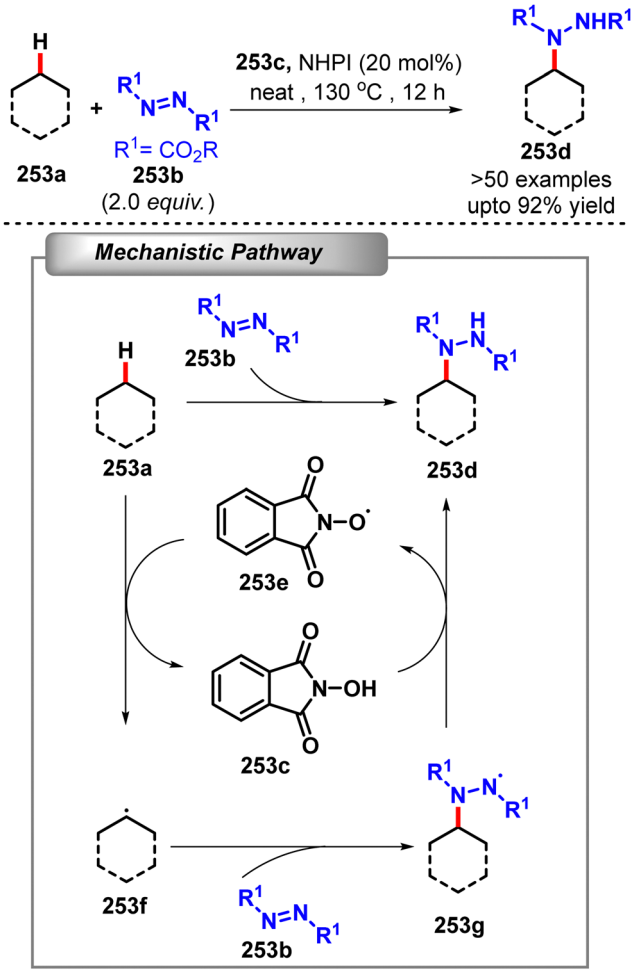

Scheme 253 Chemoselective C(sp^3)–H amination of C(sp^3)–H bonds (Amaoka *et al.*[320]).

The next year, they developed a similar metal-free radical C(sp^3)–H fluorination by employing a catalytic amount of *N*,*N*-dihydroxypyromellitimide (NDHPI) **254b** as a radical precursor and selectfluor **254c** as a fluorinating agent (Scheme 254).[321] The reaction was initiated by the generation of electrophilic *N*-oxyl radical **254e** from NDHPI **254b** by oxidation of selectfluor **254c** which helped in C(sp^3)–H bond abstraction followed by the intermolecular radical trap by selectfluor to form the C(sp^3)-F bond. Precisely, the benzylic C(sp^3)–H bonds of aromatic compounds and the tertiary C(sp^3)–H bonds of aliphatic compounds and even the secondary C(sp^3)–H bonds of alkanes were functionalized under this protocol.

In the same line, Mandal and co-workers mastered in the open-shell phenalenyl chemistry towards transition metal free catalytic C–H functionalisation reactions (Scheme 255).[322] This phenalenyl ligand (PLY) **255c** helped in the chelation-assisted single electron transfer (SET) process, which further facilitated the C–H functionalisation of unactivated arenes **255b**. It is worth mentioning that, the phenalenyl ligand can efficiently afford the incoming electrons in its non-bonding molecular orbital (NBMO) to stabilize the radical state as well as it can also release one electron from its singly occupied molecular orbital (SOMO) without any significant destabilization which favour it to act as a SET mediator under low-catalyst loading conditions. In 2016, they reported the C–H functionalisation of unactivated arenes to form the biaryl products with a diverse substrate scope using this PLY ligand.

Later in the next year, they again published a similar metal-free phenalenyl ligand (PLY) **255c** catalyzed direct C–H arylation

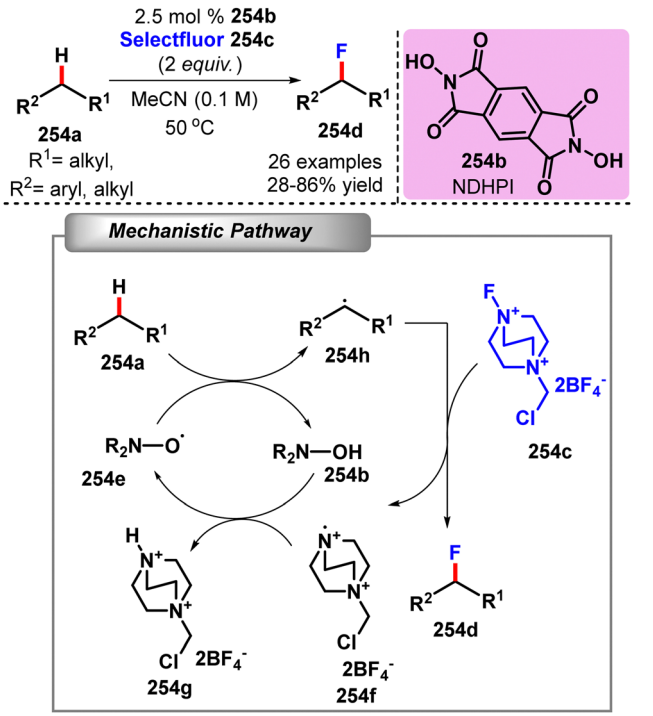

Scheme 254 Fluorination of C(sp^3)–H bonds using a catalytic *N*-oxyl radical (Amaoka *et al.*[321]).

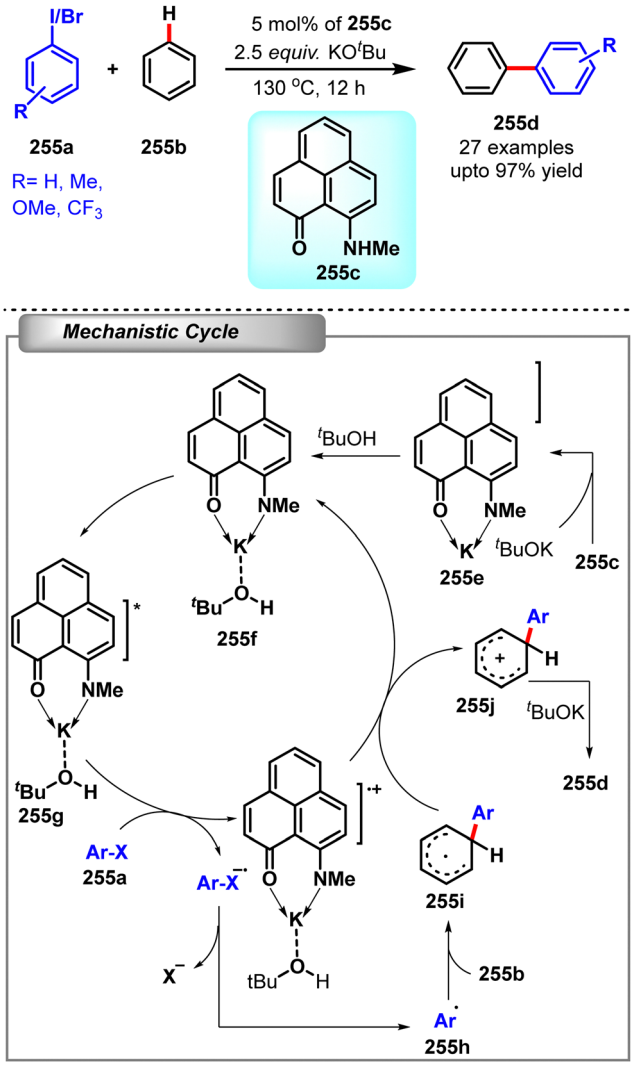

Scheme 255 Open shell phenalenyl in transition metal-free C–H functionalisation (Paira *et al.*[322]).

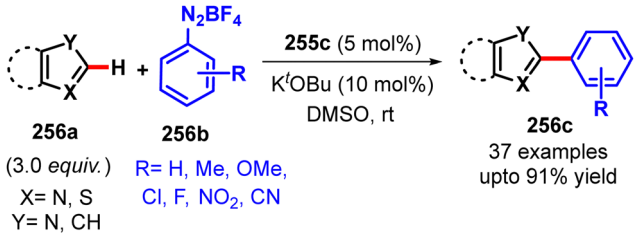

Scheme 256 Transition metal-free C–H arylation of heteroarenes at room temperature (Ahmed *et al.*[323]).

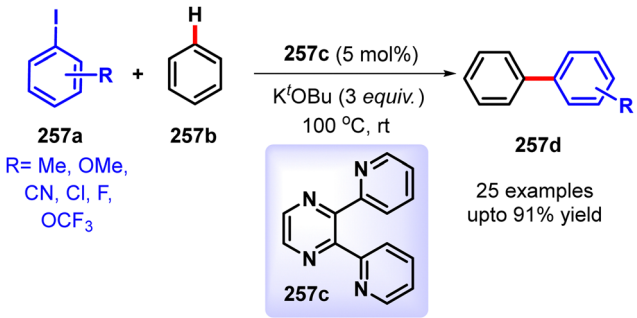

Scheme 257 Organocatalytic direct C(sp^2)–H arylation of unactivated arenes/heteroarenes (Tiwari *et al.*[324]).

of a variety of heteroarenes like azoles, furan, thiophene and pyridine at room temperature without employing any photoactivation step (Scheme 256).[323]

Recently in 2020, Chaudhary and co-workers reported 2,3-bis-(2-pyridyl) pyrazine **257c** as a new organocatalyst for the direct cross-coupling reactions of an aryl halide with unactivated arenes/heteroarenes *via* C(sp^2)–H bond activation (Scheme 257).[324]

7.6 Versatile new age C–H functionalisation

Direct C–H functionalisation now-a-days has become a useful tool for the introduction of structural and functional molecular complexity. Although this site selectivity can sometimes be achieved through appropriate directing groups or substitution patterns, the absence of such functionality usually provides more than one product isomer. Therefore, the development of the direct C–H functionalisation reaction that proceeds with high positional selectivity or installs a functional group that can serve as a synthetic linchpin for further functionalisation is highly desirable.

In this aspect, Ritter *et al.* first reported a highly selective (>99%) metal free C–H functionalisation of complex molecules as well as simple arenes **258a** by introducing an excellent linchpin group, *i.e.*, persistent sulfur-based thianthrenium salts which can be further broadly engaged in different transformations, *via* both transition-metal and photoredox catalysis (Scheme 258).[325] A plausible mechanism was proposed for this thianthrenation process by the generation of radical cations **258f** followed by formation of an aryl dicationic adduct **258g** and finally the irreversible deprotonation afforded the product **258d**. Furthermore, the generation of radical cations by comproportionation of TFT S-oxide **258b** and TFT **258c** under the reaction conditions was observed by EPR spectroscopy. Furthermore, a wide range of functionalisation was portrayed by this aryl thianthrenium cation.

The Procter group also pioneered in such metal free C–H functionalisation by utilising the concept of interrupted Pummerer reaction employing sulfoxides (Scheme 259).[326] In 2016, they disclosed metal-free C–H thioarylation of arenes and heteroarenes **259b** using methyl sulfoxides **259a** which upon activation formed sulfoxonium salts and served as excellent sulfur electrophiles for coupling with a variety of aryl–H partners for the synthesis of high value diaryl sulfides **259c**.

Later in 2020, they further developed a metal free strategy for the rapid construction of (hetero)biaryl motifs **260d** from non-pre-functionalized partners **260a** and **260c** using a combination of organophotoredox catalysis and the interrupted Pummerer reaction (Scheme 260).[327] The collaboration of the organic photoredox catalyst, 10-phenylphenothiazine (PTH), and intermediate aryldibenzothiophenium salts **260e** led to a highly selective synthesis of (hetero)biaryl motifs **260d** with a wide

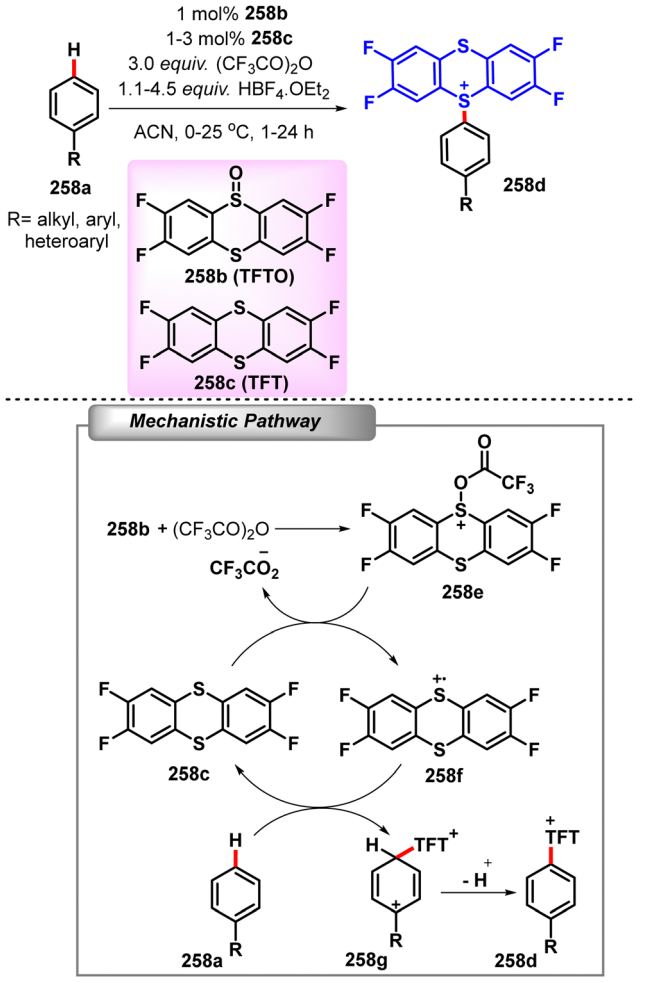

Scheme 258 Metal free thianthrenation by aryl C–H functionalisation (Berger *et al.*[325]).

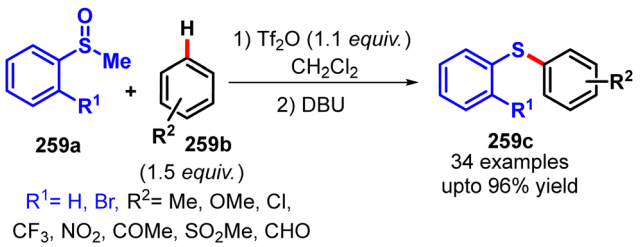

Scheme 259 Metal free C–H thioarylation of arenes using sulfoxides (Farnández-Salas *et al.*[326]).

substrate scope. The mechanism of the transformation was proposed as the initial sulfoxide activation of the nucleophilic arene moiety by an interrupted Pummerer reaction to generate the corresponding aryldibenzothiophenium salt (Ar–DBT+) **260e**. Next, a SET from the photoexcited PTH to Ar–DBT+ resulted in the expulsion of dibenzothiophene and concomitant formation of an aryl radical species **260f** which was subsequently trapped by the other arene or heteroarene **260c**. The newly formed radical species **260g** was then oxidised by SET followed by aromatization to afford the final product **260d**.

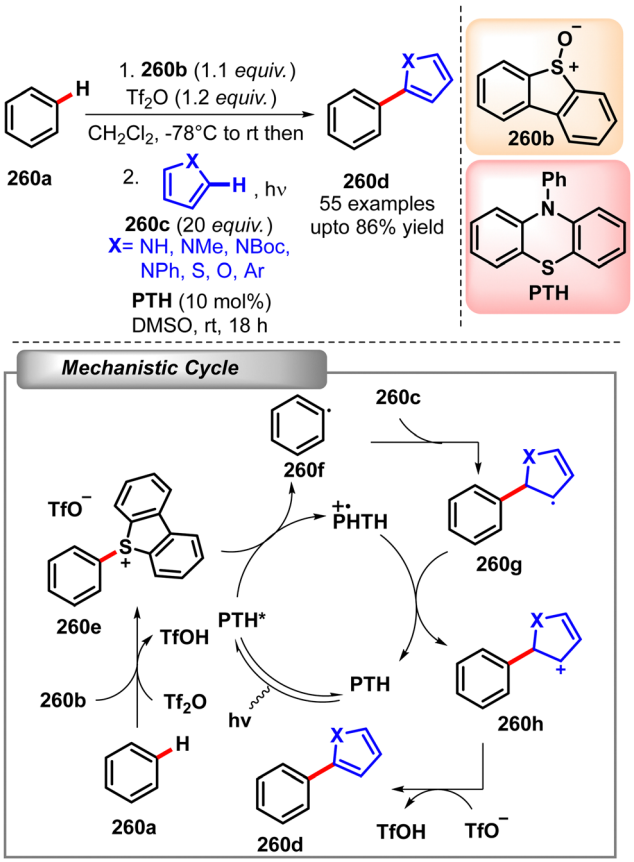

Scheme 260 Metal free formal C–H/C–H coupling of arenes enabled by interrupted Pummerer activation (Aukland *et al.*[327]).

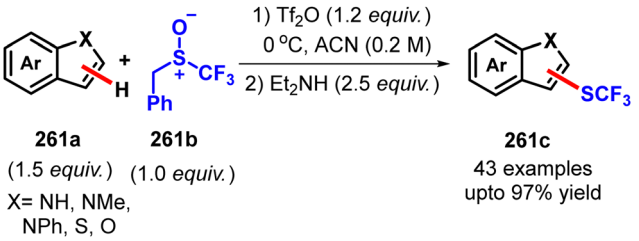

Scheme 261 Metal free C–H trifluoromethylthiolation of (hetero)arenes (Wang *et al.*[328]).

In the same year, they again disclosed metal-free C–H trifluoromethylthiolation of a range of (hetero)arenes, ligand derivatives, polyaromatics and even medicines and agrochemicals by utilising trifluoromethyl sulfoxides **261b** as a new class of trifluoromethylthiolating reagents by the similar interrupted Pummerer reaction mechanism (Scheme 261).[328]

8 Conclusions and future outlook

The field of metal free C–H functionalisation has garnered significant advancements in organic chemistry. It mitigates the major challenges associated with transition metal catalysed C–H functionalisation by increasing the practicality and contributing

environmentally benign, cost-effective, scalable, and sustainable catalytic systems. However, to consummate the pinnacle, it should go a long way to offer more general, robust catalytic systems that can replace the transition metal in true sense. Scientific progress toward sustainability has been given a boost by the recent Nobel Prize for organocatalysis. We sincerely believe that "the proper use of science is not to conquer the nature but to live in it." We hope this review will inspire the researchers in both academia and industries towards the greener and sustainable future of C–H activation.

Conflicts of interest

There are no conflicts to declare.

Acknowledgements

Financial support received from SERB TETRA (TTR/2021/000108) is gratefully acknowledged.

Notes and references

1 J. Clayden, N. Greeves and S. Warren, *Organic Chemistry*, *Oxford University Press*, 2012, pp. 1–15.
2 K. C. Nicolaou and E. J. Sorensen, *Classics in Total Synthesis: Targets, Strategies, Methods*, 1996, ISBN 978-3-527-29231-8.
3 T. F. Markle, J. W. Darcy and J. M. Mayer, *Sci. Adv.*, 2018, **4**, eaat5776.
4 T. Rogge, N. Kaplaneris, N. Chatani, J. Kim, S. Chang, B. Punji, L. L. Schafer, D. G. Musaev, J. Wencel-Delord, C. A. Roberts, R. Sarpong, Z. E. Wilson, M. A. Brimble, M. J. Johansson and L. Ackermann, *Nat. Rev. Methods Primers*, 2021, **1**, 43.
5 S. K. Sinha, S. Guin, S. Maiti, J. P. Biswas, S. Porey and D. Maiti, *Chem. Rev.*, 2022, **122**, 5682–5841.
6 U. Dutta, S. Maiti, T. Bhattacharya and D. Maiti, *Science*, 2021, **372**, 771–779.
7 J. F. Hartwig and M. A. Larsen, *ACS Cent. Sci.*, 2016, **2**, 281–292.
8 F.-L. Zhang, K. Hong, T.-J. Li, H. Park and J.-Q. Yu, *Science*, 2016, **351**, 252–256.
9 K. Godula and D. Sames, *Science*, 2006, **312**, 67–72.
10 C. C. C. Johansson Seechurn, M. O. Kitching, T. J. Colacot and V. Snieckus, *Angew. Chem., Int. Ed.*, 2012, **51**, 5062–5085.
11 J. D. Hayler, D. K. Leahy and E. M. Simmons, *Organometallics*, 2019, **38**, 36–46.
12 T. Laird, *Org. Process Res. Dev.*, 2012, **16**, 1–2.
13 C. R. McElroy, A. Constantinou, L. C. Jones, L. Summerton and J. H. Clark, *Green Chem.*, 2015, **17**, 3111–3121.
14 P. Gilding, *Nature*, 2019, **573**, 311.
15 J. D. Lasso, D. J. Castillo-Pazos and C.-J. Li, *Chem. Soc. Rev.*, 2021, **50**, 10955–10982.
16 V. N. Charushin and O. N. Chupakhin, *Topics in Heterocyclic Chemistry*, Springer, Cham, vol 37. ISBN 978-3-319-07018-6.
17 R. Samanta, K. Matcha and A. P. Antonchick, *Eur. J. Org. Chem.*, 2013, 5769–5804.
18 T. Gensch, M. N. Hopkinson, F. Glorius and J. Wencel-Delord, *Chem. Soc. Rev.*, 2016, **45**, 2900–2936.
19 T. Dalton, T. Faber and F. Glorius, *ACS Cent. Sci.*, 2021, **7**, 245–261.
20 K. M. Altus and J. A. Love, *Commun. Chem.*, 2021, **4**, 173.
21 D. W. Stephan, *Acc. Chem. Res.*, 2015, **48**, 306–316.
22 D. W. Stephan and G. Erker, *Angew. Chem., Int. Ed.*, 2015, **54**, 6400–6441.
23 B. M. Trost, *Science*, 1991, **254**, 1471–1477.
24 R. J. Fitzmaurice, J. M. Ahern and S. Caddick, *Org. Biomol. Chem.*, 2009, **7**, 235–237.
25 V. Chudasama, R. J. Fitzmaurice, J. M. Ahern and S. Caddick, *Chem. Commun.*, 2010, **46**, 133–135.
26 V. Chudasama, R. J. Fitzmaurice and S. Caddick, *Nat. Chem.*, 2010, **2**, 592–596.
27 V. Chudasama, J. M. Ahern, R. J. Fitzmaurice and S. Caddick, *Tetrahedron Lett.*, 2011, **52**, 1067–1069.
28 S. Paul and J. Guin, *Chem. – Eur. J.*, 2015, **21**, 17618–17622.
29 P. Biswas, S. Mandal and J. Guin, *Org. Lett.*, 2020, **22**, 4294–4299.
30 L. Troisi, C. Granito, L. Ronzini, F. Rosato and V. Videtta, *Tetrahedron Lett.*, 2010, **51**, 5980–5983.
31 L. Liu, S. Zhang, X. Fu and C.-H. Yan, *Chem. Commun.*, 2011, **47**, 10148–10150.
32 T. B. Nguyen, L. Ermolenko and A. Al-Mourabit, *Green Chem.*, 2013, **15**, 2713–2717.
33 C. Huo, Y. Yuan, M. Wu, X. Jia, X. Wang, F. Chen and J. Tang, *Angew. Chem., Int. Ed.*, 2014, **53**, 13544–13547.
34 G. Deng, K. Ueda, S. Yanagisawa, K. Itami and C.-J. Li, *Chem. – Eur. J.*, 2009, **15**, 333–337.
35 Z.-Q. Liu, L. Sun, J.-G. Wang, J. Han, Y.-K. Zhao and B. Zhou, *Org. Lett.*, 2009, **11**, 1437–1439.
36 T. He, L. Yu, L. Zhang, L. Wang and M. Wang, *Org. Lett.*, 2011, **13**, 5016–5019.
37 H. Richter, R. Fröhlich, C.-G. Daniliuc and O. García Mancheño, *Angew. Chem., Int. Ed.*, 2012, **51**, 8656–8660.
38 R. Xia, H.-Y. Niu, G.-R. Qu and H.-M. Guo, *Org. Lett.*, 2012, **14**, 5546–5549.
39 H. Wang, L.-N. Guo and X.-H. Duan, *Org. Lett.*, 2013, **15**, 5254–5257.
40 J. Zhao, H. Fang, P. Qian, J. Han and Y. Pan, *Org. Lett.*, 2014, **16**, 5342–5345.
41 J.-J. Cao, T.-H. Zhu, S.-Y. Wang, Z.-Y. Gu, X. Wang and S.-J. Ji, *Chem. Commun.*, 2014, **50**, 6439–6442.
42 W. Sha, J.-T. Yu, Y. Jiang, H. Yang and J. Cheng, *Chem. Commun.*, 2014, **50**, 9179–9181.
43 X.-Q. Chu, H. Meng, Y. Zi, X.-P. Xu and S.-J. Ji, *Chem. Commun.*, 2014, **50**, 9718–9721.
44 H.-Y. Huang, H.-R. Wu, F. Wei, D. Wang and L. Liu, *Org. Lett.*, 2015, **17**, 3702–3705.
45 M. Hu, J.-H. Fan, Y. Liu, X.-H. Ouyang, R.-J. Song and J.-H. Li, *Angew. Chem., Int. Ed.*, 2015, **54**, 9577–9580.
46 H. Zhang, C. Pan, N. Jin, Z. Gu, H. Hua and C. Zhu, *Chem. Commun.*, 2015, **51**, 1320–1322.
47 H. Zhang, Z. Gu, P. Xu, H. Hu, Y. Cheng and C. Zhu, *Chem. Commun.*, 2016, **52**, 477–480.

48 Y. Liu, Q.-L. Wang, C.-S. Zhou, B.-Q. Xiong, P.-L. Zhang, C. Yang and K.-W. Tang, *J. Org. Chem.*, 2017, **82**, 7394–7401.
49 M. T. Westwood, C. J. C. Lamb, D. R. Sutherland and A.-L. Lee, *Org. Lett.*, 2019, **21**, 7119–7123.
50 D. Ramesh, U. Ramulu, K. Mukkanti and Y. Venkateswarlu, *Tetrahedron Lett.*, 2012, **53**, 2904–2908.
51 J. Liu, H. Zhang, H. Yi, C. Liu and A. Lei, *Sci. China Chem.*, 2015, **58**, 1323–1328.
52 H. Wang, X. Li, F. Wu and B. Wan, *Tetrahedron Lett.*, 2012, **53**, 681–683.
53 R.-Y. Tang, Y.-X. Xie, Y.-L. Xie, J.-N. Xiang and J.-H. Li, *Chem. Commun.*, 2011, **47**, 12867–12869.
54 S.-R. Guo, S.-R. Guo, Y.-Q. Yuan and J.-N. Xiang, *Org. Lett.*, 2013, **15**, 4654–4657.
55 J. Yuan, X. Ma, H. Yi, C. Liu and A. Lei, *Chem. Commun.*, 2014, **50**, 14386–14389.
56 B. Du, B. Jin and P. Sun, *Org. Lett.*, 2014, **16**, 3032–3035.
57 J.-W. Zeng, Y.-C. Liu, P.-A. Hsieh, Y.-T. Huang, C.-L. Yi, S. S. Badsara and C.-F. Lee, *Green Chem.*, 2014, **16**, 2644–2652.
58 T. Kittikool and S. Yotphan, *Eur. J. Org. Chem.*, 2020, 961–970.
59 Y. Kita, T. Takada, M. Gyoten, H. Tohma, M. H. Zenk and J. Eichhorn, *J. Org. Chem.*, 1996, **61**, 5857–5864.
60 T. Takada, M. Arisawa, M. Gyoten, R. Hamada, H. Tohma and Y. Kita, *J. Org. Chem.*, 1998, **63**, 7698–7706.
61 Y. Kita, T. Takada, M. Gyoten, H. Tohma, M. H. Zenk and J. Eichhorn, *J. Org. Chem.*, 1996, **61**, 5857–5864.
62 J. Barluenga, M. Trincado, E. Rubio and J. M. Gonzalez, *Angew. Chem., Int. Ed.*, 2006, **45**, 3140–3143.
63 Z. Zheng, L. Dian, Y. Yuan, D. Zhang-Negrerie, Y. Du and K. Zhao, *J. Org. Chem.*, 2014, **79**, 7451–7458.
64 W. Yu, Y. Du and K. Zhao, *Org. Lett.*, 2009, **11**, 2417–2420.
65 L. Liu, H. Lu, H. Wang, C. Yang, X. Zhang, D. Zhang-Negrerie, Y. Du and K. Zhao, *Org. Lett.*, 2013, **15**, 2906–2909.
66 J. Liang, J. Chen, F. Du, X. Zeng, L. Li and H. Zhang, *Org. Let.*, 2009, **11**, 2820–2823.
67 J. Wang, Y. Yuan, R. Xiong, D. Zhang-Negrerie, Y. Du and K. Zhao, *Org. Lett.*, 2012, **14**, 2210–2213.
68 H. Wu, Y.-P. He, L. Xu, D.-Y. Zhang and L.-Z. Gong, *Angew. Chem., Int. Ed.*, 2014, **53**, 3466–3469.
69 D.-Y. Zhang, L. Xu, H. Wu and L.-Z. Gong, *Chem. – Eur. J.*, 2015, **21**, 10314–10317.
70 X. Zhen, X. Wan, W. Zhang, Q. Li, D. Zhang-Negrerie and Y. Du, *Org. Lett.*, 2019, **21**, 890–894.
71 H. Tohma, M. Iwata, T. Maegawa and Y. Kita, *Tetrahedron Lett.*, 2002, **43**, 9241–9244.
72 D. Mirk, A. Willner, R. Fröhlich and S. R. Waldvogel, *Adv. Synth. Catal.*, 2004, **346**, 675–681.
73 T. Dohi, M. Ito, K. Morimoto, M. Iwata and Y. Kita, *Angew. Chem., Int. Ed.*, 2008, **47**, 1301–1304.
74 T. Dohi, M. Ito, I. Itani, N. Yamaoka, K. Morimoto, H. Fujioka and Y. Kita, *Org. Lett.*, 2011, **13**, 6208–6211.
75 K. Morimoto, T. Dohi and Y. Kita, *Eur. J. Org. Chem.*, 2013, 1659–1662.
76 H. Tohma, M. Iwata, T. Maegawa, Y. Kiyono, A. Maruyama and Y. Kita, *Org. Biomol. Chem.*, 2003, **1**, 1647–1649.
77 T. Dohi, K. Morimoto, Y. Kiyono, A. Maruyama, H. Tohma and Y. Kita, *Chem. Commun.*, 2005, 2930–2932.
78 K. Morimoto, N. Yamaoka, C. Ogawa, T. Nakae, H. Fujioka, T. Dohi and Y. Kita, *Org. Lett.*, 2010, **12**, 3804–3807.
79 T. Dohi, K. Morimoto, A. Maruyama and Y. Kita, *Org. Lett.*, 2006, **8**, 2007–2010.
80 Y. Kita, K. Morimoto, M. Ito, C. Ogawa, A. Goto and T. Dohi, *J. Am. Chem. Soc.*, 2009, **131**, 1668–1669.
81 T. Dohi, M. Ito, N. Yamaoka, K. Morimoto, H. Fujioka and Y. Kita, *Angew. Chem., Int. Ed.*, 2010, **49**, 3334–3337.
82 L. Ackermann, M. Dell'Acqua, S. Fenner, R. Vicente and R. Sandmann, *Org. Lett.*, 2011, **13**, 2358–2360.
83 J. Wen, R.-Y. Zhang, S.-Y. Chen, J. Zhang and X.-Q. Yu, *J. Org. Chem.*, 2012, **77**, 766–771.
84 K. Morimoto, Y. Ohnishi, D. Koseki, A. Nakamura, T. Dohi and Y. Kita, *Org. Biomol. Chem.*, 2016, **14**, 8947–8951.
85 Y. Gu and D. Wang, *Tetrahedron Lett.*, 2010, **51**, 2004–2006.
86 A. Jean, J. Cantat, D. Bérard, D. Bouchu and S. Canesi, *Org. Lett.*, 2007, **9**, 2553–2556.
87 M. Ito, H. Kubo, I. Itani, K. Morimoto, T. Dohi and Y. Kita, *J. Am. Chem. Soc.*, 2013, **135**, 14078–14081.
88 K. Matcha and A. P. Antonchick, *Angew. Chem., Int. Ed.*, 2013, **52**, 2082–2086.
89 K. Morimoto, K. Sakamoto, T. Ohshika, T. Dohi and Y. Kita, *Angew. Chem., Int. Ed.*, 2016, **55**, 3652–3655.
90 S. Paul, J. H. Ha, G. E. Park and Y. R. Lee, *Adv. Synth. Catal.*, 2017, **359**, 1515–1521.
91 E. L. Du, T. Duhail, M. D. Wodrich, R. Scopelliti, F. Fadaei-Tirani, E. Anselmi, E. Magnier and J. Waser, *Chem. – Eur. J.*, 2018, **24**, 10049–10053.
92 Y. Kita, H. Tohma, K. Hatanaka, T. Takada, S. Fujita, S. Mitoh, H. Sakurai and S. Oka, *J. Am. Chem. Soc.*, 1994, **116**, 3684–3691.
93 T. C. Turner, K. Shibayama and D. L. Boger, *Org. Lett.*, 2013, **15**, 1100–1103.
94 A. P. Antonchick and L. Burgmann, *Angew. Chem., Int. Ed.*, 2013, **52**, 3267–3271.
95 J. Malmgren, S. Santoro, N. Jalalian, F. Himo and B. Olofsson, *Chem. – Eur. J.*, 2013, **19**, 10334–10342.
96 R. Narayan and A. P. Antonchick, *Chem. – Eur. J.*, 2014, **20**, 4568–4572.
97 Z. Jia, E. Gálvez, R. M. Sebastián, R. Pleixats, Á. Álvarez-Larena, E. Martin, A. Vallribera and A. Shafir, *Angew. Chem., Int. Ed.*, 2014, **53**, 11298–11301.
98 C. Sen and S. C. Ghosh, *Adv. Synth. Catal.*, 2018, **360**, 905–910.
99 X. Wu, H. Zhang, N. Tang, Z. Wu, D. Wang, M. Ji, Y. Xu, M. Wang and C. Zhu, *Nat. Commun.*, 2018, **9**, 3343–3349.
100 N. Tang, X. Wu and C. Zhu, *Chem. Sci.*, 2019, **10**, 6915–6919.
101 K. Yasuo and K. Masami, *Chem. Lett.*, 1990, 581–582.
102 A. G. Romero, W. H. Darlington, E. J. Jacobsen and J. W. Mickelson, *Tetrahedron Lett.*, 1996, **37**, 2361–2364.
103 Y. Kikugawa, A. Nagashima, T. Sakamoto, E. Miyazawa and M. Shiiya, *J. Org. Chem.*, 2003, **68**, 6739–6744.
104 J. Yu, C. Gao, Z. Song, H. Yang and H. Fu, *Eur. J. Org. Chem.*, 2015, 5869–5875.
105 S. H. Cho, J. Yoon and S. Chang, *J. Am. Chem. Soc.*, 2011, **133**, 5996–6005.

106 A. P. Antonchick, R. Samanta, K. Kulikov and J. Lategahn, *Angew. Chem., Int. Ed.*, 2011, **50**, 8605–8608.
107 R. Samanta, K. Kulikov, C. Strohmann and A. P. Antonchick, *Synthesis*, 2012, 2325–2332.
108 X. Ban, Y. Pan, Y. Lin, S. Wang, Y. Du and K. Zhao, *Org. Biomol. Chem.*, 2012, **10**, 3606–3609.
109 A. Bal, S. Maiti and P. Mal, *J. Org. Chem.*, 2018, **83**, 11278–11287.
110 M. T. Herrero, I. Tellitu, E. Domínguez, I. Moreno and R. SanMartín, *Tetrahedron Lett.*, 2002, **43**, 8273–8275.
111 A. Correa, I. Tellitu, E. Domínguez, I. Moreno and R. SanMartin, *J. Org. Chem.*, 2005, **70**, 2256–2264.
112 E. Malamidou-Xenikaki, S. Spyroudis, M. Tsanakopoulou and D. Hadjipavlou-Litina, *J. Org. Chem.*, 2009, **74**, 7315–7321.
113 X. Li, L. Yang, X. Zhang, D. Zhang-Negrerie, Y. Du and K. Zhao, *J. Org. Chem.*, 2014, **79**, 955–962.
114 X. Guoa, D. Zhang-Negreriea and Y. Du, *RSC Adv.*, 2015, **5**, 94732–94736.
115 X. Zhang, D. Zhang-Negrerie, J. Deng, Y. Du and K. Zhao, *J. Org. Chem.*, 2013, **78**, 12750–12759.
116 Y. Li, D. Zhang-Negrerie, Y. Du and K. Zhao, *Tetrahedron*, 2015, **71**, 2927–2935.
117 Z. Zhang, X. Gao, Z. Li, G. Zhang, N. Ma, Q. Liu and T. Liu, *Org. Chem. Front.*, 2017, **4**, 404–408.
118 Z. Zhang, Y. Zhang, G. Huang and G. Zhang, *Org. Chem. Front.*, 2017, **4**, 1372–1375.
119 C. Hu, Z. Zhang, W. Gao, G. Zhang, T. Liu and Q. Liu, *Tetrahedron*, 2018, **74**, 665–671.
120 D. Liang, W. Yu, N. Nguyen, J. R. Deschamps, G. H. Imler, Y. Li, A. D. MacKerell, Jr., C. Jiang and F. Xue, *J. Org. Chem.*, 2017, **82**, 3589–3596.
121 D. Liang, D. Sersen, C. Yang, J. R. Deschamps, G. H. Imler, C. Jiang and F. Xue, *Org. Biomol. Chem.*, 2017, **15**, 4390–4398.
122 S. K. Bera, Md. T. Alam and P. Mal, *J. Org. Chem.*, 2019, **84**, 12009–12020.
123 J. Huang, Y. He, Y. Wang and Q. Zhu, *Chem. – Eur. J.*, 2012, **18**, 13964–13967.
124 Y. He, J. Huang, D. Liang, L. Liu and Q. Zhu, *Chem. Commun.*, 2013, **49**, 7352–7354.
125 S. K. Alla, R. K. Kumar, P. Sadhu and T. Punniyamurthy, *Org. Lett.*, 2013, **15**, 1334–1337.
126 J.-P. Lin, F.-H. Zhang and Y.-Q. Long, *Org. Lett.*, 2014, **16**, 2822–2825.
127 D. N. Rao, S. Rasheed, R. A. Vishwakarma and P. Das, *RSC Adv.*, 2014, **4**, 25600–25604.
128 Y. Chi, W.-X. Zhang and Z. Xi, *Org. Lett.*, 2014, **16**, 6274–6277.
129 S. Maiti and P. Mal, *Adv. Synth. Catal.*, 2015, **357**, 1416–1424.
130 G. Qian, B. Liu, Q. Tan, S. Zhang and B. Xu, *Eur. J. Org. Chem.*, 2014, 4837–4843.
131 B. V. Subba Reddy, C. R. Reddy, M. R. Reddy, S. Yarlagadda and B. Sridhar, *Org. Lett.*, 2015, **17**, 3730–3733.
132 Y. Du, R. Liu, G. Linn and K. Zhao, *Org. Lett.*, 2006, **8**, 5919–5922.
133 L. Fra, A. Millán, J. A. Souto and K. Muñiz, *Angew. Chem., Int. Ed.*, 2014, **53**, 7349–7353.
134 C.-Y. Zhao, K. Li, Y. Pang, J.-Q. Li, C. Liang, G.-F. Su and D.-L. Mo, *Adv. Synth. Catal.*, 2018, **360**, 1919–1925.
135 H.-D. Xia, H.-D. Xia, Y.-D. Zhang, Y.-H. Wang and C. Zhang, *Org. Lett.*, 2018, **20**, 4052–4056.
136 D. Liang and Q. Zhu, *Asian J. Org. Chem.*, 2015, **4**, 42–45.
137 R. Fan, D. Pu, F. Wen and J. Wu, *J. Org. Chem.*, 2007, **72**, 8994–8997.
138 A. Nagashima, T. Sakamoto and Y. Kikugawa, *Heterocycles*, 2007, **74**, 273–281.
139 Y. Ye, H. Wang and R. Fan, *Org. Lett.*, 2010, **12**, 2802–2805.
140 R. Fan, H. Wang, Y. Ye and J. Gan, *Tetrahedron Lett.*, 2010, **51**, 453–456.
141 L. Mao, Y. Li, T. Xiong, K. Sun and Q. Zhang, *J. Org. Chem.*, 2013, **78**, 733–737.
142 C. Zhu, Y. Liang, X. Hong, H. Sun, W.-Y. Sun, K. N. Houk and Z. Shi, *J. Am. Chem. Soc.*, 2015, **137**, 7564–7567.
143 C. Martínez and K. Muñiz, *Angew. Chem., Int. Ed.*, 2015, **54**, 8287–8291.
144 N. R. Paz, D. Rodríguez-Sosa, H. Valdés, R. Marticorena, D. Melián, M. B. Copano, C. C. González and A. J. Herrera, *Org. Lett.*, 2015, **17**, 2370–2373.
145 E. A. Wappes, S. C. Fosu, T. C. Chopko and D. A. Nagib, *Angew. Chem., Int. Ed.*, 2016, **55**, 9974–9978.
146 D. Zhang, H. Wang, H. Cheng, J. G. Hernández and C. Bolm, *Adv. Synth. Catal.*, 2017, **359**, 4274–4277.
147 Y. Kumar, Y. Jaiswal and A. Kumar, *Org. Lett.*, 2018, **20**, 4964–4969.
148 J. Joseph, J. Y. Kim and S. Chang, *Chem. – Eur. J.*, 2011, **17**, 8294–8298.
149 H. J. Kim, J. Kim, S. H. Cho and S. Chang, *J. Am. Chem. Soc.*, 2011, **133**, 16382–16385.
150 A. A. Kantak, S. Potavathri, R. A. Barham, K. M. Romano and B. DeBoef, *J. Am. Chem. Soc.*, 2011, **133**, 19960–19965.
151 R. Samanta, J. Lategahn and A. P. Antonchick, *Chem. Commun.*, 2012, **48**, 3194–3196.
152 R. Samanta, J. O. Bauer, C. Strohmann and A. P. Antonchick, *Org. Lett.*, 2012, **14**, 5518–5521.
153 S. Manna, P. O. Serebrennikova, I. A. Utepova, A. P. Antonchick and O. N. Chupakhin, *Org. Lett.*, 2015, **17**, 4588–4591.
154 Y. Wang, Y. Wang, Z. Guo, Q. Zhang and D. Li, *Asian J. Org. Chem.*, 2016, **5**, 1438–1441.
155 D. Ji, X. He, Y. Xu, Z. Xu, Y. Bian, W. Liu, Q. Zhu and Y. Xu, *Org. Lett.*, 2016, **18**, 4478–4481.
156 A. Pialat, J. Berges, A. Sabourin, R. Vinck, B. Liegault and M. Taillefer, *Chem. – Eur. J.*, 2015, **21**, 10014–10018.
157 F. Zhao, T. Sun, H. Sun, G. Xi and K. Sun, *Tetrahedron Lett.*, 2017, **58**, 3132–3135.
158 S. Mondal, S. Samanta, S. Jana and A. Hajra, *J. Org. Chem.*, 2017, **82**, 4504–4510.
159 M. Singsardar, S. Mondal, R. Sarkar and A. Hajra, *ACS Omega*, 2018, **3**, 12505–12512.
160 N. Luan, Z. Liu, S. Han, L. Shen, J. Li, D. Zou, Y. Wu and Y. Wu, *Tetrahedron Lett.*, 2020, **61**, 151362.
161 Y. Kita, H. Tohma, M. Inagaki, K. Hatanaka and T. Yakura, *Tetrahedron Lett.*, 1991, **32**, 4321–4324.
162 P. Li, J. Zhao, C. Xia and F. Li, *Org. Chem. Front.*, 2015, **2**, 1313–1317.

163 R. Fan, W. Li, D. Pu and L. Zhang, *Org. Lett.*, 2009, **11**, 1425–1428.
164 H. M. Guo, C. Xia, H. Y. Niu, X. T. Zhang, S. N. Kong, D. C. Wang and G. R. Qu, *Adv. Synth. Catal.*, 2011, **353**, 53–56.
165 J. A. Souto, D. Zian and K. Muniz, *J. Am. Chem. Soc.*, 2012, **134**, 7242–7245.
166 I. Buslov and X. Hu, *Adv. Synth. Catal.*, 2014, **356**, 3325–3330.
167 Y. Yang, Y. Yu, Y. Wang, Q. Zhang and D. Li, *Tetrahedron*, 2018, **74**, 1085–1091.
168 Y. Kita, H. Tohma, T. Takada, S. Mitoh, S. Fujita and M. Gyoten, *Synlett*, 1994, 427–428.
169 P. Magnus, C. Hulme and W. Weber, *J. Am. Chem. Soc.*, 1994, **116**, 4501–4502.
170 W. T. Chen, L. H. Gao, W. H. Bao, W. T. Wei and H. Tohma, *Chem. Commun.*, 1998, 173–174.
171 C. M. Pedersen, L. G. Marinescua and M. Bols, *Org. Biomol. Chem.*, 2005, **3**, 816–822.
172 W. T. Chen, L. H. Gao, W. H. Bao and W. T. Wei, *J. Org. Chem.*, 2018, **83**, 11074–11079.
173 H. Hamamoto, K. Hata, H. Nambu, Y. Shiozaki, H. Tohma and Y. Kita, *Tetrahedron Lett.*, 2004, **45**, 2293–2295.
174 Y. Gu and K. Xue, *Tetrahedron Letters*, 2010, **51**, 192–196.
175 J. Li, H. Chen, D. Z. Negrerie, Y. Du and K. Zhao, *RSC Adv.*, 2013, **3**, 4311–4320.
176 X. Wang, J. G. Donaire and R. Martin, *Angew. Chem., Int. Ed.*, 2014, **53**, 11084–11087.
177 M. Ngatimin, R. Frey, C. Andrews, D. W. Lupton and O. E. Hutt, *Chem. Commun.*, 2011, **47**, 11778–11780.
178 F. V. Singh and T. Wirth, *Synthesis*, 2012, 1171–1177.
179 Z. Yu, L. Ma and W. Yu, *Synlett*, 2012, 1534–1540.
180 Y. Zheng, X. Li, C. Ren, D. Z. Negrerie, Y. Du and K. Zhao, *J. Org. Chem.*, 2012, **77**, 10353–10361.
181 J. Ranjith, N. Rajesh, B. Sridharb and P. R. Krishna, *Org. Biomol. Chem.*, 2016, **14**, 10074–10079.
182 K. Xu, R. Yang, S. Yang, C. Jiang and Z. Ding, *Org. Biomol. Chem.*, 2019, **17**, 8977–8981.
183 K. Xu, S. Yanga and Z. Ding, *Org. Chem. Front.*, 2020, **7**, 69–72.
184 R. Fan, Y. Sun and Y. Ye, *Org. Lett.*, 2009, **11**, 5174–5177.
185 Y. Cao, X. Zhang, G. Lin, D. Z. Negrerie and Y. Du, *Org. Lett.*, 2016, **18**, 5580–5583.
186 D. Sun, X. Zhao, B. Zhang, Y. Cong, X. Wan, M. Bao, X. Zhao, B. Li, D. Z. Negrerie and Y. Du, *Adv. Synth. Catal.*, 2018, **360**, 1634–1638.
187 Q. Xing, H. Liang, M. Bao, X. Li, J. Zhang, T. Bi, Y. Zhang, J. Xu, Y. Du and K. Zhao, *Adv. Synth. Catal.*, 2019, **361**, 4669–4673.
188 I. Couto, I. Tellitu and E. Domínguez, *J. Org. Chem.*, 2010, **75**, 7954–7957.
189 X. Wang, J. G. Donaire and R. Martin, *Angew. Chem., Int. Ed.*, 2014, **53**, 11084–11087.
190 N. Zhang, R. Cheng, D. Z. Negrerie, Y. Du and K. Zhao, *J. Org. Chem.*, 2014, **79**, 10581–10587.
191 N. Itoh, T. Sakamoto, E. Miyazawa and Y. Kikugawa, *J. Org. Chem.*, 2002, **67**, 7424–7428.
192 S. Maiti, T. Alam and P. Mal, *Asian J. Org. Chem.*, 2018, **7**, 715–719.
193 H. Liu, X. Wanga and Y. Gu, *Org. Biomol. Chem.*, 2011, **9**, 1614–1620.
194 H. Liu, Y. Xie and Y. Gu, *Tetrahedron Lett.*, 2011, **52**, 4324–4326.
195 S. Wang, Z. Ni, Y. Wang, Y. Pang and Y. Pan, *Tetrahedron*, 2014, **70**, 6879–6884.
196 Q. Jiang, J. Y. Wang and C. Guo, *J. Org. Chem.*, 2014, **79**, 8768–8773.
197 K. Liu, P. Wen, J. Liu and G. Huang, *Synthesis*, 2010, 3623–3626.
198 V. Soni, U. N. Patel and B. Punji, *RSC Adv.*, 2015, **5**, 57472–57481.
199 N. N. Karade, V. H. Budhewar, A. N. Katkar and G. B. Tiwari, *Arkivoc*, 2006, **xi**, 162–167.
200 N. Wang, R. Liu, Q. Xu and X. Liang, *Chem. Lett.*, 2006, **35**, 566–567.
201 F. Zhao, X. Liu, R. Qi, D. Z. Negrerie, J. Huang, Y. Du and K. Zhao, *J. Org. Chem.*, 2011, **76**, 10338–10344.
202 X. Liu, R. Cheng, F. Zhao, D. Z. Negrerie, Y. Du and K. Zhao, *Org. Lett.*, 2012, **14**, 5480–5483.
203 F. Wang, W. Sun, Y. Wang, Y. Jiang and T. P. Loh, *Org. Lett.*, 2018, **20**, 1256–1260.
204 X. Z. Shu, X. F. Xia, Y. F. Yang, K. G. Ji, X. Y. Liuand and Y. M. Liang, *J. Org. Chem.*, 2009, **74**, 7464–7469.
205 H. Zaimoku, T. Hatta, T. Taniguchi and H. Ishibashi, *Org. Lett.*, 2012, **14**, 6088–6091.
206 C. Y. Zhao, L. G. Li, Q. R. Liu, C. X. Pan, G. F. Su and D. L. Mo, *Org. Biomol. Chem.*, 2016, **14**, 6795–6803.
207 N. Doben, H. Yan, M. Kischkewitz, J. Mao and A. Studer, *Org. Lett.*, 2018, **20**, 7933–7936.
208 D. M. Chen, Y. Y. Sun, Q. Q. Han and Z. L. Wang, *Tetrahedron Lett.*, 2020, **61**, 152482.
209 V. Gouverneur and K. Seppelt, *Chem. Rev.*, 2015, **115**, 563–565.
210 Y. Ogawa, E. Tokunaga, O. Kobayashi, K. Hirai and N. Shibata, *iScience*, 2020, **23**, 101467.
211 M. M. Alauddin, *Am. J. Nucl. Med. Mol. Imamging*, 2012, **2**, 55–76.
212 M. Saito, K. Miyamoto and M. Ochiai, *Chem. Commun.*, 2011, **47**, 3410–3412.
213 T. Tian, W. H. Zhong, S. Meng, X. B. Meng and Z. J. Li, *J. Org. Chem.*, 2013, **78**, 728–732.
214 S. Hara, M. Sekiguchi, A. Ohmori, T. Fukuhara and N. Yoneda, *Chem. Commun.*, 1996, 1899–1900.
215 M. Yoshida, K. Fujikawa, S. Sato and S. Hara, *Arkivoc*, 2003, **vi**, 36–42.
216 T. Kitamura, S. Kuriki, M. H. Morshed and Y. Hori, *Org. Lett.*, 2011, **13**, 2392–2394.
217 G. C. Geary, E. G. Hope, K. Singh and A. M. Stuart, *Chem. Commun.*, 2013, **49**, 9263–9265.
218 S. Suzuki, T. Kamo, K. Fukushi, T. Hiramatsu, E. Tokunaga, T. Dohi, Y. Kita and N. Shibata, *Chem. Sci.*, 2014, **5**, 2754–2760.
219 T. Kitamura, K. Muta and K. Muta, *J. Org. Chem.*, 2014, **79**, 5842–5846.

220 T. Kitamura, K. Muta and J. Oyamada, *Synthesis*, 2015, 3241–3245.
221 L. Wang, T. Kitamura, Y. Zhou, G. Butler and V. A. Soloshonok, *J. Fluor. Chem.*, 2020, **240**, 109670.
222 M. A. Arrica and T. Wirth, *Eur. J. Org. Chem.*, 2005, 395–403.
223 C. T. Xu, Y. Weizhe, J. Qian, W. G. An and G. Li, *Eur. J. Org. Chem.*, 2018, 5972–5979.
224 Y. Lee and M. S. Kwon, *Eur. J. Org. Chem.*, 2020, 6028–6043.
225 M. H. Shaw, J. Twilton and D. W. C. MacMillan, *J. Org. Chem.*, 2016, **81**, 6898–6926.
226 D. P. Hari, P. Schroll and B. Konig, *J. Am. Chem. Soc.*, 2012, **134**, 2958–2961.
227 T. Xiao, X. Dong, Y. Tang and L. Zhou, *Adv. Synth. Catal.*, 2012, **354**, 3195–3199.
228 L. Huang and J. Zhao, *RSC Adv.*, 2013, **3**, 23377–23388.
229 I. Ghosh, T. Ghosh, J. I. Bardagi and B. König, *Science*, 2014, **346**, 725–728.
230 P. Maity, D. Kundu and B. C. Ranu, *Eur. J. Org. Chem.*, 2015, 1727–1734.
231 S. O. Poelma, G. L. Burnett, E. H. Discekici, K. M. Mattson, N. J. Treat, Y. Luo, Z. M. Hudson, S. L. Shankel, P. G. Clark, J. W. Kramer, C. J. Hawker and J. R. de Alaniz, *J. Org. Chem.*, 2016, **81**, 7155–7160.
232 A. U. Meyer, T. Slanina, C. J. Yao and B. König, *ACS Catal.*, 2016, **6**, 369–375.
233 L. Marzo, I. Ghosh, F. Esteban and B. König, *ACS Catal.*, 2016, **6**, 6780–6784.
234 A. Graml, I. Ghosh and B. König, *J. Org. Chem.*, 2017, **82**, 3552–3560.
235 K. R. Jasinska, B. Konig and D. Gryko, *Eur. J. Org. Chem.*, 2017, 2104–2107.
236 Y. S. Feng, X. S. Bu, B. Huang, C. Rong and H. J. Xu, *Tetrahedron Lett.*, 2017, **58**, 1939–1942.
237 D. Wang, C. Cheng, Q. Wu, J. Wang, Z. Kang, X. Guo, H. Wu, E. Hao and L. Jiao, *Org. Lett.*, 2019, **21**, 5121–5125.
238 R. Kapoor, R. Chawla and L. D. S. Yadav, *Tetrahedron Lett.*, 2019, **60**, 805–809.
239 M. H. Aukland, M. Siauciulis, A. West, G. J. P. Perry and D. J. Procter, *Nat. Catal.*, 2020, **3**, 163–169.
240 T. Adak, C. Hu, M. Rudolph, J. Li and A. S. K. Hashmi, *Org. Lett.*, 2020, **22**, 5640–5644.
241 A. M. M. Gualda, R. Cano, L. Marzo, R. P. Ruiz, J. L. Barrera, R. M. Balleste, A. Fraile, V. A. de la, P. OShea and J. Aleman, *Nat. Commun.*, 2019, **10**, 2634.
242 X. Li, X. Gu, Y. Li and P. Li, *ACS Catal.*, 2014, **4**, 1897–1900.
243 K. Zhao, X. C. Zhang, J. Y. Tao, X. D. Wu, J. X. Wu, W. M. Li, T. H. Zhu and T. P. Loh, *Green Chem.*, 2020, **22**, 5497–5503.
244 L. Cui, Y. Matusaki, N. Tada, T. Miura, B. Uno and A. Itoh, *Adv. Synth. Catal.*, 2013, **355**, 2203–2207.
245 S. P. Pitre, C. D. McTiernan, H. Ismaili and J. C. Scaiano, *ACS Catal.*, 2014, **4**, 2530–2535.
246 Q. Lefebvre, N. Hoffmann and M. Rueping, *Chem. Commun.*, 2016, **52**, 2493–2496.
247 S. B. Vallejo, D. E. Yerien and A. Postigo, *Eur. J. Org. Chem.*, 2015, 7869–7875.
248 J. K. Matsui, D. N. Primer and G. A. Molander, *Chem. Sci.*, 2017, **8**, 3512–3522.
249 J. K. Matsui and G. A. Molander, *Org. Lett.*, 2017, **19**, 950–953.
250 D. P. Tiwari, S. Dabral, J. Wen, J. Wiesenthal, S. Terhorst and C. Bolm, *Org. Lett.*, 2017, **19**, 4295–4298.
251 J. B. McManus and D. A. Nicewicz, *J. Am. Chem. Soc.*, 2017, **139**, 2880–2883.
252 X. Q. Dai, W. X. Xu, Y. L. Wen, X. H. Liu and J. Q. Weng, *Tetrahedron Lett.*, 2018, **59**, 2945–2949.
253 T. C. Sherwood, N. Li, A. N. Yazdani and T. G. M. Dhar, *J. Org. Chem.*, 2018, **83**, 3000–3012.
254 T. C. Sherwood, H. Y. Xiao, R. G. Bhaskar, E. M. Simmons, S. Zaretsky, M. P. Rauch, R. R. Knowles and T. G. Murali Dhar, *J. Org. Chem.*, 2019, **84**, 8360–8379.
255 P. Natarajan, D. Chuskita and Priya, *Green Chem.*, 2019, **21**, 4406–4411.
256 Z. Y. Yu, J. N. Zhao, F. Yang, X. F. Tang, Y. F. Wu, C. F. Ma, B. Song, L. Yun and Q. W. Meng, *RSC Adv.*, 2020, **10**, 4825–4831.
257 G. Pandey, K. S. Rani and G. Lakshmaiah, *Tetraheron Lett.*, 1992, **33**, 5107–5110.
258 G. Cocquet, C. Ferroud, P. Simona and P. L. Tabernaa, *J. Chem. Soc., Perkin Trans. 2*, 2000, 1147–1153.
259 D. P. Hari and B. Konig, *Org. Lett.*, 2011, **13**, 3852–3855.
260 Q. Liu, Y. N. Li, H. H. Zhang, B. Chen, C. H. Tung and L. Z. Wu, *Chem. – Eur. J.*, 2012, **18**, 620–627.
261 M. Rueping, C. Vila and T. Bootwicha, *ACS Catal.*, 2013, **3**, 1676–1680.
262 M. N. Gandy, C. L. Raston and K. A. Stubbs, *Chem. Commun.*, 2015, **51**, 11041–11044.
263 Y. Zhao, C. Zhang, K. F. Chin, O. Pytela, G. Wei, H. Liu, F. Bures and Z. Jiang, *RSC Adv.*, 2014, **4**, 30062–30067.
264 X. Liu, X. Ye, F. Bures, H. Liu and Z. Jiang, *Angew. Chem., Int. Ed.*, 2015, **54**, 11443–11447.
265 G. Wei, C. Zhang, F. Bures, X. Ye, C. H. Tan and Z. Jiang, *ACS Catal.*, 2016, **6**, 3708–3712.
266 X. Z. Fan, J. W. Rong, H. L. Wu, Q. Zhou, H. P. Deng, J. D. Tan, C. W. Xue, L. Z. Wu, H. R. Tao and J. Wu, *Angew. Chem., Int. Ed.*, 2018, **57**, 8514–8518.
267 K. G. Ghosh, D. Das, P. Chandu and D. Sureshkumar, *J. Org. Chem.*, 2021, **86**, 2644–2657.
268 T. Adak, M. Hoffmann, S. Witzel, M. Rudolph, A. Dreuw and A. S. K. Hashmi, *Chem. – Eur. J.*, 2020, **26**, 15573–15580.
269 M. J. Yi, H. X. Zhang, T. F. Xiao, J. H. Zhang, Z. T. Feng, L. P. Wei, G. Q. Xu and P. F. Xu, *ACS Catal.*, 2021, **11**, 3466–3472.
270 Y. Zhao, B. Huang, C. Yang, B. Li, B. Gou and W. Xia, *ACS Catal.*, 2017, **7**, 2446–2451.
271 N. A. Romero, K. A. Margrey, N. E. Tay and D. A. Nicewicz, *Science*, 2015, **349**, 1326–1330.
272 K. A. Margrey, A. Levens and D. A. Nicewicz, *Angew. Chem., Int. Ed.*, 2017, **56**, 15644–15648.
273 K. A. Margrey, W. L. Czaplyski, D. A. Nicewicz and E. J. Alexanian, *J. Am. Chem. Soc.*, 2018, **140**, 4213–4217.
274 W. Wei, L. Wang, P. Bao, Y. Shao, H. Yue, D. Yang, X. Yang, X. Zhao and H. Wang, *Org. Lett.*, 2018, **20**, 7125–7130.

275 J. R. Xin, Y. H. He and Z. Guan, *Org. Chem. Front.*, 2018, **5**, 1684–1688.
276 S. Saba, C. R. D. Santos, B. R. Zavarise, A. A. S. Naujorks, M. S. Franco, A. R. Schneider, M. R. Scheide, R. F. Affeldt, J. Rafique and A. L. Braga, *Chem. – Eur. J.*, 2020, **26**, 4461–4466.
277 M. Zheng, I. Ghosh, B. Konig and X. Wang, *Chem. Cat. Chem*, 2019, **11**, 703–706.
278 J. L. Hofstra, B. R. Grassbaugh, Q. M. Tran, N. R. Armada and H. J. P. de Lijser, *J. Org. Chem.*, 2015, **80**, 256–265.
279 G. Kibriya, S. Samanta, S. Jana, S. Mondal and A. Hajra, *J. Org. Chem.*, 2017, **82**, 13722–13727.
280 A. De, S. Santra, A. Hajra, G. V. Zyryanov and A. Majee, *J. Org. Chem.*, 2019, **84**, 11735–11740.
281 L. Zhao, L. Wang, Y. Gao, Z. Wang and P. Li, *Adv. Synth. Catal.*, 2019, **361**, 5363–5370.
282 X. Xu, C. Xia, X. Li, J. Suna and L. Hao, *RSC Adv.*, 2020, **10**, 2016–2026.
283 K. Luo, Y. Z. Chen, W. C. Yang, J. Zhu and L. Wu, *Org. Lett.*, 2016, **18**, 452–455.
284 P. Peng, L. Peng, G. Wang, F. Wang, Y. Luoa and A. Lei, *Org. Chem. Front.*, 2016, **3**, 749–752.
285 M. Singsardar, A. Dey, R. Sarkar and A. Hajra, *J. Org. Chem.*, 2018, **83**, 12694–12701.
286 F. Gao, K. Sun, X.-L. Chen, T. Shi, X.-Y. Li, L.-B. Qu, Y.-F. Zhao and B. Yu, *J. Org. Chem.*, 2020, **85**, 14744–14752.
287 J.-B. Xia, C. Zhu and C. Chen, *J. Am. Chem. Soc.*, 2013, **135**, 17494–17500.
288 D. Cantillo, O. de Frutos, J. A. Rincón, C. Mateos and C. O. Kappe, *J. Org. Chem.*, 2014, **79**, 8486–8490.
289 H. Zhao and J. Jin, *Org. Lett.*, 2019, **21**, 6179–6184.
290 V. Rathore and S. Kumar, *Green Chem.*, 2019, **21**, 2670–2676.
291 B. Bieszczad, L. A. Perego and P. Melchiorre, *Angew. Chem., Int. Ed.*, 2019, **58**, 16878–16883.
292 E. J. McClain, T. M. Monos, M. Mori, J. W. Beatty and C. R. J. Stephenson, *ACS Catal.*, 2020, **10**, 12636–12641.
293 M. J. James, F. Strieth-Kalthoff, F. Sandfort, F. J. R. Klauck, F. Wagener and F. Glorius, *Chem. – Eur. J.*, 2019, **25**, 8240–8244.
294 R. C. Silva, L. F. Villela, T. J. Brocksom and K. T. de Oliveira, *RSC Adv.*, 2020, **10**, 31115–31122.
295 C. Wang, R. Qi, H. Xue, Y. Shen, M. Chang, Y. Chen, R. Wang and Z. Xu, *Angew. Chem., Int. Ed.*, 2020, **59**, 7461–7466.
296 É. Rochette, M.-A. Courtemanche and F.-G. Fontaine, *Chem. – Eur. J.*, 2017, **23**, 3567–3571.
297 M.-A. Légaré, M.-A. Courtemanche, É. Rochette and F.-G. Fontaine, *Science*, 2015, **349**, 513–516.
298 S. Zhang, Y. Han, J. He and Y. Zhang, *J. Org. Chem.*, 2018, **83**, 1377–1386.
299 É. Rochette, V. Desrosiers, Y. Soltani and F.-G. Fontaine, *J. Am. Chem. Soc.*, 2019, **141**, 12305–12311.
300 J. Lv, X. Chen, X.-S. Xue, B. Zhao, Y. Liang, M. Wang, L. Jin, Y. Yuan, Y. Han, Y. Zhao, Y. Lu, J. Zhao, W.-Y. Sun, K. N. Houk and Z. Shi, *Nature*, 2019, **575**, 336–341.
301 S. A. Iqbal, J. Cid, R. J. Procter, M. Uzelac, K. Yuan and M. J. Ingleson, *Angew. Chem., Int. Ed.*, 2019, **58**, 15381–15385.
302 A. A. Toutov, W.-B. Liu, K. N. Betz1, A. Fedorov, B. M. Stoltz and R. H. Grubbs, *Nature*, 2015, **518**, 80–84.
303 C. Tortoreto, D. Rackl and H. M. L. Davies, *Org. Lett.*, 2017, **19**, 770–773.
304 C. Shu, A. Noble and V. K. Aggarwal, *Nature*, 2020, **586**, 714–719.
305 X. Wang and A. Studer, *Angew. Chem., Int. Ed.*, 2018, **57**, 11792–11796.
306 B.-H. Chen, Y.-D. Du and W. Shu, *Angew. Chem., Int. Ed.*, 2022, **61**, e2022007.
307 J. Yan, A. P. Pulis, G. J. P. Perry and D. J. Procter, *Angew. Chem., Int. Ed.*, 2019, **58**, 15675–15679.
308 L. Bering and A. P. Antonchick, *Org. Lett.*, 2015, **17**, 3134–3137.
309 R. Kumar, I. Kumar, R. Sharma and U. Sharma, *Org. Biomol. Chem.*, 2016, **14**, 2613–2617.
310 H. Xia, Y. Liu, P. Zhao, S. Gou and J. Wang, *Org. Lett.*, 2016, **18**, 1796–1799.
311 G. E. M. Crisenza, E. M. Dauncey and J. F. Bower, *Org. Biomol. Chem.*, 2016, **14**, 5820–5825.
312 X. Chen, M. Peng, H. Huang, Y. Zheng, X. Tao, C. He and Y. Xiao, *Org. Biomol. Chem.*, 2018, **16**, 6202–6205.
313 L.-Y. Xie, S. Peng, F. Liu, J.-Y. Yi, M. Wang, Z. Tang, X. Xu and W.-M. He, *Adv. Synth. Catal.*, 2018, **360**, 4259–4264.
314 A. K. Dhiman, D. Chandra, R. Kumar and U. Sharma, *J. Org. Chem.*, 2019, **84**, 6962–6969.
315 B. K. Sarmah, M. Konwar, D. Bhattacharyya, P. Adhikari and A. Das, *Adv. Synth. Catal.*, 2019, **361**, 5616–5625.
316 B. K. Sarmah, M. Konwar and A. Das, *J. Org. Chem.*, 2021, **86**, 10762–10772.
317 D. Cheng and W. Bao, *Adv. Synth. Catal.*, 2008, **350**, 1263–1266.
318 W. Tu, L. Liu and P. E. Floreancig, *Angew. Chem., Int. Ed.*, 2008, **47**, 4184–4187.
319 R. Zhou, H. Liu, H. Tao, X. Yua and J. Wu, *Chem. Sci.*, 2017, **8**, 4654–4659.
320 Y. Amaoka, S. Kamijo, T. Hoshikawa and M. Inoue, *J. Org. Chem.*, 2012, **77**, 9959–9969.
321 Y. Amaoka, M. Nagatomo and M. Inoue, *Org. Lett.*, 2013, **15**, 2160–2163.
322 R. Paira, B. Singh, P. K. Hota, J. Ahmed, S. C. Sau, J. P. Johnpeter and S. K. Mandal, *J. Org. Chem.*, 2016, **81**, 2432–2441.
323 J. Ahmed, P. Sreejyothi, G. Vijaykumar, A. Jose, M. Raj and S. K. Mandal, *Chem. Sci.*, 2017, **8**, 7798–7806.
324 M. K. Tiwari, L. Yadav and S. Chaudhary, *Chem. Select*, 2020, **5**, 11968–11975.
325 F. Berger, M. B. Plutschack, J. Riegger, W. Yu, S. Speicher, M. Ho, N. Frank and T. Ritter, *Nature*, 2019, **567**, 223–228.
326 J. A. Fernández-Salas, A. P. Pulis and D. J. Procter, *Chem. Commun.*, 2016, **52**, 12364–12367.
327 M. H. Aukland, M. Šiaučiulis, A. West, G. J. P. Perry and D. J. Procter, *Nat. Catal.*, 2020, **3**, 163–169.
328 D. Wang, C. G. Carlton, M. Tayu, J. J. W. McDouall, G. J. P. Perry and D. J. Procter, *Angew. Chem., Int. Ed.*, 2020, **59**, 15918–15922.